ELUCIDATING MOLECULAR MECHANISMS OF ERBB2/NEU-INDUCED MAMMARY TUMORIGENESIS

by

MELISSA D. LANDIS

Submitted in partial fulfillment of the requirements

For the degree of Doctor of Philosophy

Dissertation Advisor: Dr. Ruth A. Keri

Department of Pharmacology

CASE WESTERN RESERVE UNIVERSITY

January, 2006

Print out two copies of this form on 25% Cotton Bond paper, as it will accompany your thesis or dissertation. (This notice will not show up on printouts).

CASE WESTERN RESERVE UNIVERSITY

SCHOOL OF GRADUATE STUDIES

We hereby approve the thesis/dissertation of

Melissa D. Landis

candidate for the Ph.D. degree *.

(signed) John H. Nilson, Ph.D.
(chair of the committee)

Ruth A. Keri, Ph.D.

Paul N. MacDonald, Ph.D.

George R. Dubyak, Ph.D.

(date) August 26, 2005

*We also certify that written approval has been obtained for any proprietary material contained therein.

DEDICATION

I would like to dedicate my dissertation to my husband, Chris Landis. He has been able to see the final goal when I was unable to see beyond the frustration of the last failed experiment. Without his encouragement and relentless support, I would never have seen this entire process through to completion. Also, he has given me the greatest joy I have ever known in the two children we share.

Also, I would like to dedicate this work to the women in my life who have courageously battled breast cancer: my aunt, Kay Hickox, and my stepmother, Laurie King.

TABLE OF CONTENTS

LIST OF TABLES

LIST OF FIGURES

ACKNOWLEDGEMENTS

I am very grateful to the numerous people whose contributions made completion of my dissertation a reality. I would especially like to extend my gratitude to my research advisor and mentor, Ruth Keri. She is truly an amazing mentor who taught me on so many levels, both professionally and personally. She has taught me how to critically evaluate scientific data and appreciate the experimental details. She has also helped me to delve deeper into questions and in doing so challenged me to think on a whole new level. To Ruth, I am eternally grateful for her encouragement of my scientific maturation and her illustration of excellence in everything that she does.

I would also like to thank the members of my thesis committee for their continued contributions to my research. Paul MacDonald and George Dubyak have both provided constructive criticism and excellent advice throughout this Ph.D process. John Nilson has always served as a second mentor, as my so called "Grandfather of Science". He has provided the positive attitude and motivation to keep me moving on track. His door has always been open to any stragglers that might wander in, from the first time when he advised me of what a promising young investigator he saw in Ruth Keri to recent advice regarding the post-doctoral interviewing process.

The lab environment is always a changing entity. Initially when Ruth's lab first ventured out on its own, our mammary gland lab meetings included Ruth, Kristen Lozada, Erin Milliken, and myself. Without Kristen, our lab would be lost on

many levels. She not only manages our lab and our mice, but she has always been ready to dive head first into the latest ethical and political issues. Thanks for all the heartfelt discussions. Erin and I started this whole process together. We learned, laughed, and cried together a lot over the years. Thank you for your continued friendship and for continuing to helping me to evaluate and reevaluate issues both personal and scientific. As our lab has grown, so have the friendships and contributions. Thank you to Jonathan Mosley for his continued critical evaluation of our science and his generous spirit. And a special “Gracias” to Marjorie Montañez Wiscovich for her many hours of database interrogation to uncover information regarding the ever changing gene lists. After all, it was you that first noticed that all those TGF-β target genes were downregulated. That sent my research in a whole new and exciting direction. ¡Gracias! Thank you to the many members of the Nilson lab who made our lab meetings a learning experience, particularly Helai Mohammad and Tehnaz Parakh. Your strength and dedication have been inspiring. We are also eternally grateful for the “foster children” we gained from the departure of the Nilson lab. Darcie Seachrist and Jen Yori have been wonderful in sharing lab bench space, as well our pregnancies. I owe a special thanks to Darcie for her dedicated support both technically and personally. She can work magic with her hands at the bench, and she is relentless in critical evaluation of her work.

A special thanks to my family and friends who have always provided unconditional love and encouragement in all of lives’ arenas. Mom and Doug you have always made me believe that I could accomplish anything that I

desired. Dad, for many years now, you have encouraged me to embark upon math and science and have always helped me develop my goals and career path. The Landis's, Rex and Carolyn, thank you for your continued support as though I were one of your own children. Finally, to the rest of the Gang of Six, Hayley, Tosha, Caryn, Mic, and Nancy, thank you for always believing and encouraging.

ABBREVIATIONS

ActRIIB	type II Activin receptor B, also ALK4
ErbB2	also HER2 or Neu
HER2	human epidermal growth factor receptor 2, also ErbB2 or Neu
HIF-1	hypoxia induced factor - 1
LH	luteinizing hormone
MAPK	mitogen activated protein kinase
MMTV	mouse mammary tumor virus long terminal repeat
Neu	rodent form of human epidermal growth factor receptor 2 or ErbB2
NRG	neuregulin/heregulin
PI3K	phosphatidylinositol-3-kinase
PLC-γ	phospholipase C-γ
STAT	signal transducer and activator of transcriptiom
TGF-β	transforming growth factor-β
TβRI	transforming growth factor-β receptor I, also Alk5
TβRII	transforming growth factor-β receptor II
VEGF	vascular endothelial growth factor
WAP	whey acidic protein

Elucidating Molecular Mechanisms of ErbB2/Neu-Induced Mammary Tumorigenesis

Abstract

by

Melissa D. Landis

The 15-30% of human breast cancers that have upregulated HER2/ErbB2/Neu are highly aggressive and resistant to traditional treatments, resulting in poor prognosis. To identify novel therapeutic targets, we derived the transcriptomes associated with tumor progression in two independent mouse models of ErbB2/Neu-induced tumorigenesis. From MMTV-*Neu* mice, we identified 324 candidate genes unique to ErbB2/Neu-induced tumors relative to wild-type mammary glands. A subset of these genes also changed expression levels in preneoplastic mammary glands, indicating a pivotal role early in ErbB2/Neu-initiated tumorigenesis.

Downregulation of several known transforming growth factor (TGF)-β target genes in the ErbB2/Neu molecular signature suggested attenuation of the TGF-β signaling cascade in these tumors. Analysis of TGF-β-Receptor-I/ALK5 by western blot and immunohistochemistry confirmed that Smad-dependent TGF-β signaling was inactive in these tumors. Although absent in most of the tumor, colocalization of phosphorylated Smad2 and Activin-Receptor-IB/ALK4 at the tumor periphery suggested functional Activin signaling at the leading edge of

these tumors. Collectively, these data indicate intrinsic TGF-β pathway suppression in ErbB2/Neu tumors via loss of TGF-β-Receptor-I/ALK5.

Recent studies have shown that pregnancy can accelerate ErbB2/Neu tumor development, inducing a susceptible cell population in MMTV-*Neu* mammary glands. The stochastic pattern of tumor development in multiparous MMTV-*Neu* mice suggests additional events are required for ErbB2/Neu oncogenesis. It remains unclear whether such events are genetic or reflective of the dynamic, pregnancy-associated hormonal control of the gland. Bitransgenic mice generated by breeding MMTV-*Neu* mice with a model of ovarian hyperstimulation developed multifocal mammary tumors in an accelerated, synchronous manner compared to virgin MMTV-*Neu* animals. This synchrony of tumor development suggests that trophic maintenance of the mammary gland provides the additional events required for tumor formation and maintains the population of cells targeted by ErbB2/Neu for transformation.

The synchronous nature of tumor development in this bitransgenic mouse model permitted characterization of a window of commitment to tumorigenesis and subsequent identification of approximately 2800 genes that demonstrate altered expression with oncogenic commitment. Thirty-two of these genes are also changed in the preneoplastic glands of MMTV-*Neu* mice, suggesting that this subset of genes may be regulated by ErbB2/Neu and/or contribute to early events of ErbB2/Neu-induced tumorigenesis.

CHAPTER I

INTRODUCTION, REVIEW OF THE LITERATURE, AND STATEMENT OF PURPOSE

INTRODUCTION

Despite advances in cancer therapeutics over several decades, cancer accounts for 23% of all deaths in the United States each year (National Center for Health Statistics, Centers for Disease Control and Prevention, 2003). Moreover, our current systemic treatments are limited by narrow therapeutic index; the dosage at which most treatment modalities are effective generally causes toxic side effects. Thus, the quest for more targeted therapies with fewer side effects is of utmost importance.

Carcinogenesis is a multistep process attributable to progressive genetic alterations that induce transformation of normal cells to malignant cancer cells. Rationally-designed therapeutics are intended to selectively inhibit the deregulation of cellular processes that is caused by these genetic alterations in tumor cells but limit toxicity to normal cells. Recent advancement of cancer treatment by targeting specific molecular abnormalities emphasizes the significance of understanding the molecular mechanisms that cause tumor formation. The antileukemic effects of Gleevec/STI571 (Imatinib, Novartis, Basel, Switzerland), which targets the BCR-ABL kinase known to cause chronic myeloid leukemia, marked one of the first successes of rationally designed drug therapy (Druker et al., 2001). Targeted brain tumor therapy has reached a level

of success never achieved with other therapies (Lesniak and Brem, 2004). Herceptin (Trastuzmab, Genentech, San Francisco, CA), humanized monoclonal antibody targeting the HER2 receptor, has become the standard treatment for metastatic HER2-positive breast cancer (Goldenberg, 1999; Shepard et al., 1991; Sliwkowski et al., 1999). The success of each of these therapeutic approaches is attributable to a fundamental understanding of the molecular mechanisms that sustain tumor viablility.

Although recent advances of targeted therapies for cancer treatment are encouraging, continued research is necessary to improve our understanding of the molecular mechanisms that contribute to tumorigenesis and improve our therapeutic approaches. We are particularly interested in further elucidating the mechanisms that underlie induction of HER2 positive breast cancers since the 15-30% of breast tumors that express HER2 are highly aggressive and resistant to traditional therapies (Salomon et al., 1995; Slamon et al., 1989). Despite the standard use of Herceptin in treating metastatic breast disease (Goldenberg, 1999; Shepard et al., 1991; Sliwkowski et al., 1999), only 12-26% of patients respond to monotherapy (Baselga et al., 1996; Cobleigh et al., 1999; Vogel et al., 2002) and 49% respond with adjuvant therapy (Slamon et al., 2001). Thus it is imperative to improve our understanding of the oncogenic properties of HER2.

HER2/ErbB2/Neu in human breast cancer

The *HER2* gene, also known as *ErbB2* and *Neu*, is located on chromosome 17q12 and encodes a 185-kDA transmembrane protein that is a member of the

ErbB family of receptor tyrosine kinases (Coussens et al., 1985; Yamamoto et al., 1986). This family comprises four receptors with shared homology: epidermal growth factor (EGF) receptor (also termed ErbB1/HER1) (Ullrich et al., 1984), ErbB2/Neu/HER2 (Coussens et al., 1985), ErbB3/HER3 (Kraus et al., 1989), and ErbB4/HER4 (Plowman et al., 1993a). Each of these receptors is composed of three key regions. The extracellular ligand-binding domain with two critical cysteine-rich regions is relatively conserved despite the distinct ligand-binding properties of these receptors. ErbB2/Neu is a distinct member of this family in that it lacks any known ligand. Each ErbB receptor contains a hydrophobic membrane-spanning region and an intracellular domain with a highly conserved tyrosine kinase domain. ErbB3 is unique in lacking kinase activity due to mutations in its kinase domain. The kinase domain is flanked by a juxtamembrane domain and a carboxy-terminal tail with tyrosine autophosphorylation sites.

Although mutations within the human *HER2/ErbB2/Neu* gene in human breast cancer are rare (Lemoine et al., 1990; Slamon et al., 1989; Zoll et al., 1992), the entire gene is amplified in 15-30% of human breast cancers. The resultant overexpression of HER2 in tumor epithelium correlates with poor prognosis because of the highly aggressive and metastatic nature of these tumors and their resistance to traditional treatment paradigms (Carlomagno et al., 1996; De Placido et al., 2003; Houston et al., 1999; Revillion et al., 1998; Salomon et al., 1995; Slamon et al., 1987; Wright et al., 1992; Yu and Hung, 2000). The lack of effective treatment strategies and the fact that HER2 is only overexpressed in

cancerous cells have inspired development of rationally-designed therapeutics that specifically target ErbB2/Neu. Monoclonal antibodies against the ErbB2/Neu receptor, the murine mAb4D5 (Hudziak et al., 1989) and its humanized version, Trastuzumab (Herceptin) (Carter et al., 1992) prevent proliferation of tumor cells. This is most likely a direct effect of downregulation of ErbB2/Neu and subsequent inhibition of ErbB2/Neu-induced signaling cascades (Hudziak et al., 1989; Lane et al., 2000). While the antiproliferative and proapoptotic effect of Herceptin on HER2-positive tumor cells accounts for part of the response to this treatment, additional mechanisms are believed to be involved (Sliwkowski et al., 1999). In xenograft models, Herceptin stimulates recruitment of cytotoxic cells such as macrophages and monocytes (Clynes et al., 2000). Herceptin also prevents ectodomain shedding of the ErbB2/Neu receptor which has been suggested to cause constitutive signaling by HER2 (Molina et al., 2001)

Depending on the technique used to assess HER2 positive tumors, 12-26% of patients respond to single agent treatment with Trastuzumab/Herceptin (Baselga et al., 1996; Cobleigh et al., 1999; Vogel et al., 2002) Adjuvant therapy combining Herceptin with chemotherapeutics has proven to be more efficacious than treatment with chemotherapy alone (Esteva et al., 2002; Slamon et al., 2001), although combination with anthracyclines is discouraged due to cardiotoxicity (Tham et al., 2002). Most importantly, recent clinical studies in which breast cancer patients with early-stage, HER2 positive invasive tumors received adjuvant therapy combining Herceptin with chemotherapeutic agents reported a 52% decrease in disease recurrence than patients that received

chemotherapy alone (http://www.nsabp.pitt.edu/NCI_Herceptin_Press_Release_04252005.pdf) (2005). While these results are encouraging, many tumors are resistant to Herceptin treatment or eventually acquire resistance, necessitating the development of additional therapeutics.

Several drugs have been developed to combat resistance to Herceptin. Like Herceptin, Pertuzumab (Genentech) is an HER2-targeted monoclonal antibody, but it targets the dimerization arm of HER2, preventing formation of HER2-containing dimers (Franklin et al., 2004). Since it is currently being investigated in clinical trials, its efficacy is undetermined (Hynes and Lane, 2005). Additionally, several small molecule tyrosine-kinase inhibitors are currently in various stages of clinical trials including: Lapatinib (GlaxoSmithKline), AEE788 (Novartis), and CI-1033 (Pfizer) (Hynes and Lane, 2005). Current studies suggest that the most effective defense against HER2-overexpressing tumors requires combination therapy blocking multiple targets simultaneously.

HER2/ErbB2/Neu Signaling

The ErbB signaling network is multilayered

Signaling by the ErbB family of receptors is multilayered with overlap in downstream components (Marmor et al., 2004; Yarden, 2001; Yarden and Sliwkowski, 2001) (**Figure I-1**). Upon ligand binding to their extracellular domain, receptors dimerize and are activated by transphosphorylation. Resultant autophosphorylation of tyrosine residues in their cytoplasmic domains provide

docking sites for adaptor molecules which in turn induce a vast array of downstream signaling cascades.

There are three main levels of signaling that contribute to ErbB signaling complexity including the ligand-receptor interaction, receptor dimer formation, and adaptor protein activation of multiple intracellular signaling cascades. The first level of signaling complexity is achieved by combinatorial ligand-receptor interactions. The EGF-like peptide growth factors are synthesized as transmembrane precursors (Massague and Pandiella, 1993). As such, they can function as membrane-anchored growth factors to activate juxtacrine signaling; but, generally, they act as soluble growth factors, following proteolytic cleavage, to induce paracrine and autocrine signaling. This proteolytic cleavage and tissue- and developmental stage-specific expression determine ligand availability (Bates et al., 1988; Dickson et al., 1987; Dickson and Lippman, 1987; Harari et al., 1999; Martinez-Lacaci et al., 1995; Meyer and Birchmeier, 1995; Paria et al., 1999; Prenzel et al., 1999; Toyoda et al., 1995; Zhang et al., 1997). These growth factors share homology of an EGF-like domain that is composed of 45-55 amino acids with six cysteine residues that generate three intramolecular disulfide linkages (Salomon et al., 1995). These linkages form three loops in the secondary structure of each ligand. This EGF-like domain is both required and sufficient for interaction and activation with the ErbB family of receptors.

Distinct biochemical features of these growth factor ligands contribute to the signaling diversity of the ErbB network. The differential binding affinity of each of these growth factors for the different ErbB receptors influences signaling strength

and duration. Except for ErbB2/Neu, the other receptors in this family each selectively interact with high affinity ligands (Klapper et al., 1999). The EGF family of ligands can be divided into three main groups according to the receptor that they bind (Beerli and Hynes, 1996; Carraway, III et al., 1994; Chang et al., 1997; Elenius et al., 1997; Harari et al., 1999; Higashiyama et al., 1991; Johnson et al., 1993; Karunagaran et al., 1996; Pinkas-Kramarski et al., 1996; Plowman et al., 1993b; Riese et al., 1995; Riese et al., 1996a; Riese et al., 1996b; Riese and Stern, 1998; Shing et al., 1993; Shoyab et al., 1989; Toyoda et al., 1995; Zhang et al., 1997). The first group of ligands interacts specifically with EGFR and includes EGF, transforming growth factor-α, and amphiregulin. The second group of ligands share specificity for EGFR and ErbB4 and includes betacellulin, heparin-binding EGF, and epiregulin. The third group are neuregulins (NRG), also called heregulins and Neu differentiation factors, which can be subgrouped base on their ability to bind ErbB3 and ErbB4 (NRG1 and NRG2) or only ErbB4 (NRG3 and NRG4). Virally-encoded low affinity ligands have been shown to potentiate ErbB signaling by attenuating downregulation and degradation (Tzahar et al., 1998), and its possible that low affinity ligands may actually be more powerful signaling activators than high affinity ligands. The lack of a known ligand for ErbB2/Neu can be explained by two characteristics that were unveiled by recent structural analyses: 1) the unique arrangement of the extracellular domains blocks binding of soluble ligands and 2) alterations in the putative ligand-binding domain would most likely hinder ligand binding even if it were exposed (Garrett et al., 2003).

The bivalency of the EGF-like growth factors dictates which receptor pairs are induced, in turn determining which signaling cascades will be activated (Barbacci et al., 1995; Groenen et al., 1994; Jones et al., 1999; Katsuura and Tanaka, 1989; Lemmon et al., 1997; Tzahar et al., 1997). Bivalent ligands contain both a low and high affinity receptor binding site. For example, NRG1 has a high affinity site in the amino terminal region of the EGF-like domain and a low affinity site on the carboxy terminal region of the EGF-like domain (Barbacci et al., 1995; Jones et al., 1999; Pinkas-Kramarski et al., 1996; Tzahar et al., 1997), thus allowing NRG to induce a heterodimer of ErbB3 and another ErbB receptor.

Furthermore, the stability of each ligand-receptor pair is differentially influenced by pH. For example, a pH-resistant ligand-receptor interaction, i.e, EGF/EGFR, will target the ErbB receptor to the lysosome for degradation. In contrast, a pH-sensitive interaction, i.e. TGF-α/EGFR and NRG1/ErbB3, will dissociate in the endosome so that the receptor is recycled to the cell surface (French et al., 1995; Waterman et al., 1998). This is critical for receptor trafficking and, thus, signaling duration and strength.

A second level of signaling complexity is achieved by the induction of ErbB receptor dimers following ligand-receptor interaction. Oligomerization of the receptors induces transphosphorylation of the tyrosine residues located in the activation loop of the kinase domain, thus, enhancing the intrinsic kinase activity of each of the receptors in the complex (Carraway, III and Cantley, 1994; Goldman et al., 1990; Peles et al., 1993; van der et al., 1994; Wada et al., 1990). ErbB3 is unique in that it lacks kinase activity due to substitutions in its kinase

domain, thus it relies on interaction with other ErbB receptors to be activated (Guy et al., 1994). The ensuing autophosphorylation of tyrosine residues on the carboxy terminal tail of the ErbB receptors generates binding sites for adaptor proteins containing Src homology (SH2) and phosphotyrosine binding (PTB) domains, thus dictating which signaling pathways are activated.

Dimerization occurs in a hierarchy among the ErbB receptors, with ErbB2/Neu being the preferred partner for the other receptors (Graus-Porta et al., 1997; Tzahar et al., 1996). Recent success in deciphering the crystal structures of the ErbB receptors has provided explanations for some of these unique properties (Burgess et al., 2003; Cho et al., 2003; Garrett et al., 2003). ErbB2/Neu maintains a closed configuration that resembles the ligand-bound conformation of ErbB3 and EGFR, so ErbB2 is constitutively “poised” for interactions with the other ligand-bound ErbB receptors, providing a stuctural explanation as to why ErbB2/Neu is the preferred dimerization partner (Cho et al., 2003; Garrett et al., 2003).

Heterodimerization diversifies the biological response, increasing both the duration and the intensity of the signal. The simplest explanation for synergism of these receptors is that they activate complementary signaling pathways, but, actually, activation of diverse pathways potentiates the biological response. Each receptor has unique profile of adaptor proteins as determined by the pattern of phosphorylated tyrosyl residues in the carboxy terminus (Olayioye et al., 2000). For example, the ErbB3 receptor contains six p85 Src homology 2 (SH2) domain recognition sequences that serve as docking sites for the p85

subunit of PI3K; consequently, the PI3K-Akt pathway is preferentially induced when the ErbB3 receptor is activated (Soltoff et al., 1994). Accordingly, the identity of activated receptors determines which downstream signaling cascades are induced.

Induction of multiple signaling pathways by the adaptor proteins generates a third level of signaling diversification. These enzyme cascades include, but are not limited to (Olayioye et al., 2000): Ras-mitogen-activated kinase (MAPK;(Dougall et al., 1994; Olayioye et al., 2000; Yarden and Sliwkowski, 2001), the signal transducer and activator of transcription (STAT) pathways (Yu and Jove, 2004), phospholipase (PLC)-γ, phosphitidyl inositol 3-kinase (PI3K)-Akt (Soltoff et al., 1994; Yarden and Sliwkowski, 2001), mammalian target of rapamycin (mTOR) (Bjornsti and Houghton, 2004), src tyrosine kinase (Ishizawar and Parsons, 2004; Olayioye et al., 1999; Olayioye et al., 2001). In the final steps, these signaling cascades regulate transcription factors that converge on the nucleus to alter the cellular transcriptome. The Ras/MAPK, STAT, PLCγ, and PI3K/Akt pathways and their key nuclear effectors are schematically represented in **Figure I-1**. Overall, a growth factor signal is relayed from the cell surface through an ErbB receptor pair to the nucleus to alter cellular processes such as cell proliferation, survival, differentiation, motility, and death (Alroy and Yarden, 1997). The cellular outcome is determined by the complement of activated signaling pathways as well as the magnitude and duration of signaling, as determined by the specificity of interactions among the signaling moieties at each level of the cascade and regulatory mechanisms integrated into each level of signaling.

Cellular trafficking regulates ErbB Signaling

The ErbB signaling network is regulated by membrane trafficking of ErbB receptors. The specific EGFR signaling effectors are determined by the cellular location of EGFR. For example, Shc and PLC-γ are preferentially phosphorylated on the cell surface; whereas, EGFR itself and the p85 subunit of PI3K are preferentially phosphorylated in the mildly acidic early endosome (Vieira et al., 1996). Furthermore, intracellular membrane trafficking of ErbB receptors regulates the strength and duration of activated ErbB signaling pathways. Under normal physiological conditions, ligand binding induces rapid clustering of EGFR into clathrin-coated pits, and, subsequently, the cell membrane invaginates to produce endocytic vesicles. These vesicles then mature to early and late endosomes with a gradual decline of pH and accumulation of hydrolytic enzymes so that, ultimately, EGFR is degraded in the lysosome. Compared to EGFR, the other ErbB receptors are endocytically impaired (Baulida et al., 1996; Pinkas-Kramarski et al., 1996). Indeed, while EGFR homodimers are targeted to the lysosome for degradation, ErbB3 is constitutively recycled to the cell surface (Waterman et al., 1998). Moreover, heterodimerization with ErbB2/Neu slows endocytosis and increases recycling of its partners (Lenferink et al., 1998). The dependency of downregulation of receptor type indicates that potency and/or efficacy of signaling is also receptor dependent.

This differential regulation of ErbB receptors is attributed to multiple mechanisms. The rate of receptor internalization is determined by cytoplasmic motifs (Sorkin et al., 1993). For example, in studies with chimeric and normal ErbB2/Neu and

EGFR, the carboxyl-terminus of ErbB2/Neu delayed internalization 3-4 fold (Sorkin et al., 1993). However, receptor sorting in the endosomes is dependent on the pH-sensitivity of the ligand-receptor interaction. If the complex is dissociated in the mildly acidic conditions of the early endosome, such as the NRG1/ErbB3 and TGF-α/EGFR complexes, then the receptor is recycled to the cell surface (French et al., 1995; Waterman et al., 1998). Alternatively, the relatively pH-insensitive complex of EGF and EGFR dissociates much later, thus continuous activation of tyrosine phosphorylation by this complex generates phosphorylation of a docking site for an ubiquitin ligase, c-Cbl (Muthuswamy et al., 1999). c-Cbl preferentially binds and attaches polyubiquitin chains to EGFR homodimers, targeting them to the lysosome for degradation (Levkowitz et al., 1998; Levkowitz et al., 1999). Conversely, avoidance of c-Cbl-mediated degradation, allows ErbB3 and ErbB2/Neu to recycle to the cell surface (Klapper et al., 2000). The distinct mechanisms involved in downregulation of each of the ErbB receptors underscore the complexity of ErbB signaling in regulating cellular processes.

A mechanistic view of ErbB2/Neu-induced oncogenesis

Breast tumor development is a multi-step process in which epithelial cells progress through many stages including normal, hyperplastic, dysplastic, and eventually malignant (Beckmann et al., 1997; Hanahan and Weinberg, 2000). This stochastic process is reflective of multiple underlying genetic alterations that ultimately allow tumor cells to acquire several key properties that drive tumor formation. These include: “self-sufficiency in growth signals, limitless replicative

ability, evading apoptosis, insensitivity to anti-growth signals, sustained angiogenesis, tissue invasion and metastasis" (Hanahan and Weinberg, 2000). Herein, we will discuss how overexpression of ErbB2/Neu allows mammary cells to acquire these oncogenic capabilities. The oncogenic potential of ErbB2/Neu is related to its overexpression. While a mutant form of ErbB2/Neu is rare in humans, amplification of the gene and resultant overexpression is well documented and correlates with poor prognosis. Overexpression of ErbB2/Neu is believed to drive spontaneous dimer formation and, consequently, potentiate signaling by constitutive kinase activation. Aberrant ErbB2/Neu signaling circumvents multiple check points that normally protect the cell from dysregulated growth, ultimately driving transformation of mammary epithelia.

Receptor dimerization drives cellular transformation

Manipulations of ErbB2/Neu in several model systems have revealed the unique transforming capabilities of ErbB2/Neu. Overexpression of normal ErbB2/Neu confers several oncogenic properties on cells including: growth factor independence (Ignatoski et al., 1999), anchorage-independent growth (Di Fiore et al., 1987; Di Marco et al., 1990; Hudziak et al., 1987), and the gold-standard of *in vitro* transformation assays, tumor formation in nude mice (Di Fiore et al., 1987; Di Marco et al., 1990; Hudziak et al., 1987). Furthermore, MMTV-*Neu* mice that express high levels of the rat form of *ErbB2/Neu* in the mammary gland under direction of the mammary gland selective MMTV promoter develop focal mammary tumors with long latency and will eventually acquire pulmonary metastases (Guy et al., 1992). The mammary tumors are estrogen-receptor

negative, solid, nodular lesions composed of intermediate cells that histologically resemble a subset of human breast tumors (Cardiff et al., 2000; Wu et al., 2002). Alternatively, a transforming ErbB2/Neu gene with a single point mutation encoding an amino acid substitution (Valine to Glutamate) was identified in carcinogen-induced neuro/glioblastomas (Bargmann et al., 1986; Schechter et al., 1984). This oncogenic form of ErbB2/Neu, hereafter referred to as *NeuT*, transforms cells in tissue culture models and in transgenic mice. Transgenic mice that harbor an MMTV-*NeuT* expression cassette rapidly develop multifocal mammary tumors and eventually acquire pulmonary metastases (Bouchard et al., 1989; Guy et al., 1996; Muller et al., 1988).

From mechanistic analyses of these models of ErbB2/Neu-induced transformation, a common hypothesis emerged: transformation of cells is associated with constitutive kinase activity of ErbB2/Neu (Bargmann and Weinberg, 1988; Di Fiore et al., 1987; Di Marco et al., 1990; Segatto et al., 1988). Constitutive kinase activity may be driven by homodimerization of ErbB2/Neu receptors and/or heterodimerization with other ErbB receptors. The oncogenic potential of ErbB2/Neu may be related to its high level of basal autophosphorylation (Lonardo et al., 1990). Accordingly, elevated expression of ErbB2/Neu could drive homodimerization and constitutive kinase activity in the absence of heterodimerization with a ligand-bound family member (Debnath et al., 2002; Di Fiore et al., 1987; Di Marco et al., 1990). This theme of spontaneous ErbB2/Neu homodimer formation is analogous to the constitutive homodimer formation of oncogenic *NeuT* (Bargmann and Weinberg, 1988;

Schechter et al., 1984; Segatto et al., 1988). Although homodimerization alone may contribute to oncogenesis, the oncogenic capacity of ErbB2/Neu is probably related to its ability to drive heterodimerization with other ErbB receptors (Siegel et al., 1999). Autocrine activation of EGFR through upregulation of its ligands has been observed in human ErbB2/Neu-positive tumors (Salomon et al., 1995). The coexpression of ErbB2/Neu and ErbB3 in tumors derived from mouse models of ErbB2/Neu-induced mammary tumorigenesis further supports a role for cooperative transformation by ErbB receptors (DiGiovanna et al., 1998).

The oncogenic capacity of ErbB2/Neu-containing heterodimers is most likely related to the diversification of signaling by heterodimers and the potentiation of signaling by the unique properties bestowed by ErbB2/Neu in a receptor pair. Heterodimers actually have stronger mitogenic potential than their homomeric counterparts. This was first recognized by the synergistic interaction of EGFR and ErbB2/Neu in the transformation of NR6 fibroblasts (Kokai et al., 1989). Several subsequent studies corroborated this potentiation of transformation by other receptor heterodimers (Alimandi et al., 1995; Cohen et al., 1996; Zhang et al., 1996).

The oncogenic capacity of heterodimers containing ErbB2/Neu may be related to the unique ability of ErbB2/Neu to potentiate signaling by evading downregulation. As the favored heterodimerization partner of the ErbB receptor family, ErbB2/Neu imparts several unique characteristics to a receptor complex. Overexpression of ErbB2/Neu enhances and extends signaling through the MAPK pathway in cells (Karunagaran et al., 1996). Normally, receptor signaling

is rapidly inactivated by several mechanisms such as dissociation of the ligand-receptor complex, dephosphorylation, rapid internalization, and lysosomal degradation. However, overexpression of ErbB2/Neu prolongs signaling by delaying each of these steps of desensitization except for receptor dephosphorylation. ErbB2/Neu attenuates ligand-receptor dissociation. This is illustrated by the increased affinity of EGF (Karunagaran et al., 1996; Wada et al., 1990) and NRGs (Karunagaran et al., 1996; Peles et al., 1993; Sliwkowski et al., 1994; Tzahar et al., 1996) for their respective receptors in the presence of ErbB2/Neu. This increased ligand-receptor affinity is dependent on the extracellular domain of ErbB2/Neu as revealed by accelerated ligand-receptor dissociation by inhibitory antibodies directed at the extracellular domain of ErbB2/Neu (Klapper et al., 1997). Furthermore, ErbB2/Neu impedes internalization and endocytosis. Studies with chimeric proteins in cell lines showed that the carboxyl-terminus of ErbB2/Neu delays receptor internalization, and consequently receptor down-regulation and degradation (Sorkin et al., 1993). While ErbB2/Neu and EGFR coexpression does not affect EGFR internalization, overexpression of ErbB2/Neu increased EGFR recycling with concomitant delay in receptor degradation (Lenferink et al., 1998; Worthylake et al., 1999). Since recycling is the default mechanism, ErbB2/Neu appears to alter EGFR lysosomal targeting. The inefficient degradation of ErbB2/Neu containing dimers is most likely due to the weak coupling between ErbB2/Neu and the ubiquitin ligase, c-Cbl (Klapper et al., 2000; Muthuswamy et al., 1999). Conversely, c-Cbl binds EGFR very efficiently and rapidly targets it to the lysosome for degradation

(Muthuswamy et al., 1999). In conclusion, the oncogenic capacity of heterodimers containing ErbB2/Neu may be related to the unique ability of ErbB2/Neu to potentiate signaling by evading downregulation.

Overexpression of ErbB2/Neu drives tumor cell proliferation

Inhibition of ErbB2/Neu by various methods has demonstrated that sustained proliferation of ErbB2-overexpressing tumor cells is dependent on the presence of functional ErbB2/Neu. These methods included: antagonistic antibodies (Lane et al., 2000; Le et al., 2003; Yakes et al., 2002), small molecule inhibitors (Barbacci et al., 2003; Moasser et al., 2001; Motoyama et al., 2002), compounds causing ErbB2/Neu degradation (Basso et al., 2002; Munster et al., 2002), single-chain antibody (scFv)-mediated retention of ErbB2/Neu in the endoplasmic reticulum (Neve et al., 2000), and retrovirus-mediated small interfering RNA (Yang et al., 2004). Several ErbB2/Neu nuclear effectors identified by these studies regulate the G1/S transition during cell cycle progression including: myc, D-type cyclins, cyclin E/cdk2 complexes, and cyclin-dependent kinase inhibitors p27KIP1 and p21Cip1/Waf1.

The D-type cyclins, which activate CDK4 and CDK6 to promote G1/S phase cell cycle progression, show decreased expression following ErbB2/Neu inhibition (Basso et al., 2002; Lane et al., 2000; Neve et al., 2000). Conversely, in cells that are transfected with oncogenic *Neu*, or also in tumors from mice that overexpress either proto-oncogenic or oncogenic *Neu*, cyclin D1 protein is upregulated (Lee et al., 2000). Apparently, ErbB2/Neu-induced MAPK activation

induces the cyclin D1 promoter through Sp1 and E2F transcription factors (Lee et al., 2000) and stabilizes the protein through threonine phosphorylation by Akt/PKB (Diehl et al., 1998). Similar to cyclin D1 induction by ErbB2/Neu overexpression, ligand-induced activation of ErbB signaling promotes cell cycle entry by upregulating D-type cyclins (Neve et al., 2000). The loss of D-type cyclins during blockade of ErbB2/Neu expression is probably due to decreased activity of mitogenic pathways and loss of Myc expression since ectopic expression of Myc increased cyclin D expression and partially overcame the G1 block by scFv expression (Neve et al., 2000).

Inhibition of ErbB2/Neu signaling also causes downregulation of PI3K/Akt signaling and, consequently, relocalization of cyclin-dependent kinase inhibitors, p27Kip and p21Cip1/Waf1. The p27Kip cyclin-dependent kinase inhibitor is cytoplasmic, or inactive, when phosphorylated by Akt/PKB on a specific threonine residue, Threonine-187 (Le et al., 2003; Liang et al., 2002; Shin et al., 2002; Viglietto et al., 2002); however, when the Akt/PKB pathway is downregulated, p27Kip1 relocates to the nucleus where it can form inhibitory complexes with cyclin-dependent kinases and block cell cycle progression. Additionally, the loss of D-type cyclins allows redistribution of p27Kip1 to CyclinE/cdk2 complexes which causes their inactivation, contributing to a G1 block (Lane et al., 2000; Lenferink et al., 2001; Moasser et al., 2001; Yakes et al., 2002). Blockade of the PI3K/PKB/Akt pathway in ErbB2/Neu-overexpressing cells cause redistribution and decreased expression of p21Cip1/Waf1 (Hermanto et al., 2001; Zhou et al., 2001a). Conversely, ErbB2/Neu activation of Akt/PKB

induces MDM2-mediated ubiquitination and degradation of the cell cycle regulator, p53 (Zhou et al., 2001b). Ultimately, the aberrant regulation of multiple G1 phase regulators by ErbB2/Neu signaling networks drives proliferation of tumor cells and contributes to the oncogenic capacity of ErbB2/Neu overexpression.

ErbB signaling promotes cell survival

The replicative response to overexpression of cell cycle regulators normally activates apoptotic check points, but cells that overexpress ErbB2/Neu seem to concomitantly drive unlimited replication and promote cell survival (Danielsen and Maihle, 2002; Evan and Vousden, 2001; Green and Evan, 2002). One of the primary ErbB signaling pathways, PI3K/PKB/Akt, directly phosphorylates and blocks the activity of several members of the apoptotic cascade such as pro-apoptotic Bad and caspase-9 (Cardone et al., 1998; Datta et al., 1997; Zha et al., 1996). Additionally, PKB/Akt phosphorylation of members of the Forkhead family of transcription factors prevents induction of several key genes for apoptosis such as FasL, BIM, and others (Brunet et al., 2001). Furthermore, PKB/Akt ultimately activates NF-κB, which in turn induces prosurvival Bcl-X_L protein and several members of the inhibitors of apoptosis (IAP) family (Datta et al., 1999).

Overexpression of ErbB2/Neu induces multiple prosurvival mechanisms through activation of the PI3K pathway. Activation of the PKB/Akt/NF-κB pathway renders ErbB2/Neu overexpressing tumor cells resistant to Tumor Necrosis Factor-induced apoptosis (Zhou et al., 2000). Additionally, the Muc4/sialomucin

complex, an intramembrane modulator of ErbB2/Neu promotes tumor growth by suppressing apoptosis in xenotransplanted tumors (Komatsu et al., 2001). Recent work in mammospheres, a three-dimensional cell culture model of mammary acini, has shown another route through which ErbB2/Neu circumvents apoptosis. Overexpression of ErbB2/Neu, but not EGFR, causes mammospheres to gain several characteristics of early-stage tumors including loss of proliferative suppression, an absence of lumen, retention of the basement membrane, but lack of invasive properties (Muthuswamy et al., 2001). Acinar lumen formation requires apoptosis to clear epithelial cells from its center (Debnath et al., 2002), and the lack of lumen formation concomitant with overexpression of ErbB2/Neu in these mammospheres seems to be related to suppression of Bim, a proapototic protein, through activation of Erk-MAPK (Reginato et al., 2005). Moreover, ErbB2/Neu overexpressing cells are resistant to chemotherapy-induced apoptosis through transcriptional upregulation of p21Cip1/Waf1 (Yu et al., 1998b; Yu et al., 1998a). In summary, overexpression of ErbB2/Neu invokes numerous anti-apoptotic mechanisms to promote cell survival and circumvent anti-apoptotic check points.

Overexpression of ErbB2/Neu activates angiogenesis

As an increased number of tumor cells accumulate, they must eventually establish new routes to sustain oxygen access and nutrition. This requires angiogenesis, or new blood vessel formation. In this regard, ErbB-induced tumors produce several factors that influence surrounding vasculature (Azuma et al., 1994; Carter et al., 2001; Goldman et al., 1993; Hirata et al., 2002; Schreiber

et al., 1986). Under hypoxic conditions in which cells are situated too distant from vasculature, activation of the tightly monitored hypoxia-inducible transcription factor (HIF)-1 stimulates expression of vascular endothelial growth factor (VEGF) and other hypoxia-inducible genes (Harris, 2002). However, HIF-1 is also induced, independently of hypoxia, by PI3K/Akt/PKB in ErbB2/Neu-overexpressing cells (Laughner et al., 2001; Li et al., 2005). Furthermore, VEGF is induced under normoxic conditions in many tumors (Berra et al., 2000). Breast cancer cell lines with constitutive activation of ErbB2/Neu have elevated VEGF expression that is potentiated by NRG1-induced MAPK signaling (Laughner et al., 2001; Xiong et al., 2001; Yen et al., 2000; Yen et al., 2002). ErbB2/Neu induction of VEGF expression is mediated by AP-2 and Sp-1 transcription factors (Finkenzeller et al., 2004; Loureiro et al., 2005; Yen et al., 2002). The significance of ErbB2/Neu-mediated signaling in regulating VEGF is evident from the concomitant modulation of VEGF expression and/or activity with functional inactivation of ErbB2/Neu (Izumi et al., 2002; Klos et al., 2003; Yang et al., 2004). The oncogenic potential of ErbB2/Neu is related to its ability to induce angiogenic factors that drive neovascularization, thus delivering oxygen and nutrients to tumor cells.

ErbB2/Neu stimulates migration and invasion

The metastatic nature of ErbB2/Neu-induced mammary tumors in MMTV-*Neu* (Guy et al., 1992) and MMTV-*NeuT* (Muller et al., 1988; Siegel et al., 1999) mice as well as human breast tumors (Allred et al., 1992; Hynes and Stern, 1994; Salomon et al., 1995; Sjogren et al., 1998; Slamon et al., 1987) suggests that

activation of ErbB2/Neu signaling pathways stimulates migration and invasion. For tumor cells to metastasize, they must acquire several properties including the ability to migrate and invade the basement membrane. Although mechanistic studies regarding the role of overexpression of ErbB2/Neu in cell migration and invasion are lacking, several of the ErbB signaling pathways, i.e. the MAPK and PI3K/Akt pathways, regulate migration (Adam et al., 1998; Adelsman et al., 1999; Spencer et al., 2000). Furthermore, cells must degrade the extracellular matrix to invade the basement membrane. In this regard, NRG1 stimulates the serine protease uPA and its receptor (Mazumdar et al., 2001) and Matrix Metalloproteinase (MMP)-9 (Xu et al., 1997) in breast cancer cells, leading to accelerated invasiveness (Xu et al., 1997). Thus, ErbB signaling networks may target extracellular membrane proteases to initiate tumor cell invasion.

ErbB2/Neu and TGF-β

Recent studies suggest that TGF-β and ErbB2/Neu cooperate to activate both migration and invasion, thus enhancing tumor progression. Since an extensive review of the TGF-β family and its signaling pathways is beyond the scope of this dissertation, herein, I will describe the significance of TGF-β as it pertains to ErbB2/Neu-induced tumorigenesis and metastasis. The reader is referred to several TGF-β reviews for more detailed information (Derynck et al., 2001; Massague, 1998; Massague, 2000; Reiss, 1999; Siegel and Massague, 2003). In the predominant signal transduction pathway, the TGF-β receptors relay information from the cell surface through Smad proteins to the nucleus to alter cellular homeostasis. The TGF-β superfamily of ligands (TGF-β, Activin, bone

morphogenetic protein, and Nodal) induces a heterotetrameric complex containing two type I and two type II membrane spanning TGF-β receptors, activating their intrinsic serine/threonine kinases (Massague, 1998; Yue and Mulder, 2001) (**Figure I-2**). Signals are transduced from the cell surface to the nucleus by activated Smad complexes. The interaction of TGF-β, Activin, or Nodal ligands with their respective receptors selectively activates the Smad2 and Smad3 receptor-activated Smads via phosphorylation. Smad2 and Smad3 then form heteromeric complexes with the common mediator-Smad, Smad4, to enable translocation to the nucleus and transcriptional regulation of numerous genes. Of these target genes, induction of inhibitory Smads, Smad6 and Smad7, serves as a negative feedback mechanism. Several non-Smad signaling mechanisms contribute to TGF-β-inducible signaling, such as those involving EGF/MAPK and Wnt/β-catenin, adding extra layers of input and diversity of physiological output to TGF-β signaling (Derynck et al., 2001).

Physiological output from activated TGF-β signaling is cell type and context specific with potent suppression of growth and induction of apoptosis in lymphoid and normal epithelial cells (Derynck et al., 2001; Massague, 2000). In the mammary gland, the TGF-β pathway regulates normal ductal and alveolar development and remodeling during postlactational involution (Barcellos-Hoff and Ewan, 2000; Wakefield et al., 2000). This process is dependent on intimate interaction between the stromal and epithelial cell compartments. For example, in a transgenic mouse model where TβRII has been conditionally knocked out in fibroblasts, defective mammary gland development is observed with suppression

of ductal morphogenesis and terminal end bud formation (Cheng et al., 2005). Based on the role of TGF-β signaling during normal development, it is logical that dysregulated TGF-β signaling contributes to tumorigenesis.

The TGF-β pathway has a paradoxical role in mammary tumorigenesis with its activities depending on the tumor cell type and stage (Derynck et al., 2001; Reiss, 1999; Roberts and Wakefield, 2003; Tang et al., 2003). While TGF-β is growth suppressive in normal epithelium and thus acts as a tumor suppressor during early tumorigenesis (de Caestecker et al., 2000; Wakefield and Roberts, 2002; Wakefield and Sporn, 1990), it can promote invasion and metastasis later during malignant progression. Indeed, TGF-β activity is actually required for metastasis in some tumor cells (Akhurst and Derynck, 2001; Wakefield and Roberts, 2002). Until recently, the dual role of TGF-β during tumorigenesis has been inferred from studies with multiple carcinoma cell lines and various mouse models; however, the latest studies have shown both roles simultaneously within the same model of tumorigenesis.

Three recent studies have evaluated the impact of genetically manipulating the TGF-β pathway on ErbB2/Neu-induced mammary tumorigenesis in mice (Muraoka et al., 2003; Siegel et al., 2003; Yang et al., 2002) (Results summarized in **Table I-1**). These model systems are highly relevant to human breast cancers because, as mentioned above, ErbB2/Neu is overexpressed in 15-30% of human breast cancer (Slamon et al., 1987) and changes in expression of TGF-β ligands and members of its signaling pathway occurs during generalized cancer progression (Dalal et al., 1993; Gobbi et al., 1999; Gobbi et

al., 2000). All three studies reported that the TGF-β pathway promotes metastasis of ErbB2/Neu-induced mammary tumors; however, discrepancies were reported regarding primary tumor latency. Although overexpression of secreted TβRII or active TGF-β1 had no impact on primary tumor latency (Muraoka et al., 2003; Yang et al., 2002), forced expression of constitutively active TβRI in the same cells that express ErbB2/Neu delayed tumor development (Siegel et al., 2003). Conversely, suppression of TGF-β activity by overexpression of a dominant negative form of TβRII accelerated primary tumorigenesis. Multiple studies also found that forced activation of the TGF-β signaling pathway decreases the proliferative rate of ErbB2/Neu-induced tumors (Muraoka et al., 2003; Siegel et al., 2003). Collectively, these latter studies support the notion that TGF-β acts as a tumor suppressor by blocking tumor cell growth. The tumor phenotype discrepancy among these different bitransgenic mouse models may be related to the different mechanisms utilized to alter TGF-β activity, i.e. soluble factors vs. membrane bound receptors. In the models where soluble factors were manipulated (Muraoka et al., 2003; Yang et al., 2002), the same cells did not necessarily have simultaneous overexpression of ErbB2/Neu and alteration of TGF-β activity. This is very significant considering several TGF-β cellular activities are tumor cell autonomous (Roberts and Wakefield, 2003).

Despite the variation of mammary tumor development among these models, each of these studies corroborated the metastasis promoting properties of TGF-β activity. Metastasis is multi-step process wherein the tumor cells must escape the confinement of the mammary gland structure, make their way into the

vasculature, adhere to an accommodating secondary organ such as lung or bone, and extravastate from the vasculature into the target organ. Furthermore tumor cells must amplify from a single cell to a sustainable population of cells somewhere in the process. Exactly where and when this occurs is hotly debated (Al Mehdi et al., 2000; Chambers et al., 2002; MacDonald et al., 2002; Wong et al., 2002). In the MMTV-activated-*Neu* mice the total number of metastasis was not altered by expressing an activated TβRII, yet these animals had an increased number of pulmonary metastatic lesions that extravastated from the vasculature (Siegel et al., 2003). Furthermore, expression of active TGF-β enhanced the malignancy of ErbB2/Neu-induced tumor cells by increasing local invasion, circulating tumor cells, and total pulmonary metastases (Muraoka et al., 2003). Conversely, expression of a soluble TGF-β antagonist decreased the incidence of ErbB2/Neu-induced lung metastastes (Yang et al., 2002). Together, these reports support the metastasis promoting role of TGF-β during ErbB2/Neu-initiated mammary tumorigenesis.

Manipulation of TGF-β and ErbB2/Neu activation in cell culture studies with mammary epithelial cells that overexpress ErbB2/Neu (MCF10A/HER2) further corroborate the cooperativity of TGF-β and ErbB2/Neu during metastasis, revealing mechanisms for altered cell migration and invasion. In MCF10A cells that overexpress HER2, TGF-β-1 and -3 induction of cell migration required sustained activation of Erk-MAPK (Seton-Rogers et al., 2004). Furthermore, it seems that overexpression of ErbB2/Neu is actually required to “unmask” TGF-β-induced cell migration (Ueda et al., 2004). In this same mammary epithelial cell

line, MCF10A/HER2, TGF-β treatment enhanced cell motility, FAK phosphorylation, F-actin assembly, and focal adhesion formation and inhibited RhoA activity (Wang et al., 2005). These responses were dependent on receptor type protein tyrosine phosphatase kappa expression (Wang et al., 2005). This recent flurry of research surrounding the cooperativity of TGF-β and ErbB2/Neu during mammary tumor development and progression reflects the significance of these pathways and their interplay in cancer biology.

ErbB2/Neu and Activin

In contrast to the studies examining the relationship of TGF-β and ErbB2/Neu, there have been no reports of the interplay between ErbB2/Neu and Activin, another member of the TGF-β superfamily of ligands. However, recent data from our laboratory suggests a role for Activin signaling during ErbB2/Neu-induced mammary tumor development and progression. Activins are dimers of βA or βB subunits, existing as homodimers Activin A (βAβA) and Activin B (βBβB) or heterodimer AB (βAβB). Activins bind a heteromeric complex of a type I Activin (ActRI and ActRIB) and a type II Activin receptor (ActRIIA & ActRIIB), each of which contain a characteristic cytoplasmic serine/threonine kinase domain (Cameron et al., 1994; Mathews and Vale, 1993; Phillips, 2000). The Activin-binding protein, follistatin, regulates Activin activity by inhibiting Activin interaction with its receptor (Phillips and de Kretser, 1998). Like the TGF-β receptors, Activin receptors relay signals from the cell surface through Smad-2 and -3 to

1991; Welt and Crowley, Jr., 1998). Recent evaluation of expression of Activins, Activin receptors, and Smads in human breast specimens showed that these components are expressed in normal tissue and early stage cancer but suppressed in high-grade cancer, suggesting downregulation of the Activin signaling pathway is significant for tumor progression. Deciphering the role of Activin signaling in breast cancer may unveil new mechanisms of tumorigenic progression.

Hormonal modulation of ErbB2/Neu-induced tumorigenesis

Although it is well established that pregnancy and lactation provide long-term protection against breast cancer, epidemiological studies also indicate that risk for this disease is transiently elevated with parity (Kelsey et al., 1993; Lambe et al., 1994; Robertson et al., 1997). Indeed, there is a 15-year period of increased risk post-pregnancy that peaks 5 years after parturition in uniparous women and 3 years after delivery in biparous women compared to nulliparous women (Liu et al., 2002). This increased parity-associated risk suggests that the hormones that are elevated during pregnancy can adversely affect the mammary gland, possibly promoting growth of cells that have already undergone malignant transformation. Alternatively, epidemiological studies suggest that the hormonal milieu of the mammary gland during pregnancy and lactation promotes acquisition of a cell population that is particularly susceptible to transformation by HER2. HER2 expression is associated with increased parity-induced risk of breast cancer in women (Reed et al., 2003), and women that have been pregnant and have breastfed have a 4.2-fold increased risk in developing HER2 positive breast

alter transcription of targets genes in the nucleus, ultimately regulating cellular processes.

Activins have many physiological roles including regulation of cell growth and differentiation in various cell types (Ball and Risbridger, 2001; Matzuk et al., 1995). Despite several reports of Activin and Activin receptor expression in the mammary gland (Reis et al., 2004), information regarding their biological role in the mammary gland is limited. Adult female mice with βB Activin subunit deletion have limited ductal growth and alveolar differentiation, revealing a critical role for Activin in these processes and lack of functional redundancy with the βA subunit (Robinson and Hennighausen, 1997). Ex vivo studies have revealed that Activin A inhibits proliferation in isolated rat acini and final pregnancy-associated differentiation (Bussmann et al., 2004).

Activin A also blocks proliferation of breast cancer cell lines (Cocolakis et al., 2001; Kalkhoven et al., 1995; Liu et al., 1996). For this growth suppressive activity, ActRIB is required (de Winter et al., 1997), and signaling is mediated by the Smad proteins with concomitant activation of the p38-MAPK pathway and phosphorylation of the transcription factor AF2 (Cocolakis et al., 2001). These growth suppressive properties imply a potential tumor suppressor role for Activin, but, currently, biological evidence for such a role is lacking. Based on the peritumoral breast tissue-induction of immune responses and the modulation of cell-mediated immunity by Activin, Activin may also have an immunomodulatory role in breast cancer (de Kretser et al., 1999; Keelan et al., 2000; Petraglia et al.,

cancers than those that did not breastfeed (Treurniet et al., 1992). The mechanisms responsible for the increased risk of developing HER2-positive breast cancer following pregnancy remain to be elucidated.

A recent report by Wagner and colleagues (Henry et al., 2004) suggested that induction of susceptible mammary epithelial cells during pregnancy and retention of these cells following involution may account for the parity-associated acceleration of ErbB2/Neu mammary tumorigenesis. This study involved the use of the MMTV-*Neu* mouse model of ErbB2/Neu-induced breast cancer, which overexpresses the proto-oncogenic form of rat ErbB2. While pregnancy accelerates mammary tumorigenesis in MMTV-*Neu* mice compared to their nonparous littermates, tumor development remains stochastic in nature (Anisimov et al., 2003; Guy et al., 1992; Henry et al., 2004). MMTV-*Neu* tumor incidence, or multiplicity, was unaltered by a single pregnancy but increased in biparous mice and decreased by ovariectomy at 8 weeks of age (Anisimov et al., 2003). Furthermore, manipulation of hormonal milieu in various models of ErbB2/Neu overexpression further illustrates the collaborative efforts of ErbB2/Neu and hormones in the mammary gland. In mice that express *Neu* or *NeuT* under direction of a fragment of the endogenous Neu promoter (Neu-*Neu* mice), parity enhanced the proliferative mammary gland phenotype, causing incomplete regression after cessation of lactation (Weinstein et al., 2000). Furthermore, hormonal modulation, including elevated prolactin levels and lower glucocorticoid levels, promoted carcinogenesis mediated by virally-transduced *NeuT* in rats further supporting hormonal influence on ErbB2/Neu tumorigenesis

(Tai and Gould, 1995). Conversely, ovariectomy reduced ErbB2/Neu-initiated tumor occurrence on both rats and mice (Hewitt et al., 2002; Wang et al., 1992). Collectively, these data suggest that hormonal environment influences ErbB2/Neu activity in the mammary gland independent of the hormonally regulated MMTV promoter.

Estrogen has specifically been implicated in hormonal modulation of ErbB2/Neu carcinogenesis by manipulation of its activities in ErbB2/Neu-overexpressing mice (Hewitt et al., 2002) (Menard et al., 2000) (Yang et al., 2003). Exogenous estradiol exposure enhanced MMTV-Neu-induced tumorigenesis, with treatment during the reproductive period at 8 to 18 weeks of age being the most detrimental (Yang et al., 2003). In contrast, treatment with Tamoxifen, an estrogen antagonist in the breast, prior to tumor appearance reduces ErbB2/Neu tumorigenicity (Hewitt et al., 2002; Yang et al., 2003). In addition, genetically removing the estrogen receptor delays ErbB2/Neu-induced tumors (Hewitt et al., 2002). Collectively, these studies reflect the significance of hormonal modulation of ErbB2/Neu mammary tumorigenesis.

STATEMENT OF PURPOSE

The purpose of this thesis was to further elucidate the mechanisms of ErbB2/Neu-induced oncogenesis. Since overexpression of ErbB2/Neu occurs in 15-30% of human breast cancers, we utilized the MMTV-*Neu* mouse model in which overexpression of ErbB2/Neu drives mammary tumor development with long latency for these studies. The stochastic nature of tumorigenesis in this mouse model suggests that additional molecular events, above and beyond the overexpression of ErbB2/Neu, are required to progress to tumor formation. To identify these events we approached the question from two alternate directions. First to identify early molecular events of tumorigenesis, we evaluated the changes within the mammary gland transcriptome as glands progress from preneoplastic to overt tumors. Second, we manipulated the hormonal milieu of the mammary gland to determine whether this would provide the additional "hits" required to cause tumorigenesis. By Affymetrix microarray analysis, we first derived an ErbB2/Neu tumor molecular signature (**Chapter II**). The downregulation of several TGF-β-inducible target genes within the ErbB2/Neu tumor signature suggested that TGF-β activity is suppressed in ErbB2/Neu tumors; hence, we characterized the expression of several members of the TGF-β superfamily of signaling proteins in ErbB2/Neu tumors (**Chapter II**) and revealed a potential role for Activin in tumorigenic progression. Then we identified a subset of the ErbB2/Neu tumor profile genes (n=82) that are altered in preneoplastic ErbB2/Neu-overexpressing mammary glands (**Chapter II**). To determine whether altered hormonal milieu of the mammary gland promotes

tumor development, we generated a bitransgenic mouse model of ErbB2/Neu-induced tumorigenesis by breeding ovarian hormone overexpressing mice with MMTV-*Neu* mice and assessed tumor latency (**Chapter III**). The synchronous appearance of tumor in the mice permitted identification of a window of commitment to tumorigenesis and subsequent identification of genes that are altered with commitment to tumorigenesis (**Chapter III**). Collectively, these studies have provided focus for future efforts examining the oncogenic mechanisms underlying ErbB2/Neu induction of mammary tumors (**Chapter IV**).

Figure I-1. ErbB receptors activate multiple signaling pathways. [From (Marmor et al., 2004; Yarden, 2001; Yarden and Sliwkowski, 2001) with permission] EGF-like growth factor ligands induce hetero- or homodimerization of ErbB receptors, causing activation of their intrinsic kinase domains. ErbB2 and ErbB3 have distinct properties. ErbB2/Neu lacks any known ligand, whereas ErbB3 lacks kinase activity. Phosphorylated moieties serve as docking sites for adaptor proteins of multiple signaling pathways including, but not limited to, the Ras/MAPK, STATs, PLC-γ and the PI3K pathways. Signals eventually converge on the nucleus where nuclear effectors alter transcription of target genes.

Figure I-1

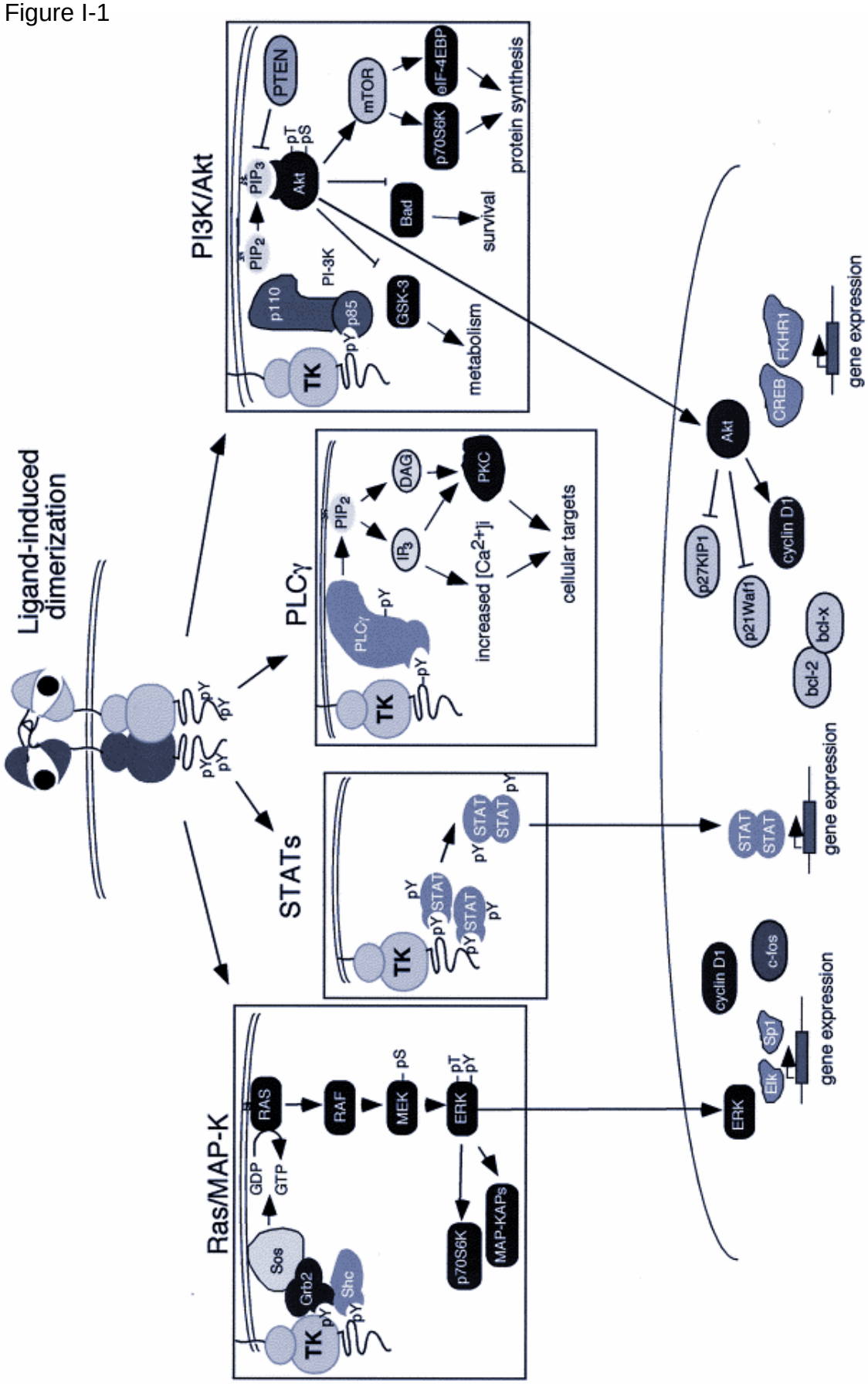
Ligand-induced dimerization
Ras/MAP-K
RAS
GDP
GTP
Sos
Grb2
Shc
RAF
MEK
ERK
pS
pT
pY
p70S6K
MAP-KAPs
STATs
STAT
PLCγ
PIP2
IP3
DAG
PKC
increased [Ca2+]i
cellular targets
PI3K/Akt
PTEN
PIP3
Akt
mTOR
p70S6K
eIF-4EBP
protein synthesis
Bad
survival
PI-3K
p110
p85
GSK-3
metabolism
TK
gene expression
cyclin D1
c-fos
Elk
Sp1
p27KIP1
p21Waf1
bcl-2
bcl-x
CREB
FKHR1

Figure I-2. TGF-β receptors relay signals from the cell surface through Smad proteins to alter transcription of target genes. Ligand binding induces a complex of type I and type II TGF-β receptors and activates their intrinsic threonine/serine kinase domains. Activated TβRI in turn activates Smads-2 and -3 which form a heteromeric complex with Smad4 to translocate to the nucleus. In the nucleus, Smad proteins interact with other transcription factors to alter expression of multiple target genes.

Figure I-2

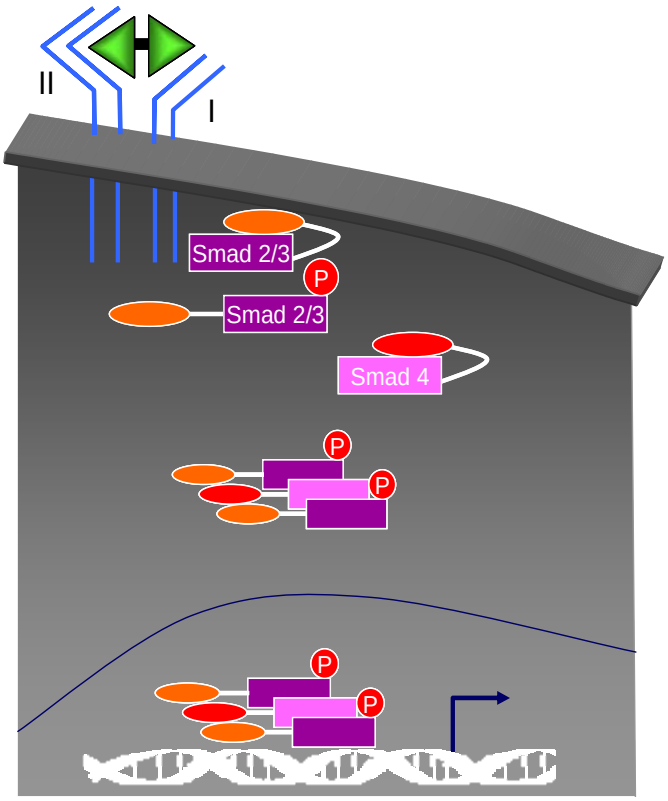

Table I-1

TGF-β	ErbB2	Primary mammary tumor onset	Invasive potential
MMTV-SR2F TGF-β antagonist (Yang *et al*., 2002)	MMTV-*Neu*	No change	decreased
MMTV-TGF-β1 Constitutively Active (Muraoka *et al.* 2003)	MMTV-*Neu*	No change, decreased proliferative ability	increased
MMTV-DN-TβRI (Siegel *et al*., 2003)	MMTV-*NeuT* (YB)	accelerated	decreased
MMTV-CA TβRI (Siegel *et al*., 2003)	MMTV-*NeuT* (YB)	delayed	No change

CHAPTER II

GENE EXPRESSION PROFILING OF CANCER PROGRESSION REVEALS INTRINSIC REGULATION OF TRANSFORMING GROWTH FACTOR-B SIGNALING IN ERBB2/NEU-INDUCED TUMORS FROM TRANSGENIC MICE

(Landis et al., 2005)

INTRODUCTION

Activation of the ErbB family of growth factor receptors and subsequent stimulation of their associated intracellular signaling pathways is a significant factor in the genesis of several human cancers (Salomon et al., 1995). Amplification of the *ErbB2* (hereafter referred to as *ErbB2/Neu*) gene and consequent protein overexpression occurs in 15-30% of primary human breast tumors (Salomon et al., 1995; Slamon et al., 1989). This overexpression is strongly associated with poor prognosis (Salomon et al., 1995), as well as resistance to endocrine and conventional chemotherapy (Wright et al., 1992). The oncogenic potential of ErbB2/Neu has been confirmed in the mammary epithelia of transgenic mice (Bouchard et al., 1989; Guy et al., 1992; Guy et al., 1996; Muller et al., 1988). Mice bearing the rat c-*neu* proto-oncogene under transcriptional control of the mouse mammary tumor virus (MMTV) promoter/enhancer (hereafter referred to as MMTV-*Neu* mice) stochastically develop focal mammary tumors and pulmonary metastases after a long latency (Guy et al., 1992). This mouse model serves as an excellent tool for deciphering the molecular pathways responsible for ErbB2/Neu-induced tumorigenesis and

identifying novel targets for both chemoprevention and chemotherapy (Boggio et al., 1998; Bulavin et al., 2004; Lenferink et al., 2000; Li et al., 1997; Shepherd et al., 2001; Yu et al., 2001).

The *ErbB2/Neu* gene is located on human chromosome 17q12 and encodes a 185-kDa member of the ErbB family of cell surface receptor tyrosine kinases (Yamamoto et al., 1986). This family of growth factor receptors is comprised of four members: epidermal growth factor receptor (also termed ErbB1/HER1), ErbB2/Neu/HER2/p185, ErbB3/HER3, and ErbB4/HER4 (Hynes and Stern, 1994). Although ErbB2/Neu is an orphan receptor with no high affinity ligand (Holbro et al., 2003), it is the preferred heterodimerization partner of the other ligand-activated family members (Graus-Porta et al., 1997; Tzahar et al., 1996). Consequent to ligand-induced formation of receptor heterodimers, each receptor subunit is activated by transphosphorylation. These phosphorylated residues serve as docking sites for a host of intracellular signaling molecules. Ultimately, these diverse signaling cascades converge on the nucleus to alter the cellular transcriptome, and the transcriptional targets of receptor activation mediate many of the physiological changes manifested by these receptors. These changes include regulation of cell growth, differentiation, motility, and death (Alroy and Yarden, 1997). As such, deregulation of any component of the pathway such as the ErbB ligands, cell surface receptors, signaling molecules, or transcriptional targets has profound implications for both normal development and malignant transformation of multiple tissues.

Development of breast cancer is a multistep process, beginning with a benign stage and progressing through intermediate stages marked by hyperproliferation of breast epithelium and ultimately resulting in invasive carcinomas (Krishnamurthy and Sneige, 2002; Wellings and Jensen, 1973). Although partial transcriptomes have been developed for ErbB2/Neu tumors, these have been limited to simple association of the gene expression profile to a specific tumor type without assessment of preneoplastic changes associated with ErbB2/Neu expression. In contrast, characterizing the early events of ErbB2/Neu-induced tumorigenesis should provide insight into the molecular mechanisms of tumorigenesis. To identify progressive changes in the transcriptome that occur during the transition from normal mammary gland to an overt ErbB2/Neu-initiated tumor, the partial transcriptomes of preneoplastic mammary glands and tumors from MMTV-*Neu* mice were compared to the partial transcriptomes of glands from wild-type mice using the Affymetrix U74Av2 GeneChip arrays. Analysis of these data revealed a subset of genes that were altered in expression during the progression from preneoplastic mammary gland to overt tumors.

In addition to identifying a transcriptional profile associated with neoplastic progression, we found that several genes downregulated in ErbB2/Neu-induced tumors were known targets of the transforming growth factor (TGF)-β signaling pathway. This suggested that the TGF-β pathway might be suppressed in ErbB2/Neu-induced mammary tumors. Normally, the TGF-β signaling pathway is activated when a member of the TGF-β superfamily of ligands (TGF-β, Activin, bone morphogenetic protein, Nodal) induces formation of a heterotetrameric

complex of two type II TGF-β-serine/threonine receptors (TβR-II) and two type I TGF-β-serine/threonine receptors (TβR-I) (Massague, 1998; Yue and Mulder, 2001). Signals are transduced from the cell surface to the nucleus by activated Smad complexes. In the canonical signaling pathway, the binding of TGF-β, Activin, or Nodal ligands to their selective receptors specifically activates the Smad2 and Smad3 receptor-activated Smads via phosphorylation. Smad2 and Smad3 then form heteromeric complexes with the common mediator-Smad, Smad4, to enable translocation to the nucleus and transcriptional regulation of numerous genes. Induction of expression of the inhibitory Smads, Smad6 and Smad7, serves as a negative feedback mechanism. In the mammary gland, the TGF-β pathway regulates normal ductal and alveolar development and remodeling during postlactational involution (Barcellos-Hoff and Ewan, 2000; Wakefield et al., 2000). The TGF-β pathway also has a paradoxical role in mammary tumorigenesis (Derynck et al., 2001; Reiss, 1999; Roberts and Wakefield, 2003; Tang et al., 2003). While TGF-β is growth suppressive during early tumorigenesis, it can promote malignancy and metastasis later during tumorigenic progression. Thus, evaluating the role of TGF-β during ErbB2/Neu tumorigenesis should yield significant insight into the processes of ErbB2/Neu tumor initiation and progression.

RESULTS

Identification of an ErbB2/Neu mammary tumor molecular signature

No previous studies have examined early changes in mammary tissues that ultimately accumulate ErbB2/Neu-initiated tumors. To identify early changes associated with ErbB2/Neu expression, we utilized the MMTV-*Neu* mouse model of mammary cancer (Guy et al., 1992). We evaluated three different mammary tissues: wild-type, preneoplastic tissue that expresses ErbB2/Neu, and ErbB2/Neu-induced tumors. The latter two were collected from the same mice. The tissue dissection is illustrated in **Figure II-1A**. To ensure the distinction between tumor and preneoplastic tissue, the tissue immediately bordering the tumor was discarded while the tumor and more distal surrounding mammary tissue (hereafter referred to as adjacent ErbB2/Neu) were used in comparative analysis of gene expression profiles. We anticipated that the mammary gland tissue surrounding ErbB2/Neu-induced tumors would express the *ErbB2/Neu* transgene and be preneoplastic but not contain an overt tumor. Northern blot analysis confirmed that the MMTV-*Neu* transgene was indeed expressed in the adjacent ErbB2/Neu mammary glands (**Figure II-1B**).

Each of the three tissue types described above were analyzed by gene expression profiling. To obtain a representative average of wild-type gene expression for baseline comparisons, RNA was isolated from 15 age-matched wild-type control mammary glands and then pooled into 3 groups of 5 samples, thus minimizing contributions due to inter-individual variation. All samples

including pooled, wild-type controls (n=3), adjacent ErbB2/Neu glands (n=4), and ErbB2/Neu tumors (n=5) were analyzed by Affymetrix U74Av2 microarrays containing 12,448 probe sets for known genes and ESTs. A subtractive approach was used to identify differentially expressed transcriptional targets in ErbB2/Neu tumors compared to wild-type tissue. Using Affymetrix Microarray Suite, data from each ErbB2/Neu tumor microarray analysis (n=5) were compared to the data collected from each pooled wild-type sample (n=3) resulting in 15 total comparisons (5 tumors $\times$ 3 wild-type) (**Figure II-1C**). Transcripts that were called "not changed" in any comparison by the Affymetrix algorithm were eliminated from the gene list. The intersection of these 15 lists contained 821 genes. This list was further reduced to 818 genes by removing any genes that were called "absent" in all analyses. The small reduction of genes by this second filter suggests that the first filtering step was sufficiently stringent to remove most genes whose expression remained unchanged when comparing tumors to wild-type samples. This list of 818 genes represents the global gene expression profile of ErbB2/Neu-induced tumors when compared to wild-type glands after interrogating the 12,488 gene set from Affymetrix and is displayed in **Table II-1**.

A subset of genes was further delineated by additional statistical analyses. First, we applied the Welch's T-test with the Benjamini and Hochberg Multiple Testing Correction (False Discovery Rate of 5%) to all 12,448 probe sets represented on the microarrays. Comparison of the 5 tumors to 3 wild-type control samples resulted in the identification of 829 transcripts that had statistically different levels

of expression in ErbB2/Neu tumor tissue compared to wild-type controls. We next evaluated the overlap in the 2 sets of genes identified by the Affymetrix algorithm (818 genes) or using the multiple testing correction (829 genes). Three-hundred and twenty-four genes were independently retained by both analytical approaches, thus delineating a filtered subset of transcripts with statistically significant alterations of gene expression (**Figure II-1D**; **Table II-2**). Genes with a p-value <0.01 are shown in **Table II-3**. At this level of significance, 23 genes were increased in tumors while 42 genes were decreased. To determine the reproducibility of the gene expression data, we analyzed two additional independent tumors by microarray analysis and found high repeatability (93% confirmed in both tumors) as indicated by the "repeated observation" column in the data tables. To further assess the accuracy of the microarray data through an independent approach, we analyzed 87 of the 324 genes that were included in the filtered gene expression profile by real time RT-PCR. This analysis involved comparisons between three additional tumors as well as 3 more wild-type control samples. The direction of alteration of gene expression (increased/decreased) in tumors compared to three wild-type controls was confirmed for 73 of the 87 genes (88%). Only three genes (3%) were changed in opposite directions when comparing the microarray and real time RT-PCR data. Overall, the data generated by real time RT-PCR provided independent confirmation of the microarray results, suggesting that the method of analysis employed for evaluating the microarray data was sufficiently stringent to

identify characteristic changes associated with ErbB2/Neu-induced mammary tumors.

We considered the possibility that a number of genes in the global tumor profile may be altered due to changes in cellularity when comparing tumors to wild-type tissue. To address this issue, we analyzed the expression changes for cytokeratins 8 and 18, both of which are epithelial cell markers. These genes were upregulated in tumors by 1.8 +/- 0.8 fold. Thus, any changes in gene expression that are less than 3.4 (the median fold change + two standard deviations), may be due to changes in cellular content. Genes that fail to surpass this cut-off are denoted within the tables.

The adjacent ErbB2/Neu tissue has preneoplastic characteristics

Once we had characterized the molecular profile associated with ErbB2/Neu-induced mammary tumors, we turned our focus to identifying gene expression changes that occur early in the tumorigenic cascade. Mammary gland tissue surrounding the ErbB2/Neu tumors was used for this analysis. Several lines of evidence suggested that this tissue expresses the *ErbB2/Neu* transgene, exhibits active ErbB2/Neu signaling, and is preneoplastic. Histological examination of the mammary gland surrounding ErbB2/Neu-induced tumors demonstrated modest focal hyperplasia and distended ducts as reported previously (Boggio et al., 1998) (**Figure II-2A**). Furthermore, immunohistochemical analysis of independent samples for phosphorylated ErbB2/Neu (Tyr-877) demonstrated activation of ErbB2/Neu signaling in adjacent ErbB2/Neu mammary tissue,

whereas wild-type tissue lacked phospho-ErbB2/Neu immunoreactivity (**Figure II-2B**). To determine whether this tissue harbored early transcriptional changes induced by active ErbB2/Neu signaling, the microarray data was inspected for known ErbB2/Neu targets. Ets variant 1 (ER81), Cyclin D1, and LIM Only-4 (LMO4) genes have previously been reported to be upregulated in ErbB2/Neu-induced mammary tumors or cell lines with activated ErbB2/Neu signaling (Lee et al., 2000; Shepherd et al., 2001; Wang et al., 2004). These genes appeared in the global ErbB2/Neu tumor molecular signature and were also upregulated in the adjacent ErbB2/Neu samples (**Table II-1**; **Figure II-2C**). Furthermore, three previously characterized ErbB2/Neu tumor markers (FXYD3, WDNM1/EXPI, casein-κ) (Morrison and Leder, 1994) were elevated in the adjacent ErbB2/Neu samples as well as in tumors (**Figure II-2C**). Confirmation of active ErbB2/Neu signaling and expression of known tumor markers in combination with the gross appearance and histological morphology of the adjacent ErbB2/Neu mammary tissue indicates that this tissue is indeed preneoplastic and, therefore, should be useful in identifying changes in gene expression associated with early carcinogenic mechanisms.

The molecular profile of the adjacent ErbB2/Neu tissue is intermediate between the profiles of tumors and control mammary tissues

To determine whether subgroups of tissue types could be identified independently based solely on their gene expression profiles, hierarchical clustering analysis (Eisen et al., 1998) was applied to the entire set of transcripts (7976 genes) that were called “present” or “marginal” on at least one of the

arrays from the three different tissue types [wild-type, adjacent ErbB2/Neu, and tumor (**Figure II-3A**)]. As expected, all tumor samples appeared on separate branches of the dendrogram from wild-type samples with one tumor appearing to be an extreme outlier of the tumor classification. Importantly, placement on the dendrogram did not correlate with somatic mutation of the transgene. Siegel et al. (Siegel et al., 1994) previously identified activating somatic deletion mutations of the *Neu* expression cassette in mammary tumors from MMTV-*Neu* mice. Although previously described as occurring in 65% of tumors in these mice, we found that only one of the seven tumors that were evaluated by the microarray analysis contained a somatic mutation of the transgene (data not shown), and this tumor is the center tumor in the dendrogram. In addition to segregating tumors from wild-type molecular signatures, this analysis revealed that the profiles from two of the adjacent ErbB2/Neu samples were more similar to the wild-type molecular profiles, whereas the other two adjacent ErbB2/Neu samples were more similar to the ErbB2/Neu tumors as indicated by their placement on the dendrogram. Hence, the adjacent ErbB2/Neu molecular profiles were intermediate between the wild-type and ErbB2/Neu tumor molecular profiles, supporting the concept that these samples and their molecular profiles reflect intermediate stages of tumorigenic progression.

Self-organizing Map (SOM) analysis reveals progressive alterations of gene expression that correlate with tumorigenic stage

Given the placement of tissue types on the hierarchical tree, we suspected that subsets of genes expressed in adjacent ErbB2/Neu samples would display

intermediate behavior between wild-type glands and tumors. To assess this directly, we used self-organizing maps (SOM) (Tamayo et al., 1999) to classify the 324 significantly altered genes (i.e. filtered tumor signature) into descriptive patterns of expression. Using the Affymetrix Data Mining Tool, we empirically determined that four nodes generated informative, non-redundant, SOM clusters. SOM cluster 1 (**Figure III-3B**; **Tables III-1, III-2** and **III-3**) contains transcripts that are more highly expressed in wild-type and adjacent ErbB2/Neu mammary glands than in the ErbB2/Neu-induced tumors. SOM clusters 2, 3, and 4 (**Figure III-3B**) reveal progressive patterns in which the expression level of genes in the adjacent ErbB2/Neu samples was intermediate between the wild-type samples and the ErbB2/Neu tumors, thus correlating with *ErbB2/Neu* transgene expression and neoplastic progression. We considered the possibility that the progressive nature of the changes of gene expression in the preneoplastic tissue was reflective of an experimental artifact due to contaminating tumor tissue in the adjacent ErbB2/Neu samples. The data in clusters 2 and 3 argue against this possibility. Expression of numerous genes in cluster 2 is high in tumors, yet the expression of many of these same genes is unchanged in the adjacent ErbB2/Neu tissues. Likewise, low expression of genes in tumors in cluster 3 should not significantly reduce expression in adjacent ErbB2/Neu tissues; however, these genes are indeed downregulated in adjacent ErbB2/Neu samples compared to wild-type controls. Neither of these clusters can be explained by minor tumor contaminants in adjacent ErbB2/Neu samples. Furthermore, we identified genes that were exclusively altered in expression in the adjacent

ErbB2/Neu samples compared to both wild-type and tumors, thus confirming the unique nature of these tissue specimens (data not shown).

To further delineate the transcriptome alterations associated with ErbB2/Neu neoplastic progression, we identified a subset of genes that were consistently changed when comparing wild-type tissue to the two adjacent ErbB2/Neu tissues that shared the most commonalities with the tumor molecular profiles. Three hundred and eighty-eight genes were consistently altered in expression in these two adjacent ErbB2/Neu samples compared to the wild-type control samples as indicated by the Affymetrix "change" parameter (6 comparisons: 2 adjacent ErbB2/Neu × 3 wild-type controls). Of these 388 genes, 230 were contained in the global ErbB2/neu Tumor molecular profile (**Table II-1**) and 82 were included in the filtered ErbB2/Neu tumor molecular signature (**Table II-2**). The data for these 82 genes are presented in **Table II-4.**

While comparisons of tumors to wild-type tissues can lead to important discoveries regarding the unique molecular signature of tumors, these studies are complicated by the difference in cellularity that exist between tumors and normal glands. We addressed this by standardizing all data to the changes observed in epithelial specific markers, cytokeratins 8 and 18. The comparison of adjacent ErbB2/Neu to wild-type control tissue described herein is not affected by this limitation because these tissues, on average, are similar in cellular composition. In comparing adjacent ErbB2/Neu microarray data to wild-type control data, we found that fat-specific markers were only slightly decreased (average 30% reduction; data not shown) while cytokeratins were marginally

increased (average 10% increase; **Table II-1**). Furthermore, western blot analysis for expression of E-cadherin, another epithelial cell marker, provided further corroboration that the wild-type control and adjacent ErbB2/Neu mammary glands have comparable epithelial cell content (**Figure II-4**). These data support the supposition that comparisons between adjacent ErbB2/Neu samples and wild-type tissues can reveal early gene expression changes that are due to overexpression of ErbB2/Neu and are not due to large changes in cellular composition. In conclusion, the progressive changes in expression of these 82 genes correlate with tumorigenic stage, suggesting that a subset of this population of genes may play a pivotal role in tumor promotion or progression.

The molecular profile of ErbB2/Neu tumors suggests that these tumors may have lost functional TGF-β signaling

During analysis of the genes contained in the filtered ErbB2/Neu tumor molecular signature, we noted that several of the genes that were decreased in tumors were known TGF-β-inducible genes. Included in this list were TGF-β-1-induced transcript 4, TGF-β-induced-microtubule-associated protein 4, dermatopontin, matrix metalloproteinase 3, serine protease 11 (IGF binding), gap junction membrane channel protein alpha 1, zinc finger homeobox 1a, and others (Chambers et al., 2003; Pimentel et al., 2002; Verrecchia et al., 2001). Although tumor cells and surrounding stroma often produce abundant TGF-β ligands (Reiss, 1999), the altered expression of these TGF-β targets lead us to hypothesize that the TGF-β pathway might be downregulated in ErbB2/Neu-induced tumors. Unfortunately, none of the canonical TGF-β intracellular

signaling pathway members satisfied the criteria required to be included in the ErbB2/Neu tumor expression profile (i.e. TGF-β1, TGF-β2, TGF-β3, TβRI, TβRII, Smad2/3, Smad4, or Smad7). To directly determine whether the TGF-β pathway is perturbed in ErbB2/Neu-induced tumors, we generated western blots with independent tumor, preneoplastic mammary gland, and wild-type samples to examine protein expression levels of multiple components of the TGF-β signaling pathway. We evaluated expression of TGF-β receptors (I/Alk5 and II) and Smad2/3 (total and phosphorylated). Western blot analyses revealed that TβRI/Alk5 protein levels were decreased in the adjacent ErbB2/Neu mammary glands and tumors relative to wild-type controls, whereas total Smad2/3 levels were increased in tumors compared to wild-type controls and adjacent ErbB2/Neu mammary glands (**Figure II-4**). Levels of phosphorylated Smad2 were unchanged to marginally decreased in tumors relative to wild-type controls. These results lead us to examine the most definitive indicator of activation of the Smad-dependent TGF-β signaling pathway: activation/phosphorylation of Smad2 within individual cells in the various tissue samples.

Smad2 is inactive throughout ErbB2/Neu-induced mammary tumors except at the tumor/stroma interface

Immunohistochemical evaluation of nuclear, phosphorylated Smad2 revealed that Smad2 is inactive in the majority of the cells of an ErbB2/Neu-induced tumor. Any activated Smad2 that was translocated to the nucleus was confined to cells in the periphery of these tumors, in areas of invagination by stromal tissue (**Figure II-5A**), and in small lobes of tumors (data not shown).

Immunohistochemical evaluation of total Smad2/3 demonstrated increased nuclear staining in the periphery of the tumors and mostly cytoplasmic staining in the rest of the tumor with some regions of negative staining (**Figure II-5A**). These data indicate that the Smad signaling pathway is quiescent in the majority of an ErbB2/Neu-induced mammary tumor.

We considered the possibility that the peripheral staining pattern of Smad2 was reflective of nonviable cells in the center of these tumors. The cells lacking Smad2 activation appeared healthy and non-necrotic. To further evaluate cell viability, proliferative indices including bromodeoxyuridine (BrdU) incorporation during DNA synthesis (**Figure II-5B**), phosphorylated-histone 3 expression (data not shown), and Ki67 expression (data not shown) were evaluated. Additionally, apoptotic cells were assessed by detection of fragmented DNA and morphological characteristics (**Figure II-5B**). These data revealed a uniform distribution of proliferating and apoptotic cells throughout the tumors, indicating that there are healthy cycling cells throughout these tumors, both in the periphery and in the center of the tumor. Thus, lack of phospho-Smad2 staining in the center of tumors is not due to loss of cell viability.

The pattern of Smad2 activation in the periphery of ErbB2/Neu-induced tumors suggested that a unique tumor microenvironment induced by proximity to the stromal compartment may lead to activation of Smad2. If so, smaller tumors with greater accessibility to the stroma may have uniform activation of Smad2. Immunohistochemical analysis for phosphorylated Smad2 in smaller tumors revealed activated Smad2 throughout the tumor (**Figure II-5C**). Together, these

data suggest that the majority of epithelial cells comprising an ErbB2/Neu-induced mammary tumor have lost Smad signaling and that accessibility to the stromal microenvironment prevents this loss.

Immunohistochemical analysis demonstrates heterogeneous activation of the ErbB2/Neu Receptor in ErbB2/Neu tumor section

To determine whether differential activation of Smad2 in the periphery versus the center of the tumor correlated with differences in activation of ErbB2/Neu signaling, ErbB2/Neu receptor phosphorylation on positions 877 or 1248 was evaluated using immunohistochemistry. As expected, the ErbB2/Neu receptor was expressed throughout most of the tumor, whereas the activated/phosphorylated receptor demonstrated positive staining in the periphery of these tumors and heterogeneous staining in the center of the tumors with interspersed regions of both positive and negative staining (**Figure II-6**). The patterns of staining for the different phosphorylated tyrosine residues (Tyr877 and Tyr1248) were consistently very similar. Generally, phosphorylated ErbB2/Neu staining overlapped with regions of positive staining for phosphorylated Smad2 at the periphery of the tumors as well as regions of negative staining in the center of the tumor, suggesting that activated Smad2 can coexist with active ErbB2/Neu signaling.

Immunohistochemical assessment reveals loss of detectable TGF-β-Receptor-I in adjacent ErbB2/Neu mammary gland and ErbB2/Neu tumor epithelia

Phosphorylated Smad2 observed in the outer rim of ErbB2/Neu tumors could be due to restricted TGF-β signaling in this area or induction by other members of TGF-β superfamily capable of activating Smad2 such as Activin (Massague, 1998). The western blot analysis (**Figure II-4**) suggested that the type I TGF-β receptor/Alk5 (TβRI) might be greatly reduced or lost in ErbB2/Neu tumors. To determine whether expression of TβRI correlated with regions of Smad2 activation, we examined the cellular localization of TβRI by immunohistochemistry. Corroborating the western blot data, staining for TβRI was mostly negative in epithelial cells of both the adjacent ErbB2/Neu tissue and in ErbB2/Neu tumors but positive in wild-type epithelial cells (**Figure II-7**). These data indicate that expression of TβRI, and hence, TGF-β signaling is suppressed in adjacent ErbB2/Neu tissue and throughout the ErbB2/Neu tumors.

Activin-Receptor-IB expression correlates with active Smad2 signaling

Loss of TβRI in the entire tumor was surprising since active Smad2 was observed in the periphery of the tumor. Smad2 can also be activated by Activin ligand binding with Activin receptors, thus we examined cellular localization of the type I Activin receptor/Alk4 (ActRIB) by immunohistochemistry. Interestingly, ActRIB staining occurred in the periphery of the tumor sections and in the adjacent ErbB2/Neu tissue (**Figure II-8**), indicating that Activin signaling may be

responsible for the activation of Smad2 at the tumor/stroma interface of ErbB2/Neu tumors.

DISCUSSION

In this study, we identified a core set of genes that are progressively altered in expression during ErbB2/Neu-induced tumorigenesis in an *in vivo* model of breast cancer. Further characterization of these genes should provide insight into the tumorigenic events associated with ErbB2/Neu overexpression and thus a more complete understanding of the underlying biological mechanisms of the ErbB2/Neu tumorigenic cascade. Due to the importance of ErbB2/Neu overexpression in human breast cancers, several groups have previously used expression profiling to identify genes associated with ErbB2/Neu expression in breast tumors and cell lines (Andrechek et al., 2003; Bertucci et al., 2004; Desai et al., 2002; Dressman et al., 2003; Kauraniemi et al., 2001; Kauraniemi et al., 2004; Kumar-Sinha et al., 2003; Mackay et al., 2003; Perou et al., 2000; Wilson et al., 2002). Importantly, none have examined the expression profiles of preneoplastic tissue to identify alterations of gene expression that are associated with tumor progression in an *in vivo* model. Indeed, Green and colleagues (Desai et al., 2002) suggested that comparative expression profiling of various developmental stages of oncogene-induced tumors would greatly increase our understanding of the progression of genetic changes associated with tumorigenesis. Accordingly, the core set of 82 genes that were described in this report whose expression is associated with ErbB2/Neu-initiated cancer

progression may provide new diagnostic and predictive markers, as well as new chemotherapeutic or chemoprevention targets.

Golub and colleagues have previously identified a seventeen gene signature associated with human breast cancer metatastasis (Ramaswamy et al., 2003). Of the metastasis genes that generated informative data in our analysis, thirty-three percent were contained within the global tumor profile (**Table II-1**). Furthermore, thirty percent of the genes encoding prognosis discriminator proteins for human breast cancer (Jacquemier et al., 2005) were also identified by our analysis of ErbB2/Neu tumors. These data support the utility of this mouse model in identifying genes that may be important in human breast tumorigenesis. Several of the 82 genes (*Etv1, Eif4ebp1, Ghr, Id2, Kai1, Tpd52*) that were progressively altered during ErbB2/Neu-induced tumorigenesis are already known to be associated with human breast cancer, highlighting the relevance of this model in evaluating alterations of the transcriptome that are associated with progression of tumorigenesis. Interestingly in previous studies, there were only a small number of genes that were common to all of the human breast tumor expression profiling experiments that identified ErbB2/Neu tumor molecular signatures, and these genes are contained in the *ErbB2/Neu* amplicon (Bertucci et al., 2004; Dressman et al., 2003; Kauraniemi et al., 2001; Perou et al., 2000; Wilson et al., 2002). The analytical approaches and perhaps the heterogeneity of human ErbB2/Neu positive breast tumors in these experiments seem to preclude identification of universal downstream targets of ErbB2/Neu

signaling. This further supports the use of the simplified ErbB2/Neu mouse model for identifying candidate genes for further analysis.

In comparing the global gene expression profile defined by our microarray analysis with previously published expression profiling data associated with ErbB2/Neu overexpression (Andrechek et al., 2003; Bertucci et al., 2004; Desai et al., 2002; Kauraniemi et al., 2004; Kumar-Sinha et al., 2003; Mackay et al., 2003; Wilson et al., 2002), we found only small subsets of overlap between the current data and these other expression profiles, and none of the genes were consistent among all of the data sets. There are several variations among the approaches used that may account for these discrepancies. These variations include: microarray formats with differential representation of the genome, analytical and statistical approaches, experimental paradigms, and starting material (i.e. cell lines vs. tissue samples). Not surprisingly, our gene expression profile shared the most commonalities with the MMTV-*Neu*-tumor signature identified by Desai et al (Desai et al., 2002). Despite the use of different microarray platforms and the collection of tumors at different time points, 70 of the 324 genes identified herein as “signature genes” were present in the list of genes reported by Desai et al. . Only four of these genes were changed in opposite directions (i.e. down- vs. up-regulated), suggesting strong concordance between the two tumor analyses. Thus, the study presented herein both confirms the data reported by Desai (Desai et al., 2002) and, extends this work by evaluating a different set of genes whose expression changes in tumors

compared to wild-type tissue and examining the transcripts associated with preneoplastic changes initiated by ErbB2/Neu expression.

The expression profiling of ErbB2/Neu tumors suggested that the TGF-β pathway may be altered in these tumors. The lack of Smad2 activation in the majority of cells within these tumors was accompanied by reduction of TβRI expression, suggesting that ErbB2/Neu-induction of tumors results in loss of at least one component of the TGF-β signaling pathway. Recently, another group reported that ErbB2/Neu can collaborate with ER81 to upregulate the expression of the inhibitory Smad7 in a breast cancer cell line (Dowdy et al., 2003), suggesting a direct mechanism for regulation of TGF-β signaling by the ErbB2/Neu pathway. Collectively, these data suggest that there are several possible mechanisms for suppression of the TGF-β pathway during ErbB2/Neu tumorigenesis. Whether loss of TβRI is due to active repression by ErbB2/Neu or an indirect mechanism remains unknown.

Three recent studies have evaluated the impact of genetically manipulating the TGF-β pathway on ErbB2/Neu-induced tumorigenesis in mice (Muraoka et al., 2003; Siegel et al., 2003; Yang et al., 2002). All three studies reported that the TGF-β pathway promotes metastasis of ErbB2/Neu-induced mammary tumors; however, discrepancies were reported regarding primary tumor latency. Whereas overexpression of secreted TβRII or active TGF-β1 had no impact on primary tumor latency, forced expression of constitutively active TβRI in the same cells that express ErbB2/Neu delayed tumor development. In addition, multiple studies also found that forced activation of the TGF-β signaling pathway

decreases the proliferative rate of ErbB2/Neu-induced tumors (Muraoka et al., 2003; Siegel et al., 2003). These data are consistent with the results reported herein indicating that intrinsic loss of TβRI provides a growth advantage for ErbB2/Neu-induced mammary tumorigenesis. It is important to note that all of the bitransgenic mouse studies discussed above focused on assessing the ability of the TGF-β pathway to alter ErbB2/Neu-induced tumorigenesis under conditions in which both pathways are exogenously regulated without evaluating whether ErbB2/Neu-induced tumors undergo spontaneous alterations in TGF-β signaling. The study presented herein is the first to our knowledge to show that ErbB2/Neu-induced mammary tumors normally lose the Smad-dependent TGF-β signaling pathway resulting from loss of TβRI.

The presence of phosphorylated Smad2 in areas of the tumor that were in close proximity to stromal tissue occurred in the apparent absence of TβRI. This suggested that another member the TGF-β superfamily might be responsible for Smad2 activation. The correlation of immunohistochemical data for phosphorylated/activated Smad2 and Activin-Receptor-IB/Alk4 suggests that ErbB2/Neu and Activin signaling can coexist within ErbB2/Neu-induced tumors, but this coexistence is limited to the subset of tumor cells that are in close apposition to the stroma. Determining the role of Activin signaling and the mechanism for suppression of TGF-β signaling during the progression of ErbB2/Neu-initiated mammary tumorigenesis will be interesting questions to pursue in future studies.

MATERIALS AND METHODS

Materials

Radiolabeled nucleotides were purchased from Perkin Elmer Life Sciences (Boston, MA). All chemicals were purchased from Sigma (St. Louis, MO). Antibodies were purchased from companies as follows: phospho-specific Smad2 (#3101), phospho-specific ErbB2/Neu (Tyr877; #2241), ErbB2/Neu (#2242) from Cell Signaling Technology, Inc. (Beverly, MA); Smad3 (FL-425), TGF-β Receptor I (sc-398), and TGF-β Receptor II (H-567) from Santa Cruz Biotechnology (Santa Cruz, CA); phospho-specific ErbB2/Neu (Tyr1248, AB-18 PN2A) from NeoMarkers (Fremont, CA); ActivinRIB (AF222) from R&D Systems (Minneapolis, MN); and anti-BrdU (Beckton Dickinson, San Jose, CA; #347580). Secondary antibodies include: horseradish peroxidase-conjugated goat anti-mouse and anti-rabbit (Santa Cruz Biotechnology) and fluorescein conjugated-goat anti-mouse (Jackson ImmunoResearch, West Grove, PA; #115-095-003).

Transgenic mice

All mice were housed in microisolator-plus units under pathogen-free conditions. Food and water were provided *ad libitum* and a 12 hr light/dark cycle was maintained. Mice [FVB/N-TgN(MMTV-*neu*)202Mul] containing the rat proto-oncogene c-*neu* transgene targeted to mammary epithelium by the MMTV-LTR promoter (Guy et al., 1992) were purchased from Jackson Laboratories (Bar Harbor, Maine) and bred to generate a colony of MMTV-*Neu* and non-transgenic, wild-type control mice. Transgenic mice were genotyped by PCR

with primers specific to the *Neu* transgene: forward: 5' CGCAACCCACATCAGGCC 3' and reverse: 5' TTCCTGCAGCAGCCTACGC 3'. Nulliparous mice were palpated weekly to detect tumors. One to three weeks after initial tumor detection, mice were killed by asphyxiation in a CO_2 chamber, cardiac blood was collected, mammary tissues were removed, and other organs were examined for metastases. All animal studies were approved by the Case Western Reserve University Institutional Animal Care and Use Committee.

Tissue isolation

Tumor and surrounding mammary gland were removed 1 to 3 wks after tumor detection (average tumor latency=37 wk) and placed in RNAlater (Ambion, Austin, TX) to prevent degradation of RNA. The adjacent, grossly non-tumorigenic mammary gland (adjacent ErbB2/Neu) was isolated, leaving a perimeter of approximately 2mm of normal tissue encasing the tumor (**Figure II-1A**). This small border of tissue surrounding the tumor was then removed and discarded. This resulted in 2 tissue samples: 1) tumors and 2) adjacent tissue that was at least 2 mm from the tumor and thus contained no overt tumor tissue. The adjacent ErbB2/Neu mammary gland and tumor tissue were frozen on dry ice and stored at -80°C. For wild-type controls, thoracic mammary glands were removed from 15 age-matched, nulliparous wild-type animals (age 31 or 41 wk). RNA isolated from each gland was pooled into three groups, each representing 5 different wild-type animals.

Microarray analysis

All data and detailed protocols have been submitted to *G*ene *E*xpression *O*mnibus (GEO; http://www.ncbi.nlm.nih.gov/geo/; Accession # GSE2528) according to Minimum Information About a Microarray Experiment (MIAME) guidelines (Brazma et al., 2001). Total RNA was extracted from tissues using the TRIzol method (Invitrogen, Carlsbad, CA). Using a 10 μg total RNA template and a custom primer containing both T7 primer sequence and oligo$(dT)_{24}$ (Genset Corp, La Jolla, CA), cDNA was synthesized (Superscript Choice System, Invitrogen, Carlsbad, CA). *In vitro* transcription (Enzo Diagnostics, Inc., Farmingdale, NY) was performed with Bio-CTP and Bio-UTP to produce biotin-labeled anti-sense cRNA. Biotinylated cRNA was purified using RNeasy spin columns (Qiagen, Inc., Valencia, CA) and delivered to the Gene Expression Array Core Facility at Case Western Reserve University (http://www.geacf.net/). Ten μg of biotinylated cRNA was fragmented and spiked with prokaryotic control RNAs followed by overnight hybridization at 45°C to the Affymetrix (Santa Clara, CA) Murine U74Av2 GeneChip Array. After washing, arrays were stained with streptavidin-phycoerythrin and scanned using an Agilent Gene Array scanner 2000 driven by the Affymetrix MicroArray Suite 5.0. The scanner PMT was set to the wide dynamic range setting.

Computational analyses were performed with Microarray Suite (v.5.0, Affymetrix), Data Mining Tool (DMT v.3.0, Affymetrix), MicroDB (v.3.0, Affymetrix), and GeneSpring (v.6.0, Silicon Genetics) software. Graphs representing values for

individual genes were generated using GraphPad Prism version 4.00 for Windows, GraphPad Software (San Diego, California; www.graphpad.com). Scanned images were analyzed using Affymetrix MAS 5.0. Four columns of data were given particular attention when assessing the results including: "signal", "detection", "signal log ratio", and "change". The microarray data generated from analysis of each tumor (n=5) sample was compared to the microarray data generated from analysis of each pooled age-matched, wild-type control sample (n=3) as illustrated in **Figure II-1C**. Probes that received an Affymetrix change call of "increased", "decreased", "marginally increased", or "marginally decreased" were retained for further analysis. Probes that were not called "present" or "marginal" by Affymetrix detection call on at least one GeneChip were removed. Application of Welch's approximate T-test with Benjamini and Hochberg multiple testing correction defined a set of probes with a false discovery rate of 5% ($p<0.05$).

Histology

Following fixation in 4% (w/v) paraformaldehyde/PBS, one inguinal mammary gland and isolated tumors from each mouse were paraffin-embedded, cut into 5-μm sections, and then stained with hematoxylin and eosin.

Northern blot analysis

Following isolation of total RNA according to the TRIzol reagent protocol (Invitrogen, Carlsbad, CA), 20μg of total RNA was separated by electrophoresis on a 1% denaturing agarose gel, transferred to Hybond-N+ Nylon membrane

(Amersham Pharmacia Biotech, Visscataway, NJ) with a Turbo Blotter (Schleicher and Scheull, Keene, NJ), and hybridized to a denatured, double-stranded DNA probe in QuikHyb solution (Stratagene, Cedar Creek, TX) according to the recommended protocol. Double-stranded DNA templates for probes were generated by PCR with the *neu* transgene primers described above and transgenic mouse genomic DNA template. Probes were radiolabeled with α-^{32}P-labeled dCTP by random priming (DECAprime II, Ambion, Austin, TX).

Real time reverse transcriptase (RT)-PCR

Ten Applied Biosystem 7900HT Gene Expression Micro Fluidic Cards, configuration 9, were designed and purchased from Applied Biosystems (Foster City, CA). Each of these 384 well cards contained 95 gene targets including controls with four replicates per target. To serve as negative controls, four wells were left empty. Total RNA was extracted from tissues using the TRIzol method (Invitrogen, Carlsbad, CA). RNA was treated to remove potential contaminating DNA according to the protocol from the DNA-*free* kit (Ambion, Austin, TX) and delivered to the Gene Expression Array Core Facility at CWRU. cDNA was generated using 3 μg of RNA in a 100 μl reaction volume in accordance with the High Capacity cDNA Archive Kit protocol (Applied Biosystems, Foster City, CA). Data was evaluated using ABI Prism SDS 2.2 software (Applied Biosystems, Foster City, CA). The following adjustable analysis settings were used: automatic Threshold Cycle (C_T), automatic outlier removal, and Relative Quantification (RQ) min/max confidence 95%. All data were calibrated relative

to an endogenous control, glyceraldehyde-3-phosphate dehydrogenase. Nine independent tissue samples were evaluated [3 different samples per experimental group (tumors, adjacent glands, or wild-type controls)].

Immunoblotting

Whole tissues were homogenized in nondenaturing protein lysis buffer (20mM Tris-HCl, pH7.5, 1% Triton X-100, 100mM NaCl, 40mM NaF, 1mM EDTA, 1mM EGTA) with additional phosphatase and protease inhibitors (1mM Na_3VO_4, 10μg/ml leupeptin, 10μg/ml aprotinin, 1mM PMSF). Following lysis on ice for 30 min, homogenates were clarified by centrifugation (12,000 × g) for 10 min at 4°C. The supernatant was retained as the whole cell lysate for subsequent western blot analysis. Proteins were quantified by Bradford Protein Assay (Biorad, Hercules, CA).

Whole cell lysate (150μg) was resolved by discontinuous SDS-PAGE, and proteins were transferred to PVDF membrane in Towbin Buffer (192mg/L Glycine, 25mg/L Trisma Base, 10-20% (vol/vol) methanol). SDS-PAGE gels were stained with Coomassie blue stain to confirm complete transfer. Membranes were blocked with 5% (w/v) skim milk in PBS with 0.05% (v/v) Tween-20 (PBS-T) (1 H, RT). Membranes were incubated with primary antibody in 5% (w/v) bovine serum albumin (overnight, 4°C) in PBS-T plus sodium azide (0.02% (v/v) followed by incubation with appropriate secondary antibody conjugated to horseradish peroxidase in 5% skim milk in PBS-T (1 H, RT).

Bound antibodies were detected by chemiluminescence (Lumiglo, Cell Signaling Technology, Inc., Beverly, MA).

Immunohistochemistry

Immunohistochemistry was performed utilizing the Dako Envision Plus HRP kit (DakoCytomation, Carpinteria, CA) with minor modifications, except for ActivinRIB for which the Vectastain ABC kit was used (Vector Laboratories; Burlingame, CA). Briefly, mammary gland sections were deparaffinized in xylene and rehydrated in 100% and 95% ethanol. Methods for antigen retrieval included: boiling in 10mM citrate buffer (pH 6.0) for 10 min (PSmad2, ActRIB), boiling in 10mM citrate buffer (pH 6.0) 20 min (Total Smad2/3), 1 min boil followed by sub-boil in 1mM EDTA (pH 8.0) for 15 min (P-ErbB2-877, P-ErbB2-1248, ErbB2), and 5 min trypsin digestion (Sigma tablets, TBRI). Sections were blocked with the blocking buffer included in the kit along with 15µl/ml normal serum and then incubated with primary antibody (overnight, 4˚C). Primary antibodies were diluted 1:100 except for PSmad2 (1:200) and ActRIB (1:25). Following incubation with secondary antibody included in the Dako or Vectastain kit, bound antibody was detected by DAB reaction. Sections were counterstained with Gill's Hematoxylin #3 (Polysciences, Inc., Washington, PA), dehydrated, cleared, and mounted in Permount. A control (blocking buffer without primary antibody) was performed for each tissue stained. Seven mammary glands with tumors from seven individual transgenic animals were analyzed.

Apoptotic cells were identified using the ApopTag Plus Peroxidase In Situ Apoptosis Detection Kit (Chemicon; Temecula, CA). For assessment of cells undergoing DNA synthesis, mice received an injection (0.1mg/g body weight) of 5-bromo-2'-deoxyuridine (BrdU) 2 h before being killed. Immunohistochemistry for BrdU was carried out as described previously (Milliken et al., 2002).

ACKNOWLEDGEMENTS

We would like to extend special thanks to Kristen Lozada for her dedicated technical support and Erin Milliken for intellectual discussions. Tumor histology was performed by the Histology Core Facility of the CASE Comprehensive Cancer Center. Microarray work was supported by the Gene Expression Array Core Facility of the CASE Comprehensive Cancer Center (P30CA43703). R.A.K. was supported by National Institutes of Health Grant (RO1-CA90398). M.D.L was supported by a Breast Cancer Research Program (BCRP) Predoctoral Traineeship Award (DAMD17-03-1-0302) and the National Institutes of Health Molecular Therapeutics Training Program (GM08803A1).

Figure II-1. Identification of an ErbB2/Neu mammary tumor molecular signature. **A**. *Experimental Design.* Three mammary gland tissue types were isolated from mice for gene expression microarray analyses including: age-matched wild-type (Wild-Type), ErbB2/Neu tumor, and tissue adjacent to, but not including, the tumor. For the ErbB2/Neu-expressing tissues, the entire mammary gland was removed from the MMTV-*Neu* mouse. The tumor plus the 2 mm border of tissue immediately surrounding the tumor were cut out. This 2 mm bordering peritumoral tissue was removed and discarded. The adjacent ErbB2/Neu gland and the tumor were retained for analysis. **B**. *Northern blot analysis confirms* ErbB2/Neu *transgene expression in adjacent ErbB2/Neu tissue.* Twenty micrograms of total RNA from microarray samples were separated by gel electrophoresis, transferred to nylon membrane, and then hybridized with a PCR-generated probe for Rat *neu*, cytokeratin-8 (epithelial cell marker), and cyclophilin (loading control). **C**. *Identification of genes with altered expression using the Affymetrix Change Call Algorithm.* Samples were analyzed by Affymetrix MGU74Av2 microarrays. The gene expression profile of each tumor (n=5) was compared to the expression profile of each pooled wild-type sample (n=3 profiles; 5 pooled tissues per profile). Only genes that were called changed in every comparison using the Affymetrix change call algorithm were retained. The intersection of these 15 comparisons (5 tumors × 3 wild-type samples) contained 821 genes and ESTs. Removal of genes that were called absent on all of the microarrays reduced the list to 818 genes and ESTs. These genes represent the global tumor expression profile for ErbB2/Neu-induced

mammary tumors. **D**. *Comparison of the Affymetrix subset of genes to the subset of genes acquired using Welch's approximate T-test with the Benjamini and Hochberg multiple testing correction.* Statistical analysis of the entire 12,448 genes identified 849 genes that were statistically different in expression levels when comparing the ErbB2/Neu tumor partial transcriptomes to the wild-type partial transcriptomes. 324 genes met both the Affymetrix algorithm and the statistical criteria, as indicated by the Venn diagram. These genes represent a filtered ErbB2/Neu tumor expression profile.

Figure II-1

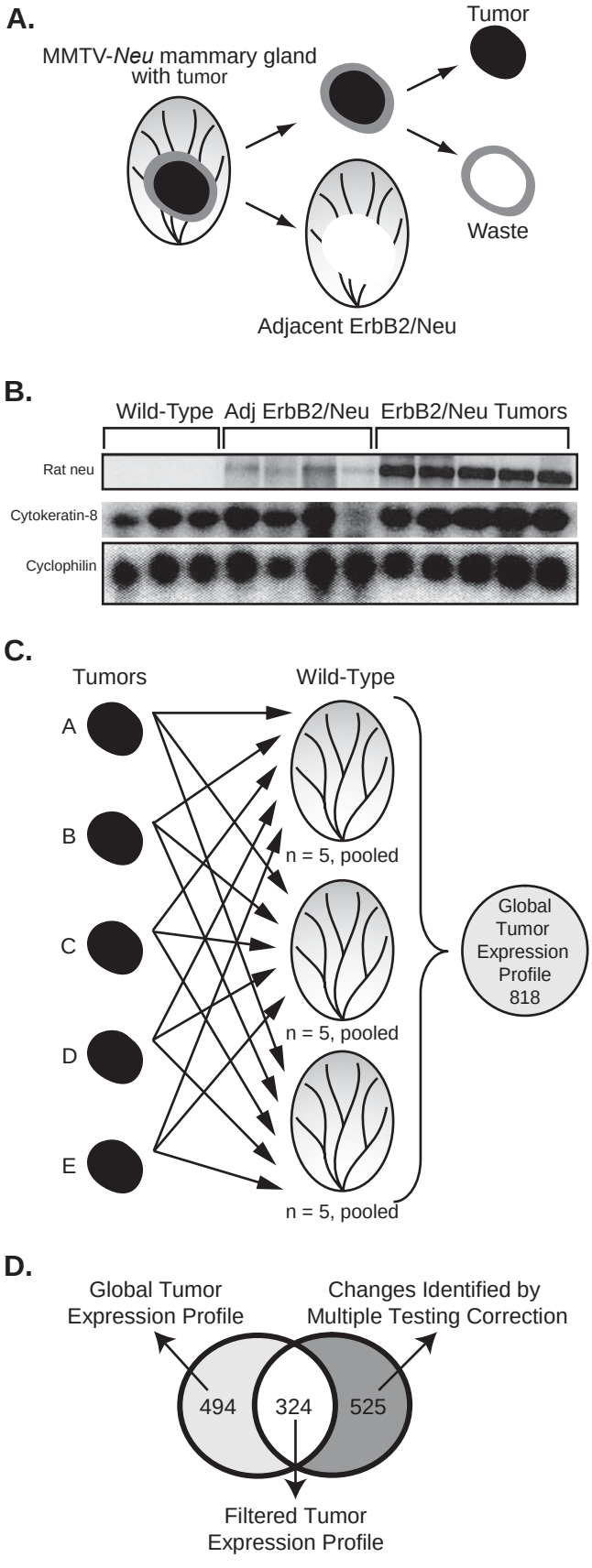
A.
MMTV-Neu mammary gland with tumor
Tumor
Waste
Adjacent ErbB2/Neu
B.
Wild-Type
Adj ErbB2/Neu
ErbB2/Neu Tumors
Rat neu
Cytokeratin-8
Cyclophilin
C.
Tumors
Wild-Type
A
B
C
D
E
n = 5, pooled
n = 5, pooled
n = 5, pooled
Global Tumor Expression Profile 818
D.
Global Tumor Expression Profile
Changes Identified by Multiple Testing Correction
494
324
525
Filtered Tumor Expression Profile

Table II-1. Global ErbB2/Neu Mammary Tumor Molecular Signature. 818 genes were changed according to Affymetrix algorithms in all tumors compared to wild-type control mammary tissues.
Note: ESTs have been annotated from public database information as of 1/2004

Gene Name	Common	Genbank	Affymetrix	Absolute call*	Fold Change§				SOM CI #†	p-value‡	Repeated Observation**	RT-PCR Confirmation§§
					ANvsWT	TUvsWT						
					Median	Median	Minimum	Max				
1-acylglycerol-3-phosphate O-acyltransferase 3	Agpat3	AW124201	160807_at		0.72	0.51	0.34	0.71			+/+	
2,4-dienoyl CoA reductase 1, mitochondrial	Decr1	AI844846	160711_at		0.55	0.21	0.14	0.25	3	0.048	+/+	
3-hydroxy-3-methylglutaryl-Coenzyme A synthase 1	Hmgcs1	AW124932	94325_at		0.53	0.28	0.19	0.41			+/+	
3-ketoacyl-CoA thiolase B	MGC29978	AW012588	99571_at	P to A	0.51	0.25	0.11	0.32	3	0.006	+/+	
3-monooxgenase/tryptophan 5-monooxgenase activation protein,	Ywhag	AW125041	95716_at		0.69	0.40	0.29	0.47		0.012	+/+	
3'-phosphoadenosine 5'-phosphosulfate synthase 1	Papss1	U34883	93298_at		1.32	2.97	1.91	4.03	2	0.040	+/+	
3'-phosphoadenosine 5'-phosphosulfate synthase 2	Papss2	AF052453	96713_at	P to A	0.71	0.22	0.12	0.43	1	0.047	+/+	
6-phosphofructo-2-kinase/fructose-2,6-biphosphatase 1	Pfkfb1	X98848	103297_at	P to A	0.34	0.07	0.04	0.09			+/+	
A kinase (PRKA) anchor protein (gravin) 12	Akap12	AB020886	95022_at		1.03	2.48	2.16	4.44	2	0.046	-/+	N
A kinase (PRKA) anchor protein (yotiao) 9	Akap9	AI561567	93464_at	A to P	1.91	13.09	3.56	26.72			-/+	
absent in melanoma 1	Aim1	AA711704	103443_at		1.39	3.66	2.13	4.26	2	0.019	+/+	
acetyl-Coenzyme A acyltransferase 2 (mitochondrial 3-oxoacyl-	Acaa2	AI849271	95064_at		0.65	0.30	0.24	0.42	3	0.005	+/+	
acetyl-Coenzyme A dehydrogenase, long-chain	Acadl	U21489	95425_at		0.65	0.43	0.27	0.59			-/+	
acetyl-Coenzyme A dehydrogenase, medium chain	Acadm	U07159	92581_at		0.66	0.26	0.16	0.38			+/+	
acetyl-Coenzyme A synthetase 2 (AMP forming)-like	Acas2l	AW125884	160921_at		1.84	2.60	1.28	4.89			-/+	
acid phosphatase 5, tartrate resistant	Acp5	M99054	98859_at		0.49	0.31	0.26	0.44			+/+	
aconitase 2, mitochondrial	Aco2	AI836740	96870_at		0.70	0.47	0.38	0.61			+/+	
actin, alpha 1, skeletal muscle	Acta1	M12347	100381_at	P to A	0.23	0.00	0.00	0.15			+/+	
actin, alpha 2, smooth muscle, aorta	Acta2	X13297	93100_at		0.87	0.18	0.11	0.26	1	0.003	+/+	
actin, beta, cytoplasmic	Actb		AFFX-b-		2.18	4.11	2.00	8.57			+/+	
actin, beta, cytoplasmic	Actb		AFFX-b-		2.00	3.12	1.84	7.73			+/+	
actin, beta, cytoplasmic	Actb		AFFX-b-		1.66	1.87	1.29	4.06			-/-	
actin-binding LIM protein 1	Ablim1	AI841606	103574_at	P to A	0.64	0.16	0.08	0.23			+/+	
actinin alpha 3	Actn3	AF093775	100879_at	P to A	0.26	0.21	0.12	0.33			+/+	
activated leukocyte cell adhesion molecule	Alcam	L25274	104407_at		1.12	0.43	0.29	0.66			+/+	
acyl-Coenzyme A oxidase 1, palmitoyl	Acox1	AF006688	101515_at		0.62	0.29	0.21	0.51			+/+	
adenylate kinase 1	Ak1	AJ010108	96801_at	P to A	0.68	0.44	0.27	2.60			-/-	
adenylate kinase 2	Ak2	AB020202	95148_at		0.54	0.29	0.25	0.37			+/+	
adipocyte complement related protein	Acrp30	U49915	99104_at		0.61	0.01	0.00	0.02			+/+	
adipsin	Adn	X04673	99671_at		0.71	0.01	0.00	0.03			+/+	
ADP-ribosylation factor GTPase activating protein 3	Arfgap3	AI844507	97811_at	A to P	1.66	3.12	2.14	4.38			+/+	
ADP-ribosylation factor-like 6 interacting protein 5	Arl6ip5	AW049647	97424_at		1.83	1.89	1.47	3.32			+/+	
ADP-ribosyltransferase 3	Art3	Y08027	98924_at	P to A	0.44	0.03	0.01	0.05			+/+	
Adrenergic receptor, beta 3	Adrb3; Adrb-3	X72862	92538_at	P to A	0.37	0.04	0.02	0.12			+/+	
Adrenergic receptor, beta 3	Adrb3; Adrb-3	X72862	92537_g_at	P to A	0.28	0.03	0.01	0.04	3	0.041	+/+	
Adrenergic receptor, beta 3	Adrb3; Adrb-3	X72862	92536_at	P to A	0.29	0.02	0.01	0.05			+/+	
aldehyde dehydrogenase family 1, subfamily A1	Aldh1a1	M74570	100068_at	P to A	0.62	0.08	0.03	0.12			+/+	
aldehyde dehydrogenase family 1, subfamily A7	Aldh1a7	U96401	94778_at	P to A	0.54	0.10	0.05	0.16	3	0.005	+/+	
aldehyde oxidase 1	Aox1	AB017482	104011_at	P to A	0.58	0.08	0.03	0.28			+/+	
aldolase 3, C isoform	Aldo3	AW121134	160546_at		4.82	14.52	9.19	24.76	2	0.023	+/+	
alpha-2-macroglobulin	A2m	AI850558	104486_at	A to P	5.93	28.25	4.26	233.94			+/+	
amine oxidase, copper containing 3	Aoc3	AF078705	102327_at		0.47	0.03	0.01	0.04			+/+	
aminoadipate-semialdehyde synthase	Aass	AJ224761	103389_at		2.98	7.67	6.11	13.74			+/+	
aminolevulinate, delta-, dehydratase	Alad	X13752	101044_at		0.57	0.26	0.14	0.32	3	0.038	+/+	
aminolevulinic acid synthase 1	Alas1	M63245	93500_at		0.79	0.52	0.37	0.66		0.021	+/-	
amphiregulin	Areg	L41352	99915_at	P to A	0.57	0.08	0.00	0.17			+/+	
amylase 1, salivary	Amy1	J00356	101058_at	P to A	0.33	0.01	0.00	0.02			+/+	
amyloid beta (A4) precursor-like protein 2	Aplp2	M97216	93498_s_at		0.64	0.41	0.28	0.53	3	0.009	+/+	
angiopoietin-like 2	Angptl2	AI840158	103556_at	P to A	0.75	0.12	0.08	0.24	1	0.010	+/+	
angiopoietin-like 4	Angptl4	AA797604	96119_s_at	P to A	0.92	0.30	0.18	0.49			-/+	
angiopoietin-like 4	Angptl4	AI326963	102114_f_at	P to A	0.80	0.24	0.13	0.44			-/+	
ankyrin 3, epithelial	Ank3	L40632	98477_s_at	A to P	4.45	9.25	2.23	18.13	4	0.023	+/+	Y
annexin A1	Anxa1	M69260	93038_f_at		0.94	0.59	0.41	0.72			-/+	
annexin A2	Anxa2	M14044	100569_at		0.71	0.43	0.32	0.63			-/+	
anthrax toxin receptor 2	Antxr2	AA612450	104761_at		0.59	0.33	0.23	0.44			+/+	
Apolipoprotein CI	Apoc1	Z22661	93354_at		0.95	1.89	0.31	7.57			-/+	
apolipoprotein A-I binding protein	Apoa1bp	AI845103	94032_at		1.13	1.59	1.22	2.07		0.023	+/+	
apolipoprotein D	Apod	X82648	93592_at	P to A	0.81	0.14	0.03	0.42			+/+	
aquaporin 1	Aqp1	L02914	93330_at	P to A	0.73	0.04	0.02	0.08			+/+	
arginase 1, liver	Arg1	U51805	93097_at		1.93	6.54	3.05	24.25			+/+	
arginine-rich, mutated in early stage tumors	Armet	AW122364	95749_at		1.24	1.88	1.39	2.35			+/+	
ATP citrate lyase	Acly	AW121639	160207_at		0.87	0.31	0.13	0.57			+/+	
ATP synthase, H+ transporting, mitochondrial F1 complex, gamma	Atp5c1	AI836694	92800_i_at		1.20	2.00	1.13	2.50			+/-	
ATPase, Ca++ transporting, cardiac muscle, fast twitch 1	Atp2a1	X67140	98126_s_at	P to A	0.12	0.03	0.02	0.15			+/+	
ATPase, Ca++ transporting, cardiac muscle, fast twitch 1	Atp2a1	AV241808	162223_f_at	P to A	0.14	0.01	0.00	0.09			+/+	
ATPase, H+ transporting, lysosomal accessory protein 2	Atp6ap2	AI845108	160202_at		1.71	2.83	1.91	3.61	2	0.027	+/+	
ATPase, H+ transporting, V1 subunit A, isoform 1	Atp6v1a1	AW123765	95746_at		1.21	2.60	2.16	3.29	2	0.007	+/+	

Table II-1. Global ErbB2/Neu Mammary Tumor Molecular Signature. 818 genes were changed according to Affymetrix algorithms in all tumors compared to wild-type control mammary tissues.
Note: ESTs have been annotated from public database information as of 1/2004

Gene Name	Common	Genbank	Affymetrix	Absolute call*	Fold Change§				SOM Cl #†	p-value‡	Repeated Observation**	RT-PCR Confirmation§§
					ANvsWT	TUvsWT						
					Median	Median	Minimum	Max				
ATPase, H+ transporting, V1 subunit A, isoform 1	Atp6v1a1	U13837	95745_g_at		1.25	2.51	1.83	3.48	2	0.023	+/+	
ATPase, H+ transporting, V1 subunit E isoform 1	Atp6v1e1	U13841	94532_at		1.16	1.91	1.44	2.79	4	0.032	+/+	
ATPase, Na+/K+ transporting, alpha 1 polypeptide	Atp1a1	AW123952	93797_g_at		5.03	7.16	2.85	16.91			+/+	
ATPase, Na+/K+ transporting, alpha 1 polypeptide	Atp1a1	AI839988	93798_at		3.47	4.92	2.85	9.51			+/+	
ATPase, Na+/K+ transporting, alpha 2 polypeptide	Atp1a2	AI839697	99481_at	P to A	0.48	0.04	0.02	4.44			+/+	
ATPase, Na+/K+ transporting, beta 3 polypeptide	Atp1b3	U59761	99579_at		0.75	0.48	0.41	0.62		0.010	+/+	
ATP-binding cassette, sub-family D (ALD), member 2	Abcd2	Z48670	92913_at	P to A	0.39	0.02	0.01	0.03			+/+	
AU RNA binding protein/enoyl-coenzyme A hydratase	Auh	AI837724	96650_at		0.73	0.57	0.45	0.67		0.019	+/+	
B lymphoma Mo-MLV insertion region 1	Bmi1	M64068	101475_at		0.66	0.50	0.33	0.73			-/-	
basic helix-loop-helix domain containing, class B2	Bhlhb2	Y07836	104701_at		1.02	2.14	1.55	4.23			+/+	
BCL2/adenovirus E1B 19kDa-interacting protein 1, NIP2	Bnip2	AF035207	93064_at		0.79	0.45	0.33	0.55	3	0.020	-/+	1of3
Bcl2-associated athanogene 2	Bag2	W71352	160962_at		1.60	2.17	1.68	2.64		0.009	+/+	
Bernardinelli-Seip congenital lipodystrophy 2 homolog (human)	Bscl2	AF069954	93080_at		0.64	0.32	0.26	0.43			+/+	
beta-1-globin	beta-1-globin	V00722	103534_at		1.17	0.35	0.16	0.68			-/+	
bladder cancer associated protein homolog (human)	Blcap	AW121500	98055_at		0.51	0.41	0.25	0.52			+/+	
brain beta spectrin (Spnb-2)	RIKEN clone:9930031C03	M74773	93571_at		0.75	0.65	0.54	0.80		0.023	+/+	
branched chain aminotransferase 2, mitochondrial	Bcat2	AF031467	100443_at		0.61	0.27	0.14	0.69	3	0.040	+/+	
branched chain ketoacid dehydrogenase E1, beta polypeptide	Bckdhb	L16992	102302_at		0.59	0.33	0.28	0.47	3	0.001	+/+	
cadherin 5	Cdh5	AI853217	104083_at		0.78	0.20	0.13	0.36			+/+	
calcitonin/calcitonin-related polypeptide, alpha	Calca	X97991	92533_at	P to A	0.34	0.02	0.01	0.11			+/+	
calcium binding protein, intestinal	Cai	Y00884	95423_at		1.54	2.17	1.82	2.58	2	0.007	+/+	
calmodulin 2	Calm2	M27844	93293_at		1.05	1.78	1.45	2.23		0.046	-/-	
calpain 12	Capn12	AI836968	96343_at		1.91	4.82	3.73	6.19	2	0.023	+/+	
calpain 2	Capn2	D38117	101040_at		0.59	0.33	0.19	0.50			+/+	
carbonic anhydrase 2	Car2	M25944	92642_at		2.58	2.36	1.45	4.06			+/+	
carbonic anhydrase 3	Car3	AJ006474	160375_at	P to A	0.70	0.01	0.01	0.03			+/+	
carbonic anhydrase 8	Car8	X61397	102773_at		1.35	4.06	1.73	7.41			+/+	
carboxyl ester lipase	Cel	U37386	99939_at	P to A	0.89	0.29	0.18	0.61			+/+	
carboxylesterase 3	Ces3	AW226939	101539_f_at	P to A	0.36	0.00	0.00	0.00			+/+	
carboxylesterase 3	Ces3	AW226939	101538_i_at	P to A	0.37	0.00	0.00	0.01	3	0.019	+/+	
carboxypeptidase A3, mast cell	Cpa3	J05118	102351_at	P to A	0.57	0.03	0.01	0.21			+/+	
carboxypeptidase D	Cpd	D85391	160655_at	A to P	1.69	5.70	3.18	16.11			+/+	
carboxypeptidase E	Cpe	X61232	99643_f_at		0.84	0.27	0.14	9.25			+/+	
carboxypeptidase E	Cpe	X61232	99642_i_at		0.96	0.24	0.12	10.34			+/+	
carnitine acetyltransferase	Crat	X85983	103646_at		0.49	0.26	0.19	0.34			+/+	
carnitine acetyltransferase	Crat	AV238359	161989_f_at	P to A	0.53	0.11	0.05	0.25			+/+	
carnitine palmitoyltransferase 2	Cpt2	U01170	95646_at		0.64	0.36	0.29	0.42	3	0.008	+/+	
casein delta	Csnd	V00740	98814_at	A to P	4.21	20.53	2.60	147.03			-/+	
casein kappa	Csnk	M10114	99065_at		2.23	2.51	1.87	4.56			-/-	
casein kinase 1, alpha 1	Csnk1a1	X90945	99650_at		1.27	1.69	1.27	2.71			+/+	
CASP2 and RIPK1 domain containing adaptor with death domain	Cradd	AJ224738	102952_g_at		1.24	2.41	1.89	3.25	2	0.006	+/+	N
CASP8 and FADD-like apoptosis regulator	Cflar	Y14041	103217_at		1.51	1.84	1.40	2.43			-/+	
caspase 1	Casp1	L28095	102064_at		1.92	6.68	2.46	7.62			+/+	
caspase 12	Casp12	Y13090	92488_at		1.57	3.53	2.25	5.24			+/+	
caspase 3, apoptosis related cysteine protease	Casp3	U54803	98436_s_at		1.43	2.36	1.42	4.63			+/+	
caspase 4, apoptosis-related cysteine protease	Casp4	Y13089	102905_at		1.68	3.16	2.28	5.28			+/+	
catechol-O-methyltransferase	Comt	AF076156	98535_at		0.59	0.22	0.16	0.29			+/+	
catenin src	Catns	Z17804	98151_s_at		1.22	2.69	1.68	4.79	2	0.043	+/+	N
cathepsin B	Ctsb	M65270	94831_at		0.64	0.48	0.32	0.77			+/+	
cathepsin C	Ctsc	U74683	101019_at		1.40	2.14	1.55	2.77	2	0.032	+/+	
cathepsin H	Ctsh	U06119	94834_at		1.30	2.07	1.27	3.10			+/+	Y
caveolin, caveolae protein	Cav	AI747654	160280_at		0.61	0.06	0.02	0.11			+/+	
Cbp/p300-interacting transactivator, with Glu/Asp-rich carboxy-terminal	Cited2	Y15163	101973_at		1.77	3.56	1.87	5.86			+/+	
CCAAT/enhancer binding protein (C/EBP), alpha	Cebpa	M62362	98447_at		0.37	0.09	0.05	0.11			+/+	
CD151 antigen	Cd151	AF033620	97930_f_at		0.77	0.59	0.50	0.74		0.050	+/+	
CD1d2 antigen	Cd1d2	M63697	101897_g_at		0.48	0.25	0.17	0.46			+/+	
CD34 antigen	Cd34	AI847784	160358_at	P to A	0.89	0.24	0.11	0.41	1	0.012	+/+	
CD36 antigen	Cd36	L23108	93332_at	P to A	0.49	0.23	0.02	0.42	3	0.031	+/+	
CD9 antigen	Cd9	L08115	95661_at		1.38	2.46	1.96	3.29		0.010	+/+	
cDNA sequence AB023957	AB023957	AB023957	96132_at	P to A	0.44	0.09	0.02	0.17			+/+	
cDNA sequence BC004728	BC004728	AW049551	94423_at		1.77	5.90	2.53	8.22	2	0.040	+/+	
cDNA sequence BC011209	BC011209	AW211793	160622_at	A to P	2.47	7.94	3.03	23.92	2	0.029	+/+	
cDNA sequence BC013529	BC013529	AI845588	103580_at	P to A	0.46	0.28	0.14	0.45			+/+	
cDNA sequence BC017133	BC017133	AW123477	96158_at		1.38	3.16	1.71	4.76			+/+	
cDNA sequence BC023239	BC023239	AA726383	160732_at	P to A	0.61	0.42	0.14	0.57			+/+	
cDNA sequence BC031468	BC031468	AA791885	160702_at		1.54	3.27	1.48	4.79			+/+	
cDNA sequence BC037006	BC037006	AI850846	104643_at		2.37	9.32	3.16	16.45			+/+	

Table II-1. Global ErbB2/Neu Mammary Tumor Molecular Signature. 818 genes were changed according to Affymetrix algorithms in all tumors compared to wild-type control mammary tissues.
Note: ESTs have been annotated from public database information as of 1/2004

Gene Name	Common	Genbank	Affymetrix	Absolute call*	Fold Change§				SOM Cl #†	p-value‡	Repeated Observation**	RT-PCR Confirmation§§
					ANvsWT	TUvsWT						
					Median	Median	Minimum	Max				
cDNA sequence BC037006	BC037006	AU017197	96518_at		1.96	4.86	2.58	7.16	2	0.032	+/+	
cDNA sequence BC054059	BC054059	AI118905	96237_at		0.65	0.19	0.08	0.45	3	0.027	+/+	
CEA-related cell adhesion molecule 10	Ceacam10	AV381191	161825_f_at	A to P	3.48	9.85	2.28	41.64			+/+	
CEA-related cell adhesion molecule 10	Ceacam10	L38422	101637_at	A to P	2.03	6.02	2.38	19.43			+/+	
cell death-inducing DNA fragmentation factor, alpha subunit-like effector	Cidea	AF041376	99994_at	P to A	0.62	0.05	0.02	0.14			+/+	
cell division cycle 2 homolog A (S. pombe)	Cdc2a	M38724	100128_at		1.43	2.28	1.39	2.83	4	0.029	+/-	
cell division cycle 34 homolog (S. cerevisiae)	Cdc34	AW120683	94048_at		0.81	0.50	0.29	0.75	3	0.030	+/+	
ceruloplasmin	Cp	U49430	92851_at		1.21	2.69	1.85	4.76			+/+	
checkpoint kinase 1 homolog (S. pombe)	Chek1	AF016583	103064_at		1.38	2.04	1.51	2.85	4	0.036	-/+	Y
chemokine (C-X-C motif) ligand 1	Cxcl1	J04596	95348_at	A to P	2.92	5.94	2.95	30.48	4	0.034	+/+	
chemokine (C-X-C motif) ligand 12	Cxcl12	L12030	100112_at	P to A	0.61	0.29	0.19	0.35	3	0.021	+/+	
chemokine (C-X-C motif) ligand 12	Cxcl12	AV139913	162234_f_at	P to A	0.58	0.12	0.05	0.32	3	0.001	+/+	
chemokine (C-X-C motif) ligand 14	Cxcl14	AW120786	96953_at		0.57	0.20	0.12	0.54			+/+	
chloride channel 3	Clcn3	AF029347	94464_at		1.56	2.45	1.36	3.66			+/+	
chloride intracellular channel 1	Clic1	AF109905	95654_at		1.39	1.77	1.56	2.57		0.047	+/+	
chondroadherin	Chad	U96626	99913_at	A to P	1.59	2.60	1.45	3.53			+/+	
chymase 2, mast cell	Cma2	M68899	95806_f_at	P to A	0.69	0.23	0.16	0.47			+/+	
citrate synthase	Cs	AW125431	99666_at		0.58	0.36	0.25	0.44			+/+	
claudin 1	Cldn1	AI604314	160415_at		1.63	2.85	2.03	5.90			+/-	
claudin 3	Cldn3	AF095905	94493_at		1.90	3.61	1.78	4.50	2	0.041	+/+	Y
claudin 3	Cldn3	AV057837	162315_f_at	A to P	1.72	2.99	1.83	4.63	4	0.049	+/+	Y
claudin 4	Cldn4	AB000713	101410_at		1.99	2.25	1.49	4.89			+/+	
claudin 5	Cldn5	U82758	104516_at	P to A	0.87	0.05	0.03	0.08			+/+	
claudin 7	Cldn7	AF087825	99561_f_at		2.02	3.71	2.77	5.06	2	0.035	+/+	Y
coagulation factor III	F3	M26071	97689_at		1.17	3.56	2.23	5.66	2	0.024	+/+	
complement component 3	C3	K02782	93497_at		0.78	0.04	0.03	0.10			+/+	
complement component factor h	Cfh	M12660	101853_f_at		0.71	0.25	0.20	0.36			+/+	
creatine kinase, mitochondrial 1, ubiquitous	Ckmt1	Z13969	160565_at		2.22	4.29	1.95	10.56			+/+	
crystallin, alpha C	Cryac	AI848798	160139_at	P to A	0.69	0.26	0.16	0.34	3	0.038	+/+	Y
C-terminal binding protein 2	Ctbp2	AW120820	160979_at		1.98	3.84	2.20	5.58	2	0.043	+/+	
C-terminal binding protein 2	Ctbp2	AF059735	92554_at		1.33	2.73	2.22	3.53	2	0.029	+/+	Y
cyclin D1	Ccnd1	M64403	94231_at	A to P	2.11	2.93	2.23	4.23	2	0.039	+/+	Y
cyclin-dependent kinase inhibitor 2C (p18, inhibits CDK4)	Cdkn2c	U19596	160638_at		0.56	0.30	0.22	0.44			+/+	
cysteine and glycine-rich protein 1	Csrp1	D88793	92608_at		3.79	4.92	1.92	11.47	2	0.027	+/+	
cysteine and glycine-rich protein 1	Csrp1	AI837625	160065_s_at		3.45	4.76	1.89	7.67	2	0.023	+/+	
cysteine dioxygenase 1, cytosolic	Cdo1	AI854020	96346_at	P to A	0.53	0.01	0.01	0.02			+/+	
cysteine-rich protein 1 (intestinal)	Crip1	M13018	94061_at		0.88	0.15	0.07	0.48	1	0.021	+/+	
cytidine monophospho-N-acetylneuraminic acid synthetase	Cmas	AJ006215	98593_at		1.71	4.66	3.12	6.28	2	0.005	+/+	
cytochrome b-5	Cyb5	AI854779	98533_at		0.69	0.44	0.32	0.50		0.012	+/+	
cytochrome b-561	Cyb561	AI846517	103423_at		1.39	2.35	1.95	3.51	4	0.025	+/+	
cytochrome c oxidase, subunit VI a, polypeptide 1	Cox6a1	U08440	99631_f_at		0.63	0.57	0.41	0.65			+/+	
cytochrome c oxidase, subunit VIIIb	Cox8b	U15541	160851_r_at		0.54	0.16	0.09	0.27			+/+	
cytochrome c oxidase, subunit VIIIb	Cox8b	AV260484	161205_at	P to A	0.52	0.10	0.06	0.26	3	0.039	+/+	
cytochrome c-1	Cyc1	AW121892	95072_at		0.70	0.54	0.46	0.68			+/+	
cytochrome P450, family 1, subfamily b, polypeptide 1	Cyp1b1	X78445	99979_at	P to A	0.68	0.06	0.01	0.42			+/+	
cytochrome P450, family 2, subfamily e, polypeptide 1	Cyp2e1	X01026	93996_at	P to A	0.58	0.06	0.03	0.10			+/+	
cytochrome P450, family 4, subfamily b, polypeptide 1	Cyp4b1	D50834	103353_f_at	P to A	0.70	0.28	0.11	0.34	1	0.042	+/+	
cytochrome P450, family 4, subfamily b, polypeptide 1	Cyp4b1	AV376161	162044_f_at	P to A	0.86	0.07	0.02	0.36	1	0.005	+/+	
cytochrome P450, family 4, subfamily v, polypeptide 3	Cyp4v3	AA212964	160611_at		0.67	0.32	0.18	0.42			+/+	
D-dopachrome tautomerase	Ddt	AF068199	100564_at		0.63	0.47	0.38	0.57			+/+	
DEAD (Asp-Glu-Ala-Asp) box polypeptide 6	Ddx6	AF038995	93964_s_at	A to P	5.03	8.46	4.17	31.78			-/+	
DEAD (Asp-Glu-Ala-Asp) box polypeptide 6	Ddx6	AF038995	93965_r_at	A to P	1.82	4.50	2.58	10.56	4	0.036	-/-	Y
DEAH (Asp-Glu-Ala-His) box polypeptide 36	Dhx36	AV299153	95944_at		1.77	2.69	1.93	22.16			+/+	
death-associated protein	Dap	AI196645	93842_at		1.29	2.11	1.79	2.71		0.008	+/+	
decorin	Dcn	X53929	93534_at		0.78	0.07	0.04	0.12			+/+	
Dehydrogenase/reductase (SDR family) member 7	2310016E22Rik	AW120882	95620_at		0.69	0.54	0.34	0.74		0.029	+/+	
deleted in polyposis 1-like 1	Dp1l1	AA755260	96134_at	P to A	0.63	0.25	0.05	0.42			+/+	
deoxycytidine kinase	Dck	X77731	98071_f_at		1.61	4.11	2.93	4.59	2	0.013	+/+	
dermatopontin	Dpt	AA717826	96742_at		0.68	0.09	0.03	0.16	3	0.006	+/+	Y
desmocollin 2	Dsc2	AW228162	103506_f_at		2.29	9.13	4.79	15.67			+/+	Y
desmoglein 2	Dsg2	AI152659	104480_at		4.11	6.11	2.75	13.00	4	0.005	+/+	
diacylglycerol O-acyltransferase 1	Dgat1	AF078752	104371_at		0.45	0.13	0.08	0.16	3	0.038	+/+	
differentially expressed in B16F10 1	Deb1	AW124231	95478_at		1.27	2.33	1.45	3.29	4	0.044	+/+	
dihydrolipoamide S-acetyltransferase (E2 component of pyruvate	Dlat	AW124813	96746_at		0.66	0.46	0.36	0.72			+/+	
dihydrolipoamide S-succinyltransferase (E2 component of 2-oxo-	Dlst	AW061024	97880_at		0.71	0.48	0.35	0.62			+/+	
dipeptidase 1 (renal)	Dpep1	D13139	103644_at	P to A	0.62	0.05	0.01	0.20	3	0.037	+/+	
DNA segment, Chr 10, ERATO Doi 214, expressed	D10Ertd214e	AI848453	94526_at		0.54	0.34	0.29	0.44			+/+	

Table II-1. Global ErbB2/Neu Mammary Tumor Molecular Signature. 818 genes were changed according to Affymetrix algorithms in all tumors compared to wild-type control mammary tissues.
Note: ESTs have been annotated from public database information as of 1/2004

Gene Name	Common	Genbank	Affymetrix	Absolute call*	Fold Change§				SOM Cl #†	p-value‡	Repeated Observation**	RT-PCR Confirmation§§
					ANvsWT	TUvsWT						
					Median	Median	Minimum	Max				
DNA segment, Chr 16, ERATO Doi 480, expressed	D16Ertd480e	AA420331	103701_at		1.14	1.46	1.06	2.33			+/+	
DNA segment, Chr 3, MJeffers 1	D3Jfr1	AI847171	92623_at		0.75	0.60	0.44	0.82			-/+	
DNA segment, Chr 3, University of California at Los Angeles 1	D3Ucla1	AI843466	95708_at		1.82	2.58	2.04	3.66	4	0.007	+/+	
DNA segment, Chr 6, Wayne State University 176, expressed	D6Wsu176e	AW125506	95541_at		1.22	2.31	1.48	3.66			+/+	
DNA segment, Chr 6, Wayne State University 176, expressed	D6Wsu176e	AA733372	97770_s_at		1.38	2.13	1.22	2.95			+/+	
DNA segment, Chr 8, ERATO Doi 594, expressed	D8Ertd594e	AW046101	93821_at		1.11	2.13	1.28	2.79			+/+	
DnaJ (Hsp40) homolog, subfamily C, member 8	Dnajc8	AI848094	95699_f_at		0.80	0.57	0.43	0.67		0.019	-/+	
DnaJ (Hsp40) homolog, subfamily D, member 1	Dnajd1	AI850983	97204_s_at		0.70	0.54	0.36	0.72			+/+	
dodecenoyl-Coenzyme A delta isomerase (3,2 trans-enoyl-Coenyme A	Dci	Z14050	98527_at		0.64	0.41	0.33	0.64			+/+	
downstream of tyrosine kinase 1	Dok1	U78818	102896_at	A to P	4.89	8.51	2.06	15.56	2	0.021	+/+	Y
dual specificity phosphatase 6	Dusp6	AI845584	93285_at		3.07	10.41	8.57	13.64	2	0.006	+/+	
dystrophia myotonica kinase, B15	Dm15	Z38015	93431_at	P to A	0.66	0.36	0.21	0.45			+/+	
ectonucleotide pyrophosphatase/phosphodiesterase 1	Enpp1	J02700	104174_at	A to P	1.64	3.43	2.45	4.92			+/+	
ectonucleotide pyrophosphatase/phosphodiesterase 2	Enpp2	AW122933	97317_at	P to A	0.59	0.01	0.00	0.01			+/+	
electron transferring flavoprotein, beta polypeptide	Etfb	AW046273	96947_at		0.50	0.24	0.19	0.33	3	0.045	+/+	
electron transferring flavoprotein, dehydrogenase	Etfdh	AI844043	97869_at		0.61	0.47	0.33	0.65			-/+	
elongation factor RNA polymerase II 2	Ell2	AI197161	103892_r_at		1.27	2.30	1.66	3.23	4	0.046	+/+	Y
ELOVL family member 6, elongation of long chain fatty acids (yeast)	Elovl6	AI839004	94418_at		0.63	0.23	0.13	0.36			+/+	
ELOVL family member 6, elongation of long chain fatty acids (yeast)	Elovl6	AW122523	103665_at		0.43	0.09	0.06	0.16			+/+	
Emu1 gene	Emu1-pending	AW122071	93689_at		2.06	5.90	2.25	7.94			+/+	
Emu1 gene	Emu1-pending	AV350190	161611_f_at		2.01	3.51	1.65	5.82			+/+	
enabled homolog (Drosophila)	Enah	D10727	100472_at	A to P	2.67	7.36	5.28	10.41	2	0.013	+/+	Y
endogenous proviral superantigen (Mtv-7 sag), and envelope protein		M90535	92780_f_at		2.35	5.06	1.97	9.06			+/+	
endoglin	Eng	X77952	100134_at	P to A	0.69	0.26	0.19	0.45			+/+	
endomucin	Emcn-pending	AB034693	93885_g_at	P to A	0.70	0.32	0.24	0.45			+/-	
endothelial-specific receptor tyrosine kinase	Tek	X71426	102720_at	P to A	0.60	0.23	0.15	0.43			+/+	
enolase 3, beta muscle	Eno3	X61600	96344_at	P to A	0.35	0.22	0.11	0.41			+/+	
enoyl coenzyme A hydratase 1, peroxisomal	Ech1	AF030343	93754_at		0.56	0.35	0.23	0.51			+/+	
enoyl Coenzyme A hydratase, short chain, 1, mitochondrial	Echs1	AW048512	95426_at		0.49	0.35	0.20	0.51			+/+	
epoxide hydrolase 2, cytoplasmic	Ephx2	Z37107	93051_at		0.49	0.13	0.07	0.23	3	0.044	+/+	
erythrocyte protein band 4.1-like 4a	Epb4.1l4a	AV308245	161603_r_at		1.49	2.64	1.44	4.20			+/+	
est	D2Ertd93e	C77278	97165_r_at	A to P	3.06	3.89	2.20	6.77	4	0.024	+/+	
est		AA419684	95184_f_at	A to P	4.24	3.39	1.93	8.46			+/-	
est		C85523	99849_at		0.72	0.30	0.22	0.46			-/+	
EST AA793972	AA793972	AA163960	160965_at	P to A	0.82	0.24	0.09	0.41			+/+	
ets homologous factor	Ehf	AF035527	102243_at	A to P	2.07	3.92	2.43	7.11	2	0.049	+/+	Y
ets variant gene 1	Etv1	L10426	92927_at	A to P	5.54	34.06	19.56	55.33	2	0.019	+/+	Y
eukaryotic translation initiation factor 4E binding protein 1	Eif4ebp1	U28656	100636_at		0.52	0.35	0.22	0.39	3	0.018	+/+	
expressed sequence AA407659	AA407659	AW048552	104434_at		1.03	1.61	1.24	2.23		0.035	+/+	
expressed sequence AI464131	AI464131	AI846672	104034_at	P to A	0.72	0.47	0.25	0.68			+/+	
expressed sequence AW112037	AW112037	AW123061	104260_at		0.64	0.37	0.30	0.42			+/+	
extracellular proteinase inhibitor	Expi	X93037	103051_at		2.79	3.58	2.97	6.77		0.035	+/+	Y
F11 receptor	F11r	U89915	103816_at		1.05	1.96	1.39	2.58	2	0.029	+/+	
faciogenital dysplasia homolog (human)	Fgd1	U22325	93674_at	A to P	2.65	4.92	2.81	19.97	4	0.030	+/+	
fasciculation and elongation protein zeta 2 (zygin II)	Fez2	AI851119	101934_at	P to A	0.97	0.47	0.26	0.63	1	0.023	+/+	
fat specific gene 27	Fsp27	M61737	102016_at	P to A	0.49	0.00	0.00	0.01	3	0.038	+/+	
fatty acid Coenzyme A ligase, long chain 2	Facl2	U15977	94507_at		0.51	0.13	0.11	0.19	3	0.033	+/+	
fatty acid synthase	Fasn	X13135	98575_at		0.76	0.11	0.06	0.18			+/+	
fatty acid-Coenzyme A ligase, long chain 4	Facl4	AB033887	104017_at	A to P	5.13	28.84	14.42	63.56			+/+	
fatty acid-Coenzyme A ligase, long chain 4	Facl4	AA619207	102381_at		5.74	19.43	11.96	31.56	2	0.021	+/+	
F-box and WD-40 domain protein 7, archipelago homolog (Drosophila)	Fbxw7	AW120511	93667_at		1.57	2.85	1.61	7.36	4	0.036	+/+	Y
Fc receptor, IgG, alpha chain transporter	Fcgrt	L17022	97533_at	P to A	0.76	0.32	0.12	0.51			+/-	
fibroblast activation protein	Fap	Y10007	92441_at	P to A	0.86	0.15	0.12	0.31			+/+	
filamin, beta	Flnb	AI838592	95637_at		1.60	3.71	2.69	5.50	2	0.018	+/+	
FK506 binding protein 11	Fkbp11	AW122851	97964_at		2.07	2.20	1.57	3.68			+/+	
folate receptor 1 (adult)	Folr1	M64782	93785_at		2.55	4.76	2.68	8.22			+/+	
folate receptor 1 (adult)	Folr1	AV035020	162302_f_at	A to P	2.18	3.66	3.10	9.19	4	0.010	+/+	
follistatin-like	Fstl	M91380	94833_at		1.16	0.36	0.24	0.61	1	0.012	-/+	Y
forkhead box A1	Foxa1	U44752	92697_at	P to A	0.58	0.07	0.03	0.14			+/+	
four and a half LIM domains 1	Fhl1	U41739	97498_at	P to A	0.48	0.05	0.02	0.16			+/+	
frizzled homolog 4 (Drosophila)	Fzd4	U43317	95772_r_at	P to A	0.54	0.04	0.03	0.29			+/+	
frizzled homolog 4 (Drosophila)	Fzd4	U43317	95771_i_at	P to A	0.52	0.05	0.02	0.34	3	0.034	+/+	Y
fucosyltransferase 8	Fut8	AB025198	98143_at		1.40	3.34	1.79	4.23	2	0.034	+/+	
FXYD domain-containing ion transport regulator 1	Fxyd1	AF091390	93040_at	P to A	0.53	0.08	0.05	0.22			+/+	
FXYD domain-containing ion transport regulator 3	Fxyd3	X93038	103059_at		1.64	3.81	3.03	5.58	2	0.031	+/+	Y
G0/G1 switch gene 2	G0s2	X95280	97531_at		0.61	0.42	0.28	2.13			+/-	
gap junction membrane channel protein alpha 1	Gja1	M63801	100064_f_at		0.81	0.15	0.09	0.46	1	0.010	+/+	Y

Table II-1. Global ErbB2/Neu Mammary Tumor Molecular Signature. 818 genes were changed according to Affymetrix algorithms in all tumors compared to wild-type control mammary tissues.
Note: ESTs have been annotated from public database information as of 1/2004

Gene Name	Common	Genbank	Affymetrix	Absolute call*	Fold Change§				SOM Cl #†	p-value‡	Repeated Observation**	RT-PCR Confirmation§§
					ANvsWT	TUvsWT						
					Median	Median	Minimum	Max				
gap junction membrane channel protein beta 2	Gjb2	M81445	98423_at		0.97	0.27	0.13	0.51	1	0.010	+/+	N
gelsolin	Gsn	J04953	93750_at		0.60	0.03	0.02	0.04			+/+	
germline IgH chain	Iga	J00475	102843_s_at	P to A	0.52	0.09	0.06	0.29			+/+	
glucan (1,4-alpha-), branching enzyme 1	Gbe1	AW210370	96803_at		0.46	0.27	0.14	0.32	3	0.026	+/+	
glucose regulated protein	Grp58	M73329	101060_at		2.07	3.27	1.60	5.62			+/+	Y
glucose-6-phosphate dehydrogenase X-linkec	G6pdx	Z11911	94966_at		0.54	0.45	0.35	0.60			+/+	
glutamate-ammonia ligase (glutamine synthase)	Glul	U09114	94852_at	P to A	0.98	0.15	0.12	0.33			+/+	
glutamyl aminopeptidase	Enpep	M29961	102373_at	P to A	0.32	0.02	0.02	0.06			+/+	
glutaredoxin 1 (thioltransferase)	Glrx1	AB013137	95722_at		1.19	2.30	1.49	3.48			+/+	
glutathione peroxidase 3	Gpx3	U13705	101676_at		0.33	0.04	0.02	0.08	3	0.000	+/+	
glutathione S-transferase kappa 1	Gstk1	AI841295	96670_at		0.56	0.34	0.20	0.48			+/+	
glutathione S-transferase, alpha 4	Gsta4	L06047	96085_at	P to A	0.66	0.12	0.06	0.71			+/+	
glutathione S-transferase, mu 2	Gstm2	J04696	93009_at		0.54	0.17	0.12	0.71			+/+	
glutathione transferase zeta 1 (maleylacetoacetate isomerase)	Gstz1	AW060750	160350_at		0.56	0.14	0.10	0.19	3	0.030	+/+	
glycerol phosphate dehydrogenase 2, mitochondrial	Gpd2	D50430	98984_f_at		0.57	0.20	0.11	0.28	3	0.000	+/+	
glycerol-3-phosphate acyltransferase, mitochondrial	Gpam	U11680	101867_at		0.38	0.17	0.13	0.19	3	0.003	+/+	
glycerol-3-phosphate dehydrogenase 1 (soluble)	Gpd1	AV290060	161753_f_at	P to A	0.65	0.08	0.04	0.17	1	0.048	+/+	
glycerol-3-phosphate dehydrogenase 1 (soluble)	Gpd1	M25558	92592_at	P to A	0.52	0.08	0.04	0.12			+/+	
glycine decarboxylase	Gldc	AW123955	95603_at	A to P	2.72	11.24	2.38	45.57			-/+	
glycogenin 1	Gyg1	AW049730	100597_at		0.51	0.31	0.22	0.44	3	0.005	+/+	
golgi phosphoprotein 3	Golph3	AW060175	160688_at		1.36	2.25	1.48	3.05		0.010	+/+	
growth arrest specific 6	Gas6	X59846	99067_at		0.86	0.31	0.16	0.59	3	0.027	+/+	2of3
growth hormone receptor	Ghr	M31680	99107_at		0.42	0.13	0.07	0.28			+/+	
growth hormone receptor	Ghr	U15012	99108_s_at		0.36	0.07	0.05	0.10	3	0.032	+/+	Y
guanine nucleotide binding protein, alpha 14	Gna14	M80631	95364_at	A to P	1.85	3.18	1.72	21.71			+/+	
guanine nucleotide binding protein, alpha inhibiting 1	Gnai1	AI153412	104412_at	P to A	0.38	0.02	0.01	0.05	3	0.036	+/+	
hairy/enhancer-of-split related with YRPW motif 1	Hey1	AJ243895	95671_at	A to P	1.82	6.87	3.16	10.48			+/+	
haptoglobin	Hp	M96827	96092_at		1.41	0.12	0.07	0.30			+/+	
heat shock protein 2	Hspa2	M20567	99816_at	A to P	1.75	4.76	1.96	10.41			+/+	
heme oxygenase (decycling) 1	Hmox1	X56824	160101_at		1.41	2.30	1.87	3.20			+/+	
hemoglobin alpha, adult chain 1	Hba-a1	AV003378	162457_f_at		1.21	0.44	0.26	0.64			+/+	
hemoglobin alpha, adult chain 1	Hba-a1	V00714	94781_at		0.94	0.27	0.14	0.52			+/+	
Hemoglobin, beta adult major chain	Hbb-b1	J00413	101869_s_at		1.00	0.32	0.15	0.64			-/+	
hephaestin	Heph	AF082567	104194_at		0.40	0.16	0.09	0.32	1	0.010	+/+	
hexokinase 2	Hk2	Y11666	94375_at		0.42	0.21	0.12	0.34			+/+	
hexose-6-phosphate dehydrogenase (glucose 1-dehydrogenase	H6pd	AA939571	104148_at		0.67	0.46	0.30	0.67	1	0.036	+/+	
histocompatibility 2, class II antigen A, alpha	H2-Aa	X52643	92866_at		0.94	0.46	0.16	0.71	3	0.033	+/+	
histocompatibility 2, Q region locus 1	H2-Q1	U96752	92222_f_at		1.32	2.10	1.54	4.76			+/+	
histocompatibility 2, T region locus 23	H2-T23	Y00629	98472_at		1.22	2.11	1.48	4.20			+/+	
histocompatibility 47	H47	AW125865	94245_at		1.25	1.89	1.42	2.48			+/+	
histone H2A.1	H2A.1	M33988	94805_f_at		1.35	2.27	1.58	3.71			-/-	
hnRNP-associated with lethal yellow	Raly	L17076	98511_at		3.31	2.81	1.26	5.03			+/+	
homeodomain interacting protein kinase 2	Hipk2	AF077659	103833_at	P to A	0.65	0.08	0.05	0.15			+/+	
homer homolog 2 (Drosophila)	Homer2	AF093259	160695_i_at	A to P	2.63	7.16	3.63	13.36	4	0.028	+/+	
hydroxyacyl-Coenzyme A dehydrogenase/3-ketoacyl-Coenzyme A	Hadhb	AW122615	96913_at		0.45	0.17	0.15	0.21	3	0.037	+/+	
hydroxysteroid (17-beta) dehydrogenase 4	Hsd17b4	X89998	97515_at		0.54	0.36	0.20	0.52			+/+	
hydroxysteroid 11-beta dehydrogenase 1	Hsd11b1	X83202	97867_at	P to A	0.39	0.08	0.05	0.17			+/+	
hypothetical protein 6330505N24	6330505N24	AI430272	104207_at		1.54	2.99	2.39	4.32	2	0.005	+/+	
hypothetical protein B230364F10	B230364F10	AI536457	103321_at		1.30	1.71	1.52	2.58		0.030	+/+	
hypothetical protein D930024E11	D930024E11	AI226337	161075_at		1.51	3.39	1.88	6.11			+/+	
hypothetical protein MGC18837	MGC18837	AI835706	95442_at		0.76	0.57	0.52	0.70		0.017	-/+	
IgK chain	IgM	M80423	102156_f_at		0.51	0.02	0.01	0.04			+/+	
Ig-kappa light chain V-J kappa 5 joining region		X00652	96971_f_at	P to A	0.54	0.13	0.04	0.30			+/+	
imilar to CUB and Sushi multiple domains 2 (LOC381556)	C77080	AV232292	161696_f_at		1.44	2.58	1.77	3.71	2	0.038	-/+	
immediate early response 2	Ier2	M59821	99109_at		1.46	2.38	1.83	2.91	2	0.030	+/+	
immediate early response 3	Ier3	X67644	94384_at		3.03	14.93	9.85	22.78	2	0.048	+/+	Y
immediate early response 5	Ier5	AF079528	92773_at		0.99	0.34	0.24	0.56	1	0.029	+/+	N
immediate early response, erythropoietin 4	Ierepo4-pending	AW125150	160251_at		1.15	1.54	1.27	1.87		0.040	+/+	
immune associated nucleotide 1	Ian1	AA795946	96172_at	P to A	0.84	0.31	0.20	0.43			+/+	
immunoglobulin heavy chain		AF042798	97563_f_at	P to A	0.61	0.18	0.08	0.55			+/+	
immunoglobulin heavy chain variable region precursor		AF036736	97574_f_at	P to A	0.73	0.07	0.03	0.19			+/+	
immunoglobulin heavy chain variable region precursor		AF025445	100376_f_at	P to A	0.77	0.07	0.03	0.21			+/+	
immunoglobulin heavy chain VDJ region		AF059706	93904_f_at	P to A	0.77	0.25	0.13	0.40			+/+	
immunoglobulin heavy chain (J558 family)	Igh-VJ558	J00475	100583_at	P to A	0.57	0.06	0.04	0.14			+/+	
immunoglobulin heavy chain 4 (serum IgG1)	Igh-4	L33954	93927_f_at	P to A	0.60	0.08	0.01	0.18			+/+	
immunoglobulin heavy chain 4 (serum IgG1)	Igh-4	X88902	101871_f_at	P to A	0.61	0.06	0.03	0.11			-/+	
immunoglobulin heavy chain 4 (serum IgG1)	Igh-4	V00793	101870_at	P to A	0.43	0.03	0.01	0.10			+/+	

Table II-1. Global ErbB2/Neu Mammary Tumor Molecular Signature. 818 genes were changed according to Affymetrix algorithms in all tumors compared to wild-type control mammary tissues.
Note: ESTs have been annotated from public database information as of 1/2004

Gene Name	Common	Genbank	Affymetrix	Absolute call*	Fold Change§				SOM Cl #†	p-value‡	Repeated Observation**	RT-PCR Confirmation§§
					ANvsWT	TUvsWT						
					Median	Median	Minimum	Max				
immunoglobulin heavy chain 4 (serum IgG1)	Igh-4	X94418	99420_at	P to A	0.35	0.03	0.01	0.07			+/+	
immunoglobulin joining chain	Igj	M90766	102372_at		0.60	0.10	0.07	0.17	3	0.047	+/+	
immunoglobulin kappa chain variable 8 (V8)	Igk-V8	X00651	96972_f_at	P to A	0.53	0.19	0.11	0.61			+/+	
immunoglobulin kappa chain variable 8 (V8)	Igk-V8	AB017349	102585_f_at	P to A	0.52	0.16	0.10	0.47			+/+	
immunoglobulin kappa chain variable 8 (V8)	Igk-V8	U19315	101718_f_at	P to A	0.57	0.16	0.07	0.42			+/+	
immunoglobulin kappa chain variable 8 (V8)	Igk-V8	AF045024	97566_f_at	P to A	0.48	0.14	0.03	0.62			+/+	
immunoglobulin kappa chain variable 8 (V8)	Igk-V8	AF045026	97567_f_at	P to A	0.48	0.11	0.04	0.41			+/+	
immunoglobulin kappa chain variable 8 (V8)	Igk-V8	U55576	100299_f_at	P to A	0.56	0.10	0.02	0.40			+/+	
immunoglobulin kappa chain variable 8 (V8)	Igk-V8	M15593	101640_f_at	P to A	0.49	0.06	0.03	0.23			+/+	
immunoglobulin kappa chain variable 8 (V8)	Igk-V8	M18237	93086_at		0.61	0.03	0.02	0.06			+/+	
immunoglobulin kappa chain variable 8 (V8)	Igk-V8	M15520	102157_f_at	P to A	0.58	0.02	0.02	0.16			+/+	
immunoglobulin kappa chain variable 8 (V8)	Igk-V8	U55641	101331_f_at	P to A	0.49	0.01	0.00	0.06			+/+	
immunoglobulin superfamily, member 8	Igsf8	AW061299	160820_at		1.25	1.72	1.21	2.03			+/+	
inactive X specific transcripts	Xist	L04961	99126_at		2.05	11.31	4.59	28.05	2	0.047	+/+	
inhibitor of DNA binding 1	Idb1	M31885	100050_at	P to A	0.62	0.20	0.09	0.33			+/+	
inhibitor of DNA binding 2	Idb2	AF077861	93013_at		2.07	3.73	2.48	6.36	4	0.046	+/+	Y
inhibitor of DNA binding 3	Idb3	M60523	92614_at	P to A	0.51	0.22	0.15	0.42			+/+	
inhibitor of DNA binding 4	Idb4	AJ001972	96144_at	P to A	0.81	0.10	0.05	0.33			+/+	
inositol 1,4,5-triphosphate receptor 1	Itpr1	X15373	94977_at		1.36	2.11	1.93	3.61			+/+	
inositol 1,4,5-triphosphate receptor 5	Itpr5	AF031127	101441_i_at		1.95	4.69	2.95	10.20	2	0.009	+/+	Y
inositol polyphosphate phosphatase-like 1	Inppl1	U92477	102988_at	A to P	1.71	2.07	1.58	2.41		0.023	+/+	
insulin-like growth factor 1	Igf1	X04480	95546_g_at	P to A	0.48	0.08	0.02	0.13			+/+	
insulin-like growth factor 2 receptor	Igf2r	U04710	95117_at		1.34	2.45	1.75	3.46		0.010	+/+	Y
insulin-like growth factor binding protein 4	Igfbp4	X76066	101571_g_at	P to A	0.77	0.14	0.03	0.30			+/+	
insulin-like growth factor binding protein 5	Igfbp5	L12447	100566_at		1.45	2.58	1.62	4.41			+/+	
insulin-like growth factor binding protein 6	Igfbp6	X81584	103904_at	P to A	0.62	0.04	0.03	0.12	1	0.023	+/+	Y
integral membrane protein 2A	Itm2a	L38971	93511_at		0.88	0.13	0.07	0.27			+/+	
integrin beta 1 binding protein 1	Itgb1bp1	AJ001373	100990_g_at		0.56	0.29	0.22	0.37			+/+	
integrin beta 4	Itgb4	L04678	103305_at	A to P	1.43	2.19	1.55	3.29			+/+	
interferon activated gene 205	Ifi205	M74123	94224_s_at		0.91	0.29	0.10	0.46			+/+	
interferon dependent positive acting transcription factor 3 gamma	Isgf3g	U51992	103634_at		1.26	1.96	1.36	2.77			+/+	
interferon inducible protein 1	Ifi1	U19119	97409_at		1.46	3.41	1.54	4.56			+/+	
interferon regulatory factor 6	Irf6	U73029	92440_at		1.35	2.79	2.03	4.06	2	0.036	+/+	Y
interferon stimulated gene 12		AI158810	92718_at		0.53	0.15	0.04	0.23			+/+	
interferon stimulated gene 12		AA763004	104467_at		1.61	4.03	2.73	8.22			+/+	
interferon, alpha-inducible protein	G1p2	AV152244	161511_f_at	A to P	3.63	13.09	3.73	38.85			+/+	
interferon, alpha-inducible protein	G1p2	X56602	98822_at	A to P	1.92	5.43	2.41	8.06			+/+	
interferon-induced protein with tetratricopeptide repeats 1	Ifit1	U43084	100981_at	A to P	1.22	5.50	2.95	17.63			+/+	
interleukin 25	Il25	AW045739	96318_at		1.37	1.69	1.54	2.23		0.005	+/+	
interleukin 6 signal transducer	Il6st	AI843709	94345_at		0.67	0.17	0.10	0.34			+/+	
IQ motif containing GTPase activating protein 1	Iqgap1	AW209098	100561_at		1.66	2.08	1.48	3.84			+/+	
Iroquois related homeobox 3 (Drosophila)	Irx3	Y15001	99034_at		1.48	2.31	1.47	3.53	4	0.027	+/+	Y
isocitrate dehydrogenase 1 (NADP+), soluble	Idh1	AF020039	160571_at		0.70	0.41	0.32	0.67	3	0.015	-/+	
isocitrate dehydrogenase 2 (NADP+), mitochondrial	Idh2	U51167	95693_at		0.73	0.43	0.25	0.63	3	0.050	+/+	
isocitrate dehydrogenase 3 (NAD+), gamma	Idh3g	U68564	93029_at		0.66	0.58	0.49	0.74			-/-	
isovaleryl coenzyme A dehydrogenase	Ivd	AW047743	104153_at		0.57	0.36	0.26	0.44	3	0.032	+/+	
kangai 1 (suppression of tumorigenicity 6, prostate)	Kai1	D14883	99584_at		2.31	3.10	1.96	4.14	4	0.013	+/+	
keratin complex 1, acidic, gene 18	Krt1-18	M22832	94270_at		1.43	1.91	1.37	4.63			+/+	
keratin complex 1, acidic, gene 19	Krt1-19	M36120	92550_at	P to A	0.91	0.00	0.00	0.17	1	0.049	+/+	
keratin complex 1, acidic, gene 19	Krt1-19	AU040563	102121_f_at	P to A	1.18	0.04	0.02	0.09	1	0.042	+/+	Y
keratin complex 2, basic, gene 8	Krt2-8	X15662	101009_at		1.27	1.73	1.30	2.62		0.037	+/+	
Kinesin family member 16B	RIKEN clone:7030401O13	AW122699	103998_at		1.32	2.64	1.75	3.94			+/+	
kit oncogene	Kit	Y00864	99956_at		1.62	4.29	2.11	10.48			+/+	
Kruppel-like factor 4 (gut)	Klf4	U20344	99622_at		0.69	0.23	0.19	0.44	3	0.003	+/+	Y
L-3-hydroxyacyl-Coenzyme A dehydrogenase, short chain	Hadhsc	D29639	95485_at		0.71	0.45	0.39	0.58	3	0.005	+/+	
lactotransferrin	Ltf	J03298	101115_at		1.48	0.24	0.09	8.22			+/+	
laminin B1 subunit 1	Lamb1-1	X05212	101948_at		0.67	0.24	0.14	0.41	1	0.018	+/+	
laminin, alpha 2	Lama2	U12147	92366_at	P to A	0.67	0.10	0.05	0.20			+/+	
latent transforming growth factor beta binding protein 2	Ltbp2	AF004874	92335_at		2.10	7.36	1.43	10.27			+/+	
latent transforming growth factor beta binding protein 4	Ltbp4	AA838868	97347_at	P to A	0.57	0.22	0.16	0.30			+/+	
latexin	Lxn	D88769	96065_at		1.71	3.41	2.33	3.84	2	0.009	+/+	
lectin, galactose binding, soluble 1	Lgals1	X15986	99669_at		0.63	0.16	0.09	0.29			+/+	
lectin, mannose-binding, 1	Lman1	AW108371	160270_at		1.38	2.51	1.65	3.27	2	0.037	+/+	
leptin	Lep	AI882416	98443_at	P to A	0.45	0.17	0.10	0.39			+/+	
leptin	Lep	AI882416	98444_g_at	P to A	0.47	0.03	0.02	0.09			+/+	
leucine rich repeat (in FLII) interacting protein 1	Lrrfip1	AI891475	92564_at		1.83	3.92	2.17	6.73	4	0.034	+/+	
leukotriene C4 synthase	Ltc4s	U27195	92401_at	P to A	0.61	0.20	0.10	0.35			+/+	

Table II-1. Global ErbB2/Neu Mammary Tumor Molecular Signature. 818 genes were changed according to Affymetrix algorithms in all tumors compared to wild-type control mammary tissues.
Note: ESTs have been annotated from public database information as of 1/2004

Gene Name	Common	Genbank	Affymetrix	Absolute call*	Fold Change§				SOM Cl #†	p-value‡	Repeated Observation**	RT-PCR Confirmation§§
					ANvsWT	TUvsWT						
					Median	Median	Minimum	Max				
Ligase III, DNA, ATP-dependent	1700051E09Rik	AW123157	96220_at		1.35	3.71	1.57	6.54			+/+	
ligase III, DNA, ATP-dependent	Lig3	U66058	102803_at		1.31	2.19	1.55	2.58	4	0.025	+/+	Y
LIM domain only 4	Lmo4	AF074600	98122_at		2.00	4.56	2.46	8.00	2	0.043	+/+	Y
lipase, hormone sensitive	Lipe	U69543	103083_at	P to A	0.77	0.06	0.02	0.11			+/+	
lipin 1	Lpin1	AI846934	98892_at		0.46	0.18	0.11	0.24	3	0.022	+/+	
lipocalin 2	Lcn2	X81627	160564_at		2.68	6.92	4.35	9.65		0.011	+/+	
lipocalin 2	Lcn2	AV210775	161684_r_at		1.64	2.87	1.39	5.50			+/-	
lipopolysaccharide binding protein	Lbp	X99347	96123_at		1.88	4.35	3.05	7.11			+/+	
lipoprotein lipase	Lpl	M63335	160083_at	P to A	1.25	0.06	0.05	0.09			+/+	
lipoprotein lipase	Lpl	AA726364	95611_at		0.64	0.02	0.02	0.04			+/+	
liver-specific bHLH-Zip transcription factor	Lisch7-pending	U49507	99452_at		1.57	2.06	1.71	2.89	2	0.045	+/+	Y
LPS-induced TN factor	Litaf	AI852632	93753_at		1.38	2.57	1.97	3.63	2	0.033	+/+	
lumican	Lum	AF013262	93353_at		0.90	0.07	0.03	0.20	1	0.010	+/+	
lymphoblastomic leukemia	Lyl1	X57687	100468_g_at		0.86	0.31	0.25	0.51	1	0.012	+/+	2of3
lymphocyte antigen 6 complex, locus A	Ly6a	X04653	93078_at		0.93	0.19	0.09	0.66	1	0.021	+/+	
lymphocyte cytosolic protein 1	Lcp1	D37837	94278_at		1.67	3.71	1.55	4.26			+/+	
lysozyme	Lyzs	M21050	100611_at		1.04	0.40	0.27	1.62			-/-	
major urinary protein group 1	Mup1; Up-1; Ltn-1; Mup-1; Mup-a; Lvtn-1	M17818	101566_f_at	P to A	1.34	0.07	0.02	0.31			+/+	
mammary tumor virus clone 66B env precursor (env) and vSAG		AF043689	93928_f_at		2.97	7.46	2.27	33.36			+/+	
manic fringe homolog (Drosophila)	Mfng	AF015769	100508_at		0.68	0.31	0.25	0.40	3	0.025	+/+	Y
mannose receptor, C type 1	Mrc1	Z11974	103226_at		1.07	0.21	0.16	0.36	1	0.039	+/+	
mannosidase 1, alpha	Man1a	AI021125	160579_at	P to A	0.95	0.13	0.02	0.39	1	0.038	+/+	
mannoside acetylglucosaminyltransferase 2	Mgat2	AI117848	95417_at		1.61	2.79	1.69	3.73			+/+	
MAP kinase-interacting serine/threonine kinase 2	Mknk2	AI845732	101007_at		0.61	0.29	0.17	0.43	3	0.050	+/+	
MARCKS-like protein	Mlp	X61399	97203_at		1.60	2.51	1.52	4.17			+/+	
mast cell protease 5	Mcpt5	M68898	102407_at		0.57	0.11	0.04	0.24			+/+	
matrilin 2	Matn2	U69262	98475_at	P to A	0.61	0.22	0.07	0.42			+/+	
matrix metalloproteinase 15	Mmp15	D86332	93612_at		1.77	3.46	2.00	7.57			+/+	
matrix metalloproteinase 3	Mmp3	X66402	98833_at		0.98	0.08	0.01	0.45	1	0.018	+/+	Y
melanoma cell adhesion molecule	Mcam	AI853261	160458_at		0.57	0.30	0.21	0.38			+/+	
melanoma inhibitory activity	Mia	X94322	101453_at		1.61	4.23	3.29	12.91			+/+	
membrane glycoprotein		Z22552	92779_f_at		2.73	7.01	3.68	25.63			+/+	
membrane glycoprotein		Z22552	92778_i_at		2.09	3.36	1.67	6.02			+/+	
membrane bound C2 domain containing protein	Mbc2	AF098633	96767_at		0.69	0.48	0.35	0.66			+/+	
mesenchyme homeobox 2	Meox2	Z16406	99937_at	P to A	0.64	0.02	0.01	0.04			+/+	
methylcrotonoyl-Coenzyme A carboxylase 1 (alpha)	Mccc1	AW123316	94940_at		0.46	0.26	0.18	0.37	3	0.035	+/+	
methylmalonyl-Coenzyme A mutase	Mut	X51941	99613_at		0.74	0.53	0.40	0.68	3	0.010	+/+	
microfibrillar associated protein 5	Mfap5-pending	AW121179	99518_at		1.21	0.34	0.25	0.62			+/+	
microsomal glutathione S-transferase 3	Mgst3	AI843448	96258_at		0.57	0.36	0.21	0.54			+/+	
microtubule-associated protein 4	Mtap4	M72414	92795_at		0.77	0.47	0.30	0.57	3	0.014	+/+	2of3
mitogen activated protein kinase 8 interacting protein	Mapk8ip	AF003115	104170_at	A to P	1.78	2.60	1.58	4.00	4	0.043	+/+	
mitogen activated protein kinase kinase kinase 1	Map3k1	AI317205	103021_r_at		1.51	3.36	1.54	6.87			+/+	
moderate similarity to protein pir:B42856 (H.sapiens) B42856 ubiquitin	6720465F12Rik	AI837415	94274_at		2.27	2.58	1.64	3.56			+/+	
moderate similarity to protein sp:P25962 (M.musculus) B3AR_MOUSE		AV373835	161900_f_at	P to A	0.43	0.01	0.01	0.05			+/+	
molybdenum cofactor synthesis 2	Mocs2	AW060325	160637_at		0.81	0.28	0.18	0.40	1	0.037	+/+	
monoglyceride lipase	Mgll	AI846600	97511_at		0.52	0.17	0.09	0.24			+/+	
mucin 10, submandibular gland salivary mucin	Muc10	U37531	101139_r_at	A to P	5.86	8.57	1.59	34.54			+/+	
Mus musculus 12 days embryo male wolffian duct includes surrounding		AA212897	96532_at	A to P	2.87	4.50	1.84	17.63			-/+	
Mus musculus mRNA similar to SHB (Src homology 2 domain	IMAGE:4488005	AI835278	102979_at	A to P	2.75	9.92	5.90	20.97			+/+	
Mus musculus Sestrin 1, mRNA (cDNA clone MGC:67135	IMAGE:6414521	AI843106	95731_at		0.70	0.48	0.34	0.55			-/-	
Mus musculus transcribed sequence with strong similarity to protein		AI553024	92202_g_at		1.23	0.24	0.01	0.57			+/+	
Mus musculus transcribed sequences		AA958903	100944_at		0.77	0.23	0.09	0.57	1	0.020	+/+	
Mus musculus, clone IMAGE:4196918, mRNA		AI841800	103456_at		0.77	0.37	0.24	0.51			+/+	
muscle glycogen phosphorylase	Pygm	AI850363	160754_at	P to A	0.16	0.02	0.01	0.09			+/+	
mutL homolog 1 (E. coli)	Mlh1	AA920621	104577_at		1.67	2.23	1.58	2.97		0.027	+/+	
myeloblastosis oncogene	Myb	M12848	92644_s_at		0.74	0.28	0.06	0.37			+/+	
myosin heavy chain 11, smooth muscle	Myh11	D85923	97990_at	P to A	0.67	0.03	0.01	0.06			+/+	
myosin, heavy polypeptide 1, skeletal muscle, adult	Myh1	AJ002522	98308_at	P to A	0.15	0.03	0.00	0.12			+/+	
myosin, heavy polypeptide 4, skeletal muscle	Myh4	AJ223361	98488_at	P to A	0.12	0.00	0.00	0.10			+/+	
myosin, light polypeptide 1, alkali; atrial, embryonic	Myl1	X12973	92541_at	P to A	0.22	0.05	0.02	0.14			+/+	
myosin, light polypeptide 9, regulatory	Myl9	AI842649	96939_at		0.79	0.40	0.23	0.54	1	0.019	+/+	
myristoylated alanine rich protein kinase C substrate	Marcks	M60474	96865_at		0.90	0.35	0.27	0.50	3	0.009	+/+	
N-acetylneuraminic acid synthase (sialic acid synthase)	Nans	AW122052	104147_at		1.57	2.19	1.39	4.03			+/+	
NADH dehydrogenase (ubiquinone) 1 alpha subcomplex, 3	Ndufa3	AA879764	96915_f_at		0.67	0.62	0.55	0.71			+/+	
NADH dehydrogenase (ubiquinone) 1, alpha/beta subcomplex, 1	Ndufab1	AI849803	96909_at		0.62	0.53	0.34	0.60	3	0.016	+/+	
NADH dehydrogenase (ubiquinone) Fe-S protein 1	Ndufs1	AI835051	93572_at		0.70	0.52	0.44	0.68			+/+	
NADH dehydrogenase (ubiquinone) Fe-S protein 2	Ndufs2	AI837493	93972_at		0.67	0.45	0.36	0.67			+/+	

Table II-1. Global ErbB2/Neu Mammary Tumor Molecular Signature. 818 genes were changed according to Affymetrix algorithms in all tumors compared to wild-type control mammary tissues.
Note: ESTs have been annotated from public database information as of 1/2004

Gene Name	Common	Genbank	Affymetrix	Absolute call*	Fold Change§				SOM Cl #†	p-value‡	Repeated Observation**	RT-PCR Confirmation§§
					ANvsWT	TUvsWT						
					Median	Median	Minimum	Max				
NADH dehydrogenase (ubiquinone) Fe-S protein 5	Ndufs5	AI852355	99593_at		0.74	0.61	0.51	0.76		0.040	-/-	
NADH dehydrogenase (ubiquinone) flavoprotein 1	Ndufv1	AI846127	96267_at		0.68	0.48	0.42	0.62		0.023	+/+	
necdin	Ndn	D76440	101059_at	P to A	0.56	0.06	0.03	0.15			+/+	
Nephronectin		AA592182	103721_at	A to P	6.83	49.87	23.26	93.70	2	0.042	+/+	Y
nestin	Nes	AW061260	103549_at		2.32	5.62	2.39	12.21			+/+	
neuroepithelial cell transforming gene 1	Net1	AJ010045	94223_at		0.68	0.39	0.25	0.56		0.016	+/+	N
neuronatin	Nnat	X83569	97520_s_at	P to A	0.27	0.02	0.01	0.05			+/+	
neuropeptide Y	Npy	AI848386	103235_at	A to P	4.58	43.41	9.45	298.17			+/+	
neuropilin	Nrp	D50086	95016_at		0.82	0.18	0.13	0.31	3	0.004	+/+	
nicotinamide N-methyltransferase	Nnmt	U86108	101473_at	P to A	0.54	0.03	0.02	0.05			+/+	
nidogen 1	Nid1	L17324	100120_at		0.62	0.14	0.09	0.25			+/+	
nidogen 2	Nid2	AB017202	93563_s_at	P to A	0.56	0.19	0.01	0.39			+/-	
Niemann Pick type C2	Npc2	AB021289	160344_at		0.60	0.54	0.44	0.63		0.019	+/+	
nitric oxide synthase 3, endothelial cell	Nos3	U53142	94167_at	P to A	0.19	0.07	0.05	0.15			+/+	
N-myc downstream regulated 2	Ndr2	AV349686	161610_at	P to A	0.64	0.20	0.09	0.40			+/+	
N-myc downstream regulated 2	Ndr2	AB033921	96088_at	P to A	0.55	0.11	0.04	0.32			+/+	
nuclear factor I/X	Nfix	AA002843	100307_at		2.30	3.86	2.69	8.88			+/+	
nuclear factor of kappa light chain gene enhancer in B-cells inhibitor,	Nfkbia	U57524	101554_at		1.20	0.50	0.38	0.68			-/-	
nuclear protein 95	Np95	D87908	99564_at		1.12	1.91	1.26	2.93			-/+	
nuclear receptor subfamily 1, group H, member 3	Nr1h3	AF085745	104381_at	P to A	0.57	0.10	0.08	0.13	3	0.039	+/+	Y
nuclear receptor subfamily 4, group A, member 1	Nr4a1	X16995	102371_at	A to P	1.56	3.51	2.06	6.06	2	0.040	+/+	
nucleobindin 2	Nucb2	AJ222586	102197_at		2.59	6.32	2.75	11.47	2	0.038	+/+	
orosomucoid 1	Orm1	M27008	100437_g_at	P to A	0.42	0.02	0.01	0.03			+/+	
orosomucoid 1	Orm1	M27008	100436_at	P to A	0.38	0.01	0.01	0.04			+/+	
osteoblast specific factor 2 (fasciclin I-like)	Osf2-pending	D13664	92593_at		1.11	0.15	0.08	0.54	1	0.024	+/+	Y
osteocalcin-related protein	Bglap-rs1; ORG; mOC-X	L24430	102801_at		1.55	4.17	2.06	9.06			+/+	
osteoglycin	Ogn	D31951	99549_at	P to A	0.67	0.08	0.04	0.16			+/+	
osteoglycin	Ogn	AA647799	160877_at	P to A	0.68	0.06	0.03	0.12			+/+	
oxoglutarate dehydrogenase (lipoamide)	Ogdh	AI852338	96879_at		0.56	0.41	0.30	0.48			+/+	
oxysterol binding protein-like 11	Osbpl11	AW124363	94439_at		0.70	0.47	0.33	0.55			+/-	
P450 (cytochrome) oxidoreductase	Por	D17571	99019_at		0.77	0.30	0.17	0.34			+/+	
p53 apoptosis effector related to Pmp22	Perp-pending	AI854029	97825_at		1.86	4.03	3.14	4.63	2	0.010	+/+	Y
parathyroid hormone receptor 1	Pthr1	X78936	98482_at	P to A	0.68	0.07	0.05	0.21			+/+	
PDZ and LIM domain 3	Pdlim3	AF002283	101089_at	P to A	0.88	0.12	0.04	0.17			+/+	
peripheral myelin protein	Pmp22	Z38110	102395_at		0.56	0.21	0.11	0.34			+/+	
peroxisome proliferator activated receptor gamma	Pparg	U10374	97926_s_at	P to A	0.42	0.02	0.01	0.04			+/+	Y
phenylalkylamine Ca2+ antagonist (emopamil) binding protein	Ebp	X97755	96627_at		1.16	1.65	1.31	1.93		0.041	+/+	
phosphatidic acid phosphatase 2a	Ppap2a	D84376	98508_s_at	P to A	0.62	0.32	0.05	0.48	3	0.015	+/-	
Phosphatidylinositol glycan, class R	pigr	AB001489	99926_at		2.59	2.79	2.20	7.73			+/+	
phosphodiesterase 8A	Pde8a	AF067806	160941_at	P to A	0.82	0.19	0.09	0.30	1	0.005	+/+	Y
phosphodiesterase 9A	Pde9a	AF031147	102338_at	A to P	1.56	4.20	2.58	7.52			+/+	
phosphoenolpyruvate carboxykinase 1, cytosolic	Pck1	AF009605	160481_at	P to A	0.36	0.01	0.01	0.04			+/+	
phosphoglucomutase 2	Pgm2	AI842432	104313_at		0.52	0.29	0.23	0.33	3	0.006	+/+	
phosphogluconate dehydrogenase	Pgd	AW120625	95420_at		0.71	0.52	0.40	0.71			+/+	
phosphoglycerate mutase 2	Pgam2	AF029843	92599_at	P to A	0.11	0.03	0.01	0.07			+/+	
phospholipid transfer protein	Pltp	U28960	100927_at	P to A	0.57	0.08	0.04	0.14			+/+	
phosphorylase kinase alpha 2	Phka2	AA822296	104003_at	P to A	0.57	0.23	0.15	0.38			+/+	
phytanoyl-CoA hydroxylase	Phyh	AF023463	96608_at		0.72	0.44	0.28	0.73	3	0.010	+/+	
placenta-specific 8	Plac8	AA790307	98092_at		0.93	0.33	0.17	0.54	1	0.040	+/+	
plasma membrane associated protein, S3-12	S3-12-pending	AF064748	102763_at	P to A	0.48	0.00	0.00	0.01			+/+	
platelet derived growth factor receptor, alpha polypeptide	Pdgfra	M57683	95079_at	P to A	0.72	0.14	0.10	0.29			+/+	
platelet derived growth factor receptor, beta polypeptide	Pdgfrb	X04367	160867_at	P to A	0.86	0.41	0.27	0.64			+/-	
pleckstrin homology-like domain, family A, member 1	Phlda1	U44088	160829_at		2.00	3.97	2.48	8.88			+/+	
pleckstrin homology-like domain, family A, member 3	Phlda3	AI846214	98056_at		0.59	0.17	0.06	0.33			+/+	
pleiotrophin	Ptn	D90225	97474_r_at	P to A	0.80	0.06	0.02	0.10			+/+	
potassium channel, subfamily K, member 1	Kcnk1	AF033017	102335_at		1.83	3.94	2.87	6.15			+/+	
potassium channel, subfamily K, member 2	Kcnk2	AI849601	104652_at	P to A	0.48	0.17	0.12	0.26			+/+	
potassium intermediate/small conductance calcium-activated channel,	Kcnn4	AF042487	102198_at		2.98	10.06	5.62	13.18	2	0.031	+/+	
preproenkephalin 1	Penk1	M55181	94516_f_at		0.56	0.20	0.08	0.26	3	0.010	+/+	
prion protein	Prnp	M18070	100606_at		0.74	0.49	0.32	0.65			+/-	
procollagen, type I, alpha 1	Col1a1	U03419	94305_at		0.93	0.25	0.16	0.64	1	0.043	+/+	
procollagen, type I, alpha 2	Col1a2	X58251	101130_at		1.01	0.30	0.14	0.62			+/+	
procollagen, type III, alpha 1	Col3a1	X52046	98331_at		1.18	0.18	0.11	0.41			+/+	
procollagen, type III, alpha 1	Col3a1	AA655199	102990_at		1.05	0.14	0.10	0.46	1	0.010	+/+	
procollagen, type IV, alpha 1	Col4a1	M15832	101093_at		0.81	0.47	0.33	0.68	3	0.019	+/+	
procollagen, type IV, alpha 2	Col4a2	X04647	101039_at		0.69	0.30	0.20	0.51			+/+	
procollagen, type IX, alpha 1	Col9a1	L12215	104483_at	A to P	4.29	13.36	7.84	37.01			+/+	

Table II-1. Global ErbB2/Neu Mammary Tumor Molecular Signature. 818 genes were changed according to Affymetrix algorithms in all tumors compared to wild-type control mammary tissues.
Note: ESTs have been annotated from public database information as of 1/2004

Gene Name	Common	Genbank	Affymetrix	Absolute call*	Fold Change§				SOM Cl #†	p-value‡	Repeated Observation**	RT-PCR Confirmation§§
					ANvsWT	TUvsWT						
					Median	Median	Minimum	Max				
procollagen, type IX, alpha 2	Col9a2	Z22923	98027_at		1.65	2.62	1.75	3.71			+/+	
procollagen, type V, alpha 1	Col5a1	AA796989	93472_at		0.89	0.50	0.37	0.75	1	0.046	+/+	
procollagen, type VI, alpha 1	Col6a1	X66405	95493_at		0.83	0.30	0.18	0.50			+/+	
procollagen, type VI, alpha 1	Col6a1	AV010209	162459_f_at	P to A	1.09	0.24	0.13	0.57	1	0.035	+/+	Y
procollagen, type VI, alpha 2	Col6a2	Z18272	93517_at		0.70	0.22	0.13	0.44			+/+	
procollagen, type VI, alpha 3	Col6a3	AF064749	101110_at		0.60	0.17	0.13	0.36	3	0.009	+/+	
procollagen, type XI, alpha 1	Col11a1	D38162	100481_at	A to P	4.03	13.27	6.36	23.10			+/+	
procollagen, type XV	Col15a1	AF011450	99637_at		0.62	0.21	0.15	0.38			+/+	
procollagen, type XVIII, alpha 1	Col18a1	L22545	101881_g_at	P to A	0.68	0.07	0.05	0.21	3	0.019	+/+	2of3
progressive ankylosis	ank	AW049351	100948_at		0.95	1.85	1.39	2.51	2	0.040	+/+	
properdin factor, complement	Pfc	X12905	101468_at	P to A	1.11	0.21	0.14	0.55	1	0.046	+/+	
prostaglandin E receptor 3 (subtype EP3)	Ptger3	D10204	96588_at	P to A	0.50	0.01	0.00	0.07			+/+	
prostaglandin E synthase	Ptges	AI060798	104406_at	P to A	0.71	0.08	0.02	0.18	1	0.010	+/+	
protease, serine, 11 (Igf binding)	Prss11	AW125478	96920_at		0.54	0.08	0.04	0.16	3	0.000	+/+	Y
protein distantly related to to the gamma subunit family	Pr1	AI849587	95465_s_at		1.27	2.62	1.41	4.50			+/+	
protein phosphatase 1, catalytic subunit, beta isoform	Ppp1cb	M27073	100088_at		1.59	2.36	1.39	3.66	4	0.045	+/+	
protein phosphatase 2, regulatory subunit B (B56), alpha isoform	Ppp2r5a	AI956230	93826_at		0.57	0.16	0.11	0.20	3	0.041	+/+	Y
protein phosphatase 3, catalytic subunit, alpha isoform	Ppp3ca	J05479	95092_at		1.79	3.39	1.91	5.28	4	0.047	+/+	
protein tyrosine phosphatase 4a3	Ptp4a3	AF035645	160862_at	P to A	0.84	0.26	0.08	0.43			+/+	
protein tyrosine phosphatase, non-receptor type 2	Ptpn2	M80739	101996_at		1.40	2.97	1.92	5.86	2	0.027	+/+	2of3
protein tyrosine phosphatase, receptor type, B	Ptprb	X58289	92289_at	P to A	0.37	0.04	0.03	0.06	3	0.031	+/+	Y
protein-tyrosine sulfotransferase 1	Tpst1	AF038008	103032_at	P to A	0.66	0.15	0.06	0.28			+/+	
prothymosin alpha	Ptma	X56135	100718_at		1.28	1.84	1.44	2.57			+/+	
protocadherin alpha 4	Pcdha4	D86916	160610_at	P to A	0.48	0.16	0.03	0.34			+/+	
PTK7 protein tyrosine kinase 7	Ptk7	AI326889	92325_at	A to P	3.96	4.86	2.28	12.30	4	0.020	+/+	
pyruvate carboxylase	Pcx		AFFX-		0.49	0.09	0.04	0.14			+/+	
pyruvate carboxylase	Pcx	M97957	93308_s_at	P to A	0.43	0.07	0.03	0.17			+/+	
pyruvate dehydrogenase (lipoamide) beta	Pdhb	AW125336	94806_at		0.55	0.36	0.31	0.49			+/+	
pyruvate dehydrogenase E1 alpha 1	Pdha1	M76727	98102_at		0.61	0.43	0.34	0.52	3	0.034	+/+	
pyruvate dehydrogenase kinase, isoenzyme 4	Pdk4	AJ001418	102049_at	P to A	0.68	0.10	0.05	0.26			+/+	
quaking	Qk	U44940	160726_at		0.70	0.19	0.12	0.30	1	0.011	+/+	
quiescin Q6	Qscn6	AW123556	96603_at		2.07	2.71	1.46	4.32			+/+	
RAB10, member RAS oncogene family	Rab10	AI841543	160149_at		1.60	2.60	1.80	4.06	4	0.036	+/+	
RAB18, member RAS oncogene family	Rab18	L04966	94319_at		1.16	1.75	1.46	2.14		0.005	+/+	2of3
RAB34, member of RAS oncogene family	Rab34	AI835712	160317_at	P to A	0.52	0.33	0.11	0.38	3	0.035	+/+	Y
RAB3D, member RAS oncogene family	Rab3d	M89777	97415_at		1.39	3.05	1.60	4.50			+/+	
RAS p21 protein activator 1	Rasa1	AI846922	99467_at		1.20	2.30	1.89	2.95			+/+	
RAS p21 protein activator 3	Rasa3	U20238	93319_at		0.64	0.16	0.09	0.21			+/+	
RAS, dexamethasone-induced 1	Rasd1	AF009246	99032_at	P to A	0.57	0.06	0.02	0.10			+/+	
Ras-related GTP binding C	Rragc	AB017616	98950_at		0.72	0.55	0.38	0.66		0.020	-/-	
receptor (calcitonin) activity modifying protein 2	Ramp2	AJ250490	99444_at	P to A	0.63	0.21	0.16	0.32			+/+	
recombinant antineuraminidase single chain Ig VH and VL domains	LOC56304	U10410	100721_f_at	P to A	0.70	0.13	0.06	0.28			+/+	
ref:NP_062775.1 - open reading frame 18; thymic dendritic cell-derived	1110001M20Rik	AW125185	95477_at		1.17	2.43	1.35	3.46			+/+	
ref:NP_076015.1 - kappaB-Ras1 protein	2400004O09Rik	AI846893	160991_at		0.55	0.40	0.31	0.60	3	0.038	+/+	
ref:NP_080832.1 - dynein light chain 2; RIKEN cDNA 1700064A15 gene	6720463E02Rik	AI836322	101929_at		4.18	3.18	1.39	7.78			+/+	
resistin	Retn	AA718169	102366_at	P to A	0.51	0.00	0.00	0.02			+/+	
reticulocalbin 2	Rcn2	AF049125	93281_at		1.33	3.18	2.30	5.28	4	0.023	+/+	
reticulon 1	Rtn1	AW123115	94545_at		2.18	6.82	3.61	13.09			+/+	
retinol binding protein 4, plasma	Rbp4	U63146	96047_at	P to A	0.45	0.01	0.00	0.01			+/+	
Rho guanine nucleotide exchange factor (GEF) 5	Arhgef5	AA726063	160977_at		1.40	2.19	1.84	2.87	2	0.023	+/+	
rhophilin, Rho GTPase binding protein 2	C230052I12Rik	AI850288	98485_at		1.96	3.01	1.78	7.78			+/+	
rhotekin	Rtkn	U54638	160864_at		1.53	1.92	1.53	2.91	4	0.027	+/+	
ribonuclease, RNase A family 4	Rnase4	AI840339	96038_at		0.74	0.15	0.07	0.21			+/+	
ribonucleotide reductase M2	Rrm2	M14223	102001_at		1.75	2.93	1.79	3.48	4	0.013	+/+	Y
RIKEN cDNA 0610007L05 gene	0610007L05Rik	AI842828	97835_at	P to A	0.47	0.03	0.01	0.09			+/+	
RIKEN cDNA 0610010O12 gene	0610010O12Rik	AI849011	97242_at		1.45	2.93	2.25	4.14	2	0.019	+/+	
RIKEN cDNA 0610013D04 gene	0610013D04Rik	AF110520	96785_at	P to A	0.55	0.13	0.07	0.22			+/+	
RIKEN cDNA 0610013D04 gene	0610013D04Rik	AA879929	96786_s_at	P to A	0.29	0.08	0.04	0.16			+/+	
RIKEN cDNA 0610039C21 gene	0610039C21Rik	AW121217	96348_at		0.54	0.15	0.10	0.21			+/+	
RIKEN cDNA 0610039N19 gene	0610039N19Rik	AW047688	95026_at	P to A	0.54	0.23	0.16	0.41			+/+	
RIKEN cDNA 0710001O03 gene	0710001O03Rik	AI853364	160391_at		0.84	0.31	0.15	0.61	1	0.031	+/+	
RIKEN cDNA 1100001H23 gene	1100001H23Rik	AA710132	98033_at		0.54	0.24	0.17	0.37			+/+	
RIKEN cDNA 1110001C20 gene	1110001C20Rik	AW121960	95458_s_at		1.48	1.95	1.42	3.32			+/+	
RIKEN cDNA 1110001I14 gene	1110001I14Rik	AW047554	104605_at		0.45	0.26	0.18	0.38	3	0.001	+/+	
RIKEN cDNA 1110003O22 gene	1110003O22Rik	AI847054	96662_at		0.64	0.51	0.23	0.66			+/+	
RIKEN cDNA 1110004P15 gene	1110004P15Rik	AA657044	160255_at		0.69	0.19	0.10	0.43	1	0.019	+/+	
RIKEN cDNA 1110015E22 gene	1110015E22Rik	AW045753	104217_at		0.62	0.11	0.08	0.67	3	0.039	-/-	

Table II-1. Global ErbB2/Neu Mammary Tumor Molecular Signature. 818 genes were changed according to Affymetrix algorithms in all tumors compared to wild-type control mammary tissues.
Note: ESTs have been annotated from public database information as of 1/2004

Gene Name	Common	Genbank	Affymetrix	Absolute call*	Fold Change§				SOM Cl #†	p-value‡	Repeated Observation**	RT-PCR Confirmation§§
					ANvsWT	TUvsWT						
					Median	Median	Minimum	Max				
RIKEN cDNA 1110020B03 gene	1110020B03Rik	AI851387	102922_at		1.18	2.53	1.88	3.53	2	0.013	+/+	
RIKEN cDNA 1110020K19 gene	1110020K19Rik	AW047874	103773_at		0.48	0.35	0.21	0.61			+/+	
RIKEN cDNA 1110020P15 gene	1110020P15Rik	AW046239	94078_at		0.78	0.59	0.41	0.69	3	0.019	+/+	
RIKEN cDNA 1110021N07 gene	1110021N07Rik	AI846382	93983_at	P to A	0.58	0.38	0.29	0.45	3	0.008	+/+	
RIKEN cDNA 1110025G12 gene	1110025G12Rik	AI461631	104325_at	P to A	0.59	0.02	0.01	0.11			+/+	
RIKEN cDNA 1110032O19 gene	1110032O19Rik	AI853294	97386_at		0.57	0.30	0.16	0.42	3	0.010	+/+	
RIKEN cDNA 1190002H23 gene	1190002H23Rik	AI854358	160359_at		0.55	0.14	0.10	0.32			+/+	
RIKEN cDNA 1190002N15 gene	1190002N15Rik	AW125453	98594_at	P to A	0.69	0.30	0.17	0.40			+/+	
RIKEN cDNA 1190006E07 gene	1190006E07Rik	AI852865	160112_at		1.39	2.30	1.95	3.05	4	0.019	+/+	
RIKEN cDNA 1200002G13 gene	1200002G13Rik	AW120643	96708_at		1.42	1.93	1.43	2.20	2	0.040	+/+	
RIKEN cDNA 1200015A22 gene	1200015A22Rik	AI854863	98633_at	P to A	0.44	0.24	0.18	0.31	3	0.009	+/+	
RIKEN cDNA 1200015G06 gene	1200015G06Rik	AI844370	93590_at		2.28	2.77	1.87	4.20	2	0.006	+/+	
RIKEN cDNA 1300002F13 gene	1300002F13Rik	AI853531	93975_at		1.43	3.51	2.41	4.79	2	0.016	+/+	
RIKEN cDNA 1300002F13 gene	1300002F13Rik	AW212475	93974_at		1.59	2.68	1.32	6.50			+/+	
RIKEN cDNA 1300003D03 gene	1300003D03Rik	AA871791	102052_at		0.65	0.40	0.19	0.76	3	0.041	+/+	
RIKEN cDNA 1500040F11 gene	1500040F11Rik	AW061302	93844_at		0.59	0.34	0.26	0.43			+/+	
RIKEN cDNA 1600023A02 gene	1600023A02Rik	AW121336	96643_at	P to A	0.69	0.11	0.04	0.39			+/+	
RIKEN cDNA 1600029D21 gene	1600029D21Rik	AI121305	97413_at		4.19	8.63	3.92	16.80	4	0.040	+/+	
RIKEN cDNA 1620401E04 gene	1620401E04Rik	AW125480	96900_at		0.66	0.49	0.35	0.70	3	0.009	+/+	
RIKEN cDNA 1700012G19 gene	1700012G19Rik	AI848173	98890_at		1.95	3.81	2.64	6.23			+/+	
RIKEN cDNA 1700051C09 gene	1700051C09Rik	AV260411	161227_r_at		2.92	5.21	3.51	7.11	4	0.025	+/+	
RIKEN cDNA 1810015C04 gene	1810015C04Rik	AW122893	95518_at		1.68	3.53	2.39	4.53	2	0.013	+/+	
RIKEN cDNA 1810044O22 gene	1810044O22Rik	AI850017	103619_at		0.62	0.24	0.18	0.32	3	0.043	+/+	
RIKEN cDNA 2300006M17 gene	2300006M17Rik	AW045317	97933_at		1.55	3.20	2.16	4.76			+/+	
RIKEN cDNA 2310005P05 gene	2310005P05Rik	AI838150	160916_at	P to A	0.39	0.06	0.03	0.20			+/+	
RIKEN cDNA 2310009N05 gene	2310009N05Rik	AW061073	160801_at		1.59	3.10	2.04	3.51	2	0.019	+/+	
RIKEN cDNA 2310016A09 gene	2310016A09Rik	AW049373	96122_at		0.42	0.08	0.04	0.11			+/+	
RIKEN cDNA 2310020A21 gene	2310020A21Rik	AI173973	100043_f_at	A to P	1.88	2.81	1.42	4.72	4	0.047	+/-	
RIKEN cDNA 2310047E01 gene	2310047E01Rik	AI314958	103905_at	A to P	4.07	15.67	5.31	23.75			+/+	
RIKEN cDNA 2310075E07 gene	2310075E07Rik	AI845915	104100_at		0.40	0.06	0.05	0.09			+/+	
RIKEN cDNA 2400003B06 gene	2400003B06Rik	AW046723	100074_at		1.96	2.51	1.54	4.35			+/+	
RIKEN cDNA 2410091N08 gene	2410091N08Rik	AW046563	103912_at	P to A	0.52	0.48	0.23	0.70			+/+	
RIKEN cDNA 2610001E17 gene	2610001E17Rik	AW122012	160298_at		0.59	0.08	0.05	0.22	1	0.039	+/+	
RIKEN cDNA 2610019F03 gene	2610019F03Rik	AI846549	100902_at	P to A	0.50	0.26	0.21	0.33			+/+	
RIKEN cDNA 2610025P08 gene	2610025P08Rik	AI853551	104146_at	P to A	0.84	0.08	0.04	0.15			+/+	
RIKEN cDNA 2610042L04 gene	2610042L04Rik	AI853444	93569_f_at	P to A	1.18	0.10	0.03	0.28			+/+	
RIKEN cDNA 2610042L04 gene	2610042L04Rik	AI853444	93568_i_at	P to A	1.26	0.08	0.01	0.28	1	0.006	+/+	
RIKEN cDNA 2610207I16 gene	2610207I16Rik	AI648018	96096_f_at		0.65	0.38	0.21	0.56			+/+	
RIKEN cDNA 2610207I16 gene	2610207I16Rik	AI648018	96095_i_at		0.54	0.31	0.20	0.45			-/+	
RIKEN cDNA 2610509I15 gene	2610509I15Rik	AW121399	103939_at		0.60	0.30	0.24	0.46			+/+	
RIKEN cDNA 2700030M23 gene	2700030M23Rik	AW011791	96935_at		1.69	2.58	1.75	4.08			+/+	
RIKEN cDNA 3110001A13 gene	3110001A13Rik	AI644158	96640_at	P to A	1.02	0.44	0.30	0.61	1	0.019	+/+	
RIKEN cDNA 3110003A17 gene	3110003A17Rik	AA833425	96135_at		1.70	2.31	1.65	3.01	4	0.016	+/+	
RIKEN cDNA 3110038L01 gene	3110038L01Rik	AI844396	95135_at		0.50	0.26	0.19	0.33			+/+	
RIKEN cDNA 3110043O21 gene	3110043O21Rik	AI840585	100464_at		0.45	0.19	0.13	0.24			+/+	
RIKEN cDNA 3930401E15 gene	3930401E15Rik	AI846109	160183_f_at		1.30	2.04	1.37	2.33			+/+	
RIKEN cDNA 4631408O11 gene	4631408O11Rik	AW046694	104445_at		0.55	0.08	0.03	0.13			+/+	
RIKEN cDNA 4921515A04 gene	4921515A04Rik	AI642098	104494_at		0.53	0.33	0.15	0.54	3	0.008	+/+	
RIKEN cDNA 4930488L10 gene	4930488L10Rik	AA727410	97349_at		0.89	0.47	0.33	0.75			+/+	
RIKEN cDNA 4931406C07 gene	4931406C07Rik	AI255972	96090_g_at		1.21	2.66	1.89	3.39	2	0.028	+/+	
RIKEN cDNA 4931406C07 gene	4931406C07Rik	AI255972	96089_at		0.97	2.06	1.56	2.99			+/+	
RIKEN cDNA 5530401C11 gene	5530401C11Rik	AI155273	160785_at		1.30	2.58	1.24	3.58			+/+	
RIKEN cDNA 5530600A18 gene	5530600A18Rik	AW125433	94955_at	P to A	0.58	0.44	0.04	0.80			-/-	
RIKEN cDNA 5730551F12 gene	5730551F12Rik	AW125340	160193_at		1.28	1.77	1.57	2.03		0.019	+/+	
RIKEN cDNA 6030432N09 gene	6030432N09Rik	AI851332	95413_at		1.32	1.61	1.30	2.14			+/+	
RIKEN cDNA 6330514M23 gene	6330514M23Rik	AW048944	97496_f_at		0.63	0.16	0.09	0.51	1	0.020	+/+	
RIKEN cDNA 6430402H10 gene	6430402H10Rik	AI837615	97279_at		0.63	0.54	0.41	0.78			-/-	
RIKEN cDNA 9130009C22 gene	9130009C22Rik	AA959954	103446_at		1.48	2.39	1.56	4.20			+/+	
RIKEN cDNA 9130415E20 gene	9130415E20Rik	AI848868	95020_at		0.72	0.32	0.19	0.46			+/+	
RIKEN cDNA 9630044O09 gene	9630044O09Rik	AI835624	160236_at	A to P	3.04	6.28	2.69	30.27	2	0.019	+/+	
RIKEN cDNA A230075M04 gene	A230075M04Rik	AW061234	103697_at		0.70	0.35	0.20	0.45			+/+	
RIKEN cDNA A430096B05 gene	A430096B05Rik	AI465965	97826_at		0.60	0.05	0.03	0.13	3	0.012	+/+	
RIKEN cDNA B430320C24 gene	B430320C24Rik	AI606967	97711_at	P to A	0.34	0.11	0.03	0.26			+/+	
RIKEN cDNA B430320C24 gene	B430320C24Rik	AA717225	160989_r_at	P to A	0.46	0.07	0.04	0.09			+/+	
RIKEN cDNA C030048H19 gene	C030048H19Rik	AW122114	92526_f_at		1.04	2.23	1.33	3.63			-/+	
RIKEN cDNA C330027C09 gene	C330027C09Rik	AA590345	160973_at		1.51	2.31	1.58	3.27	4	0.042	+/+	
RIKEN cDNA C730036B01 gene	C730036B01Rik	AA690483	103257_at		0.66	0.27	0.16	0.40			+/-	

Table II-1. Global ErbB2/Neu Mammary Tumor Molecular Signature. 818 genes were changed according to Affymetrix algorithms in all tumors compared to wild-type control mammary tissues.
Note: ESTs have been annotated from public database information as of 1/2004

Gene Name	Common	Genbank	Affymetrix	Absolute call*	Fold Change§				SOM Cl #†	p-value‡	Repeated Observation**	RT-PCR Confirmation§§
					ANvsWT	TUvsWT						
					Median	Median	Minimum	Max				
RIKEN cDNA D330037A14 gene	D330037A14Rik	AI854506	96206_at	P to A	0.69	0.25	0.18	0.49	1	0.005	+/+	
ring finger protein 149	Rnf149	AI849082	98915_at		1.31	1.66	1.47	1.91		0.013	-/+	
RNA binding motif, single stranded interacting protein 1	Rbms1	AB026569	94972_at		1.35	1.83	1.54	2.33			-/-	
S100 calcium binding protein A10 (calpactin)	S100a10	M16465	92539_at		0.76	0.35	0.25	0.49			-/+	
S100 calcium binding protein A13	S100a13	AV007820	161121_f_at		0.63	0.50	0.31	0.76			+/+	
S100 calcium binding protein A6 (calcyclin)	S100a6	X66449	92770_at		0.90	0.27	0.12	0.71	1	0.045	+/+	
sarcoglycan, epsilon	Sgce	AF031919	101861_at	P to A	0.47	0.10	0.04	0.17			+/+	
sarcospan	Sspn	U02487	102378_at	P to A	0.71	0.34	0.12	0.38			+/+	
schlafen 2	Slfn2	AF099973	92472_f_at	A to P	2.67	3.27	1.43	7.31			+/+	
scrapie responsive gene 1	Scrg1	AJ223206	94181_at	A to P	7.32	64.00	13.93	111.43			+/+	
SEC23A (S. cerevisiae)	Sec23a	AI843665	104709_at		0.73	0.57	0.45	0.75		0.039	-/-	
secreted acidic cysteine rich glycoprotein	Sparc	X04017	97160_at		0.75	0.17	0.09	0.28			+/+	
secreted phosphoprotein 1	Spp1	X13986	97519_at		1.02	0.14	0.06	3.27			+/+	
septin 4	38234	X61452	94079_at	P to A	0.55	0.16	0.05	0.31			+/+	
serine (or cysteine) proteinase inhibitor, clade A, member 3C	Serpina3c	X61597	102707_f_at	P to A	0.73	0.21	0.08	0.29			+/+	
serine (or cysteine) proteinase inhibitor, clade A, member 3N	Serpina3n	M64086	104374_at	P to A	0.74	0.31	0.17	0.70			-/+	
serine (or cysteine) proteinase inhibitor, clade E, member 2	Serpine2	X70296	97487_at		1.87	6.15	2.62	13.00			+/+	
serine (or cysteine) proteinase inhibitor, clade F), member 1	Serpinf1	AF036164	93574_at		0.68	0.11	0.06	0.27			+/+	
serine (or cysteine) proteinase inhibitor, clade G, member 1	Serping1	AF010254	99081_at		0.52	0.10	0.06	0.21			+/+	
serine protease inhibitor, Kunitz type 1	Spint1	AW230369	97206_at		1.71	3.43	2.93	5.10	2	0.038	+/+	Y
serine/threonine kinase 39, STE20/SPS1 homolog (yeast)	Stk39	AF099988	160806_at		1.76	5.70	2.91	9.65	2	0.038	+/+	Y
serum deprivation response	Sdpr	AI839175	160373_i_at		0.54	0.18	0.13	0.45	3	0.006	+/+	Y
shroom	Shrm	AI641895	100024_at		2.19	4.92	2.79	9.78	4	0.020	+/+	Y
sialyltransferase 10 (alpha-2,3-sialyltransferase VI)	Siat10	AI153959	102208_at	P to A	0.48	0.18	0.11	0.30	3	0.042	+/+	
sialyltransferase 7 ((alpha-N-acetylneuraminyl 2,3-betagalactosyl-1,3)-N-	Siat7d	Y15780	96682_at	A to P	2.53	9.99	2.85	20.68	2	0.042	+/+	
sialyltransferase 7 ((alpha-N-acetylneuraminyl 2,3-betagalactosyl-1,3)-N-	Siat7e	AB030836	92403_at	P to A	0.40	0.12	0.08	0.21			+/+	
sialyltransferase 8 (alpha-2, 8-sialyltransferase) D	Siat8d	X86000	102318_at	P to A	0.87	0.28	0.18	0.58			+/+	
sialyltransferase 9 (CMP-NeuAc:lactosylceramide alpha-2,3-sialyltransferase)	Siat9	Y15003	98596_s_at	A to P	6.42	23.75	12.55	37.01	2	0.041	+/+	
signal recognition particle 19	Srp19	AI848458	160343_at		1.52	1.91	1.57	3.20		0.034	+/+	
signal sequence receptor, beta	Ssr2	AI845293	101061_at		1.31	1.66	1.43	2.08			+/+	
SIMILAR TO MOLYBDENUM COFACTOR SULFURASE [Homo	1110018O12Rik	AA839813	96151_at		1.29	2.14	1.49	6.41			+/+	
Similar to protein kinase, lysine deficient 1	IMAGE:4193361	AW124781	95952_at	A to P	1.94	3.20	1.73	4.76	4	0.019	-/+	
similar to SW:WDNM_RAT P14730 WDNM1 PROTEIN PRECURSOR	1100001G20Rik	AI019679	101912_at	P to A	1.00	0.16	0.04	0.26			+/+	
SKI interacting protein	Skiip	AW046671	104158_at		3.48	4.20	2.45	13.00			+/+	
small chemokine (C-C motif) ligand 11	Ccl11	U77462	92742_at	P to A	0.58	0.15	0.04	0.33	3	0.010	+/+	
small nuclear ribonucleoprotein D3	Snrpd3	AA796831	98077_at		3.34	3.94	2.01	8.00			+/+	
SNF related kinase	Snrk	AW048113	97429_at		0.74	0.37	0.12	0.53	3	0.021	+/+	
solute carrier family 1, member 7	Slc1a7	L42115	92582_at	P to A	0.38	0.03	0.01	0.06			+/+	
solute carrier family 12, member 2	Slc12a2	U13174	99500_at		1.55	3.97	2.14	6.54	2	0.041	+/+	
solute carrier family 2 (facilitated glucose transporter), member 4	Slc2a4	M23383	102314_at	P to A	0.52	0.10	0.02	0.20			+/+	
solute carrier family 25 (mitochondrial carrier; citrate transporter),	Slc25a1	AI848354	94807_at		0.87	0.28	0.13	0.37			+/+	
solute carrier family 25 (mitochondrial carrier; citrate transporter),	Slc25a1	AV218217	162358_i_at		0.59	0.18	0.09	0.27			+/+	
solute carrier family 25 (mitochondrial carrier; dicarboxylate transporter),	Slc25a10	AA683883	99112_at	P to A	0.67	0.27	0.06	0.43			+/+	
solute carrier family 27 (fatty acid transporter), member 1	Slc27a1	U15976	93486_at	P to A	0.69	0.05	0.03	0.08	1	0.025	+/+	
solute carrier family 29 (nucleoside transporters), member 1	Slc29a1	AI838274	95733_at		1.55	3.94	3.10	5.78	2	0.045	+/+	Y
solute carrier family 35 (CMP-sialic acid transporter), member 1	Slc35a1	Z71268	104380_at		1.48	2.83	1.24	3.68			+/+	
solute carrier family 5 (sodium-dependent vitamin transporter), member	Slc5a6	AW048729	104200_at	P to A	0.55	0.11	0.05	0.47			+/+	
solute carrier family 7 (cationic amino acid transporter, y+ system),	Slc7a5	AB017189	104221_at		1.56	2.68	1.59	3.43			+/+	
sorbin and SH3 domain containing 1	Sorbs1	U58883	160320_at		0.59	0.12	0.08	0.15	3	0.044	+/+	
sorting nexin 1	Snx1	AW121324	94550_at		1.21	2.00	1.57	2.39			+/+	Y
sp:Q9D4V0 - EKI1_MOUSE Ethanolamine kinase	4930555L11Rik	AI853226	160393_at		1.89	7.11	4.99	10.20	2	0.020	+/+	
SP22_MOUSE Microsomal signal peptidase 23 kDa subunit	6530401D17Rik	AI839718	95523_at		0.37	0.04	0.03	0.07			+/+	
spectrin alpha 2	Spna2	AW046708	103345_at		1.08	2.08	1.54	2.75	2	0.026	+/+	
spermatid perinuclear RNA binding protein	Spnr	AI838709	103330_at		1.52	2.64	2.01	3.46	2	0.023	+/+	Y
spermatogenesis associated 6	Spata6	AF032967	101520_at		1.39	1.85	1.55	2.41			+/+	
spermidine/spermine N1-acetyl transferase 1	Sat1	L10244	96657_at		1.11	1.89	1.38	2.55			+/-	
S-phase kinase-associated protein 1A	Skp1a	Z47088	99607_at		1.95	3.05	2.46	7.57	4	0.025	+/+	2of3
spindlin	Spin	AW122015	99528_at		1.59	2.28	1.20	4.06			+/+	
Src activating and signaling molecule	Srcasm	AI840130	104063_at		1.28	2.68	2.22	3.32	2	0.012	+/+	
SRY-box containing gene 10	Sox10	AF047389	102856_at		1.89	3.76	1.74	5.24			+/+	
SRY-box containing gene 4	Sox4	X70298	160109_at		1.75	3.39	2.22	4.89	2	0.031	+/+	Y
stearoyl-Coenzyme A desaturase 1	Scd1	M21285	94057_g_at		0.86	0.35	0.16	0.69			+/+	
sterol carrier protein 2-pseudogene	Scp2-ps2	X87685	95787_s_at		0.55	0.41	0.23	0.73	3	0.048	-/-	
stromal cell derived factor receptor 2	Sdfr2	D50464	103421_at		2.29	3.05	2.16	4.66	4	0.022	+/+	
succinate dehydrogenase complex, subunit A, flavoprotein (Fp)	Sdha	AI835718	94080_at		0.53	0.30	0.25	0.40			+/+	
succinate dehydrogenase complex, subunit B, iron sulfur (Ip)	Sdhb	AA674669	95053_s_at		0.53	0.32	0.19	0.43			+/+	

Table II-1. Global ErbB2/Neu Mammary Tumor Molecular Signature. 818 genes were changed according to Affymetrix algorithms in all tumors compared to wild-type control mammary tissues.
Note: ESTs have been annotated from public database information as of 1/2004

Gene Name	Common	Genbank	Affymetrix	Absolute call*	Fold Change§				SOM Cl #†	p-value‡	Repeated Observation**	RT-PCR Confirmation§§
					ANvsWT	TUvsWT						
					Median	Median	Minimum	Max				
succinate-CoA ligase, GDP-forming, alpha subunit	Suclg1	AI840979	96268_at		0.72	0.44	0.35	0.58			+/+	
sulfide quinone reductase-like (yeast)	Sqrdl	AW208628	94515_at		0.58	0.37	0.29	0.64	3	0.041	+/+	
sulfotransferase family 1A, phenol-preferring, member 1	Sult1a1	L02331	103087_at	P to A	0.61	0.02	0.01	0.04	3	0.042	+/+	
superoxide dismutase 3, extracellular	Sod3	U38261	94902_at		0.60	0.32	0.23	0.51			+/-	
suppressor of cytokine signaling 2	Socs2	U88327	99475_at		2.26	14.22	5.74	19.56	2	0.034	+/+	
sushi-repeat-containing protein	Srpx	AB028049	103568_at	P to A	0.68	0.10	0.06	0.25	1	0.008	+/+	Y
synaptonemal complex protein 3	Sycp3	AW212131	93994_at		0.54	0.15	0.12	0.22	3	0.007	+/+	
synovial sarcoma, X breakpoint 2 interacting protein	Ssx2ip	AW122911	96723_f_at		1.49	2.04	1.60	2.58			+/+	
Syntaxin 8	BC019633	AA645293	97977_at		1.37	2.04	1.54	2.53			-/+	
synuclein, gamma	Sncg	AV062363	161859_f_at		0.49	0.13	0.07	0.23			+/+	
synuclein, gamma	Sncg	AF017255	104280_at	P to A	0.43	0.01	0.00	0.02			+/+	
TCDD-inducible poly(ADP-ribose) polymerase	AW558171	AW120868	93985_at	P to A	0.57	0.21	0.06	0.85			+/-	
T-cell immunoglobulin and mucin domain containing 2	Timd2	AA986114	103794_i_at		2.60	4.59	1.93	7.01	4	0.030	+/+	
T-cell immunoglobulin and mucin domain containing 2	Timd2	AA795198	97335_at		1.52	2.38	1.64	3.14	4	0.010	+/-	
T-cell lymphoma invasion and metastasis 1	Tiam1	U05245	102283_at		1.51	2.06	1.77	2.66	4	0.040	+/+	Y
tensin like C1 domain-containing phosphatase	Tenc1	AI854794	96825_at	P to A	0.62	0.18	0.03	0.40			+/+	
tetranectin (plasminogen binding protein)	Tna	X79199	92224_at	P to A	1.13	0.06	0.03	0.17	1	0.041	+/+	
TG interacting factor	Tgif	X89749	101502_at		1.33	3.36	1.37	4.86			+/+	
thioether S-methyltransferase	Temt	M88694	97402_at	P to A	0.88	0.05	0.03	0.13			+/+	
thrombomodulin	Thbd	X14432	104601_at	P to A	0.84	0.29	0.18	0.41	1	0.033	+/+	
thrombospondin 1	Thbs1	M62470	160469_at		1.96	4.92	1.88	9.51			+/+	Y
thrombospondin type 1 domain containing gene	Rspondin-pending	AB016768	98312_at	P to A	1.04	0.03	0.02	0.04	1	0.000	+/+	
thymus cell antigen 1, theta	Thy1	M12379	99057_at	P to A	1.17	0.18	0.05	0.37			+/+	
thyroid hormone responsive SPOT14 homolog (Rattus)	Thrsp	X95279	160306_at		0.72	0.07	0.04	0.19			+/+	
thyroid stimulating hormone receptor	Tshr	U02602	98328_at	P to A	0.40	0.03	0.01	0.16			+/+	
tissue inhibitor of metalloproteinase 3	Timp3	U26437	160519_at		0.83	0.29	0.18	0.38			+/+	
Tnf receptor associated factor 4	Traf4	AV109962	162482_at		1.40	2.10	1.88	2.51	2	0.037	+/+	Y
Tnf receptor associated factor 4	Traf4	X92346	100005_at		1.48	2.04	1.45	2.48		0.016	+/+	Y
transaldolase 1	Taldo1	U67611	95066_at		0.77	0.42	0.32	0.61			+/+	
transcobalamin 2	Tcn2	AF090686	93736_at		1.43	3.12	2.25	4.79			+/+	
transcription factor AP-2, gamma	Tcfap2c	X94694	92275_at		1.48	4.23	2.69	5.98	2	0.040	+/+	Y
transforming growth factor alpha	Tgfa	M92420	92369_at	A to P	1.72	4.82	2.50	7.31	2	0.050	+/+	Y
transforming growth factor beta 1 induced transcript 4	Tgfb1i4	X62940	93728_at		0.82	0.38	0.31	0.48	1	0.009	-/+	1of3
transforming growth factor, beta induced	Tgfbi	L19932	92877_at		0.87	0.34	0.23	0.54	1	0.013	+/+	Y
transgelin	Tagln	Z68618	93541_at		0.93	0.18	0.13	0.31			+/+	
transketolase	Tkt	U05809	101964_at		0.71	0.30	0.19	0.53			+/+	
translocating chain-associating membrane protein 1	Tram1	AI844979	98956_at		1.19	2.20	1.60	2.60			+/+	
transmembrane 4 superfamily member 3	Tm4sf3	AI047972	103494_at	A to P	3.92	24.25	14.52	31.78	2	0.014	+/+	
troponin T3, skeletal, fast	Tnnt3	L48989	92885_at	P to A	0.20	0.02	0.01	0.12			+/+	
tryptophan hydroxylase 1	Tph1	J04758	99972_at	P to A	0.98	0.05	0.01	0.10			+/+	
TSG118.1	2310008H09Rik	AF034580	160872_f_at		1.61	2.43	1.79	3.78	4	0.024	+/+	
tuftelin 1	Tuft1	AF047704	102043_at	A to P	1.85	2.83	2.19	3.84	2	0.035	+/+	
tumor differentially expressed 1	Tde1	L29441	100151_at		1.44	2.41	1.36	2.99		0.038	+/+	
tumor necrosis factor receptor superfamily, member 11a	Tnfrsf11a	AF019046	101632_at		1.61	2.73	1.62	5.74			+/+	
tumor protein D52	Tpd52	U44426	160249_at		1.76	2.89	2.20	4.35	4	0.036	+/+	
tumor protein D52-like 1	Tpd52l1	AF004428	101446_at	A to P	2.72	12.13	7.26	21.41	2	0.006	+/+	Y
tumor-associated calcium signal transducer 1	Tacstd1	M76124	99582_at		2.09	6.15	3.78	9.32	4	0.016	+/+	Y
twist gene homolog 1 (Drosophila)	Twist1	M63649	98028_at	P to A	0.73	0.04	0.02	0.09			+/+	
tyrosine 3-monooxygenase/tryptophan 5-monooxygenase activation	Ywhaq	AW215489	97061_g_at		0.99	1.41	1.12	1.96			-/-	
tyrosine kinase receptor 1	Tie1	AV235418	161184_f_at		0.85	0.24	0.16	0.39			+/+	
tyrosyl-tRNA synthetase	C77080	AW045507	160697_at		1.28	1.96	1.30	2.60			+/+	
U2 small nuclear ribonucleoprotein auxiliary factor (U2AF) 1	U2af1	AA693246	97486_at		1.93	2.17	1.82	3.48			+/+	
ubiquinol-cytochrome c reductase core protein 1	Uqcrc1	AW125380	101989_at		0.67	0.47	0.29	0.74			-/-	
ubiquitin specific protease 18	Usp18	AW047653	95024_at	A to P	0.92	5.66	2.51	13.93			+/+	
UDP glycosyltransferase 1 family, polypeptide A6	Ugt1a6	U16818	99580_s_at	P to A	0.64	0.12	0.09	0.26	3	0.000	+/+	
UDP-Gal:betaGlcNAc beta 1,3-galactosyltransferase, polypeptide 2	B3galt2	AF029791	92341_at	P to A	0.31	0.03	0.02	0.05			+/+	
UDP-Gal:betaGlcNAc beta 1,3-galactosyltransferase, polypeptide 3	B3galt3	AF029792	98960_s_at	P to A	0.51	0.11	0.06	0.21			+/+	
UDP-Gal:betaGlcNAc beta 1,4-galactosyltransferase, polypeptide 6	B4galt6	AW125314	102936_at		2.38	7.46	4.35	11.55	2	0.036	+/+	
UDP-N-acetyl-alpha-D-galactosamine:(N-acetylneuraminyl)-	Galgt1	U18975	103367_at		1.51	2.81	1.54	3.68			+/+	
UDP-N-acetyl-alpha-D-galactosamine:polypeptide N-	Galnt10	AW121380	102352_at		1.77	4.03	2.35	6.73			+/+	
UDP-N-acetyl-alpha-D-galactosamine:polypeptide N-	Galnt3	U70538	99011_at		2.12	7.16	4.56	12.13	2	0.030	+/+	
UDP-N-acetyl-alpha-D-galactosamine:polypeptide N-	Galnt3	AV055653	162313_f_at		2.02	5.13	2.33	8.11	4	0.030	+/+	
uncoupling protein 1, mitochondrial	Ucp1	AV294354	161422_f_at		0.58	0.19	0.13	0.32			+/+	
uncoupling protein 1, mitochondrial	Ucp1	M21247	99507_at	P to A	0.25	0.01	0.00	0.01			+/+	
uridine monophosphate kinase	Umpk	L31783	94381_at		0.58	0.51	0.37	0.68	3	0.010	+/+	
variable light chain		X88903	94725_f_at	P to A	0.54	0.22	0.12	0.53			+/+	
vascular cell adhesion molecule 1	Vcam1	U12884	92559_at	P to A	0.58	0.34	0.24	0.45			-/+	

Table II-1. Global ErbB2/Neu Mammary Tumor Molecular Signature. 818 genes were changed according to Affymetrix algorithms in all tumors compared to wild-type control mammary tissues.
Note: ESTs have been annotated from public database information as of 1/2004

Gene Name	Common	Genbank	Affymetrix	Absolute call*	Fold Change§				SOM Cl #†	p-value‡	Repeated Observation**	RT-PCR Confirmation§§
					ANvsWT	TUvsWT						
					Median	Median	Minimum	Max				
vascular endothelial growth factor B	Vegfb	U43836	103001_at		0.53	0.35	0.29	0.47			+/+	
v-erb-b2 erythroblastic leukemia viral oncogene homolog 3 (avian)	Erbb3	AI006228	96771_at		1.66	3.73	1.71	5.46	2	0.045	+/+	
V-erb-bt2 erythroblastic leukemia viral oncogene homolog 2,	1810046J19Rik	AI852571	94453_at		1.05	1.93	1.27	2.73		0.049	+/+	
vesicle-associated membrane protein 5	Vamp5	AF035643	92496_at	P to A	0.55	0.14	0.08	0.27			-/-	
villin 2	Vil2	X60671	100084_at		1.68	2.71	2.35	3.71	4	0.022	+/+	Y
vitamin D receptor	Vdr	AW061016	99964_at		1.71	1.89	1.39	2.36	2	0.039	-/+	
Von Willebrand factor homolog	Vwf	AI843063	103499_at	P to A	0.56	0.03	0.01	0.06	3	0.043	+/+	
WD-40-repeat-containing protein with a SOCS box 2	Wsb2-pending	AF033188	160296_at		1.24	1.73	1.59	2.11		0.005	+/+	
wee 1 homolog (S. pombe)	Wee1	D30743	101458_at		1.63	3.27	2.17	7.11	2	0.022	+/+	Y
WW domain binding protein 5	Wbp5	U92454	100523_r_at		1.67	2.99	1.73	4.89			+/+	
WW domain binding protein 5	Wbp5	U92454	100522_s_at		1.72	2.75	1.79	4.41	4	0.020	+/+	
xanthine dehydrogenase	Xdh	X75129	97950_at	A to P	12.90	13.45	7.36	47.84			+/+	
X-box binding protein 1	Xbp1	AW123880	94821_at		1.46	2.71	2.23	3.66		0.032	+/+	Y
zinc finger homeobox 1a	Zfhx1a	D76432	99052_at		0.72	0.31	0.15	0.53	1	0.024	+/+	Y
zinc finger protein 106	Zfp106	AW048037	95533_at		1.65	2.77	1.91	6.02			+/+	

* Absolute call is the Affymetrix parameter that measures detection. P=present A=absent. "A to P" indicates that a gene was called "absent" in control and "present" in tumor. If a gene changes from absent to present or vice versa, the fold change is irrelevant.

§ Fold change was derived from the Affymetrix signal log ratio (SLR). AN= adjacent *neu*, WT=wild-type control, and TU=tumor. The shaded areas denote <3.4 fold changed TuvsWT.

† "SOM CL #" = self-organizing map cluster number. Clusters are shown in Figure 3B.

‡ p-value was calculated for average tumor versus average control using Welch's t-test with the Benjamini and Hochberg Multiple Testing Correction (False Discovery Rate of 5%).

** Repeated observation indicates whether the gene was confirmed by microarray data from 2 additional independent tumor samples. "+/+" indicates confirmed by both tumors analyzed; "+/-" or "-/+" by one tumor; and "-/-" by neither tumor.

§§ Direction (increased/decreased) of expression confirmed by RealTime RT-PCR. "Y"=yes confirmed in 3 tumors, "2of3"= confirmed in 2 of 3 tumors,"1of3"= confirmed in 1 of 3 tumors "N"=not confirmed. If blank, then not assayed.

Table II-2. Filtered ErbB2/Neu Mammary Tumor Molecular Signature.

Gene Name	Common	Genbank	Affymetrix	Absolute call*	Fold Change§				SOM Cl #†	p-value‡	Repeated Observation**	RT-PCR Confirmation§§
					ANvsWT	TUvsWT						
					Median	Median	Minimum	Max				
	D2Ertd93e	C77278	97165_r_at	A to P	3.06	3.89	2.20	6.77	4	0.0236	+/+	
	Scp2-ps2	X87685	95787_s_at		0.55	0.41	0.23	0.73	3	0.0480	-/-	
	Adrb3; Adrb-3	X72862	92537_g_at	P to A	0.28	0.03	0.01	0.04	3	0.0410	+/+	
2,4-dienoyl CoA reductase 1, mitochondrial	Decr1	AI844846	160711_at		0.55	0.21	0.14	0.25	3	0.0480	+/+	
3-ketoacyl-CoA thiolase B	Acaa	AW012588	99571_at	P to A	0.51	0.25	0.11	0.32	3	0.0060	+/+	
3-monooxgenase/tryptophan 5-monooxgenase activation protein, gamma polypeptide	Ywhag	AW125041	95716_at		0.69	0.40	0.29	0.47		0.0122	+/+	
3'-phosphoadenosine 5'-phosphosulfate synthase 1	Papss1	U34883	93298_at		1.32	2.97	1.91	4.03	2	0.0404	+/+	
3'-phosphoadenosine 5'-phosphosulfate synthase 2	Papss2	AF052453	96713_at	P to A	0.71	0.22	0.12	0.43	1	0.0467	+/+	
A kinase (PRKA) anchor protein (gravin) 12	Akap12	AB020886	95022_at		1.03	2.48	2.16	4.44	2	0.0456	-/+	N
absent in melanoma 1		AA711704	103443_at		1.39	3.66	2.13	4.26	2	0.0186	+/+	
acetyl-Coenzyme A acyltransferase 2 (mitochondrial 3-oxoacyl-Coenzyme A thiolase)	0610011L04Rik	AI849271	95064_at		0.65	0.30	0.24	0.42	3	0.0050	+/+	
actin, alpha 2, smooth muscle, aorta	Acta2	X13297	93100_at		0.87	0.18	0.11	0.26	1	0.0031	+/+	
aldehyde dehydrogenase family 1, subfamily A7	Aldh1a7	U96401	94778_at	P to A	0.54	0.10	0.05	0.16	3	0.0050	+/+	
aldolase 3, C isoform	Aldo3	AW121134	160546_at		4.82	14.52	9.19	24.76	2	0.0230	+/+	
aminolevulinate, delta-, dehydratase	Alad	X13752	101044_at		0.57	0.26	0.14	0.32	3	0.0375	+/+	
aminolevulinic acid synthase 1	Alas1	M63245	93500_at		0.79	0.52	0.37	0.66		0.0208	+/-	
amyloid beta (A4) precursor-like protein 2	Aplp2	M97216	93498_s_at		0.64	0.41	0.28	0.53	3	0.0085	+/+	
angiopoietin-like 2	AW260363	AI840158	103556_at	P to A	0.75	0.12	0.08	0.24	1	0.0101	+/+	
ankyrin 3, epithelial	Ank3	L40632	98477_s_at	A to P	4.45	9.25	2.23	18.13	4	0.0233	+/+	Y
apolipoprotein A-I binding protein	AA087124	AI845103	94032_at		1.13	1.59	1.22	2.07		0.0227	+/+	
ATPase, H+ transporting, lysosomal accessory protein 2	5730403E06Rik	AI845108	160202_at		1.71	2.83	1.91	3.61	2	0.0267	+/+	
ATPase, H+ transporting, V1 subunit A, isoform 1	Atp6a1	AW123765	95746_at		1.21	2.60	2.16	3.29	2	0.0069	+/+	
ATPase, H+ transporting, V1 subunit A, isoform 1	Atp6a1; Atp6a2	U13837	95745_g_at		1.25	2.51	1.83	3.48	2	0.0225	+/+	
ATPase, H+ transporting, V1 subunit E isoform 1	Atp6e	U13841	94532_at		1.16	1.91	1.44	2.79	4	0.0317	+/+	
ATPase, Na+/K+ transporting, beta 3 polypeptide	Atp1b3	U59761	99579_at		0.75	0.48	0.41	0.62		0.0097	+/+	
AU RNA binding protein/enoyl-coenzyme A hydratase	Auh	AI837724	96650_at		0.73	0.57	0.45	0.67		0.0187	+/+	
BCL2/adenovirus E1B 19kDa-interacting protein 1, NIP2	Bnip2	AF035207	93064_at		0.79	0.45	0.33	0.55	3	0.0196	-/+	1of3
Bcl2-associated athanogene 2		W71352	160962_at		1.60	2.17	1.68	2.64		0.0085	+/+	
branched chain aminotransferase 2, mitochondrial	Bcat2	AF031467	100443_at		0.61	0.27	0.14	0.69	3	0.0403	+/+	
branched chain ketoacid dehydrogenase E1, beta polypeptide	Bckdhb	L16992	102302_at		0.59	0.33	0.28	0.47	3	0.0014	+/+	
calcium binding protein, intestinal	Cai	Y00884	95423_at		1.54	2.17	1.82	2.58	2	0.0070	+/+	
calmodulin 2	CaM	M27844	93293_at		1.05	1.78	1.45	2.23		0.0460	-/-	
calpain 12	Actn4	AI836968	96343_at		1.91	4.82	3.73	6.19	2	0.0234	+/+	
carboxylesterase 3	Ces3	AW226939	101538_i_at	P to A	0.37	0.00	0.00	0.01	3	0.0189	+/+	
carnitine palmitoyltransferase 2	Cpt2; CPTII; AI323697	U01170	95646_at		0.64	0.36	0.29	0.42	3	0.0083	+/+	
CASP2 and RIPK1 domain containing adaptor with death domain	Cradd	AJ224738	102952_g_at		1.24	2.41	1.89	3.25	2	0.0064	+/+	N
catenin src	Catns	Z17804	98151_s_at		1.22	2.69	1.68	4.79	2	0.0425	+/+	N
cathepsin C	Ctsc	U74683	101019_at		1.40	2.14	1.55	2.77	2	0.0317	+/+	
CD151 antigen	Peta3	AF033620	97930_f_at		0.77	0.59	0.50	0.74		0.0499	+/+	
CD34 antigen	Cd34	AI847784	160358_at	P to A	0.89	0.24	0.11	0.41	1	0.0123	+/+	
CD36 antigen	Cd36	L23108	93332_at	P to A	0.49	0.23	0.02	0.42	3	0.0306	+/+	
CD9 antigen	Cd9	L08115	95661_at		1.38	2.46	1.96	3.29		0.0098	+/+	
cDNA sequence BC004728		AW049551	94423_at		1.77	5.90	2.53	8.22	2	0.0401	+/+	
cDNA sequence BC011209		AW211793	160622_at	A to P	2.47	7.94	3.03	23.92	2	0.0289	+/+	
cDNA sequence BC037006	AU017197	AU017197	96518_at		1.96	4.86	2.58	7.16	2	0.0317	+/+	
cDNA sequence BC054059		AI118905	96237_at		0.65	0.19	0.08	0.45	3	0.0270	+/+	
cell division cycle 2 homolog A (S. pombe)	Cdc2a	M38724	100128_at		1.43	2.28	1.39	2.83	4	0.0289	+/-	
cell division cycle 34 homolog (S. cerevisiae)	AI327276	AW120683	94048_at		0.81	0.50	0.29	0.75	3	0.0295	+/+	
checkpoint kinase 1 homolog (S. pombe)	Chek1	AF016583	103064_at		1.38	2.04	1.51	2.85	4	0.0356	-/+	Y
chemokine (C-X-C motif) ligand 1	Gro1	J04596	95348_at	A to P	2.92	5.94	2.95	30.48	4	0.0343	+/+	

Table II-2. Filtered ErbB2/Neu Mammary Tumor Molecular Signature.

Gene Name	Common	Genbank	Affymetrix	Absolute call*	Fold Change§				SOM Cl #†	p-value‡	Repeated Observation**	RT-PCR Confirmation§§
					ANvsWT	TUvsWT						
					Median	Median	Minimum	Max				
chemokine (C-X-C motif) ligand 12	Sdf1	L12030	100112_at	P to A	0.61	0.29	0.19	0.35	3	0.0208	+/+	
chemokine (C-X-C motif) ligand 12	Sdf1	AV139913	162234_f_at	P to A	0.58	0.12	0.05	0.32	3	0.0008	+/+	
chloride intracellular channel 1		AF109905	95654_at		1.39	1.77	1.56	2.57		0.0467	+/+	
claudin 3	Cldn3	AF095905	94493_at		1.90	3.61	1.78	4.50	2	0.0408	+/+	Y
claudin 3	Cldn3	AV057837	162315_f_at	A to P	1.72	2.99	1.83	4.63	4	0.0493	+/+	Y
claudin 7	Cldn7	AF087825	99561_f_at		2.02	3.71	2.77	5.06	2	0.0349	+/+	Y
coagulation factor III	F3	M26071	97689_at		1.17	3.56	2.23	5.66	2	0.0242	+/+	
crystallin, alpha C	Cryac	AI848798	160139_at	P to A	0.69	0.26	0.16	0.34	3	0.0378	+/+	Y
C-terminal binding protein 2		AW120820	160979_at		1.98	3.84	2.20	5.58	2	0.0428	+/+	
C-terminal binding protein 2	Ctbp2	AF059735	92554_at		1.33	2.73	2.22	3.53	2	0.0289	+/+	Y
cyclin D1	Ccnd1	M64403	94231_at	A to P	2.11	2.93	2.23	4.23	2	0.0394	+/+	Y
cysteine and glycine-rich protein 1	Csrp	D88793	92608_at		3.79	4.92	1.92	11.47	2	0.0267	+/+	
cysteine and glycine-rich protein 1	Csrp	AI837625	160065_s_at		3.45	4.76	1.89	7.67	2	0.0234	+/+	
cysteine-rich protein 1 (intestinal)	Crip	M13018	94061_at		0.88	0.15	0.07	0.48	1	0.0208	+/+	
cytidine monophospho-N-acetylneuraminic acid synthetase	Cmas	AJ006215	98593_at		1.71	4.66	3.12	6.28	2	0.0050	+/+	
cytochrome b-5	0610009N12Rik	AI854779	98533_at		0.69	0.44	0.32	0.50		0.0121	+/+	
cytochrome b-561	Cyb561	AI846517	103423_at		1.39	2.35	1.95	3.51	4	0.0248	+/+	
cytochrome c oxidase, subunit VIIIb	Cox8b	AV260484	161205_at	P to A	0.52	0.10	0.06	0.26	3	0.0394	+/+	
cytochrome P450, family 4, subfamily b, polypeptide 1	Cyp4b1	D50834	103353_f_at	P to A	0.70	0.28	0.11	0.34	1	0.0421	+/+	
cytochrome P450, family 4, subfamily b, polypeptide 1	Cyp4b1	AV376161	162044_f_at	P to A	0.86	0.07	0.02	0.36	1	0.0050	+/+	
DEAD (Asp-Glu-Ala-Asp) box polypeptide 6	Ddx6	AF038995	93965_r_at	A to P	1.82	4.50	2.58	10.56	4	0.0362	-/-	Y
death-associated protein	4921531N22Rik	AI196645	93842_at		1.29	2.11	1.79	2.71		0.0083	+/+	
deoxycytidine kinase	Dck	X77731	98071_f_at		1.61	4.11	2.93	4.59	2	0.0133	+/+	
dermatopontin	Dpt	AA717826	96742_at		0.68	0.09	0.03	0.16	3	0.0064	+/+	Y
desmoglein 2	AA408168	AI152659	104480_at		4.11	6.11	2.75	13.00	4	0.0049	+/+	
diacylglycerol O-acyltransferase 1	Dgat1	AF078752	104371_at		0.45	0.13	0.08	0.16	3	0.0378	+/+	
differentially expressed in B16F10 1	1110020I04Rik	AW124231	95478_at		1.27	2.33	1.45	3.29	4	0.0437	+/+	
dipeptidase 1 (renal)	Dpep1	D13139	103644_at	P to A	0.62	0.05	0.01	0.20	3	0.0368	+/+	
DNA segment, Chr 3, University of California at Los Angeles 1	D3Ucla1	AI843466	95708_at		1.82	2.58	2.04	3.66	4	0.0070	+/+	
DnaJ (Hsp40) homolog, subfamily C, member 8	Dnajc8	AI848094	95699_f_at		0.80	0.57	0.43	0.67		0.0187	-/+	
downstream of tyrosine kinase 1	Dok1	U78818	102896_at	A to P	4.89	8.51	2.06	15.56	2	0.0208	+/+	Y
dual specificity phosphatase 6	Dusp6	AI845584	93285_at		3.07	10.41	8.57	13.64	2	0.0060	+/+	
electron transferring flavoprotein, beta polypeptide	0610009I16Rik	AW046273	96947_at		0.50	0.24	0.19	0.33	3	0.0445	+/+	
elongation factor RNA polymerase II 2	Ell2	AI197161	103892_r_at		1.27	2.30	1.66	3.23	4	0.0456	+/+	Y
enabled homolog (Drosophila)	Enah	D10727	100472_at	A to P	2.67	7.36	5.28	10.41	2	0.0133	+/+	Y
epoxide hydrolase 2, cytoplasmic	Ephx2	Z37107	93051_at		0.49	0.13	0.07	0.23	3	0.0437	+/+	
ets homologous factor	Ehf	AF035527	102243_at	A to P	2.07	3.92	2.43	7.11	2	0.0490	+/+	Y
ets variant gene 1	Etv1	L10426	92927_at	A to P	5.54	34.06	19.56	55.33	2	0.0187	+/+	Y
eukaryotic translation initiation factor 4E binding protein 1	Eif4ebp1	U28656	100636_at		0.52	0.35	0.22	0.39	3	0.0178	+/+	
expressed sequence AA407659		AW048552	104434_at		1.03	1.61	1.24	2.23		0.0345	+/+	
expressed sequence C77080	C77080	AV232292	161696_f_at		1.44	2.58	1.77	3.71	2	0.0375	-/+	
extracellular proteinase inhibitor	Expi	X93037	103051_at		2.79	3.58	2.97	6.77		0.0352	+/+	Y
F11 receptor	Jcam1	U89915	103816_at		1.05	1.96	1.39	2.58	2	0.0289	+/+	
faciogenital dysplasia homolog (human)	Fgd1	U22325	93674_at	A to P	2.65	4.92	2.81	19.97	4	0.0297	+/+	
fasciculation and elongation protein zeta 2 (zygin II)	D17Ertd315e	AI851119	101934_at	P to A	0.97	0.47	0.26	0.63	1	0.0227	+/+	
fat specific gene 27	Fsp27	M61737	102016_at	P to A	0.49	0.00	0.00	0.01	3	0.0382	+/+	
fatty acid Coenzyme A ligase, long chain 2	Facl2	U15977	94507_at		0.51	0.13	0.11	0.19	3	0.0330	+/+	
fatty acid-Coenzyme A ligase, long chain 4	AU018108	AA619207	102381_at		5.74	19.43	11.96	31.56	2	0.0210	+/+	
F-box and WD-40 domain protein 7, archipelago homolog (Drosophila)		AW120511	93667_at		1.57	2.85	1.61	7.36	4	0.0357	+/+	Y
filamin, beta	AL024016	AI838592	95637_at		1.60	3.71	2.69	5.50	2	0.0181	+/+	
folate receptor 1 (adult)	Folr1	AV035020	162302_f_at	A to P	2.18	3.66	3.10	9.19	4	0.0098	+/+	

Table II-2. Filtered ErbB2/Neu Mammary Tumor Molecular Signature.

Gene Name	Common	Genbank	Affymetrix	Absolute call*	Fold Change§				SOM Cl # †	p-value‡	Repeated Observation**	RT-PCR Confirmation§§
					ANvsWT	TUvsWT						
					Median	Median	Minimum	Max				
follistatin-like	Fstl	M91380	94833_at		1.16	0.36	0.24	0.61	1	0.0124	-/+	Y
frizzled homolog 4 (Drosophila)	Fzd4	U43317	95771_i_at	P to A	0.52	0.05	0.02	0.34	3	0.0343	+/+	Y
fucosyltransferase 8	Fut8	AB025198	98143_at		1.40	3.34	1.79	4.23	2	0.0344	+/+	
FXYD domain-containing ion transport regulator 3	Fxyd3	X93038	103059_at		1.64	3.81	3.03	5.58	2	0.0308	+/+	Y
gap junction membrane channel protein alpha 1	Gja1	M63801	100064_f_at		0.81	0.15	0.09	0.46	1	0.0102	+/+	Y
gap junction membrane channel protein beta 2	Cx26	M81445	98423_at		0.97	0.27	0.13	0.51	1	0.0102	+/+	N
glucan (1,4-alpha-), branching enzyme 1	Gbe1	AW210370	96803_at		0.46	0.27	0.14	0.32	3	0.0257	+/+	
glutathione peroxidase 3	Gpx3	U13705	101676_at		0.33	0.04	0.02	0.08	3	0.0001	+/+	
glutathione transferase zeta 1 (maleylacetoacetate isomerase)	Gstz1	AW060750	160350_at		0.56	0.14	0.10	0.19	3	0.0301	+/+	
glycerol phosphate dehydrogenase 2, mitochondrial	Gdm1	D50430	98984_f_at		0.57	0.20	0.11	0.28	3	0.0001	+/+	
glycerol-3-phosphate acyltransferase, mitochondrial	Gpam; GPAT	U11680	101867_at		0.38	0.17	0.13	0.19	3	0.0028	+/+	
glycerol-3-phosphate dehydrogenase 1 (soluble)	Gdc1	AV290060	161753_f_at	P to A	0.65	0.08	0.04	0.17	1	0.0479	+/+	
glycogenin 1	Gyg1	AW049730	100597_at		0.51	0.31	0.22	0.44	3	0.0049	+/+	
golgi phosphoprotein 3	Golph3	AW060175	160688_at		1.36	2.25	1.48	3.05		0.0098	+/+	
growth arrest specific 6	Gas6	X59846	99067_at		0.86	0.31	0.16	0.59	3	0.0267	+/+	2of3
growth hormone receptor	Ghr	U15012	99108_s_at		0.36	0.07	0.05	0.10	3	0.0317	+/+	Y
guanine nucleotide binding protein, alpha inhibiting 1	Gnai1	AI153412	104412_at	P to A	0.38	0.02	0.01	0.05	3	0.0364	+/+	
hephaestin	Heph	AF082567	104194_at		0.40	0.16	0.09	0.32	1	0.0097	+/+	
hexose-6-phosphate dehydrogenase (glucose 1-dehydrogenase)	AI785303	AA939571	104148_at		0.67	0.46	0.30	0.67	1	0.0359	+/+	
histocompatibility 2, class II antigen A, alpha	H2-Aa	X52643	92866_at		0.94	0.46	0.16	0.71	3	0.0330	+/+	
homer homolog 2 (Drosophila)	Homer2-pending	AF093259	160695_i_at	A to P	2.63	7.16	3.63	13.36	4	0.0276	+/+	
hydroxyacyl-Coenzyme A dehydrogenase/3-ketoacyl-Coenzyme A thiolase/enoyl-Coenzyme A hydratase (trifunctional protein), beta subunit	AW122615	96913_at		0.45	0.17	0.15	0.21	3	0.0365	+/+	
hypothetical protein 6330505N24		AI430272	104207_at		1.54	2.99	2.39	4.32	2	0.0050	+/+	
hypothetical protein B230364F10		AI536457	103321_at		1.30	1.71	1.52	2.58		0.0295	+/+	
hypothetical protein MGC18837	Rab3d	AI835706	95442_at		0.76	0.57	0.52	0.70		0.0170	-/+	
immediate early response 2	Ier2	M59821	99109_at		1.46	2.38	1.83	2.91	2	0.0295	+/+	
immediate early response 3	Ier3	X67644	94384_at		3.03	14.93	9.85	22.78	2	0.0481	+/+	Y
immediate early response 5	Ier5	AF079528	92773_at		0.99	0.34	0.24	0.56	1	0.0289	+/+	N
immediate early response, erythropoietin 4	Ierepo4-pending	AW125150	160251_at		1.15	1.54	1.27	1.87		0.0397	+/+	
immunoglobulin joining chain	Igj	M90766	102372_at		0.60	0.10	0.07	0.17	3	0.0470	+/+	
inactive X specific transcripts	Xist	L04961	99126_at		2.05	11.31	4.59	28.05	2	0.0467	+/+	
inhibitor of DNA binding 2	helix-loop-helix protein Id2	AF077861	93013_at		2.07	3.73	2.48	6.36	4	0.0462	+/+	Y
inositol 1,4,5-triphosphate receptor 5	Itpr2	AF031127	101441_i_at		1.95	4.69	2.95	10.20	2	0.0085	+/+	Y
inositol polyphosphate phosphatase-like 1	Inppl1	U92477	102988_at	A to P	1.71	2.07	1.58	2.41		0.0234	+/+	
insulin-like growth factor 2 receptor	Igf2r	U04710	95117_at		1.34	2.45	1.75	3.46		0.0099	+/+	Y
insulin-like growth factor binding protein 6	Igfbp6	X81584	103904_at	P to A	0.62	0.04	0.03	0.12	1	0.0230	+/+	Y
interferon regulatory factor 6	Irf6	U73029	92440_at		1.35	2.79	2.03	4.06	2	0.0357	+/+	Y
interleukin 25	Il25	AW045739	96318_at		1.37	1.69	1.54	2.23		0.0050	+/+	
Iroquois related homeobox 3 (Drosophila)	Irx3	Y15001	99034_at		1.48	2.31	1.47	3.53	4	0.0267	+/+	Y
isocitrate dehydrogenase 1 (NADP+), soluble	Idh1	AF020039	160571_at		0.70	0.41	0.32	0.67	3	0.0153	-/+	
isocitrate dehydrogenase 2 (NADP+), mitochondrial	Idh2	U51167	95693_at		0.73	0.43	0.25	0.63	3	0.0499	+/+	
isovaleryl coenzyme A dehydrogenase	Ivd	AW047743	104153_at		0.57	0.36	0.26	0.44	3	0.0320	+/+	
kangai 1 (suppression of tumorigenicity 6, prostate)	Kai1	D14883	99584_at		2.31	3.10	1.96	4.14	4	0.0133	+/+	
keratin complex 1, acidic, gene 19	keratin 19	M36120	92550_at	P to A	0.91	0.00	0.00	0.17	1	0.0485	+/+	
keratin complex 1, acidic, gene 19	Krt1-19	AU040563	102121_f_at	P to A	1.18	0.04	0.02	0.09	1	0.0423	+/+	Y
keratin complex 2, basic, gene 8	Krt2-8; K8; EndoA; Krt-2.8; AA960620; AL022697; AU019895	X15662	101009_at		1.27	1.73	1.30	2.62		0.0365	+/+	
Kruppel-like factor 4 (gut)	Klf4	U20344	99622_at		0.69	0.23	0.19	0.44	3	0.0028	+/+	Y

Table II-2. Filtered ErbB2/Neu Mammary Tumor Molecular Signature.

Gene Name	Common	Genbank	Affymetrix	Absolute call*	Fold Change§				SOM Cl #†	p-value‡	Repeated Observation**	RT-PCR Confirmation§§
					ANvsWT	TUvsWT						
					Median	Median	Minimum	Max				
L-3-hydroxyacyl-Coenzyme A dehydrogenase, short chain	Hadhsc	D29639	95485_at		0.71	0.45	0.39	0.58	3	0.0049	+/+	
laminin B1 subunit 1	Lamb1-1	X05212	101948_at		0.67	0.24	0.14	0.41	1	0.0178	+/+	
latexin	Lxn	D88769	96065_at		1.71	3.41	2.33	3.84	2	0.0085	+/+	
lectin, mannose-binding, 1	Lman1	AW108371	160270_at		1.38	2.51	1.65	3.27	2	0.0365	+/+	
leucine rich repeat (in FLII) interacting protein 1	AU024550	AI891475	92564_at		1.83	3.92	2.17	6.73	4	0.0343	+/+	
ligase III, DNA, ATP-dependent	Lig3	U66058	102803_at		1.31	2.19	1.55	2.58	4	0.0252	+/+	Y
LIM domain only 4	Lmo4	AF074600	98122_at		2.00	4.56	2.46	8.00	2	0.0425	+/+	Y
lipin 1	Lpin1	AI846934	98892_at		0.46	0.18	0.11	0.24	3	0.0219	+/+	
lipocalin 2	24p3	X81627	160564_at		2.68	6.92	4.35	9.65		0.0111	+/+	
liver-specific bHLH-Zip transcription factor	Lisch7-pending	U49507	99452_at		1.57	2.06	1.71	2.89	2	0.0445	+/+	Y
LPS-induced TN factor	Litaf-pending	AI852632	93753_at		1.38	2.57	1.97	3.63	2	0.0333	+/+	
lumican	Ldc	AF013262	93353_at		0.90	0.07	0.03	0.20	1	0.0095	+/+	
lymphoblastomic leukemia	Lyl1	X57687	100468_g_at		0.86	0.31	0.25	0.51	1	0.0124	+/+	2of3
lymphocyte antigen 6 complex, locus A	Ly6a	X04653	93078_at		0.93	0.19	0.09	0.66	1	0.0210	+/+	
manic fringe homolog (Drosophila)	Mfng	AF015769	100508_at		0.68	0.31	0.25	0.40	3	0.0245	+/+	Y
mannose receptor, C type 1	Mrc1	Z11974	103226_at		1.07	0.21	0.16	0.36	1	0.0387	+/+	
mannosidase 1, alpha	Man1a	AI021125	160579_at	P to A	0.95	0.13	0.02	0.39	1	0.0375	+/+	
MAP kinase-interacting serine/threonine kinase 2	Gprk7	AI845732	101007_at		0.61	0.29	0.17	0.43	3	0.0499	+/+	
matrix metalloproteinase 3	Mmp3	X66402	98833_at		0.98	0.08	0.01	0.45	1	0.0179	+/+	Y
methylcrotonoyl-Coenzyme A carboxylase 1 (alpha)	Mccc1	AW123316	94940_at		0.46	0.26	0.18	0.37	3	0.0350	+/+	
methylmalonyl-Coenzyme A mutase	Mut	X51941	99613_at		0.74	0.53	0.40	0.68	3	0.0104	+/+	
microtubule-associated protein 4	Mtap4	M72414	92795_at		0.77	0.47	0.30	0.57	3	0.0141	+/+	2of3
mitogen activated protein kinase 8 interacting protein	Mapk8ip	AF003115	104170_at	A to P	1.78	2.60	1.58	4.00	4	0.0428	+/+	
molybdenum cofactor synthesis 2	Mocs2	AW060325	160637_at		0.81	0.28	0.18	0.40	1	0.0365	+/+	
Mus musculus adult female vagina cDNA, RIKEN full-length enriched library, clone:9930031C03 product:beta-spectrin 2, non-erythrocytic, full insert sequence	Spnb-2	M74773	93571_at		0.75	0.65	0.54	0.80		0.0229	+/+	
Mus musculus transcribed sequences	AW112010	AA958903	100944_at		0.77	0.23	0.09	0.57	1	0.0201	+/+	
Mus musculus transcribed sequences	Npnt	AA592182	103721_at	A to P	6.83	49.87	23.26	93.70	2	0.0419	+/+	Y
Mus musculus, Similar to protein kinase, lysine deficient 1, clone IMAGE:4193361, mRNA, partial cds	1810073P09Rik	AW124781	95952_at	A to P	1.94	3.20	1.73	4.76	4	0.0187	-/+	
mutL homolog 1 (E. coli)	Mlh1	AA920621	104577_at		1.67	2.23	1.58	2.97		0.0267	+/+	
myosin, light polypeptide 9, regulatory	Trrp2	AI842649	96939_at		0.79	0.40	0.23	0.54	1	0.0186	+/+	
myristoylated alanine rich protein kinase C substrate	Macs	M60474	96865_at		0.90	0.35	0.27	0.50	3	0.0087	+/+	
NADH dehydrogenase (ubiquinone) 1, alpha/beta subcomplex, 1	2310039H15Rik	AI849803	96909_at		0.62	0.53	0.34	0.60	3	0.0155	+/+	
NADH dehydrogenase (ubiquinone) Fe-S protein 5	AI256693	AI852355	99593_at		0.74	0.61	0.51	0.76		0.0397	-/-	
NADH dehydrogenase (ubiquinone) flavoprotein 1	Ndufv1	AI846127	96267_at		0.68	0.48	0.42	0.62		0.0234	+/+	
neuroepithelial cell transforming gene 1	Net1	AJ010045	94223_at		0.68	0.39	0.25	0.56		0.0155	+/+	N
neuropilin	Nrp	D50086	95016_at		0.82	0.18	0.13	0.31	3	0.0038	+/+	
Niemann Pick type C2	Npc2	AB021289	160344_at		0.60	0.54	0.44	0.63		0.0189	+/+	
nuclear receptor subfamily 1, group H, member 3	Nr1h3	AF085745	104381_at	P to A	0.57	0.10	0.08	0.13	3	0.0390	+/+	Y
nuclear receptor subfamily 4, group A, member 1	N10	X16995	102371_at	A to P	1.56	3.51	2.06	6.06	2	0.0404	+/+	
nucleobindin 2	Nucb2	AJ222586	102197_at		2.59	6.32	2.75	11.47	2	0.0375	+/+	
osteoblast specific factor 2 (fasciclin I-like)	Osf2-pending	D13664	92593_at		1.11	0.15	0.08	0.54	1	0.0235	+/+	Y
p53 apoptosis effector related to Pmp22	Perp-pending	AI854029	97825_at		1.86	4.03	3.14	4.63	2	0.0097	+/+	Y
phenylalkylamine Ca2+ antagonist (emopamil) binding protein	Ebp	X97755	96627_at		1.16	1.65	1.31	1.93		0.0408	+/+	
phosphatidic acid phosphatase 2a	Ppap2a	D84376	98508_s_at	P to A	0.62	0.32	0.05	0.48	3	0.0148	+/-	
phosphodiesterase 8A	Pde8a	AF067806	160941_at	P to A	0.82	0.19	0.09	0.30	1	0.0050	+/+	Y
phosphoglucomutase 2	2610020G18Rik	AI842432	104313_at		0.52	0.29	0.23	0.33	3	0.0062	+/+	
phytanoyl-CoA hydroxylase	Phyh	AF023463	96608_at		0.72	0.44	0.28	0.73	3	0.0097	+/+	
placenta-specific 8		AA790307	98092_at		0.93	0.33	0.17	0.54	1	0.0396	+/+	

Table II-2. Filtered ErbB2/Neu Mammary Tumor Molecular Signature.

Gene Name	Common	Genbank	Affymetrix	Absolute call*	Fold Change§				SOM Cl #†	p-value‡	Repeated Observation**	RT-PCR Confirmation§§
					ANvsWT	TUvsWT						
					Median	Median	Minimum	Max				
potassium intermediate/small conductance calcium-activated channel, subfamily N, member 4	Kcnn4	AF042487	102198_at		2.98	10.06	5.62	13.18	2	0.0306	+/+	
preproenkephalin 1	Penk1; ENK; PPA; AI326464	M55181	94516_f_at		0.56	0.20	0.08	0.26	3	0.0098	+/+	
procollagen, type I, alpha 1	Col1a1	U03419	94305_at		0.93	0.25	0.16	0.64	1	0.0431	+/+	
procollagen, type III, alpha 1	Col3a1	AA655199	102990_at		1.05	0.14	0.10	0.46	1	0.0100	+/+	
procollagen, type IV, alpha 1	Col4a1	M15832	101093_at		0.81	0.47	0.33	0.68	3	0.0187	+/+	
procollagen, type V, alpha 1	AI413331	AA796989	93472_at		0.89	0.50	0.37	0.75	1	0.0464	+/+	
procollagen, type VI, alpha 1	Col6a1	AV010209	162459_f_at	P to A	1.09	0.24	0.13	0.57	1	0.0350	+/+	Y
procollagen, type VI, alpha 3	Col6a3	AF064749	101110_at		0.60	0.17	0.13	0.36	3	0.0088	+/+	
procollagen, type XVIII, alpha 1	Col18a1	L22545	101881_g_at	P to A	0.68	0.07	0.05	0.21	3	0.0193	+/+	2of3
progressive ankylosis	ank	AW049351	100948_at		0.95	1.85	1.39	2.51	2	0.0402	+/+	
properdin factor, complement	Pfc	X12905	101468_at	P to A	1.11	0.21	0.14	0.55	1	0.0456	+/+	
prostaglandin E synthase	Ptges	AI060798	104406_at	P to A	0.71	0.08	0.02	0.18	1	0.0097	+/+	
protease, serine, 11 (Igf binding)	Prss11	AW125478	96920_at		0.54	0.08	0.04	0.16	3	0.0001	+/+	Y
protein phosphatase 1, catalytic subunit, beta isoform	Ppp1cb	M27073	100088_at		1.59	2.36	1.39	3.66	4	0.0447	+/+	
protein phosphatase 2, regulatory subunit B (B56), alpha isoform		AI956230	93826_at		0.57	0.16	0.11	0.20	3	0.0409	+/+	Y
protein phosphatase 3, catalytic subunit, alpha isoform	Ppp3ca	J05479	95092_at		1.79	3.39	1.91	5.28	4	0.0466	+/+	
protein tyrosine phosphatase, non-receptor type 2	Ptpn2	M80739	101996_at		1.40	2.97	1.92	5.86	2	0.0267	+/+	2of3
protein tyrosine phosphatase, receptor type, B	Ptprb	X58289	92289_at	P to A	0.37	0.04	0.03	0.06	3	0.0308	+/+	Y
PTK7 protein tyrosine kinase 7	8430404F20Rik	AI326889	92325_at	A to P	3.96	4.86	2.28	12.30	4	0.0201	+/+	
pyruvate dehydrogenase E1 alpha 1	Pdha1	M76727	98102_at		0.61	0.43	0.34	0.52	3	0.0339	+/+	
quaking	qk	U44940	160726_at		0.70	0.19	0.12	0.30	1	0.0111	+/+	
RAB10, member RAS oncogene family	AW107754	AI841543	160149_at		1.60	2.60	1.80	4.06	4	0.0357	+/+	
RAB18, member RAS oncogene family	Rab18	L04966	94319_at		1.16	1.75	1.46	2.14		0.0052	+/+	2of3
RAB34, member of RAS oncogene family	Rab34	AI835712	160317_at	P to A	0.52	0.33	0.11	0.38	3	0.0345	+/+	Y
Ras-related GTP binding C	Gtr2	AB017616	98950_at		0.72	0.55	0.38	0.66		0.0196	-/-	
reticulocalbin 2	Rcn2	AF049125	93281_at		1.33	3.18	2.30	5.28	4	0.0233	+/+	
Rho guanine nucleotide exchange factor (GEF) 5	Arhgef5	AA726063	160977_at		1.40	2.19	1.84	2.87	2	0.0226	+/+	
rhotekin	Rtkn	U54638	160864_at		1.53	1.92	1.53	2.91	4	0.0273	+/+	
ribonucleotide reductase M2	Rrm2	M14223	102001_at		1.75	2.93	1.79	3.48	4	0.0130	+/+	Y
RIKEN cDNA 0610010O12 gene	0610010O12Rik	AI849011	97242_at		1.45	2.93	2.25	4.14	2	0.0187	+/+	
RIKEN cDNA 0710001O03 gene	0710001O03Rik	AI853364	160391_at		0.84	0.31	0.15	0.61	1	0.0308	+/+	
RIKEN cDNA 1110001I14 gene	AI115388	AW047554	104605_at		0.45	0.26	0.18	0.38	3	0.0013	+/+	
RIKEN cDNA 1110004P15 gene	AA589382	AA657044	160255_at		0.69	0.19	0.10	0.43	1	0.0187	+/+	
RIKEN cDNA 1110015E22 gene	1110015E22Rik	AW045753	104217_at		0.62	0.11	0.08	0.67	3	0.0387	-/-	
RIKEN cDNA 1110020B03 gene	AI851387	AI851387	102922_at		1.18	2.53	1.88	3.53	2	0.0128	+/+	
RIKEN cDNA 1110020P15 gene		AW046239	94078_at		0.78	0.59	0.41	0.69	3	0.0193	+/+	
RIKEN cDNA 1110021N07 gene	AI195141	AI846382	93983_at	P to A	0.58	0.38	0.29	0.45	3	0.0084	+/+	
RIKEN cDNA 1110032O19 gene	AI430822	AI853294	97386_at		0.57	0.30	0.16	0.42	3	0.0100	+/+	
RIKEN cDNA 1190006E07 gene	1190006E07Rik	AI852865	160112_at		1.39	2.30	1.95	3.05	4	0.0185	+/+	
RIKEN cDNA 1200002G13 gene	1200002G13Rik	AW120643	96708_at		1.42	1.93	1.43	2.20	2	0.0403	+/+	
RIKEN cDNA 1200015A22 gene	1200015A22Rik	AI854863	98633_at	P to A	0.44	0.24	0.18	0.31	3	0.0085	+/+	
RIKEN cDNA 1200015G06 gene	1200015G06Rik	AI844370	93590_at		2.28	2.77	1.87	4.20	2	0.0056	+/+	
RIKEN cDNA 1300002F13 gene	1300002F13Rik	AI853531	93975_at		1.43	3.51	2.41	4.79	2	0.0155	+/+	
RIKEN cDNA 1300003D03 gene	1300003D03Rik	AA871791	102052_at		0.65	0.40	0.19	0.76	3	0.0407	+/+	
RIKEN cDNA 1600029D21 gene	1600029D21Rik	AI121305	97413_at		4.19	8.63	3.92	16.80	4	0.0403	+/+	
RIKEN cDNA 1620401E04 gene	Als2	AW125480	96900_at		0.66	0.49	0.35	0.70	3	0.0085	+/+	
RIKEN cDNA 1700051C09 gene	Becn1	AV260411	161227_r_at		2.92	5.21	3.51	7.11	4	0.0252	+/+	
RIKEN cDNA 1810015C04 gene	1810015C04Rik	AW122893	95518_at		1.68	3.53	2.39	4.53	2	0.0133	+/+	
RIKEN cDNA 1810044O22 gene	1810044O22Rik	AI850017	103619_at		0.62	0.24	0.18	0.32	3	0.0434	+/+	
RIKEN cDNA 1810046J19 gene	1810046J19Rik	AI852571	94453_at		1.05	1.93	1.27	2.73		0.0494	+/+	

Table II-2. Filtered ErbB2/Neu Mammary Tumor Molecular Signature.

Gene Name	Common	Genbank	Affymetrix	Absolute call*	Fold Change§				SOM Cl #†	p-value‡	Repeated Observation**	RT-PCR Confirmation§§
					ANvsWT	TUvsWT						
					Median	Median	Minimum	Max				
RIKEN cDNA 2310008H09 gene	2310008H09Rik	AF034580	160872_f_at		1.61	2.43	1.79	3.78	4	0.0241	+/+	
RIKEN cDNA 2310009N05 gene	2310009N05Rik	AW061073	160801_at		1.59	3.10	2.04	3.51	2	0.0189	+/+	
RIKEN cDNA 2310016E22 gene	2310016E22Rik	AW120882	95620_at		0.69	0.54	0.34	0.74		0.0289	+/+	
RIKEN cDNA 2310020A21 gene	2310020A21Rik	AI173973	100043_f_at	A to P	1.88	2.81	1.42	4.72	4	0.0465	+/-	
RIKEN cDNA 2400004O09 gene	2400004O09Rik	AI846893	160991_at		0.55	0.40	0.31	0.60	3	0.0375	+/+	
RIKEN cDNA 2610001E17 gene	2610001E17Rik	AW122012	160298_at		0.59	0.08	0.05	0.22	1	0.0394	+/+	
RIKEN cDNA 2610042L04 gene	2610042L04Rik	AI853444	93568_i_at	P to A	1.26	0.08	0.01	0.28	1	0.0056	+/+	
RIKEN cDNA 3110001A13 gene	3110001A13Rik	AI644158	96640_at	P to A	1.02	0.44	0.30	0.61	1	0.0187	+/+	
RIKEN cDNA 3110003A17 gene	3110003A17Rik	AA833425	96135_at		1.70	2.31	1.65	3.01	4	0.0161	+/+	
RIKEN cDNA 4921515A04 gene	AI874685	AI642098	104494_at		0.53	0.33	0.15	0.54	3	0.0083	+/+	
RIKEN cDNA 4930555L11 gene	AI195356	AI853226	160393_at		1.89	7.11	4.99	10.20	2	0.0195	+/+	
RIKEN cDNA 4931406C07 gene	4931406C07Rik	AI255972	96090_g_at		1.21	2.66	1.89	3.39	2	0.0279	+/+	
RIKEN cDNA 5730551F12 gene	0610012C09Rik	AW125340	160193_at		1.28	1.77	1.57	2.03		0.0190	+/+	
RIKEN cDNA 6330514M23 gene	3110015B12Rik	AW048944	97496_f_at		0.63	0.16	0.09	0.51	1	0.0197	+/+	
RIKEN cDNA 9630044O09 gene		AI835624	160236_at	A to P	3.04	6.28	2.69	30.27	2	0.0187	+/+	
RIKEN cDNA A430096B05 gene		AI465965	97826_at		0.60	0.05	0.03	0.13	3	0.0119	+/+	
RIKEN cDNA C330027C09 gene	AA408511	AA590345	160973_at		1.51	2.31	1.58	3.27	4	0.0420	+/+	
RIKEN cDNA D330037A14 gene		AI854506	96206_at	P to A	0.69	0.25	0.18	0.49	1	0.0050	+/+	
ring finger protein 149	1600023E10Rik	AI849082	98915_at		1.31	1.66	1.47	1.91		0.0128	-/+	
S100 calcium binding protein A6 (calcyclin)	S100a6	X66449	92770_at		0.90	0.27	0.12	0.71	1	0.0445	+/+	
SEC23A (S. cerevisiae)	Sec23a	AI843665	104709_at		0.73	0.57	0.45	0.75		0.0394	-/-	
serine protease inhibitor, Kunitz type 1	Spint1	AW230369	97206_at		1.71	3.43	2.93	5.10	2	0.0375	+/+	Y
serine/threonine kinase 39, STE20/SPS1 homolog (yeast)	Stk39	AF099988	160806_at		1.76	5.70	2.91	9.65	2	0.0382	+/+	Y
serum deprivation response	Sdpr	AI839175	160373_i_at		0.54	0.18	0.13	0.45	3	0.0062	+/+	Y
shroom	shrm	AI641895	100024_at		2.19	4.92	2.79	9.78	4	0.0197	+/+	Y
sialyltransferase 10 (alpha-2,3-sialyltransferase VI)	Siat10	AI153959	102208_at	P to A	0.48	0.18	0.11	0.30	3	0.0415	+/+	
sialyltransferase 7 ((alpha-N-acetylneuraminyl 2,3-betagalactosyl-1,3)-N-acetyl galactosaminide alpha-2,6-sialyltransferase) D	ST6GalNAc IV	Y15780	96682_at	A to P	2.53	9.99	2.85	20.68	2	0.0419	+/+	
sialyltransferase 9 (CMP-NeuAc:lactosylceramide alpha-2,3-sialyltransferase)	ST3Gal V	Y15003	98596_s_at	A to P	6.42	23.75	12.55	37.01	2	0.0412	+/+	
signal recognition particle 19	2310020D23Rik	AI848458	160343_at		1.52	1.91	1.57	3.20		0.0339	+/+	
small chemokine (C-C motif) ligand 11	Scya11	U77462	92742_at	P to A	0.58	0.15	0.04	0.33	3	0.0098	+/+	
SNF related kinase	Snrk	AW048113	97429_at		0.74	0.37	0.12	0.53	3	0.0210	+/+	
solute carrier family 12, member 2	Slc12a2	U13174	99500_at		1.55	3.97	2.14	6.54	2	0.0410	+/+	
solute carrier family 27 (fatty acid transporter), member 1	Slc27a1	U15976	93486_at	P to A	0.69	0.05	0.03	0.08	1	0.0248	+/+	
solute carrier family 29 (nucleoside transporters), member 1	Slc29a1	AI838274	95733_at		1.55	3.94	3.10	5.78	2	0.0453	+/+	Y
sorbin and SH3 domain containing 1	Sh3d5	U58883	160320_at		0.59	0.12	0.08	0.15	3	0.0444	+/+	
spectrin alpha 2	2610027H02Rik	AW046708	103345_at		1.08	2.08	1.54	2.75	2	0.0256	+/+	
spermatid perinuclear RNA binding protein	Spnr	AI838709	103330_at		1.52	2.64	2.01	3.46	2	0.0230	+/+	Y
S-phase kinase-associated protein 1A	Tceb1l	Z47088	99607_at		1.95	3.05	2.46	7.57	4	0.0248	+/+	2of3
Src activating and signaling molecule	Srcasm	AI840130	104063_at		1.28	2.68	2.22	3.32	2	0.0119	+/+	

Table II-2. Filtered ErbB2/Neu Mammary Tumor Molecular Signature.

Gene Name	Common	Genbank	Affymetrix	Absolute call*	Fold Change§				SOM Cl #†	p-value‡	Repeated Observation**	RT-PCR Confirmation§§
					ANvsWT	TUvsWT						
					Median	Median	Minimum	Max				
SRY-box containing gene 4	Sox4	X70298	160109_at		1.75	3.39	2.22	4.89	2	0.0308	+/+	Y
stromal cell derived factor receptor 2	Sdfr2	D50464	103421_at		2.29	3.05	2.16	4.66	4	0.0218	+/+	
sulfide quinone reductase-like (yeast)	Sqrdl	AW208628	94515_at		0.58	0.37	0.29	0.64	3	0.0410	+/+	
sulfotransferase family 1A, phenol-preferring, member 1	Sult1a1	L02331	103087_at	P to A	0.61	0.02	0.01	0.04	3	0.0419	+/+	
suppressor of cytokine signaling 2	Cish2	U88327	99475_at		2.26	14.22	5.74	19.56	2	0.0343	+/+	
sushi-repeat-containing protein	Srpx	AB028049	103568_at	P to A	0.68	0.10	0.06	0.25	1	0.0080	+/+	Y
synaptonemal complex protein 3		AW212131	93994_at		0.54	0.15	0.12	0.22	3	0.0069	+/+	
T-cell immunoglobulin and mucin domain containing 2	C78111	AA986114	103794_i_at		2.60	4.59	1.93	7.01	4	0.0295	+/+	
T-cell immunoglobulin and mucin domain containing 2	Timd2	AA795198	97335_at		1.52	2.38	1.64	3.14	4	0.0098	+/-	
T-cell lymphoma invasion and metastasis 1	Tiam1	U05245	102283_at		1.51	2.06	1.77	2.66	4	0.0397	+/+	Y
tetranectin (plasminogen binding protein)	Tna	X79199	92224_at	P to A	1.13	0.06	0.03	0.17	1	0.0407	+/+	
thrombomodulin	Thbd	X14432	104601_at	P to A	0.84	0.29	0.18	0.41	1	0.0330	+/+	
thrombospondin type 1 domain containing gene	R-spondin	AB016768	98312_at	P to A	1.04	0.03	0.02	0.04	1	0.0001	+/+	
Tnf receptor associated factor 4	Traf4	AV109962	162482_at		1.40	2.10	1.88	2.51	2	0.0371	+/+	Y
Tnf receptor associated factor 4	Traf4	X92346	100005_at		1.48	2.04	1.45	2.48		0.0155	+/+	Y
transcription factor AP-2, gamma	Tcfap2c	X94694	92275_at		1.48	4.23	2.69	5.98	2	0.0401	+/+	Y
transforming growth factor alpha	Tgfa	M92420	92369_at	A to P	1.72	4.82	2.50	7.31	2	0.0498	+/+	Y
transforming growth factor beta 1 induced transcript 4	Tgfb1i4	X62940	93728_at		0.82	0.38	0.31	0.48	1	0.0085	-/+	1of3
transforming growth factor, beta induced	Tgfbi	L19932	92877_at		0.87	0.34	0.23	0.54	1	0.0133	+/+	Y
transmembrane 4 superfamily member 3		AI047972	103494_at	A to P	3.92	24.25	14.52	31.78	2	0.0141	+/+	
tuftelin 1	Tuft1	AF047704	102043_at	A to P	1.85	2.83	2.19	3.84	2	0.0354	+/+	
tumor differentially expressed 1	Tde1	L29441	100151_at		1.44	2.41	1.36	2.99		0.0379	+/+	
tumor protein D52	Tpd52	U44426	160249_at		1.76	2.89	2.20	4.35	4	0.0356	+/+	
tumor protein D52-like 1	Tpd52l1	AF004428	101446_at	A to P	2.72	12.13	7.26	21.41	2	0.0057	+/+	Y
tumor-associated calcium signal transducer 1	Tacstd1	M76124	99582_at		2.09	6.15	3.78	9.32	4	0.0155	+/+	Y
UDP glycosyltransferase 1 family, polypeptide A6	Ugt1a6	U16818	99580_s_at	P to A	0.64	0.12	0.09	0.26	3	0.0001	+/+	
UDP-Gal:betaGlcNAc beta 1,4-galactosyltransferase, polypeptide 6	B4galt6	AW125314	102936_at		2.38	7.46	4.35	11.55	2	0.0361	+/+	
UDP-N-acetyl-alpha-D-galactosamine:polypeptide N-acetylgalactosaminyltransferase 3	Galnt3	U70538	99011_at		2.12	7.16	4.56	12.13	2	0.0295	+/+	
UDP-N-acetyl-alpha-D-galactosamine:polypeptide N-acetylgalactosaminyltransferase 3	Galnt3	AV055653	162313_f_at		2.02	5.13	2.33	8.11	4	0.0295	+/+	
uridine monophosphate kinase	Umpk	L31783	94381_at		0.58	0.51	0.37	0.68	3	0.0100	+/+	
v-erb-b2 erythroblastic leukemia viral oncogene homolog 3 (avian)	C76256	AI006228	96771_at		1.66	3.73	1.71	5.46	2	0.0445	+/+	
villin 2	Vil2	X60671	100084_at		1.68	2.71	2.35	3.71	4	0.0218	+/+	Y
vitamin D receptor	Vdr	AW061016	99964_at		1.71	1.89	1.39	2.36	2	0.0393	-/+	
Von Willebrand factor homolog	AI551257	AI843063	103499_at	P to A	0.56	0.03	0.01	0.06	3	0.0431	+/+	
WD-40-repeat-containing protein with a SOCS box 2	AA673511	AF033188	160296_at		1.24	1.73	1.59	2.11		0.0050	+/+	
wee 1 homolog (S. pombe)	Wee1	D30743	101458_at		1.63	3.27	2.17	7.11	2	0.0218	+/+	Y
WW domain binding protein 5	Wbp5	U92454	100522_s_at		1.72	2.75	1.79	4.41	4	0.0201	+/+	
X-box binding protein 1	Xbp1	AW123880	94821_at		1.46	2.71	2.23	3.66		0.0323	+/+	Y
zinc finger homeobox 1a	Zfhx1a	D76432	99052_at		0.72	0.31	0.15	0.53	1	0.0241	+/+	Y

* Absolute call is the Affymetrix parameter that measures detection. P=present A=absent. "A to P" indicates that a gene was called "absent" in control and "present" in tumor. If a gene changes from absent to present or vice versa, the fold change is irrelevant.

§ Fold change was derived from the Affymetrix signal log ratio (SLR). AN= adjacent*neu* WT=wild-type control TU=tumor. The shaded areas denote <3.4 fold changed TuvsWT.

† "SOM CL #" = self-organizing map cluster number, clusters are shown in Figure 3B.

‡ p-value was calculated for average tumor versus average control using Welch's t-test with the Benjamini and Hochberg Multiple Testing Correction (False Discovery Rate of 5%).

** Repeated observation indicates whether the gene was confirmed by microarray data from 2 additional independent tumor samples. "+/+" indicates confirmed by both tumors analyzed; "+/-" or "-+" by one tumor; and "-/-" by neither tumor.

§§ Direction (increased/decreased) of expression confirmed by RealTime RT-PCR. "Y"=yes confirmed in 3 tumors, "2of3"= confirmed in 2 of 3 tumors,"1of3"= confirmed in 1 of 3 tumors "N"=not confirmed. If blank, then not assayed.

Table II-3. Sixty-Six Genes Consistently Demonstrated Significant (p<0.01) Alterations of Gene Expression in ErbB2/Neu-Induced Mammary Tumors. Relative to Age-Matched Wild-Type Control Mammary Glands

Gene Name	Genbank Accession	Affymetrix Accession	Abs Call*	Fold Change§ ANvsWT	Fold Change§ TUvsWT	SOM Cl #†	Rep Obs‡	RT-PCR**
Increased in Tumors								
tumor protein D52-like 1	AF004428	101446_at	A to P	2.7	12.1	2	+/+	Y
dual specificity phosphatase 6	AI845584	93285_at		3.1	10.4	2	+/+	
desmoglein 2	AI152659	104480_at		4.1	6.1	4	+/+	
inositol 1,4,5-triphosphate receptor 5	AF031127	101441_i_at		2.0	4.7	2	+/+	Y
cytidine monophospho-N-acetylneuraminic acid synthetase	AJ006215	98593_at		1.7	4.7	2	+/+	
p53 apoptosis effector related to Pmp22	AI854029	97825_at		1.9	4.0	2	+/+	Y
folate receptor 1 (adult)	AV035020	162302_f_at	A to P	2.2	3.7	4	+/+	
latexin	D88769	96065_at		1.7	3.4	2	+/+	
hypothetical protein 6330505N24	AI430272	104207_at		1.5	3.0	2	+/+	
RIKEN cDNA 1200015G06 gene	AI844370	93590_at		2.3	2.8	2	+/+	
ATPase, H+ transporting, V1 subunit A, isoform 1	AW123765	95746_at		1.2	2.6	2	+/+	
DNA segment, Chr 3, UCLA 1	AI843466	95708_at		1.8	2.6	4	+/+	
CD9 antigen	L08115	95661_at		1.4	2.5		+/+	
insulin-like growth factor 2 receptor	U04710	95117_at		1.3	2.5		+/+	Y
CASP2 and RIPK1 domain containing adaptor with death domain	AJ224738	102952_g_at		1.2	2.4	2	+/+	N
T-cell immunoglobulin and mucin domain containing 2	AA795198	97335_at		1.5	2.4	4	+/-	
golgi phosphoprotein 3	AW060175	160688_at		1.4	2.3		+/+	
calcium binding protein, intestinal	Y00884	95423_at		1.5	2.2	2	+/+	
Bcl2-associated athanogene 2	W71352	160962_at		1.6	2.2		+/+	
death-associated protein	AI196645	93842_at		1.3	2.1		+/+	
RAB18, member RAS oncogene family	L04966	94319_at		1.2	1.8		+/+	2of3
WD-40-repeat-containing protein with a SOCS box 2	AF033188	160296_at		1.2	1.7		+/+	
interleukin 25	AW045739	96318_at		1.4	1.7		+/+	
Decreased in Tumors								
RIKEN cDNA 1620401E04 gene	AW125480	96900_at		0.66	0.49	3	+/+	
ATPase, Na+/K+ transporting, beta 3 polypeptide	U59761	99579_at		0.75	0.48		+/+	
L-3-hydroxyacyl-Coenzyme A dehydrogenase, short chain	D29639	95485_at		0.71	0.45	3	+/+	
phytanoyl-CoA hydroxylase	AF023463	96608_at		0.72	0.44	3	+/+	
amyloid beta (A4) precursor-like protein 2	M97216	93498_s_at		0.64	0.41	3	+/+	
transforming growth factor beta 1 induced transcript 4	X62940	93728_at		0.82	0.38	1	-/+	
RIKEN cDNA 1110021N07 gene	AI846382	93983_at	P to A	0.58	0.38	3	+/+	
carnitine palmitoyltransferase 2	U01170	95646_at		0.64	0.36	3	+/+	
myristoylated alanine rich protein kinase C substrate	M60474	96865_at		0.90	0.35	3	+/+	
branched chain ketoacid dehydrogenase E1, beta polypeptide	L16992	102302_at		0.59	0.33	3	+/+	
RIKEN cDNA 4921515A04 gene	AI642098	104494_at		0.53	0.33	3	+/+	
glycogenin 1	AW049730	100597_at		0.51	0.31	3	+/+	
acetyl-Coenzyme A acyltransferase 2	AI849271	95064_at		0.65	0.30	3	+/+	
phosphoglucomutase 2	AI842432	104313_at		0.52	0.29	3	+/+	
RIKEN cDNA 1110001J14 gene	AW047554	104605_at		0.45	0.26	3	+/+	
3-ketoacyl-CoA thiolase B	AW012588	99571_at	P to A	0.51	0.25	3	+/+	
RIKEN cDNA D330037A14 gene	AI854506	96206_at	P to A	0.69	0.25	1	+/+	
RIKEN cDNA 1200015A22 gene	AI854863	98633_at	P to A	0.44	0.24	3	+/+	
Kruppel-like factor 4 (gut)	U20344	99622_at		0.69	0.23	3	+/+	Y
glycerol phosphate dehydrogenase 2, mitochondrial	D50430	98984_f_at		0.57	0.20	3	+/+	
preproenkephalin 1	M55181	94516_f_at		0.56	0.20	3	+/+	
phosphodiesterase 8A	AF067806	160941_at	P to A	0.82	0.19	1	+/+	Y
actin, alpha 2, smooth muscle, aorta	X13297	93100_at		0.87	0.18	1	+/+	
neuropilin	D50086	95016_at		0.82	0.18	3	+/+	
serum deprivation response	AI839175	160373_i_at		0.54	0.18	3	+/+	Y
procollagen, type VI, alpha 3	AF064749	101110_at		0.60	0.17	3	+/+	
glycerol-3-phosphate acyltransferase, mitochondrial	U11680	101867_at		0.38	0.17	3	+/+	
hephaestin	AF082567	104194_at		0.40	0.16	1	+/+	
small chemokine (C-C motif) ligand 11	U77462	92742_at	P to A	0.58	0.15	3	+/+	
synaptonemal complex protein 3	AW212131	93994_at		0.54	0.15	3	+/+	
UDP glycosyltransferase 1 family, polypeptide A6	U16818	99580_s_at	P to A	0.64	0.12	3	+/+	
chemokine (C-X-C motif) ligand 12	AV139913	162234_f_at	P to A	0.58	0.12	3	+/+	
aldehyde dehydrogenase family 1, subfamily A7	U96401	94778_at	P to A	0.54	0.10	3	+/+	
sushi-repeat-containing protein	AB028049	103568_at	P to A	0.68	0.10	1	+/+	Y
dermatopontin	AA717826	96742_at		0.68	0.09	3	+/+	Y
prostaglandin E synthase	AI060798	104406_at	P to A	0.71	0.08	1	+/+	
protease, serine, 11 (Igf binding)	AW125478	96920_at		0.54	0.08	3	+/+	Y
RIKEN cDNA 2610042L04 gene	AI853444	93568_i_at	P to A	1.26	0.08	1	+/+	
lumican	AF013262	93353_at		0.90	0.07	1	+/+	
cytochrome P450, family 4, subfamily b, polypeptide 1	AV376161	162044_f_at	P to A	0.86	0.07	1	+/+	
glutathione peroxidase 3	U13705	101676_at		0.33	0.04	3	+/+	
thrombospondin type 1 domain containing gene	AB016768	98312_at	P to A	1.04	0.03	1	+/+	

* Absolute call is the Affymetrix parameter that measures detection. P=present A=absent. "A to P" indicates that a gene was called "absent" in control and "present" in tumor. If a gene changes from absent to present or vice versa, the fold change is irrelevant.

§ Fold change was derived from the Affymetrix signal log ratio (SLR) AN= adjacent *neu*, WT=wild-type control, and TU=tumor. The gray shaded rows denotes <3.4 fold change for TU vs. AMWT.

† "SOM CL #" = self-organizing map cluster number. Clusters are shown in Figure 3B.

‡ Repeated observation indicates whether the gene was confirmed by microarray data from 2 additional independent tumor samples. "+/+" indicates confirmed by both tumors analyzed and "+/-" or "-/+" by one tumor.

** Direction (increased/decreased) of expression confirmed by RealTime RT-PCR. "Y"=yes confirmed in 3 tumors, "2of3"= confirmed in 2 of 3 tumors,and "N"=not confirmed. If blank, then not assayed.

Figure II-2. The adjacent ErbB2/Neu tissue has preneoplastic characteristics. A. *Mammary gland tissue adjacent to ErbB2/Neu-induced tumors displays focal hyperplasia*. Representative sections of wild-type control mammary gland and tissue adjacent to an ErbB2/Neu-induced tumor are shown (H&E, 40X). **B.** *Adjacent ErbB2/Neu Mammary Epithelia Demonstrate Active ErbB2/Neu Signaling.* Representative sections (400X) of immunohistochemical staining for phosphorylated ErbB2/Neu (Tyr-877) in wild-type mammary gland tissue (top panel) and adjacent ErbB2/Neu tissue (bottom panel) are shown. Note the selective membrane staining in the adjacent ErbB2/Neu tissue. **C**. *Known targets of ErbB2/Neu and previously characterized ErbB2/Neu tumor markers are expressed in the adjacent ErbB2/Neu samples.* The signal intensity from microarray data is depicted on the y-axis with the tissue type on the x-axis. The expression values for individual samples are represented with the mean value for each group being indicated by a horizontal line.

Figure II-2

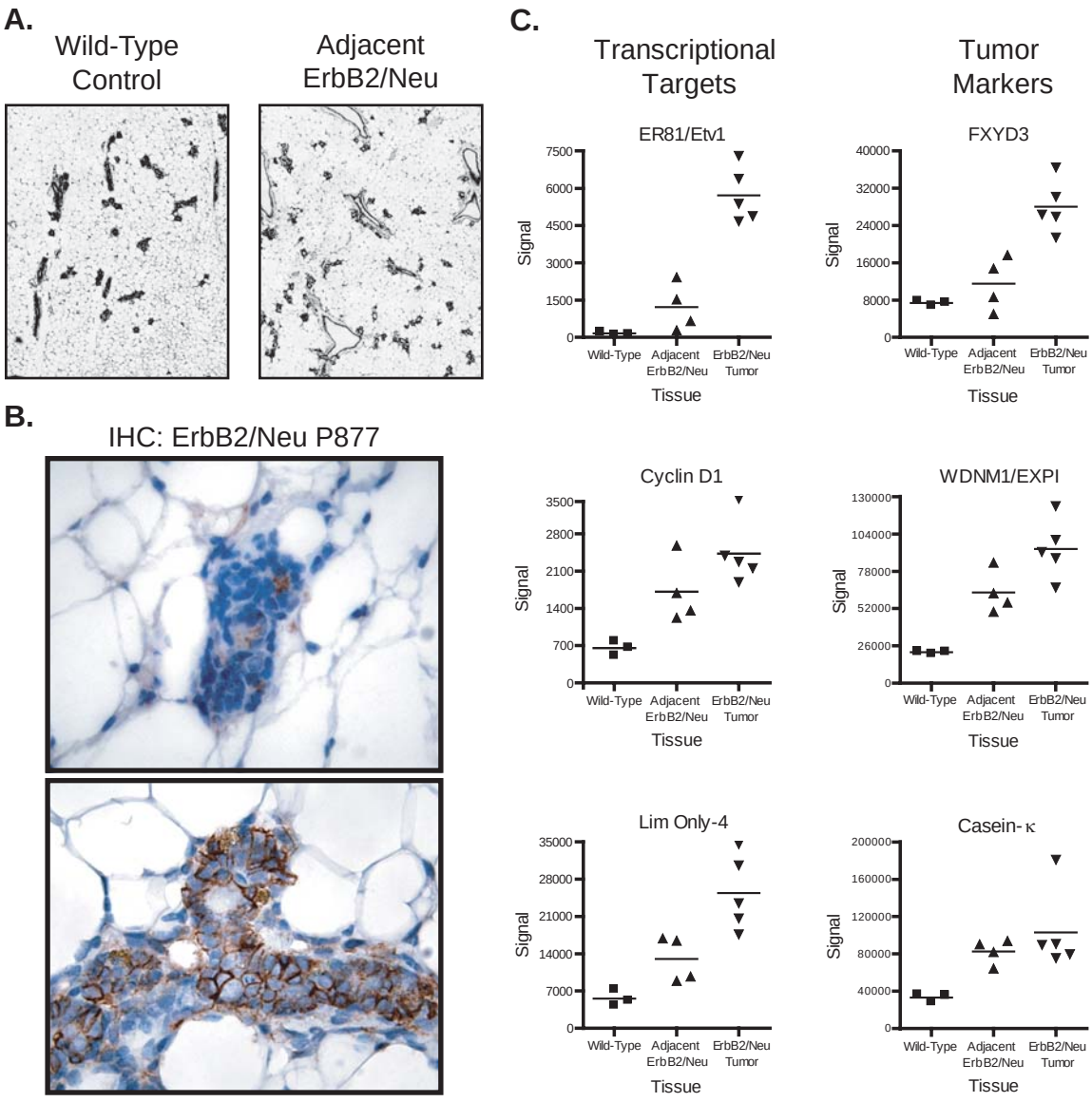
A.
Wild-Type Control
Adjacent ErbB2/Neu
B.
IHC: ErbB2/Neu P877
C.
Transcriptional Targets
Tumor Markers
ER81/Etv1
FXYD3
Cyclin D1
WDNM1/EXPI
Lim Only-4
Casein-κ
Signal
Wild-Type
Adjacent ErbB2/Neu
ErbB2/Neu Tumor
Tissue

Figure II-3. The molecular profile of the adjacent ErbB2/Neu tissue is intermediate between the profiles of tumors and control mammary tissues. **A**. A dendrogram derived by 2-way hierarchical clustering analysis of 7976 genes that were called “present” or “marginal” on at least one microarray is shown. Tissue types are grouped vertically, and genes are grouped horizontally. The arms of the tree are color coded by tissue type (pink = wild-type control (n=3); green = adjacent ErbB2/Neu (n=4); blue = ErbB2/Neu tumor (n=5)). Expression levels are displayed as red = high, yellow = intermediate, and blue = low expression. **B**. *Self-organizing Map (SOM) analysis reveals progressive alterations of gene expression that correlate with tumorigenic stage.* The y-axis represents the signal intensity derived from microarray analyses. For individual genes, values were normalized to the median value across all the samples and expression of individual genes is represented by a thin vertical line for each gene. Each bar represents a compression of all genes in an individual sample. The sample type is color coded (pink = wild-type control (n=3); green = adjacent ErbB2/Neu (n=4); blue = tumor (n=5)). The clusters have been numbered from 1 to 4 (i.e. Cluster 1 to Cluster 4) with the total number of genes represented in each cluster indicated in the top right corner. Genes within individual clusters are identified in Tables II-1, II-2, II-3, and II-4.

Figure II-3

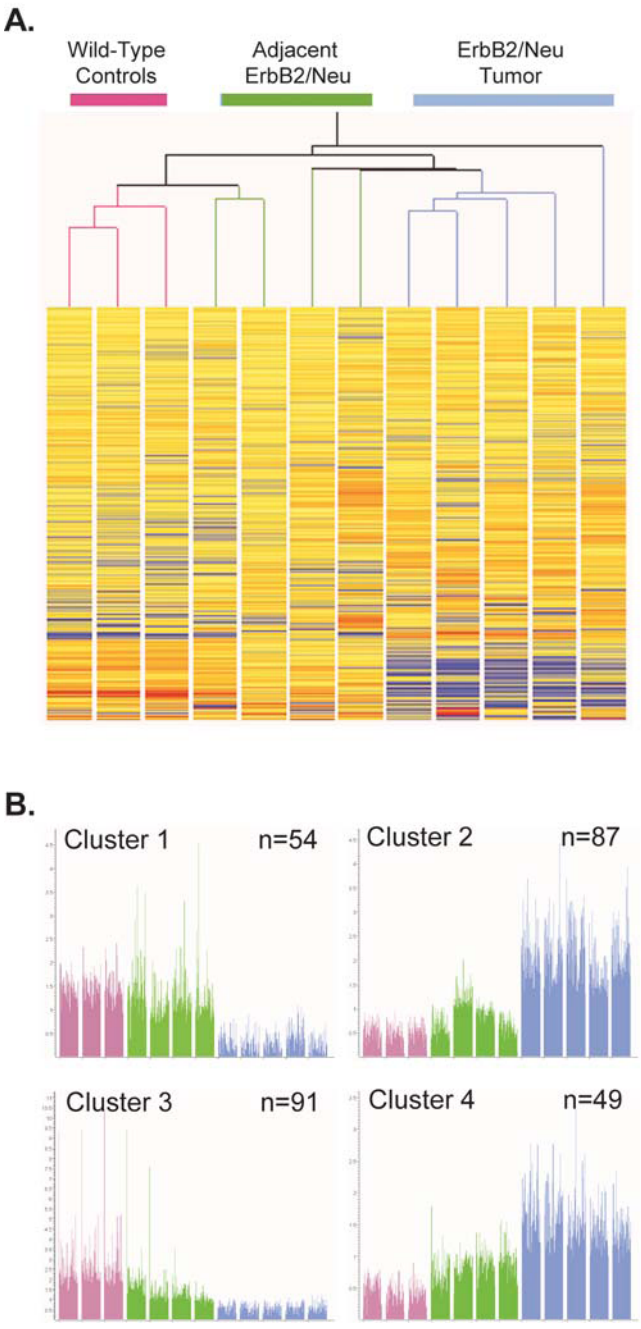
A.
Wild-Type Controls
Adjacent ErbB2/Neu
ErbB2/Neu Tumor
B.
Cluster 1
n=54
Cluster 2
n=87
Cluster 3
n=91
Cluster 4
n=49

Table II-4. Identification of Genes Whose Expression Changes During the Transition from Wild-Type to Preneoplastic Mammary Tissue and is Retained in Overt Tumors.

Gene Name	Genbank Accession	Affymetrix Accession	Abs Call*	Fold Change§ ANvsWT	Fold Change§ TUvsWT	SOM Cl #†	p-value‡	Rep Obs**
*Increased in Adjacent erbB2/*neu *Samples*								
Nephronectin	AA592182	103721_at	A to P	6.8	49.9	2	0.0419	+/+
fatty acid-Coenzyme A ligase, long chain 4	AA619207	102381_at		5.7	19.4	2	0.0210	+/+
ets variant gene 1	L10426	92927_at	A to P	5.5	34.1	2	0.0187	+/+
downstream of tyrosine kinase 1	U78818	102896_at	A to P	4.9	8.5	2	0.0208	+/+
RIKEN cDNA 1600029D21 gene	AI121305	97413_at		4.2	8.6	4	0.0403	+/+
desmoglein 2	AI152659	104480_at		4.1	6.1	4	0.0049	+/+
est	C77278	97165_r_at	A to P	3.1	3.9	4	0.0236	+/+
potassium intermediate/small conductance calcium-activated channel, subfamily N, member 4	AF042487	102198_at		3.0	10.1	2	0.0306	+/+
RIKEN cDNA 1700051C09 gene	AV260411	161227_r_at		2.9	5.2	4	0.0252	+/+
extracellular proteinase inhibitor	X93037	103051_at		2.8	3.6		0.0352	+/+
lipocalin 2	X81627	160564_at		2.7	6.9		0.0111	+/+
homer homolog 2 (Drosophila)	AF093259	160695_i_at	A to P	2.6	7.2	4	0.0276	+/+
kangai 1 (suppression of tumorigenicity 6, prostate	D14883	99584_at		2.3	3.1	4	0.0133	+/+
stromal cell derived factor receptor 2	D50464	103421_at		2.3	3.1	4	0.0218	+/+
inhibitor of DNA binding 2	AF077861	93013_at		2.1	3.7	4	0.0462	+/+
UDP-N-acetyl-alpha-D-galactosamine:polypeptide N-acetylgalactosaminyltransferase 3	AV055653	162313_f_at		2.0	5.1	4	0.0295	+/+
S-phase kinase-associated protein 1A	Z47088	99607_at		2.0	3.1	4	0.0248	+/+
tumor protein D52	U44426	160249_at		1.8	2.9	4	0.0356	+/+
ribonucleotide reductase M2	M14223	102001_at		1.8	2.9	4	0.0130	+/+
WW domain binding protein 5	U92454	100522_s_at		1.7	2.8	4	0.0201	+/+
RIKEN cDNA 3110003A17 gene	AA833425	96135_at		1.7	2.3	4	0.0161	+/+
RIKEN cDNA 2310009N05 gene	AW061073	160801_at		1.6	3.1	2	0.0189	+/+
checkpoint kinase 1 homolog (S. pombe	AF016583	103064_at		1.4	2.0	4	0.0356	-/+
RIKEN cDNA 2610042L04 gene	AI853444	93568_i_at		1.3	0.1	1	0.0056	+/+
*Decreased in Adjacent erbB2/*neu *Samples*								
RIKEN cDNA 1110020P15 gene	AW046239	94078_at		0.8	0.6	3	0.0193	+/+
ATPase, Na+/K+ transporting, beta 3 polypeptide	U59761	99579_at		0.8	0.5		0.0097	+/+
Dehydrogenase/reductase (SDR family) member 7	AW120882	95620_at		0.7	0.5		0.0289	+/+
NADH dehydrogenase (ubiquinone) flavoprotein 1	AI846127	96267_at		0.7	0.5		0.0234	+/+
RIKEN cDNA 1620401E04 gene	AW125480	96900_at		0.7	0.5	3	0.0085	+/+
RIKEN cDNA 1300003D03 gene	AA871791	102052_at		0.7	0.4	3	0.0407	+/+
acetyl-Coenzyme A acyltransferase 2 (mitochondrial 3-oxoacyl-Coenzyme A thiolase	AI849271	95064_at		0.7	0.3	3	0.0050	+/+
amyloid beta (A4) precursor-like protein 2	M97216	93498_s_at		0.6	0.4	3	0.0085	+/+
carnitine palmitoyltransferase 2	U01170	95646_at		0.6	0.4	3	0.0083	+/+
RIKEN cDNA 1110015E22 gene	AW045753	104217_at		0.6	0.1	3	0.0387	-/-
insulin-like growth factor binding protein 6	X81584	103904_at		0.6	0.0	1	0.0230	+/+
NADH dehydrogenase (ubiquinone) 1, alpha/beta subcomplex, 1	AI849803	96909_at		0.6	0.5	3	0.0155	+/+
MAP kinase-interacting serine/threonine kinase 2	AI845732	101007_at		0.6	0.3	3	0.0499	+/+
branched chain aminotransferase 2, mitochondria	AF031467	100443_at		0.6	0.3	3	0.0403	+/+
pyruvate dehydrogenase E1 alpha 1	M76727	98102_at		0.6	0.4	3	0.0339	+/+
chemokine (C-X-C motif) ligand 12	L12030	100112_at		0.6	0.3	3	0.0208	+/+
immunoglobulin joining chair	M90766	102372_at		0.6	0.1	3	0.0470	+/+
Niemann Pick type C2	AB021289	160344_at		0.6	0.5		0.0189	+/+

Table II-4. Identification of Genes Whose Expression Changes During the Transition from Wild-Type to Preneoplastic Mammary Tissue and is Retained in Overt Tumors.

Gene Name	Genbank Accession	Affymetrix Accession	Abs Call*	Fold Change§ ANvsWT	Fold Change§ TUvsWT	SOM Cl #†	p-value‡	Rep Obs**
*Decreased in Adjacent erbB2/*neu *Samples (cont.)*								
procollagen, type VI, alpha 3	AF064749	101110_at		0.6	0.2	3	0.0088	+/+
branched chain ketoacid dehydrogenase E1, beta polypeptide	L16992	102302_at		0.6	0.3	3	0.0014	+/+
uridine monophosphate kinase	L31783	94381_at		0.6	0.5	3	0.0100	+/+
protein phosphatase 2, regulatory subunit B (B56), alpha isoform	AI956230	93826_at		0.6	0.2	3	0.0409	+/+
nuclear receptor subfamily 1, group H, member 3	AF085745	104381_at		0.6	0.1	3	0.0390	+/+
aminolevulinate, delta-, dehydratase	X13752	101044_at		0.6	0.3	3	0.0375	+/+
RIKEN cDNA 1110032O19 gene	AI853294	97386_at		0.6	0.3	3	0.0100	+/+
glycerol phosphate dehydrogenase 2, mitochondria	D50430	98984_f_at		0.6	0.2	3	0.0001	+/+
glutathione transferase zeta 1 (maleylacetoacetate isomerase	AW060750	160350_at		0.6	0.1	3	0.0301	+/+
preproenkephalin 1	M55181	94516_f_at		0.6	0.2	3	0.0098	+/+
sterol carrier protein 2-pseudogene	X87685	95787_s_at		0.6	0.4	3	0.0480	-/-
2,4-dienoyl CoA reductase 1, mitochondria	AI844846	160711_at		0.6	0.2	3	0.0480	+/+
synaptonemal complex protein 3	AW212131	93994_at		0.5	0.2	3	0.0069	+/+
aldehyde dehydrogenase family 1, subfamily A7	U96401	94778_at		0.5	0.1	3	0.0050	+/+
protease, serine, 11 (Igf binding)	AW125478	96920_at		0.5	0.1	3	0.0001	+/+
RIKEN cDNA 4921515A04 gene	AI642098	104494_at		0.5	0.3	3	0.0083	+/+
RAB34, member of RAS oncogene family	AI835712	160317_at		0.5	0.3	3	0.0345	+/+
eukaryotic translation initiation factor 4E binding protein 1	U28656	100636_at		0.5	0.4	3	0.0178	+/+
phosphoglucomutase 2	AI842432	104313_at		0.5	0.3	3	0.0062	+/+
3-ketoacyl-CoA thiolase B	AW012588	99571_at		0.5	0.3	3	0.0060	+/+
glycogenin 1	AW049730	100597_at		0.5	0.3	3	0.0049	+/+
electron transferring flavoprotein, beta polypeptide	AW046273	96947_at		0.5	0.2	3	0.0445	+/+
fat specific gene 27	M61737	102016_at		0.5	0.0	3	0.0382	+/+
CD36 antigen	L23108	93332_at		0.5	0.2	3	0.0306	+/+
sialyltransferase 10 (alpha-2,3-sialyltransferase VI	AI153959	102208_at		0.5	0.2	3	0.0415	+/+
methylcrotonoyl-Coenzyme A carboxylase 1 (alpha	AW123316	94940_at		0.5	0.3	3	0.0350	+/+
glucan (1,4-alpha-), branching enzyme 1	AW210370	96803_at		0.5	0.3	3	0.0257	+/+
lipin 1	AI846934	98892_at		0.5	0.2	3	0.0219	+/+
diacylglycerol O-acyltransferase 1	AF078752	104371_at		0.5	0.1	3	0.0378	+/+
hydroxyacyl-Coenzyme A dehydrogenase/3-ketoacyl-Coenzyme A thiolase/enoyl-Coenzyme A hydratase (trifunctional protein), beta subuni	AW122615	96913_at		0.5	0.2	3	0.0365	+/+
RIKEN cDNA 1110001I14 gene	AW047554	104605_at		0.5	0.3	3	0.0013	+/+
RIKEN cDNA 1200015A22 gene	AI854863	98633_at		0.4	0.2	3	0.0085	+/+
guanine nucleotide binding protein, alpha inhibiting	AI153412	104412_at		0.4	0.0	3	0.0364	+/+
glycerol-3-phosphate acyltransferase, mitochondria	U11680	101867_at		0.4	0.2	3	0.0028	+/+
protein tyrosine phosphatase, receptor type, E	X58289	92289_at	P to A	0.4	0.0	3	0.0308	+/+
carboxylesterase 3	AW226939	101538_i_at		0.4	0.0	3	0.0189	+/+
growth hormone receptor	U15012	99108_s_at		0.4	0.1	3	0.0317	+/+
glutathione peroxidase 3	U13705	101676_at		0.3	0.0	3	0.0001	+/+
Adrenergic receptor, beta 3	X72862	92537_g_at		0.3	0.0	3	0.0410	+/+

* Absolute call is the Affymetrix parameter that measures detection. P=present A=absent. "A to P" indicates that a gene was called "absent" in control and "present" in adjacent *erbB2/neu* tissue. If a gene changes from absent to present or vice versa, then the fold change is irrelevant.

§ Fold change was derived from the Affymetrix signal log ratio (SLR). AN= adjacent *neu* , WT=wild-type control, and TU=tumor. The gray shaded rows denote <2.0 fold change for AN vs. WT.

† SOM CL # = self-organizing map cluster number. Clusters are shown in Figure 3B.

‡ p-value was calculated for average tumor versue average control using Welch's t-test with the Benjamini and Hochberg Multiple Testing Correction (False Discovery Rate of 5%).

** Repeated observation indicates whether the gene was confirmed by microarray data from 2 additional independent tumor samples. "+/+" indicates confirmed by both tumors analyzed, "+/-" or "-/+" by one tumor, and "-/-" by neither.

Figure II-4. Western blot analysis confirms alterations in components of the TGF-β pathway in ErbB2/Neu-induced mammary tumors. 150μg of whole cell lysate from mammary gland tissue was resolved by SDS-PAGE and transferred to PVDF membrane. Membranes were sequentially evaluated for the presence/absence of several TGF-β pathway components. E-cadherin was included as a marker for epithelial cell content and the IgG band represents a loading control.

Figure II-4

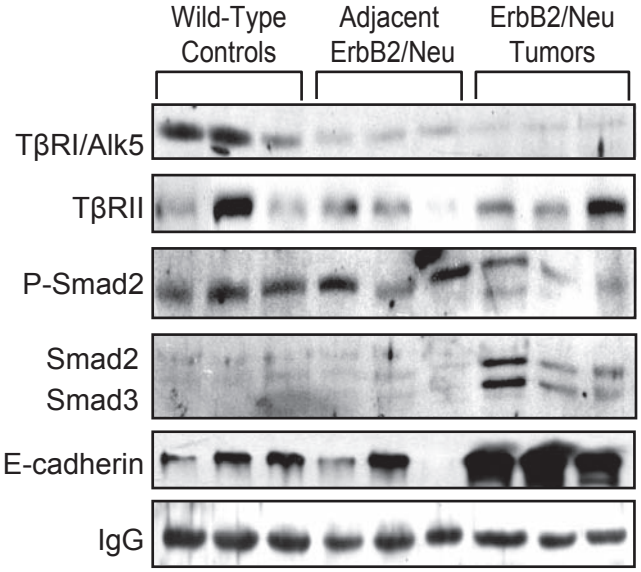
Wild-Type Controls
Adjacent ErbB2/Neu
ErbB2/Neu Tumors
TβRI/Alk5
TβRII
P-Smad2
Smad2
Smad3
E-cadherin
IgG

Figure II-5. Smad2 is inactive throughout ErbB2/Neu-induced mammary tumors except at the tumor/stroma interface. A. *Immunohistochemical analysis of phosphorylated and total Smad2 in ErbB2/Neu-induced tumors.* The top panels are representative immunohistochemical analyses for phosphorylated Smad2 and total Smad2/3 on ErbB2/Neu tumor sections (40X). The bottom panels are a higher magnification (200X) of the boxed area from the panels above. Note the selective nuclear staining (brown) in the enlarged sections, identifying cells with activated Smad2. Sections were counterstained with Gill's Hematoxylin (blue). Seven independent tumors from *ErbB2/neu* mice. These tumors were comparable to the size of tumors that were evaluated by microarray analyses and utilized for subsequent immunohistochemical analysis. **B**. *Assessment of DNA synthesis and apoptosis reveals cycling cells throughout ErbB2/Neu-induced mammary tumors.* The top panel (100X) is representative staining for BrdU (green). Nuclei were counterstained with DAPI (blue). The bottom panel (200X) is representative *in situ* analysis for apoptosis. The brown cells (indicated by arrows) are apoptotic cells. **C.** *Smad2 is activated throughout small ErbB2/Neu tumors*. The top panel is a representative immunohistochemical analysis for phosphorylated Smad2 on sections of small ErbB2/Neu tumors (40X). The bottom panel is a higher magnification (200X) of the boxed area from the panel on top. Note the selective nuclear staining (brown) in the enlarged section, identifying cells with activated Smad2. Sections were counterstained with Gill's Hematoxylin (blue).

Figure II-5

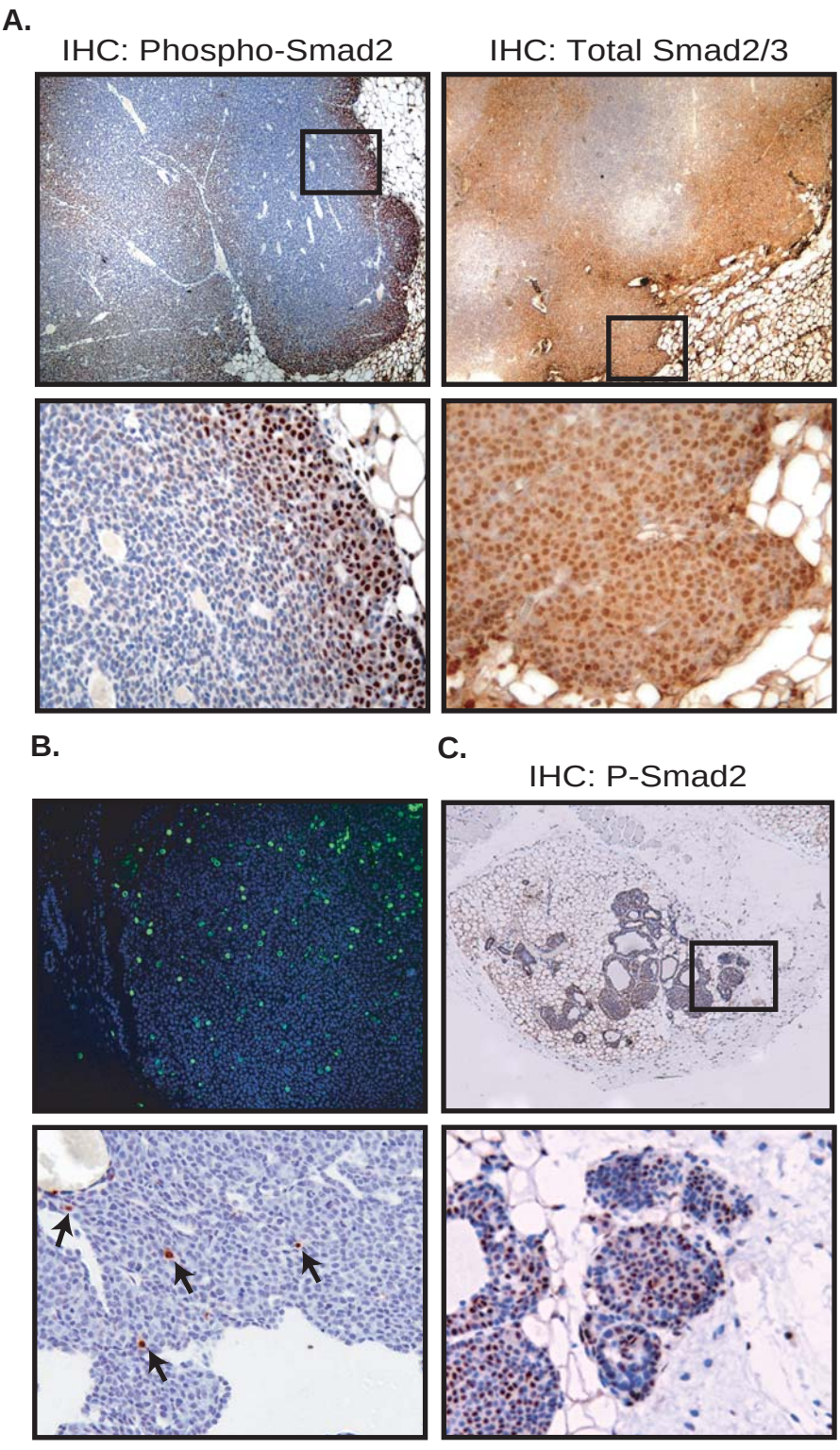

Figure II-6. **Immunohistochemical analysis demonstrates heterogeneous activation of the ErbB2/Neu Receptor in ErbB2/Neu tumor sections**. The top panels (40X) are representative ErbB2/Neu tumor sections that were incubated with antibodies to total ErbB2/Neu and phosphorylated ErbB2/Neu (P-877 and P-1248). The bottom panels (400X) are higher magnifications of the boxed areas in the top panels. Note the selective membrane staining (brown). Sections were counterstained with Gill's Hematoxylin (blue).

Figure II-6

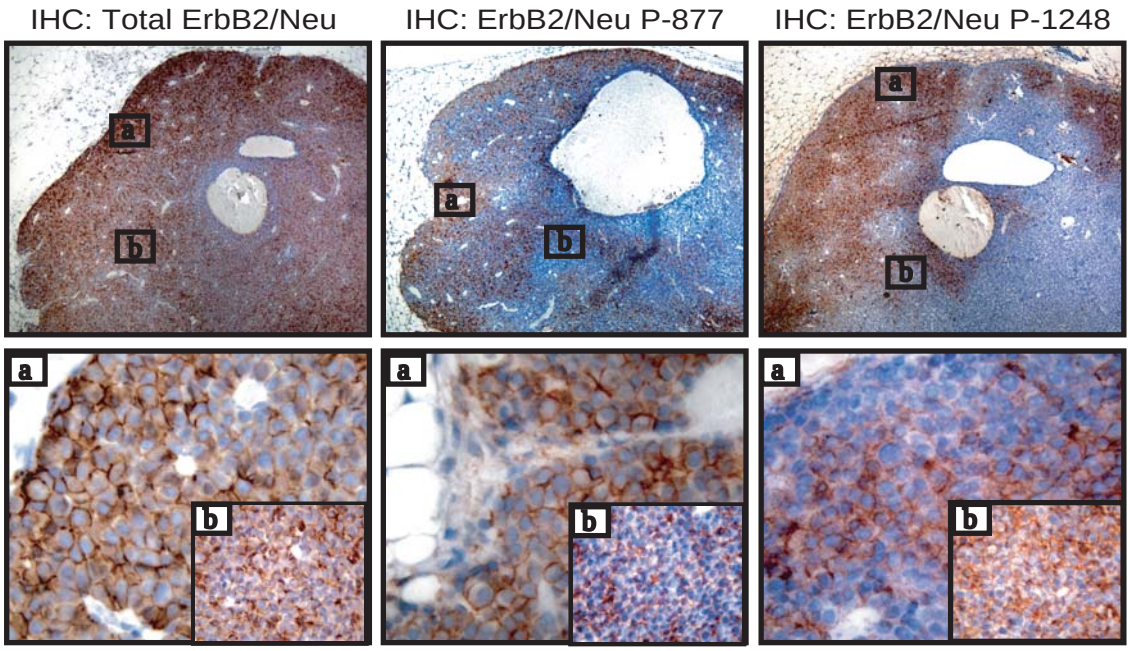
IHC: Total ErbB2/Neu
IHC: ErbB2/Neu P-877
IHC: ErbB2/Neu P-1248
a
b
a
b
a
b
a
b
a
b
a
b

Figure II-7. Immunohistochemical assessment reveals loss of detectable TGF-β-Receptor-I in adjacent ErbB2/Neu mammary gland and ErbB2/Neu Tumor Epithelia. The panels contain representative immunohistochemical staining for TGF-β-Receptor-I/ALK5 in wild-type control tissue sections (**a**, 200X), adjacent ErbB2/Neu tissues (**b**, 200X), and the ErbB2/Neu tumor tissues (**c**, 200X). Note the brown epithelial cells (arrow) in wild-type glands and the loss of this staining in epithelial cells in adjacent glands and tumors (arrows).

Figure II-7

IHC: TGFβRI/Alk5

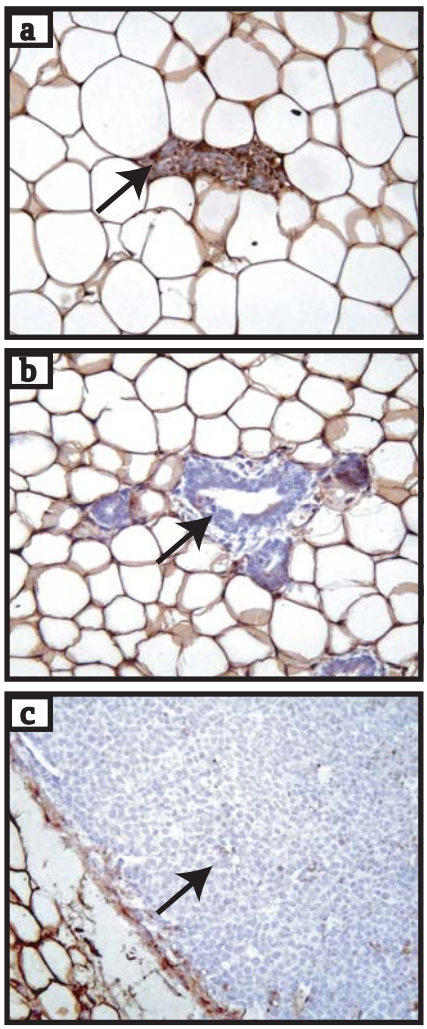

Figure II-8. Activin-Receptor-IB/ALK4 expression correlates with active Smad2 signaling. The panels contain representative immunohistochemical staining for Activin-Receptor-IB on wild-type mammary glands (**a**, 200X), adjacent ErbB2/Neu mammary glands (**b**, 200X), and ErbB2/Neu tumor sections (**c**, 40X). The bottom panel is a higher magnification (**d**, 200X) of the boxed area from the ErbB2/Neu tumor panel above. Sections were counterstained with Gill'sHematoxylin (blue).

Figure II-8

IHC: ActRIB/Alk4

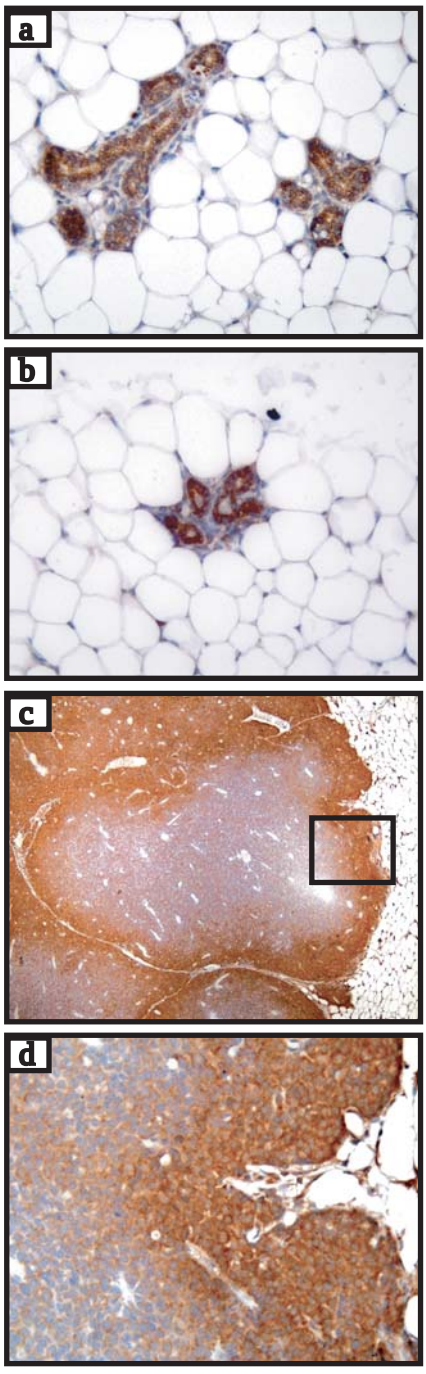

CHAPTER III

SUSTAINED TROPHISM OF THE MAMMARY GLAND IS SUFFICIENT TO ACCELERATE AND SYNCHRONIZE DEVELOPMENT OF ERBB2/NEU-INDUCED TUMORS

(Landis, M.D., Seachrist, D.D., Abdul-Karim, F., and R.A. Keri. 2006, *In Press, Oncogene*)

INTRODUCTION

Although it is well established that pregnancy and lactation provide long-term protection against breast cancer, epidemiological studies also indicate that risk for this disease is transiently elevated with parity (Kelsey et al., 1993; Lambe et al., 1994; Robertson et al., 1997). Indeed, there is a 15-year period of increased risk post-pregnancy that peaks 5 years after parturition in uniparous women and 3 years after delivery in biparous women compared to nulliparous women (Liu et al., 2002). This increased parity-associated risk suggests that the hormones that are elevated during pregnancy can adversely affect the mammary gland, possibly promoting growth of cells that have already undergone malignant transformation. Alternatively, epidemiological studies suggest that the hormonal milieu of the mammary gland during pregnancy and lactation promotes acquisition of a cell population that is particularly susceptible to transformation by HER2, also known as ErbB2 or Neu. HER2 expression is associated with increased parity-induced risk of breast cancer in women (Reed et al., 2003), and women that have been pregnant and have breastfed acquire a 4.2-fold increased risk of developing

HER2 positive breast cancers than their counterparts that never breastfed (Treurniet et al., 1992). The mechanisms responsible for the increased risk of developing HER2-positive breast cancer following pregnancy and lactation remain to be elucidated.

A recent report by Wagner and colleagues (Henry et al., 2004) suggested that induction of susceptible mammary epithelial cells during pregnancy and retention of these cells following involution may account for the parity-associated acceleration of ErbB2/Neu mammary tumorigenesis. This study involved the use of the MMTV-*Neu* mouse model of ErbB2/Neu-induced breast cancer, which overexpresses the proto-oncogenic form of rat ErbB2, *Neu*, under control of the mouse mammary tumor virus (MMTV) promoter. These transgenic mice acquire mammary tumors with long latency and eventually develop pulmonary metastases (Guy et al., 1992). The mammary tumors are estrogen-receptor negative (Wu et al., 2002), solid, nodular lesions composed of intermediate cells that histologically resemble a subset of human breast tumors (Cardiff et al., 2000). While parity accelerates mammary tumorigenesis in MMTV-*Neu* mice compared to their nonparous littermates, tumor development remains stochastic in nature (Anisimov et al., 2003; Guy et al., 1992; Henry et al., 2004).

Breast tumorigenesis is a multi-step process, as reflected by the stochastic kinetics of tumor development (Beckmann et al., 1997; Hanahan and Weinberg, 2000). The stochastic nature of tumor development in multiparous, MMTV-*Neu*

mice suggests that mechanisms above and beyond overexpression of ErbB2/Neu and the stimulus of pregnancy hormones are required to cause malignant transformation of mammary epithelial cells. What are these additional events or "hits" that contribute to ErbB2/Neu-induced tumorigenesis and can they be attributed to factors other than random genetic events? We postulated that the timing of pregnancy may significantly impact the formation of tumor-susceptible cells because it has previously been shown that terminal end buds, which form during puberty, are particularly susceptible to oncogenic insults (Russo and Russo, 1996; Singletary et al., 1991). Alternatively, we surmised that chronic hormonal maintenance, rather than broad fluctuations that occur during the brief mouse pregnancy, may provide a milieu that contributes more significantly to susceptibility.

To examine these possibilities, we carried out two independent tumor palpation studies. To examine the effects of timing of pregnancy on ErbB2/Neu-mediated tumor development, we maintained MMTV-*Neu* female mice in a pregnant or lactating state beginning at three weeks of age. This correlates with the onset of puberty when terminal end buds are just beginning to form (Hennighausen and Robinson, 2001). To determine whether chronic trophic maintenance of the mammary epithelial cells would modulate ErbB2/Neu-initiated tumorigenesis, we bred the MMTV-*Neu* mice with a model of ovarian hyperstimulation (LH-overexpressing mice; (Risma et al., 1995). The LH-overexpressing mice have elevated serum levels of estradiol and progesterone by 5 weeks of age. This

results in an ovary-dependent hyperproliferative mammary gland phenotype reflective of a mid-pregnant gland at both the morphological and molecular level (Milliken et al., 2002). In addition to permitting an assessment of chronic trophism on ErbB2/Neu-induced tumor susceptibility, the bitransgenic mice generated by these breedings allowed us to identify critical time points for evaluation of molecular events that contribute to early events of the ErbB2/Neu-mediated tumorigenic cascade.

RESULTS AND DISCUSSION

Early pregnancy accelerates ErbB2/Neu-induced mammary tumorigenesis

During puberty, the developing mammary gland is particularly susceptible to carcinogenesis (Hancock et al., 1993; Land et al., 2003; Russo and Russo, 1998; Tokunaga et al., 1979). Since adult pregnancy increases susceptibility to ErbB2/Neu-induced tumorigenesis, we postulated that chronic pregnancy/lactation initiated at puberty may provide a further increase in the susceptible cell population for ErbB2/Neu-induced transformation, possibly leading to synchronous tumor formation. To determine whether timing of pregnancy affects ErbB2/Neu-mediated tumorigenesis, MMTV-*Neu* female mice were superovulated and then continuously housed with male mice to maintain the females in a pregnant or lactating state beginning at three weeks of age. Following weekly palpation to detect developing mammary tumors, tumor latency in the multiparous, superovulated MMTV-*Neu* mice was compared to that of virgin MMTV-*Neu* mice. The multiparous, superovulated MMTV-*Neu* mice

demonstrated accelerated tumor development (**Figure III-1**, 25.1 ± 5.0 weeks) compared to virgin MMTV-*Neu* mice (34.0 ± 10.1 weeks). The acceleration of tumorigenesis by early pregnancy is consistent with the window of increased vulnerability during early reproductive age identified by chemical carcinogenic studies in rodent models (reviewed in (Russo and Russo, 1998) and human epidemiological studies (Hancock et al., 1993; Land et al., 2003; Tokunaga et al., 1979). However, tumor development remained somewhat stochastic within the population, suggesting that other rate-limiting steps are necessary for the formation of an ErbB2/Neu tumor. We speculated that such events may simply involve sustained trophism of the gland as opposed to the vast hormonal fluctuations that occur during repeated pregnancy and lactation.

Trophic maintenance of the mammary gland causes accelerated, synchronous development of ErbB2/Neu-induced mammary tumors

To determine whether chronic trophic maintenance of mammary epithelial cells would provide the necessary support to bypass the rate-limiting, stochastic step in tumor formation, we generated bitransgenic mice by breeding the MMTV-*Neu* mice with a model of ovarian hyperstimulation (LH-overexpressing mice) which have elevated circulating estradiol, progesterone, and prolactin, display a chronic mid-pregnancy-like mammary gland phenotype, and ultimately develop pathologically diverse mammary tumors at a late age (Milliken et al., 2002). Bi- and single transgenic mice were assessed for mammary tumor development by weekly palpation. Tumors were 3-4 mm in diameter upon palpation and confirmed histologically. Tumor development in the bitransgenic mice was

accelerated (**Figure III-2A**, 17.7 ± 2.0 weeks) compared to virgin (34.1 ± 10.1 weeks) or multiparous, superovulated MMTV-*Neu* mice (25.1 ± 5.0 weeks) or LH-overexpressing mice (43.0 ± 7.4 weeks). The bitransgenic mice also had an increase in the multiplicity of tumors, yielding a greater tumor burden compared to the MMTV-*Neu* single transgenics (**Figure III-2B**). The increased multiplicity and short range of tumor development (S.D. = 2.0 weeks) indicates that tumors are forming in the bitransgenic mice in a much more synchronous manner. These results suggest that trophic maintenance of the mammary gland is sufficient to promote ErbB2/Neu-induced tumorigenesis and removes the requirement for additional stochastic insults prior to tumor development.

Bitransgenic mammary tumors are analogous to ErbB2/Neu-induced tumors, both morphologically and molecularly

It was possible that accelerated tumor development in the bitransgenic mice was due to activation of distinct tumorigenic pathways compared to those that occurred in mice with just the MMTV-*Neu* transgene. If so, one would expect that either the morphological appearance or the molecular profile of the tumors from these two strains of mice would be distinct. MMTV-*Neu* mice develop signature solid, nodular tumors composed of intermediate cells (Cardiff et al., 2000; Cardiff and Wellings, 1999). However, more aggressive tumors have been reported for MMTV-*Neu* mice that were chronically treated with high levels of 17β-estradiol (Yang et al., 2003). To determine whether the bitransgenic mammary tumors were indeed ErbB2/Neu-induced tumors or whether they were derived by alternative, perhaps hormonally-induced, pathways we examined both

the histopathology and the molecular profiles of these tumors. Tumor pathology was evaluated according to the guidelines of the Annapolis Pathology Panel (Cardiff et al., 2000). Bitransgenic mice developed solid, nodular mammary tumors that were morphologically identical to the characteristic MMTV-*Neu* tumors (**Figure III-3A**). While histologically both MMTV-*Neu* and bitransgenic tumors remain well circumscribed, pulmonary metastases formation provides evidence for the malignant nature of these tumors. The incidence of pulmonary metastases occurring in both MMTV-*Neu* and bi-transgenic mice was highly variable and no obvious difference in the number of metastases was observed between these groups (data not shown). Gene expression profiling provided further evidence that the bitransgenic tumors were very similar to the MMTV-*Neu* tumors. Affymetrix MGU74Av2 arrays were used to evaluate the gene expression pattern of mammary tumors from bitransgenic, MMTV-*Neu*, and LH-overexpressing mice. Microarray data was generated for three individual bitransgenic tumors and compared to the microarray data of two tumors from LH-overexpressing mice and five MMTV-*Neu* tumors that we reported previously (Landis et al., 2005). Hierarchical clustering analysis of this data positioned the bitransgenic tumor samples interspersed among the MMTV-*Neu* tumor samples within the same arm of the hierarchical dendrogram (**Figure III-3B**), indicating that the bitransgenic tumors are no more different from MMTV-*Neu* tumors than MMTV-*Neu* tumors are from each other. The tumors from the LH-overexpressing mice were placed on an entirely separate arm of the hierarchical dendrogram from the ErbB2/Neu-derived tumors, indicating their very distinct molecular

signature. Hence, the bitransgenic mice develop characteristic MMTV-*Neu* mammary tumors, signifying that ErbB2/Neu-induced mechanisms of tumorigenesis dominate in bitransgenic tumors and that the accelerated tumorigenesis in this model is not due to alternative mechanisms of tumorigenesis induced by the hormonal milieu in the bitransgenic mice.

Accelerated and synchronous tumorigenesis in bitransgenic mice compared to pregnant and/or virgin MMTV-*Neu* mice is not due to altered expression or mutagenesis of the MMTV-*Neu* transgene

The hormonally-responsive MMTV promoter is induced during late pregnancy and lactation (reviewed in (Gunzburg and Salmons, 1992). Thus, accelerated tumor development in bitransgenic mice could simply be due to increased expression of the transgene in these animals. To determine whether elevated transgene expression is responsible for the more synchronous development of mammary tumors in the bitransgenic mice compared to parous MMTV-*Neu* mice, we examined MMTV-*Neu* transgene expression by northern blot analysis of RNA from bitransgenic mammary glands and pregnant MMTV-*Neu* mammary glands (**Figure III-4A**). MMTV-*Neu* transgene expression was similar or even lower in the bitransgenic mammary glands compared to the pregnant MMTV-*Neu* mammary glands. This suggests that higher transgene expression is not responsible for the shift in latency between these hormonally driven states. In considering alternative mechanisms for enhanced tumorigenesis in bitransgenic mice, we explored the possibility that bitransgenic mice might accumulate mutations in the MMTV-*Neu* transgene. Activating mutations within the

MMTV-*Neu* transgene have previously been reported by Siegel et al. (Siegel et al., 1994). These mutations involve a deletion within the juxtamembrane domain and have been reported to occur in ~65% of tumors. This has led to the assumption that tumor formation in the majority of MMTV-*Neu* mice requires such mutations. To determine if the altered hormonal milieu in bi-transgenic mice might promote mutations within the transgene, we assessed tumor mRNA from both bitransgenic and MMTV-*Neu* mice for presence of these activating mutations. From sequencing (data not shown) and RT-PCR analysis of the MMTV-*Neu* transgene (**Figure III-4B**), we found that no MMTV-*Neu* single transgenic tumors contained evidence of somatic mutations in the transgene and only 1 of 4 bitransgenic tumors contained a deletion in the MMTV-*Neu* transgene. In summary, these data reveal that mechanisms other than altered transgene expression or somatic mutations within the transgene are responsible for the synchrony of tumor development in the bitransgenic mice. We propose that such mechanisms involve trophic stimulation and maintenance of the susceptible cell population that has previously been identified by Wagner and colleagues (Henry et al., 2004).

The bitransgenic mammary gland becomes committed to tumorigenesis during a three-week window

To determine how long chronic hormonal stimulation is required for enhancing tumor susceptibility, we performed ovariectomy experiments on the bitransgenic mice to remove hormonal contributions of the ovary and assessed mammary gland morphology as well as tumor development. Mammary glands from

bitransgenic mice that were ovariectomized at 8 weeks of age had sustained hyperplasia two weeks following the surgery (**Figure III-5**). This suggests that irreversible events have already occurred by this age, maintaining hyperplasia in an ovarian hormone-independent state after only a few weeks of chronic hormonal input. Furthermore, animals ovariectomized at 8-weeks still developed mammary tumors more rapidly (25.0 ± 21.8) than the virgin MMTV-*Neu* mice (34.1 ± 10.0), but delayed compared to sham-operated bitransgenic mice (19.5 ± 2.2; **Figure III-6**). Importantly, tumor development across the cohort regained a stochastic pattern. This further supports the conclusion that chronic trophism by ovarian hormones can provide an environment that eliminates the need for numerous random events prior to tumor formation.

In a similar experiment involving ovariectomy at 5 weeks of age, only thirty percent of mice developed palpable tumors by two years of age (Figure III-6). This indicates that the mammary epithelial cells from 5-week-old bitransgenic mice have not yet become transformed at the time of ovariectomy or that additional tumorigenic insults fail to occur in these mice following removal of the ovaries. Furthermore, these ovariectomy/palpation experiments suggest that the bitransgenic mammary gland becomes committed to tumorigenesis between 5 and 8 weeks of age. Attempts to narrow this window further by ovariectomizing mice at 6 and 7 weeks of age generated intermediate tumor curves between the 5- and 8-week-ovariectomy tumor curves (data not shown). From these data, we conclude that only a three-week window of trophic support (i.e. from 5 to 8 weeks of age) is required for commitment to ErbB2/Neu-induced mammary

tumorigenesis. Defining this window permitted the identification of two temporally distinct physiological stages of the bitransgenic mammary gland: non-committed and committed to tumorigenesis.

Identification of genes whose expression changes during the transition from normal to preneoplastic mammary tissue

While significant progress has been made regarding understanding the processes of late stages of breast tumorigenesis and characterization of tumor types, mechanisms underlying earlier steps ranging from normal to preneoplastic and ultimately to overt tumors are not well understood. The window of commitment to ErbB2/Neu-induced tumorigenesis that we identified herein provided two critical time points in which to examine molecular changes that occur in the progression from normal (before 5-weeks) to preneoplastic (after 8-weeks) mammary glands.

To identify genes that may facilitate early steps of ErbB2/Neu-mediated mammary tumorigenesis, we performed comparative microarray analysis of 5- and 10-week bitransgenic mammary glands from ovary-intact mice in triplicate. Ten week glands were used as the preneoplastic time point because preliminary experiments with glands from 8-week-old mice failed to detect a significant number of expression changes. This is probably due to the small size of the preneoplastic cell population at 8 weeks of age. Importantly, 10 week glands do not contain overt tumors as determined by whole mount analysis (data not shown). We analyzed 3 pooled RNA samples that represented 3 animals for

each time point so that a total of 9 bitransgenic animals were analyzed per time point. From this analysis, 2793 of 45101 analyzed probe sets were identified as changed according to the Affymetrix change call parameter in all of the 10-week samples compared to the 5-week bitransgenic samples. This data has been submitted to GEO omnibus (http://www.ncbi.nlm.nih.gov/geo).

We compared the list of genes that changed expression during the transition from non-committed to committed mammary tissue in this report with those identified in our previous study of ErbB2/Neu-expressing preneoplastic mammary glands and tumors (Landis et al., 2005) and identified the expression changes that are consistent between the two approaches. Previously, we identified an ErbB2/Neu-induced mammary tumor molecular signature by comparing the partial transcriptomes of tumors from MMTV-*Neu* mice to those of mammary glands from age-matched, wild-type animals (Landis et al., 2005). Of the 324 genes contained in the molecular signature for ErbB2/Neu-induced mammary tumors, 119 were also changed in the comparison of 10-week committed mammary glands versus the 5-week non-committed glands reported herein (**Table III-1**), indicating that these genes are altered during early events of tumorigenesis and maintained in overt tumors. We, also, previously identified genes whose expression was altered in preneoplastic mammary gland tissue and retained in the ErbB2/Neu tumor signature. In that study, the adjacent mammary gland that housed, but did not directly contact, a palpable ErbB2/Neu-induced mammary tumor in MMTV-Neu mice was used to represent preneoplastic mammary tissue. Of the 82 preneoplasia genes identified previously, 32 were

observed in the current comparison of committed (10-week-old) versus non-committed (5-week-old) mammary glands (**Table III-2**). Identification of these genes by two independent approaches using different mouse models strongly supports the notion that these genes may be transcriptional targets of ErbB2/Neu and/or that they contribute to early neoplastic events of ErbB2/Neu-induced mammary tumorigenesis.

Several (Idb2, Tpd52, Ghr, Ppp2r) of the 32 genes identified by both approaches have previously been associated with human breast cancer (Boutros et al., 2004; Calin et al., 2000; Gebre-Medhin et al., 2001; Stighall et al., 2005), corroborating this method for identifying genes involved in early stages of mammary gland tumorigenesis. In addition, 44% of the genes identified by this approach have known roles in cellular metabolism. Acyl-CoA synthetase (Acsl4) expression is elevated in both hepatocellular carcinoma and colonadenocarcinoma and has been shown to block apoptosis and promote colon carcinogenesis (Cao et al., 2000; Cao et al., 2001; Kurokawa et al., 2004; Liang et al., 2005; Sung et al., 2003). The downregulation of several genes involved in fatty acid oxidation (Decr1, Adipor2), electron transfer (Etfb, Nr1h3), triglyceride synthesis (Dgat1), diversion from glycolysis (Pgm2), and inhibition of insulin-like growth factor (Igfbp6) may be reflective of the well described alteration of energy metabolism in human tumors (Board et al., 1990; Dutu et al., 1980; Hennipman et al., 1987; Macheda et al., 2005; Mazurek et al., 2002; Warburg, 1956). Malignant cells have increased glycolysis, suppression of mitochondrial energy production, increased nucleogenesis, increased *de novo* fatty acid synthesis with decreased

triglyceride production, activated glutaminolysis, and activated serinolysis (Mazurek et al., 2002) which is consistent with the early expression changes we have observed in tissues committed to form an ErbB2/Neu tumor. Moreover, these metabolic changes precede morphological changes in human carcinogenesis (McDermott et al., 1990). The identification of altered expression of these metabolic enzymes in preneoplastic mammary glands substantiates the ability of this microarray approach to identify early events of tumorigenesis. Further investigation of the genes described herein that undergo a change in expression with commitment to tumorigenesis should improve our understanding of early events of ErbB2/Neu-induced neoplasia.

The data presented herein reveal that trophic maintenance of mammary epithelial cells is sufficient to generate synchronous growth of ErbB2/Neu-mediated mammary tumors, suggesting that hormonal input provides the secondary events necessary for tumor formation in this model. How does chronic trophism cause synchronous tumor formation? Two experiments in this report oppose the presumption that elevated transgene expression is the sole contributing factor. Northern blot analysis indicated that the transgene is expressed at similar levels in the bitransgenic mammary gland compared to pregnant MMTV-*Neu* glands, yet multiparous MMTV-*Neu* mice develop tumors in a stochastic manner (Anisimov et al., 2003; Guy et al., 1992; Henry et al., 2004). Furthermore, early pregnancy, which would induce the transgene in the multiparous/superovulated MMTV-*Neu* mice at a vulnerable age, accelerated tumorigenesis, but, again, the tumor curve remained stochastic in nature. These

results indicate that hormonal stimulation of transgene expression does not provide the requisite mechanisms for synchronous tumor development. Alternatively, Wagner and colleagues have identified a parity-induced target population of cells that are susceptible to ErbB2/Neu transformation (Henry et al., 2004). Since the mammary glands of LH-overexpressing mice are highly similar to mid-pregnancy glands (Milliken et al., 2002), it is likely that a similar susceptible cell population is induced and maintained in the hormonal environment of these mice. Elevated expression of whey acidic protein, the marker of this ErbB2/Neu-targeted cell population, occurs in the mammary glands of LH-overexpressing mice (Milliken et al., 2002), further corroborating this supposition. Determining whether this parity-induced population of cells exists in LH-overexpressing mice is the subject of ongoing studies.

In conclusion, we have found that chronic trophic input to the mammary gland is sufficient to convert the stochastic pattern of ErbB2/Neu-induced tumorigenesis in virgin mice to a more rapid and synchronous pattern. This indicates that secondary events required for ErbB2/Neu-induced tumor development may take the form of hormonal stimulation rather than complex multi-step genetic events that are followed by natural selection. Hormonal stimulation for just 3 weeks is sufficient for acceleration of tumor formation. However, chronic stimulation is required for the apparent synchronous formation of tumors. This suggests that in addition to pregnancy hormones inducing a susceptible cell population as described by Henry, et al., (2004), chronic maintenance of this cell population contributes substantially to overt tumor susceptibility.

MATERIALS AND METHODS

Materials

Radiolabeled nucleotides were purchased from Perkin Elmer Life Sciences (Boston, MA, USA). All chemicals were purchased from Sigma (St. Louis, MO, USA). Primers were synthesized by Genosys (The Woodlands, TX, USA).

Mice

All animals were housed in micro-isolator plus units under pathogen-free conditions with a 12-hour light/dark cycle. Food and water were provided *ad libitum*. Mice harboring the mouse mammary tumor virus (MMTV)-*Neu* transgene (FVB/N-Tg(MMTVneu)202Mul/J) (Guy et al., 1992) were purchased from Jackson Laboratories (Bar Harbor, ME, USA) and bred with luteinizing hormone (LH)-overexpressing mice (Risma et al., 1995) to generate a colony of bitransgenic mice. The bitransgenic mice were hemizygous for the MMTV-*Neu* transgene. The LH-overexpressing mice (CF-1 genetic background) were bred at least 4 generations into the MMTV-*Neu* (FVB/N) strain. The genotypes of the mice were determined by PCR amplification of tail DNA with transgene-specific primers as previously reported (Kero et al., 2000); (Landis et al., 2005). Mice were palpated weekly to detect mammary tumors. By external caliper assessment, tumors were approximately 3-4 mm in diameter when detected. Graphs of tumor data were generated and statistically evaluated using Kaplan-Meier survival analysis. Most mice that developed tumors were euthanized to isolate tissues following palpation. In some cases, mice were kept for 4-6 weeks

after initial tumor detection for collection of larger tumors, assessment of multiplicity, and analysis of metastatic progression.

For tumor multiplicity and lung metastastes evaluation, mice with a primary tumor volume ranging from 340-1654mm^2 were killed as described above and total primary tumor numbers were counted. Lungs were harvested and fixed overnight in 4% paraformaldehyde at 4˚C and held in PBS until processed for paraffin sectioning. Every 10th section of lung was collected and stained hematoxylin and eosin until 10 slides were obtained from each lung. Total number of metastases and pulmonary emboli were counted in each section. All animal studies were approved by the Case Western Reserve University Institutional Animal Care and Use Committee.

Superovulation

To induce early/simultaneous ovulation, pregnant mares' serum gonadotropin (PMSG) (Sigma, St. Louis, MO, USA; 5 i.u. PMSG and 0.05 mg bovine serum albumin per ml sterile saline) followed by human chorionic gonadotropin (5 USP units in sterile saline; Ayerst APL, New York, New York, USA) 48 hours later was administered to three-week-old female mice. The superovulated mice were then housed with male mice and copulation was verified by presence of vaginal plugs. To maintain these mice in a pregnant or lactating state, they were continuously housed with male mice.

Ovariectomy

Ovariectomy and sham surgeries were performed under avertin anesthesia as described (Milliken et al., 2002). The mice were 5, 6, 7, or 8 weeks of age. Subsequently, mice were either killed by CO_2 asphyxiation 2 weeks following surgery to isolate tissues for histological and whole mount analysis or palpated weekly to detect developing mammary tumors.

Microarray analysis

All microarray data has been submitted to Gene Expression Omnibus (GEO, http://www.ncbi.nlm.nih.gov/geo; Accession # GSE3501) according to according to Minimum Information About a Microarray Experiment (MIAME) guidelines (Brazma et al., 2001). Microarray analyses were carried out as described (Landis et al., 2005). Briefly, for each mammary gland age group, RNA was isolated from the thoracic mammary glands of nine animals and pooled into 3 groups, each representing three individual animals. Biotinylated cRNA was synthesized from 10 μg of total RNA and hybridized to the Affymetrix Murine 430v2 GeneChip Arrays (Santa Clara, CA, USA) which contains 45101 probe sets. For tumor data, total RNA was isolated from three individual tumors and the biotinylated cRNA probes were hybridized to three Affymetrix Murine U74Av2 GeneChip Arrays (Santa Clara, CA, USA) which contains 12488 probe sets. Computational analyses were performed with Microarray Suite (v.5.0, Affymetrix), Data Mining Tool (DMT v.3.0, Affymetrix), MicroDB (v.3.0, Affymetrix), and GeneSpring (v.6.0, Silicon Genetics) software. For comparison to our previous

study (Landis et al., 2005), we identified probe sets that were included on both microarray platforms and determined which of these genes exhibited changes in expression level. 10038 probe sets on the MOE430v2 array were represented by probe sets on the Murine U74Av2 according to Affymetrix "good match" criteria (http://www.affymetrix.com/support/technical/). Because these studies were performed on different microarray platforms, the fold change values can not be directly compared.

Northern blot analysis

Northern blot analysis was performed as described (Landis et al., 2005). Briefly, 20 μg of TRIzol purified (Invitrogen, Carlsbad, CA, USA) total RNA was separated by gel electrophoresis on a 1% denaturing agarose gel and then transferred to Hybond-N+ Nylon membrane (Amersham Pharmacia Biotech, Visscataway, NJ, USA). Membranes were hybridized with a radio-labeled, double-stranded DNA probe to rat *Neu* (α-^{32}P-dCTP; DECAprime II, Ambion, Austin, TX, USA) in QuikHyb solution (Stratagene, Cedar Creek, TX, USA) according to the manufacturer's protocol. The DNA probe was PCR amplified with the *Neu* transgene primers (Landis et al., 2005).

Reverse transcription (RT)–PCR assessment of transgene mutations

The synthesis of single stranded cDNA from tumor samples was performed as previously described (Siegel et al., 1994) with minor modifications. PCR was performed to amplify a 237 base-pair region encompassing the area of multiple deletion mutations in the rat Neu cDNA (Siegel et al., 1994) using the following

primers: NeuF1842: 5'-GAAACCGGACCTCTCCTACA-3' and NeuR2079: 5'-CGGATCTTCTGTCTCCTTCG-3'. The PCR cycling conditions were: 95˚C for 5 min; (95˚C for 1.5min, 60˚C for 2min, 72˚C for 3min) x 35 cycles, 72˚C for 8 min for elongation and held at 4˚C until electrophoresis. PCR products were separated on an 8% acrylamide gel, dried, and exposed to film for 18 hours.

Morphological examination

Whole mounts and histology of abdominal (#4 or #9) mammary glands were prepared as described (Milliken et al., 2002). Briefly, for whole mount analysis, glands were preserved in Kahle's fixative, stained with Carmine Alum stain (2% carmine (w/v), 5% aluminum potassium sulfate (w/v) in water) overnight, cleared in xylene, and mounted on glass slides with Permount. For histological analysis, glands were fixed in 4% (w/v) paraformaldehyde/PBS overnight, paraffin-embedded, cut into 5-μm sections, and stained with hematoxylin and eosin.

ACKNOWLEDGEMENTS

We extend our gratitude to John Nilson for providing the LH-overexpressing mice and to Kristen Lozada for her dedicated technical support. Histology and microarray hybridization were provided by the core facilities of the CASE Comprehensive Cancer Center (P30CA43703). This work was supported by a National Institutes of Health Grant (RO1-CA90398, RAK), a USAMRMC Breast Cancer Research Program Predoctoral Traineeship Award (DAMD17-03-1-0302, MDL), and the National Institutes of Health Molecular Therapeutics Training Program (GM08803, MDL).

Figure III-1. Early pregnancy accelerates ErbB2/Neu-induced mammary tumorigenesis. MMTV-*Neu* female mice were superovulated and then continuously housed with male mice to maintain female mice pregnant or lactating starting at three weeks of age. Mammary tumor development was assessed by weekly palpation. Statistical analysis and graphical representation of tumor development was generated by Kaplan-Meier survival analysis. Sensored events, or animals that were removed from the study for reasons unrelated to tumor development, were included in the analysis. The median tumor latencies for the multiparous, superovulated MMTV-*Neu* (■, n = 16, sensored = 0) and virgin MMTV-*Neu* (●, n = 37, sensored = 6) animals were 25.1 ± 5.0 and 34.0 ± 10.1 (median ± S.D.) weeks, respectively. Tumor curves for superovulated and virgin MMTV-*Neu* mice were significantly different (log rank test Chi Square = 27.4, $p < 0.0001$).

Figure III-1

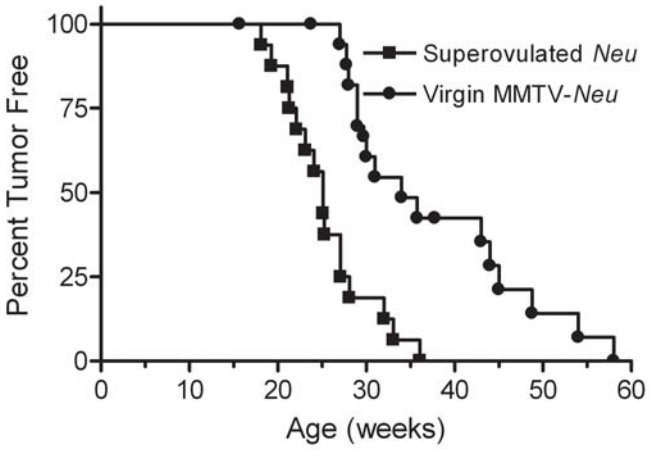
Percent Tumor Free
100
75
50
25
0
0
10
20
30
40
50
60
Age (weeks)
Superovulated *Neu*
Virgin MMTV-*Neu*

Figure III-2. Trophic maintenance of the mammary gland causes accelerated, synchronous development of ErbB2/Neu-induced mammary tumors. **A**. *MMTV*-Neu *mice were bred with LH-overexpressing mice to generate bitransgenic and control (MMTV*-Neu *and LH-overexpressing) animals. Mammary tumor development was assessed by weekly palpation*. Statistical analysis and graphical representation of tumor development was generated by Kaplan-Meier survival analysis. Sensored events, or animals that were removed from the study for reasons unrelated to tumor development, were included in the analysis. The median tumor latencies for the bitransgenic (▲, n = 20, sensored = 0) and LH-overexpressing mice (♦, n = 16, sensored = 6) were 17.7 ± 2.0 and 43.0 ± 7.4 (median ± S.D.) weeks, respectively. The bitransgenic tumor curve is significantly different than the tumor curves for both the virgin MMTV-*Neu* mice (log rank test Chi Square = 76.0, $p < 0.0001$) and the superovulated MMTV-*Neu* mice (log rank test Chi Square = 32.1, $p < 0.0001$). Note that the virgin MMTV-*Neu* tumor curve from III-1 is shown in gray for comparison. **B**. *Bitransgenic mice have increased tumor burden compared to MMTV*-Neu *single transgenics*. Mice with primary tumor volumes ranging from 340-1654mm^2 were killed and total primary tumor numbers were counted. Tumor burden was significantly greater (two-tailed t-test, $p < 0.05$) in the bitransgenic mice (n = 4; 8.2 ± 1.6) compared to MMTV-Neu single transgenics (n = 4; 3.0 ± 0.7).

.

Figure III-2

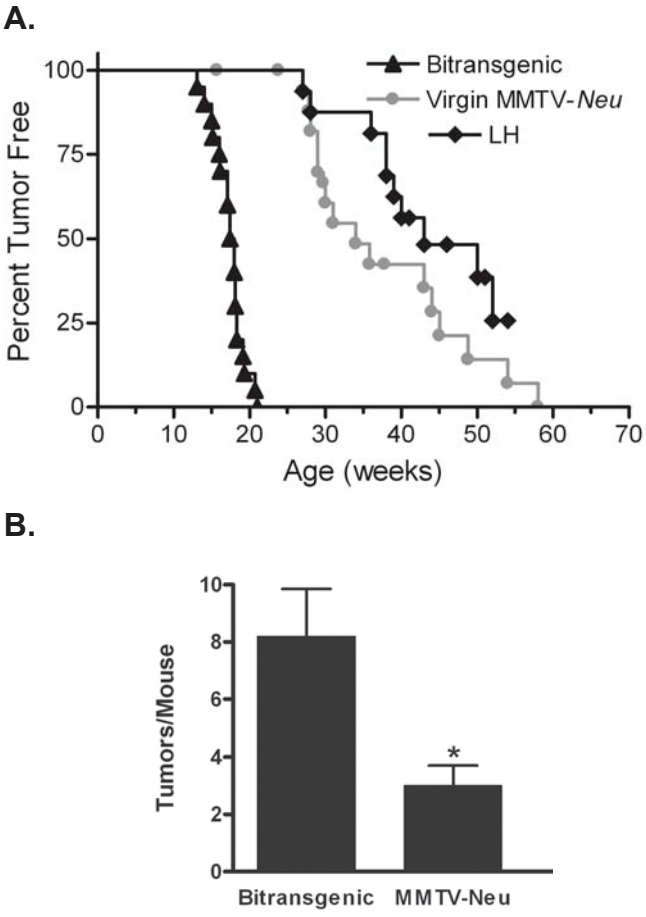
A.
Bitransgenic
Virgin MMTV-Neu
LH
Percent Tumor Free
100
75
50
25
0
0
10
20
30
40
50
60
70
Age (weeks)
B.
Tumors/Mouse
10
8
6
4
2
0
*
Bitransgenic
MMTV-Neu

Figure III-3. Bitransgenic mammary tumors are analogous to ErbB2/Neu-induced tumors, both morphologically and molecularly. **A**. *Bitransgenic and MMTV-Neu mice develop identical nodular mammary adenocarcinomas*. Five micron sections of paraffin-embedded tumor tissue were stained with Hematoyxlin and Eosin. Representative images (100X) are shown. **B**. *Gene expression microarray analysis reveals that the molecular profiles of bitransgenic and MMTV-Neu tumors are very similar*. A dendrogram derived from two-way hierarchical clustering analysis of the 12488 probe sets included on the Affymetrix Murine U74Av2 GeneChip is shown. Tumor types are grouped vertically, and genes are grouped horizontally. The arms of the tree are color coded by tumor type (blue = MMTV-*Neu* tumor (n = 5), green = bitransgenic tumor (n = 3); pink = LH-overexpressing tumor (n = 2). Expression levels are displayed as red = high, yellow = intermediate, and blue = low expression.

Figure III-3

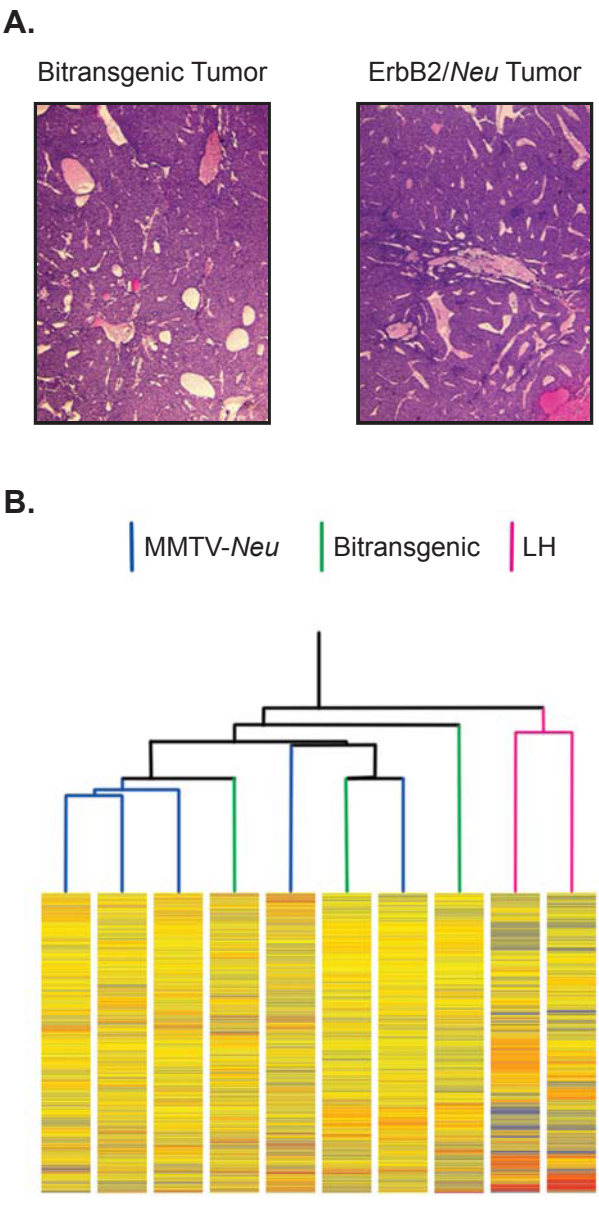
A.
Bitransgenic Tumor
ErbB2/*Neu* Tumor
B.
MMTV-*Neu*
Bitransgenic
LH

Figure III-4. Accelerated and synchronous tumorigenesis in bitransgenic mice compared to pregnant and/or virgin MMTV-Neu mice is not due to altered expression or mutagenesis of the MMTV-Neu transgene. A. Northern blots were generated with twenty micrograms of total RNA isolated from the mammary glands of 14-week-old bitransgenic, virgin MMTV-*Neu*, and pregnancy d14 (Pd14) MMTV-*Neu* mice. A radiolabeled, double-stranded DNA probe specific for the MMTV-*Neu* transgene was hybridized with the northern blot. The 28S ribosomal RNA band served as a loading control. **B**. RT-PCR analysis was carried out on total RNA isolated from bitransgenic (n = 4) and MMTV-*Neu* single transgenic (n = 3) mammary tumors. The 237 base pair (b.p.) product (upper band) represents the wild type MMTV-*Neu* transgene, whereas smaller RT-PCR products represent deletions within the transgene (lower band).

Figure III-4

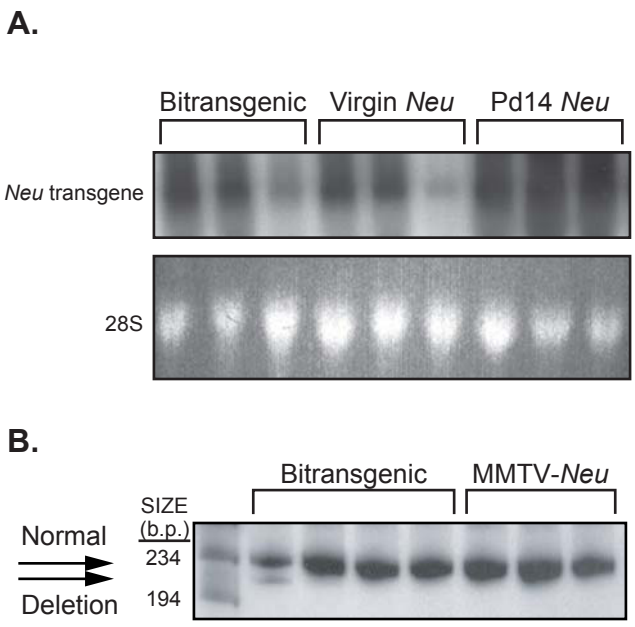
A.
Bitransgenic
Virgin *Neu*
Pd14 *Neu*
Neu transgene
28S
B.
Bitransgenic
MMTV-*Neu*
SIZE
(b.p.)
Normal
234
194
Deletion

Figure III-5. The mammary glands from bitransgenic mice that were ovariectomized at 8 weeks of age have sustained hyperplasia of the mammary gland. Bitransgenic (n = 3), LH-overexpressing (n = 3), MMTV-*Neu* (n = 3), and wild-type mice (n = 3) were ovariectomized at 8 weeks of age. At 10 weeks of age, all of the mice were killed, and mammary glands were prepared for whole mount analysis. Images (63X) of comparable regions above the lymph node of each abdominal (#4/#9) mammary gland are shown.

Figure III-5

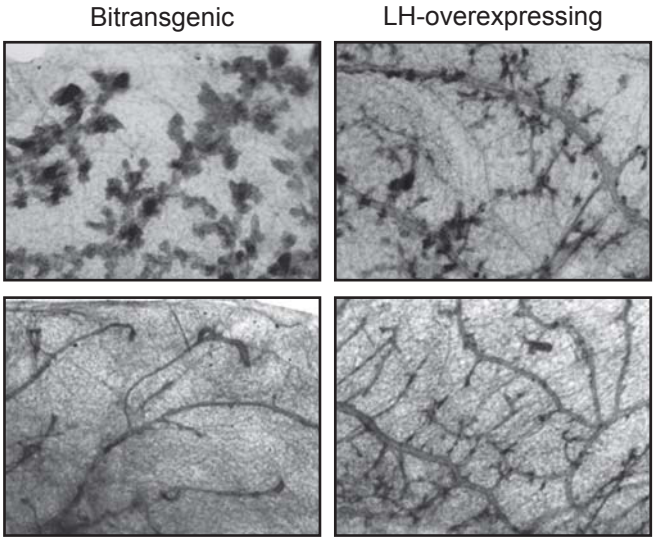

Figure III-6. The bitransgenic mammary gland becomes committed to tumorigenesis during a three-week window. Bitransgenic mice were divided into three cohorts including: 5-week ovariectomized (■, n = 9, sensored = 6 after 60 weeks), 8-week ovariectomized (●, n = 19, sensored = 0), or sham-operated controls (▲, n = 16, sensored = 0). Following either ovariectomy (OVX) or sham surgery, mice were palpated weekly to detect mammary tumor development. Statistical analysis and graphical representation of tumor development was generated by Kaplan-Meier survival analysis. Sensored events, or animals that were removed from the study for reasons unrelated to tumor development, were included in the analysis. The arrows at 5 and 8 weeks indicate the age at time of surgery. The median tumor latency for the 8-week ovariectomized and sham-operated animals was 25.0 ± 21.8 and 19.5 ± 2.2 (median ± S.D.) weeks, respectively. The median tumor latency for the 5-week ovariectomized animals can not be calculated because only thirty percent of these mice developed palpable tumors by two years of age. All curves shown were significantly different from each other [(5wk vs 8wk OVX: log rank test Chi Square = 20.1, $p < 0.0001$) (5wk OVX vs sham: log rank test Chi Square = 20.2, $p < 0.0001$) (8wk OVX vs sham: log rank test Chi Square = 11.6, $p < 0.0007$)].

Figure III-6

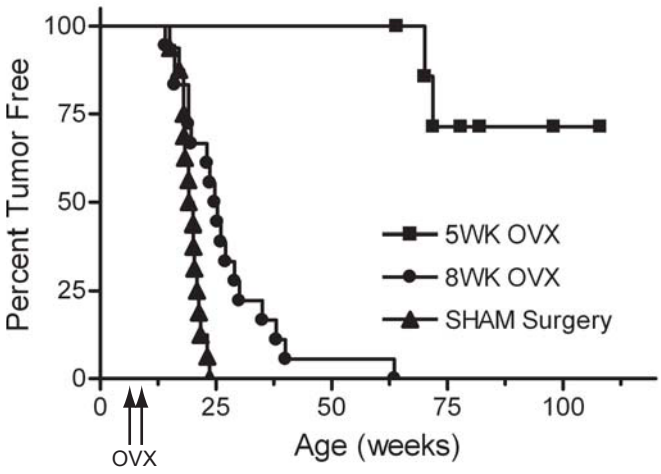
Percent Tumor Free
100
75
50
25
0
0
25
50
75
100
Age (weeks)
OVX
5WK OVX
8WK OVX
SHAM Surgery

Table III-1. Identification of Genes Whose Expression Changes During the Transition from Normal to Preneoplastic Mammary Tissue and is Maintained in Tumors.

Gene Name	Gene Symbol	Genbank Accession	Probe Set		Fold Change[a]	
			MOE430v2	U74Av2	10vs5wk	TUvsWT[b]
Increased in preneoplastic tissue and tumors						
RIKEN cDNA 1190006E07 gene	1190006E07Rik	AA881383	1428252_at	160112_at	1.7	2.3
RIKEN cDNA 1600029D21 gene	1600029D21Rik	BC022950	1423933_a_at	97413_at	2.5	8.6
RIKEN cDNA 1810015C04 gene	1810015C04Rik	BC019494	1424683_at	95518_at	2.4	3.5
RIKEN cDNA 2310009N05 gene	2310009N05Rik	AW061073	1426567_a_at	160801_at	2.0	3.1
RIKEN cDNA 2310009N05 gene	2310009N05Rik	AK009256	1430125_s_at	160801_at	2.2	3.1
fatty acid-Coenzyme A ligase, long chain 4	Acsl4	BQ174545	1433531_at	102381_at	3.6	19.4
absent in melanoma 1	Aim1	BM233292	1426942_at	103443_at	1.9	3.7
aldolase 3, C isoform	Aldo3	BC008184	1451461_a_at	160546_at	2.4	14.5
Rho guanine nucleotide exchange factor (GEF) 5	Arhgef5	BC025127	1452304_a_at	160977_at	2.0	2.2
ATPase, H+ transporting, lysosomal accessory protein 2	Atp6ap2	BC014706	1423662_at	160202_at	1.8	2.8
ATPase, H+ transporting, V1 subunit A, isoform 1	Atp6v1a1	NM_007508	1422508_at	95746_at	1.7	2.6
cDNA sequence BC037006	BC037006	AU017197	1420008_s_at	96518_at	2.2	4.9
claudin 3*	Cldn3	AW611462	1460569_x_at	94493_at	2.1	3.6
claudin 3*	Cldn3	BC012650	1451701_x_at	94493_at	2.2	3.6
claudin 3*	Cldn3	AW611462	1434651_a_at	94493_at	2.3	3.6
claudin 7	Cldn7	BC008104	1448393_at	99561_f_at	2.1	3.7
cytidine monophospho-N-acetylneuraminic acid synthetase	Cmas	AJ006215	1426662_at	98593_at	1.9	4.7
cytochrome b-561	Cyb561	BC006732	1417507_at	103423_at	2.5	2.4
DNA segment, Chr 3, University of California at Los Angeles 1	D3Ucla1	BF658806	1415827_a_at	95708_at	1.7	2.6
death-associated protein	Dap	BC024876	1423790_at	93842_at	1.6	2.1
differentially expressed in B16F10 1	Deb1	AK003863	1427955_a_at	95478_at	1.7	2.3
desmoglein 2	Dsg2	C79957	1449740_s_at	104480_at	2.4	6.1
phenylalkylamine Ca2+ antagonist (emopamil) binding protein	Ebp	NM_007898	1416667_at	96627_at	1.7	1.7
ets homologous factor	Ehf	BC008249	1419474_a_at	102243_at	2.3	3.9
elongation factor RNA polymerase II 2	Ell2	NM_138953	1450744_at	103892_r_at	2.6	2.3
FXYD domain-containing ion transport regulator 3	Fxyd3	NM_008557	1418374_at	103059_at	1.8	3.8
UDP-N-acetyl-alpha-D-galactosamine:polypeptide N-acetylgalactosamii	Galnt3	AK019995	1417588_at	99011_at	2.6	7.2
golgi phosphoprotein 3	Golph3	AW413496	1420116_s_at	160688_at	1.6	2.3
inhibitor of DNA binding 2	Idb2	BF019883	1435176_a_at	93013_at	2.0	3.7
interferon regulatory factor 6	Irf6	NM_016851	1418301_at	92440_at	2.2	2.8
Iroquois related homeobox 3 (Drosophila)	Irx3	NM_008393	1418517_at	99034_at	1.8	2.3
kangai 1 (suppression of tumorigenicity 6, prostate)	Kai1	NM_007656	1416401_at	99584_at	2.5	3.1
potassium intermediate/small conductance calcium-activated channel, s	Kcnn4	NM_008433	1421038_a_at	102198_at	2.4	10.1

Table III-1. Identification of Genes Whose Expression Changes During the Transition from Normal to Preneoplastic Mammary Tissue and is Maintained in Tumors.

Gene Name	Gene Symbol	Genbank Accession	Probe Set		Fold Change[a]	
			MOE430v2	U74Av2	10vs5wk	TUvsWT[b]
Increased in preneoplastic tissue and tumors (cont.)						
lipocalin 2	Lcn2	X14607	1427747_a_at	160564_at	2.0	6.9
liver-specific bHLH-Zip transcription factor	Lisch7	BC004672	1451255_at	99452_at	2.0	2.1
LPS-induced TN factor	Litaf	AV360881	1416303_at	93753_at	2.0	2.6
leucine rich repeat (in FLII) interacting protein 1	Lrrfip1	BG069059	1433842_at	92564_at	1.7	3.9
nucleobindin 2	Nucb2	NM_016773	1418355_at	102197_at	5.3	6.3
ring finger protein 149	Rnf149	T12280	1429321_at	98915_at	2.5	1.7
shroom	Shrm	NM_015756	1422629_s_at	100024_at	2.3	4.9
SRY-box containing gene 4	Sox4	AI428101	1419156_at	160109_at	1.5	3.4
serine protease inhibitor, Kunitz type 1	Spint1	NM_016907	1416627_at	97206_at	3.4	3.4
signal recognition particle 19	Srp19	W08076	1450891_at	160343_at	1.5	1.9
spermatid perinuclear RNA binding protein	Strbp	AK006314	1452061_s_at	103330_at	2.0	2.6
transcription factor AP-2, gamma	Tcfap2c	BB550860	1436392_s_at	92275_at	1.8	4.2
transcription factor AP-2, gamma	Tcfap2c	BC003778	1418147_at	92275_at	1.9	4.2
T-cell immunoglobulin and mucin domain containing 2*	Timd2	BC028829	1418766_s_at	103794_i_at	3.5	4.6
T-cell immunoglobulin and mucin domain containing 2*	Timd2	BC028829	1418765_at	97335_at	4.5	2.4
tumor protein D52	Tpd52	BC002036	1419493_a_at	160249_at	2.2	2.9
vitamin D receptor	Vdr	AV290079	1418176_at	99964_at	4.0	1.9
X-box binding protein 1*	Xbp1	C77390	1420011_s_at	94821_at	2.0	2.7
X-box binding protein 1*	Xbp1	NM_013842	1420886_a_at	94821_at	2.1	2.7
Decreased in preneoplastic tissue and tumors						
RIKEN cDNA 2310047C17 gene	1110004P15Rik	BE570050	1452217_at	160255_at	0.7	0.2
RIKEN cDNA 1110021N07 gene	1110021N07Rik	AV310010	1433563_s_at	93983_at	0.6	0.4
RIKEN cDNA 2610001E17 gene	2610001E17Rik	BG074158	1424186_at	160298_at	0.5	0.1
procollagen, type V, alpha 1	AI413331	AV246911	1434479_at	93472_at	0.3	0.5
aminolevulinate, delta-, dehydratase	Alad	BC018236	1424877_a_at	101044_at	0.7	0.3
aminolevulinic acid synthase 1	Alas1	BC022110	1424126_at	93500_at	0.5	0.5
602117651F1; cDNA clone IMAGE:3468684	Angptl2	BF681826	1455090_at	103556_at	0.3	0.1
cDNA sequence BC054059	BC054059	AY092026	1424729_at	96237_at	0.5	0.2
branched chain ketoacid dehydrogenase E1, beta polypeptide	Bckdhb	AW047304	1427153_at	102302_at	0.6	0.3
BCL2/adenovirus E1B 19kDa-interacting protein 1, NIP2	Bnip2	AV144704	1422490_at	93064_at	0.6	0.5
CD34 antigen	Cd34	NM_133654	1416072_at	160358_at	0.4	0.2
procollagen, type XVIII, alpha 1	Col18a1	NM_009929	1418237_s_at	101881_g_at	0.2	0.1

Table III-1. Identification of Genes Whose Expression Changes During the Transition from Normal to Preneoplastic Mammary Tissue and is Maintained in Tumors.

Gene Name	Gene Symbol	Genbank Accession	Probe Set		Fold Change[a]	
			MOE430v2	U74Av2	10vs5wk	TUvsWT[b]
Decreased in preneoplastic tissue and tumors (cont.)						
procollagen, type I, alpha 1	Col1a1	U08020	1423669_at	94305_at	0.4	0.3
procollagen, type III, alpha 1	Col3a1	AW550625	1427884_at	102990_at	0.5	0.1
procollagen, type IV, alpha 1	Col4a1	BF158638	1452035_at	101093_at	0.7	0.5
procollagen, type VI, alpha 3	Col6a3	AF064749	1424131_at	101110_at	0.5	0.2
cysteine-rich protein 1 (intestinal)	Crip1	NM_007763	1416326_at	94061_at	0.6	0.2
chemokine (C-X-C motif) ligand 12	Cxcl12	NM_013655	1417574_at	100112_at	0.3	0.3
RIKEN cDNA 1110001I14 gene	D6Ucla1e	BG074607	1434329_s_at	104605_at	0.6	0.3
2,4-dienoyl CoA reductase 1, mitochondrial	Decr1	NM_026172	1419367_at	160711_at	0.6	0.2
diacylglycerol O-acyltransferase 1	Dgat1	BC003717	1418295_s_at	104371_at	0.6	0.1
dehydrogenase/reductase (SDR family) member 7	Dhrs7	AK009385	1426440_at	95620_at	0.6	0.5
dipeptidase 1 (renal)	Dpep1	AI647687	1435943_at	103644_at	0.5	0.1
dermatopontin	Dpt	NM_019759	1418511_at	96742_at	0.5	0.1
epoxide hydrolase 2, cytoplasmic	Ephx2	NM_007940	1448499_a_at	93051_at	0.4	0.1
electron transferring flavoprotein, beta polypeptide	Etfb	BI692487	1428181_at	96947_at	0.6	0.2
fasciculation and elongation protein zeta 2 (zygin II)	Fez2	BM206792	1434348_at	101934_at	0.6	0.5
fat specific gene 27	Fsp27	BB221402	1452260_at	102016_at	0.4	0.0
follistatin-like 1	Fstl1	BI452727	1448259_at	94833_at	0.3	0.4
602109129F1 NCI_CGAP_Kid14 cDNA clone IMAGE:4237519	Fzd4	BF783030	1419301_at	95771_i_at	0.5	0.1
growth arrest specific 6	Gas6	NM_019521	1417399_at	99067_at	0.4	0.3
growth hormone receptor	Ghr	BC024375	1451501_a_at	99108_s_at	0.5	0.1
BB039269 RIKEN cDNA clone 6030441J06*	Gja1	BB039269	1437992_x_at	100064_f_at	0.4	0.2
BB142324 RIKENcDNA clone 9930014N10*	Gja1	BB142324	1438945_x_at	100064_f_at	0.4	0.2
gap junction membrane channel protein alpha 1*	Gja1	M63801	1415800_at	100064_f_at	0.4	0.2
gap junction membrane channel protein alpha 1*	Gja1	AV330726	1438650_x_at	100064_f_at	0.4	0.2
guanine nucleotide binding protein, alpha inhibiting 1	Gnai1	BQ174580	1454959_s_at	104412_at	0.6	0.0
glycerol-3-phosphate acyltransferase, mitochondrial	Gpam	NM_008149	1419499_at	101867_at	0.6	0.2
hexose-6-phosphate dehydrogenase (glucose 1-dehydrogenase)	H6pd	BC027358	1452145_at	104148_at	0.4	0.5
hephaestin	Heph	NM_010417	1448696_at	104194_at	0.2	0.2
heat shock 27kDa protein 8	Hspb8	AF250139	1417013_at	160139_at	0.4	0.3
isocitrate dehydrogenase 1 (NADP+), soluble*	Idh1	NM_010497	1422433_s_at	160571_at	0.4	0.4
isocitrate dehydrogenase 1 (NADP+), soluble*	Idh1	AI788952	1419821_s_at	160571_at	0.5	0.4
insulin-like growth factor binding protein 6	Igfbp6	NM_008344	1417933_at	103904_at	0.3	0.0
Kruppel-like factor 4 (gut)	Klf4	BG069413	1417394_at	99622_at	0.5	0.2
laminin B1 subunit 1*	Lamb1-1	BG970109	1424113_at	101948_at	0.5	0.2

Table III-1. Identification of Genes Whose Expression Changes During the Transition from Normal to Preneoplastic Mammary Tissue and is Maintained in Tumors.

Gene Name	Gene Symbol	Genbank Accession	Probe Set		Fold Change[a]	
			MOE430v2	U74Av2	10vs5wk	TUvsWT[b]
Decreased in preneoplastic tissue and tumors (cont.)						
laminin B1 subunit 1*	Lamb1-1	BG970109	1424114_s_at	101948_at	0.5	0.2
lumican	Lum	AK014312	1423607_at	93353_at	0.5	0.1
mannosidase 1, alpha	Man1a	BB070019	1417111_at	160579_at	0.7	0.1
manic fringe homolog (Drosophila)	Mfng	NM_008595	1416992_at	100508_at	0.5	0.3
3-ketoacyl-CoA thiolase B	MGC29978	BC019882	1424451_at	99571_at	0.5	0.3
mannose receptor, C type 1	Mrc1	NM_008625	1450430_at	103226_at	0.5	0.2
microtubule-associated protein 4	Mtap4	BB000894	1416091_at	92795_at	0.5	0.5
nuclear receptor subfamily 1, group H, member 3	Nr1h3	NM_013839	1450444_a_at	104381_at	0.6	0.1
neuropilin*	Nrp	AK011144	1418084_at	95016_at	0.4	0.2
neuropilin*	Nrp	AK011144	1448943_at	92773_at	0.6	0.3
BB220000 RIKEN cDNA clone A530058E15	Pde8a	BB220000	1418406_at	160941_at	0.6	0.2
preproenkephalin 1	Penk1	M13227	1427038_at	94516_f_at	0.2	0.2
phosphoglucomutase 2	Pgm2	BC008527	1451149_at	104313_at	0.5	0.3
phytanoyl-CoA hydroxylase	Phyh	NM_010726	1460194_at	96608_at	0.4	0.4
placenta-specific 8	Plac8	AF263458	1451335_at	98092_at	0.3	0.3
protein phosphatase 2, regulatory subunit B (B56), alpha isoform	Ppp2r5a	BC023062	1423911_at	93826_at	0.6	0.2
protein kinase C, delta binding protein	Prkcdbp	BC009660	1423771_at	97496_f_at	0.4	0.2
protease, serine, 11 (Igf binding)	Prss11	NM_019564	1416749_at	96920_at	0.4	0.1
quaking	Qk	NM_021881	1417073_a_at	160726_at	0.5	0.2
RAB34, member of RAS oncogene family*	Rab34	AF327929	1416590_a_at	160317_at	0.5	0.3
RAB34, member of RAS oncogene family*	Rab34	AF327929	1416591_at	160317_at	0.7	0.3
S100 calcium binding protein A6 (calcyclin)	S100a6	NM_011313	1421375_a_at	92770_at	0.4	0.3
sialyltransferase 10 (alpha-2,3-sialyltransferase VI)	Siat10	NM_018784	1449078_at	102208_at	0.4	0.2
sorbin and SH3 domain containing 1	Sorbs1	AF078667	1425826_a_at	160320_at	0.5	0.1
sulfide quinone reductase-like (yeast)	Sqrdl	AF174535	1420641_a_at	94515_at	0.5	0.4
sushi-repeat-containing protein	Srpx	AB028050	1451939_a_at	103568_at	0.2	0.1
RIKEN clone:0610030E04	Sult1a1	AK002700	1427345_a_at	103087_at	0.5	0.0
transforming growth factor, beta induced	Tgfbi	NM_009369	1448123_s_at	92877_at	0.6	0.3
thrombomodulin	Thbd	NM_009378	1448529_at	104601_at	0.4	0.3
tetranectin (plasminogen binding protein)	Tna	NM_011606	1449466_at	92224_at	0.5	0.1
uridine monophosphate kinase	Umpk	BC025146	1424399_at	94381_at	0.5	0.5
Von Willebrand factor homolog	Vwf	BB667216	1435386_at	103499_at	0.3	0.0
zinc finger homeobox 1a	Zfhx1a	NM_011546	1418926_at	99052_at	0.5	0.3

Table III-1. Identification of Genes Whose Expression Changes During the Transition from Normal to Preneoplastic Mammary Tissue and is Maintained in Tumors.

Gene Name	Gene Symbol	Genbank Accession	Probe Set		Fold Change[a]	
			MOE430v2	U74Av2	10vs5wk	TUvsWT[b]

[a] Fold change was derived from the Affymetrix signal log ratio (SLR). 10wk = committed and 5wk = precommitted bitransgenic mammary glands.

[b] TU = MMTV-*Neu* tumors WT = wild-type control. TUvsWT was previously published and is shown here for comparison (Landis et al., 2005)

* Multiple probe sets represent these genes on the MG430v2 GeneChip.

Table III-2. Identification of Genes Whose Expression Changes During the Transition from Normal to Preneoplastic Mammary Tissue.

Gene Name	Gene Symbol	Genbank Accession	Probe Set		Fold Change[a]	
			MOE430v2	U74Av2	10vs5wk	ANvsWT[b]
Increased in committed mammary tissue						
PQ loop repeat containing 1*	Pqlc1	AW061073	1426567_a_at	160801_at	2.0	1.6
inhibitor of DNA binding 2	Idb2	BF019883	1435176_a_at	93013_at	2.0	2.1
lipocalin 2	Lcn2	X14607	1427747_a_at	160564_at	2.0	2.7
PQ loop repeat containing 1*	Pqlc1	AK009256	1430125_s_at	160801_at	2.2	1.6
tumor protein D52	Tpd52	BC002036	1419493_a_at	160249_at	2.2	1.8
potassium intermediate/small conductance calcium-activated channel	Kcnn4	NM_008433	1421038_a_at	102198_at	2.4	3.0
desmoglein 2	Dsg2	C79957	1449740_s_at	104480_at	2.4	4.1
kangai 1 (suppression of tumorigenicity 6, prostate)	Kai1	NM_007656	1416401_at	99584_at	2.5	2.3
RIKEN cDNA 1600029D21 gene	1600029D21Rik	BC022950	1423933_a_at	97413_at	2.5	4.2
fatty acid-Coenzyme A ligase, long chain 4	Acsl4	BQ174545	1433531_at	102381_at	3.6	5.7
Decreased in committed mammary tissue						
aminolevulinate, delta-, dehydratase	Alad	BC018236	1424877_a_at	101044_at	0.7	0.6
RAB34, member of RAS oncogene family*	Rab34	AF327929	1416591_at	160317_at	0.7	0.5
electron transferring flavoprotein, beta polypeptide	Etfb	BI692487	1428181_at	96947_at	0.6	0.5
guanine nucleotide binding protein, alpha inhibiting 1	Gnai1	BQ174580	1454959_s_at	104412_at	0.6	0.4
2,4-dienoyl CoA reductase 1, mitochondrial	Decr1	NM_026172	1419367_at	160711_at	0.6	0.6
dehydrogenase/reductase (SDR family) member 7	Dhrs7	AK009385	1426440_at	95620_at	0.6	0.7
glycerol-3-phosphate acyltransferase, mitochondrial	Gpam	NM_008149	1419499_at	101867_at	0.6	0.4
nuclear receptor subfamily 1, group H, member 3	Nr1h3	NM_013839	1450444_a_at	104381_at	0.6	0.6
adiponectin receptor 2	Adipor2	BG074607	1434329_s_at	104605_at	0.6	0.5
branched chain ketoacid dehydrogenase E1, beta polypeptide	Bckdhb	AW047304	1427153_at	102302_at	0.6	0.6
protein phosphatase 2, regulatory subunit B (B56), alpha isoform	Ppp2r5a	BC023062	1423911_at	93826_at	0.6	0.6
diacylglycerol O-acyltransferase 1	Dgat1	BC003717	1418295_s_at	104371_at	0.6	0.5
RAB34, member of RAS oncogene family*	Rab34	AF327929	1416590_a_at	160317_at	0.5	0.5
procollagen, type VI, alpha 3	Col6a3	AF064749	1424131_at	101110_at	0.5	0.6
3-ketoacyl-CoA thiolase B	MGC29978	BC019882	1424451_at	99571_at	0.5	0.5
growth hormone receptor	Ghr	BC024375	1451501_a_at	99108_s_at	0.5	0.4
phosphoglucomutase 2	Pgm2	BC008527	1451149_at	104313_at	0.5	0.5
uridine monophosphate kinase	Umpk	BC025146	1424399_at	94381_at	0.5	0.6
protease, serine, 11 (Igf binding)	Prss11	NM_019564	1416749_at	96920_at	0.4	0.5
fat specific gene 27	Fsp27	BB221402	1452260_at	102016_at	0.4	0.5
sialyltransferase 10 (alpha-2,3-sialyltransferase VI)	Siat10	NM_018784	1449078_at	102208_at	0.4	0.5
chemokine (C-X-C motif) ligand 12	Cxcl12	NM_013655	1417574_at	100112_at	0.3	0.6
insulin-like growth factor binding protein 6	Igfbp6	NM_008344	1417933_at	103904_at	0.3	0.6
preproenkephalin 1	Penk1	M13227	1427038_at	94516_f_at	0.2	0.6

[a] Fold change was derived from the Affymetrix signal log ratio (SLR). 10wk = committed and 5wk = non-committed bitransgenic mammary glands.

[b] AN = preneoplastic adjacent Neu tissue, WT = wild-type control. ANvsWT was previously published (Landis et al., 2005).

* Multiple probe sets represent these genes on the MG430v2 GeneChip.

CHAPTER IV

SUMMARY AND FUTURE DIRECTIONS

SUMMARY

The goal of this thesis was to elucidate mechanisms of ErbB2/Neu oncogenesis. In **Chapter II**, I described the derivation of an ErbB2/Neu tumor molecular signature. Identification of subset of these genes by microarray analyses of preneoplastic ErbB2/Neu-overexpressing tissue from two independent mouse models strongly supports a role for these genes in early events of ErbB2/Neu-induced tumorigenesis (**Chapters II and III**). Future examination of these candidate genes should divulge information regarding ErbB2/Neu acquisition of oncogenic capabilities.

Further analysis of the genes contained in the ErbB2/Neu tumor signature revealed intrinsic suppression of the TGF-β signaling pathway (**Chapter II**) and subsequent confirmation of TβRI downregulation suggests that ErbB2/Neu suppresses TGF-β activity to overcome its growth inhibitory abilities during tumor development. Also, active Smad signaling colocalized with expression of Activin receptor, implicating Activin signaling in ErbB2/Neu tumorigenesis. Additional investigation regarding the role of Activin and TGF-β activity in ErbB2/Neu tumorigenesis and the mechanisms for cross-talk between each of these pathways and ErbB2/Neu signaling should be interesting areas to pursue further.

The discovery that hormonal environment may maintain a population of cells that are targeted for ErbB2/Neu-initiated tumorigenesis (**Chapter III**) has intriguing implications for hormonal modulation of ErbB2/Neu-induced tumorigenesis. In whole, this work has lead to development of numerous hypotheses that can be the subject for future investigation of ErbB2/Neu oncogenic mechanisms. In this chapter (**Chapter IV**), I will outline several experimental approaches to explore these prospective oncogenic mechanisms.

FUTURE DIRECTIONS

Derivation of the ErbB2/Neu tumor molecular signature and subsequent verification of a subset of these genes by real-time RT-PCR was described in **Chapter II**. Since a subset of these genes was also changed in preneoplastic tissue from two different transgenic mouse models of ErbB2/Neu-initiated tumorigenesis, we postulate that those genes are involved in early events of ErbB2/Neu-initiated tumorigenesis. Microarray analysis is a hypotheses generating tool. As such, in this chapter, I have outlined several hypotheses that were generated from our microarray analyses and described different experimental approaches to examine these.

One of our goals in performing extensive microarray analysis was to identify transcriptional targets of ErbB2/Neu that contribute to ErbB2/Neu-induced tumorigenesis. While we identified genes that change expression level in ErbB2/Neu tumors and in ErbB2/Neu-overexpressing preneoplastic mammary tissue, further experimentation is required to determine whether these genes are

indeed targets of ErbB2/Neu and whether they contribute to ErbB2/Neu tumor progression.

Hypothesis:* Gene X *is a target of ErbB2/Neu signaling

Which genes from the ErbB2/Neu tumor molecular signature and the preneoplastic gene list are targets of ErbB2/Neu signaling? Since a large number of genes (n=324) are contained in the ErbB2/Neu tumor molecular signature (**Chapter II**), it will be necessary to utilize high throughput approaches to determine which of these genes are indeed ErbB2/Neu transcriptional targets. To this end, microarray analysis of mammary epithelial cell lines following treatment with EGF-like ligands should be performed. This can be accomplished by activating ErbB2/Neu signaling with the EGF-like growth factor ligands NRG and EGF in normal mouse mammary epithelial cells. NRG and EGF were chosen because they will activate ErbB3 and EGFR signaling, respectively (Klapper et al., 1999). To determine whether signaling occurs through ErbB2/Neu, for each experimental group, a control group should be included in which the cells are pretreated with an ErbB2/Neu-targeted antibody. RNA should be collected at early timepoints to identify primary transcriptional targets. Each of these samples should then be used to generate labeled cRNA probes for hybridization with Affymetrix 430v2 GeneChips, and comparative analysis should be performed to identify the genes that change expression with activation of ErbB signaling pathways. Removal of the genes that do not change expression with ErbB2/Neu-targeted antibody preincubation should eliminate genes that are targets of ErbB3 or EGFR but not ErbB2/Neu signaling. The genes that are

identified by these analyses should then be compared to the ErbB2/Neu tumor molecular signature genes as well as the preneoplastic gene list to determine which of those genes are ErbB2/Neu targets.

Is the protein product of Gene X *altered by ErbB2/Neu signaling?* To determine whether the encoded protein product for *Gene X* changes expression, whole cell lysate should be collected at multiple time points as described above for the microarray analysis. Sequential western blot analysis should be carried out with commercially available antibodies against the proteins of interest.

Hypothesis: Gene X contributes to ErbB2/Neu-induced mammary tumorigenesis.

Which genes will be interesting candidates to pursue further? After identifying numerous genes by microarray analysis, we researched each gene individually to identify "interesting" genes. Interesting candidate genes for contribution to ErbB2/Neu tumor progression are transcription factors and genes involved in cellular processes that become deregulated during tumorigenesis such as cell cycle, cell growth, differentiation, genomic stability, apoptosis, cell adhesion, and cell migration. We are particularly interested in transcription factors because altering expression of a single transcription factor will change the entire transcriptome of the cell and have far reaching affects. In considering the biological relevance of candidate genes, several approaches can be utilized.

Is candidate Gene X *expression altered in human breast cancer? Does expression of the protein encoded by* Gene X *correlate with ErbB2/Neu*

expression in human breast cancer specimens? To determine whether expression of candidate genes correlates with *ErbB2/Neu* expression in human breast specimens, *in situ* hybridization with labeled probes specific for candidate genes and *ErbB2/Neu* mRNA should be performed on human breast tissue arrays containing tumor specimens and normal adjacent tissue. To examine protein expression, immunohistochemistry with commercially available antibodies should be carried out on human breast tissue arrays containing tumor tissue and adjacent normal tissue. Expression of *Gene X* should be correlated with ErbB2/Neu expression and activation.

Does alteration of candidate Gene X *expression affect ErbB2/Neu oncogenic capabilities* in vitro *and* in vivo*?* To determine whether the genes identified by our microarray analysis do indeed contribute to ErbB2/Neu-initiated tumorigenesis several strategies could be employed. First, in normal epithelial cell lines that overexpress ErbB2/Neu such as MCF10A/HER2 cells (Ueda et al., 2004; Wang et al., 2005), the expression of *Gene X* should be manipulated by knock-down strategies such as pharmacological inhibitors or siRNA or overexpression approachess. The method of manipulation will be dependent on whether the gene was increased or decreased in the microarray data. If it was increased in the microarray data, it should be blocked. Alternatively, if it was decreased in microarray data, it should be induced. Then several *in vitro* transformation assays should be utilized including: 1) colony formation assays, 2) growth on soft agar, and 3) growth in nude mice. If Gene X contributes to ErbB2/Neu tumor progression, one would expect to see decreased tumorigenicity

by manipulating *Gene X* expression. Ultimately, bitransgenic mouse models should be generated to assess the contribution of *Gene X* to ErbB2/Neu-initiated tumorigenesis *in vivo*. Depending on the direction of expression change in the microarray data, the MMTV-*Neu* mice should be bred with an overexpressing or knock-down mouse model for *Gene X*. If Gene X contributes to ErbB2/Neu tumor progression, primary mammary tumor latency or incidence and/or pulmonary metastasis would be altered. In our laboratory, these types of studies have already been initiated for three candidate transcription factor genes: LMO4, Id2, and GKLF.

Hypothesis: ErbB2/Neu suppresses TGF-β activity to prevent its growth inhibitory affects during tumor development.

Is the TGF-β signaling pathway indeed inactive in ErbB2/Neu-induced tumors? Investigation of the genes contained in the ErbB2/Neu tumor signature revealed that the expression of gene targets of the TGF-β signaling pathway was decreased in ErbB2/Neu tumors, suggesting the TGF-β signaling pathway is suppressed during ErbB2/Neu tumor development (**Chapter II**). Subsequent western blot and immunohistochemical analyses for components of the TGF-β pathway confirmed that TβRI is suppressed in ErbB2/Neu tumors (**Chapter II**). To determine whether the TGF-β pathway is intact and capable of signaling in ErbB2/Neu tumors, we have attempted two different experimental approaches. The goal of the first approach was to inject TGF-β ligand directly into ErbB2/Neu tumors in MMTV-Neu mice and then perform immunohistochemistry for phosphorylated Smad2 on sections of these tumors. We found that it was much

too difficult to carefully mark the injection site and then locate it in 5 micron sections from paraffin-embedded blocks of tumors (data not shown). Alternatively, we performed “quadrant” tumor studies in which we grossly quartered tumors and treated each quadrant with either TGF-β ligand or vehicle in cell culture media. We were unable to consistently detect phosphorylated Smad2 by immunohistochemistry even in our control samples (data not shown). Based on the technical issues that arose with these approaches, I propose a third approach involving culture of primary tumor cells followed by *in vitro* treatment with TGF-β ligand in cell culture media. Immunocytochemistry for phosphorylated Smad2 should be used as a measure of active TGF-β signaling. We would expect tumor cells to be nonresponsive to TGF-β treatment due to downregulation of TβRI. Of course, one caveat is that culturing conditions may change the intrinsic properties of these tumor cells.

What is the cellular outcome of TGF-β suppression? Based on the growth inhibitory role of TGF-β, we postulate that ErbB2/Neu gains oncogenic capabilities by suppressing TGF-β signaling and thus preventing the growth inhibitory activities of TGF-β in tumor cells. To test this hypothesis, we could replace TβRI in primary tumor cell cultures by viral-infection with constructs encoding TβRI, treat with TGF-β, and measure cell growth. We would expect replacement of TβRI to allow cells to respond appropriately to TGF-β by growth inhibition. Alternatively, other components of the TGF-β pathway may be altered in tumor cells, so replacement of TβRI alone may not be sufficient to restore TGF-β activity. This possibility will be discussed further, below.

What components of the TGF-β pathway does ErbB2/Neu signaling regulate? We suspect that the ErbB2/Neu pathway suppresses TGF-β signaling through multiple routes. Recently, another group reported that ErbB2/Neu can collaborate with ER81 to upregulate the expression of the inhibitory Smad7 in breast cancer cells (Dowdy et al., 2003). To determine the mechanism(s) for suppression of the TGF-β signaling pathway, we can first examine expression of ErbB2/Neu and components of the TGF-β signaling pathway including TGF-β1, TGF-β2, TGF-β2, TβRI, TβRII, Smad2, Smad3, Smad4, inhibitory Smads 6 and 7, and ErbB2/Neu in MMTV-*Neu* tumor cell primary cultures. We can also assess activation by immunocytochemistry for phosphorylation of ErbB2/Neu, Smad2, and Smad3. If additional components of the TGF-β signaling pathway are altered in expression, each of these proteins could be added back, individually and in combinations, by viral-infection to determine whether they can restore TGF-β responsiveness. Once expression levels and activation status are determined, we could treat with various ErbB receptor-specific inhibitors to determine which ErbB pathways regulate expression and/or activation of the TGF-β signaling pathway.

Alternatively, since the TGF-β pathway can be regulated on multiple levels (Derynck et al., 2001; Massague, 1998; Massague, 2000; Reiss, 1999; Siegel and Massague, 2003), it is possible that ErbB2/Neu signaling does not actually alter expression levels of TGF-β pathway components, but regulates TGF-β signaling by other mechanisms. For example, TGF-β ligands are produced in latent forms that must be processed before binding TGF-β receptors. It is

possible that ErbB2/Neu alters processing of the TGF-β ligands and thus alters TGF-β signaling. Or perhaps ErbB2/Neu alters stability of components of the TGF-β signaling pathway. Thus, alternative mechanisms for cross-talk between these signling pathways should be addressed in future experiments.

Hypothesis: Activin signaling is active in ErbB2/Neu tumors

We found that ActRIB and phosphorylated Smad2 are both present in the periphery of ErbB2/Neu tumors, suggesting that Activin signaling is active in this region of these tumors (**Chapter II**). To determine whether the Activin signaling pathway is indeed intact in ErbB2/Neu tumors, we could examine expression of components of the Activin signaling pathway in primary cultures of MMTV-*Neu* tumor cells. We could also treat with the Activin inhibitor, Follistatin (Phillips and de Kretser, 1998), and determine whether phosphorylation of Smad2 is attenuated, indicating that the phosphorylated Smad2 in these tumors is caused by Activin signaling.

Hypothesis: Activin signaling alters ErbB2/Neu tumor progression.

Recent cancer cell line data suggests a growth suppressive role for Activin (Cocolakis et al., 2001; Kalkhoven et al., 1995; Liu et al., 1996), but biological data are currently lacking. To determine whether Activin alters ErbB2/Neu tumor progression, we could initially determine how co-stimulation of ErbB2/Neu and Activin signaling affects *in vitro* tumorigenicity and migration assays in normal mammary epithelial cells. Ultimately, we could generate bitransgenic mice by breeding MMTV-*Follistatin* overexpressing mice with MMTV-*Neu* mice and

measuring primary tumor latency and pulmonary metastasis. If Activin suppresses ErbB2/Neu-induced tumorigenesis, we would expect Activin inhibition by Follistatin in these bitransgenic mice to accelerate tumorigenesis or enhance metastasis. It is possible that Activin has dual roles like TGF-β during mammary gland tumorigenesis, both suppressing primary tumor growth and promoting metastasis. If so, manipulation of Activin and its signaling pathways might be advantageous in our efforts to treat or prevent breast cancer, especially ErbB2/Neu positive tumors.

Hypothesis: Hormonal environment maintains ErbB2/Neu target cell population.

Recent studies have shown that pregnancy can accelerate development of ErbB2/Neu tumors, inducing a susceptible cell population in MMTV-*Neu* mammary glands (Henry et al., 2004). Multiparous MMTV-Neu mice develop mammary tumors in a stochastic manner with long latency (Anisimov et al., 2003; Guy et al., 1992; Henry et al., 2004). The stochastic nature of tumor development in these mice indicates that additional "hits" are required to produce tumors. We generated a bitransgenic mouse model of ErbB2/Neu-induced tumorigenesis by breeding the MMTV-*Neu* mice with a model of ovarian hyperstimulation, LH-overexpressing mice (**Chapter III**). These mice developed mammary tumors in a more accelerated and synchronous manner than MMTV-*Neu* mice alone, suggesting that the hormonal milieu in these bitransgenic mice provides the additional "hits" required to develop overt tumors. We postulate that the pregnancy-inducible susceptible cell population described

by Wagner and colleagues (Henry et al., 2004) is maintained by trophic hormonal support in our bitransgenic mouse model. Since the mammary glands of LH-overexpressing mice are highly similar to mid-pregnancy glands (Milliken et al., 2002), it is likely that a similar susceptible cell population is induced and maintained in the hormonal environment of these mice. Elevated expression of whey acidic protein, the marker of this ErbB2/Neu-targeted cell population, occurs in the mammary glands of LH-overexpressing mice (Milliken et al., 2002), further corroborating this supposition.

To test this hypothesis, we should generate triple transgenic mice by breeding the LH-overexpressing mice with the reporter mice utilized to originally identify the MMTV-*Neu* susceptible cell population (Henry et al., 2004). Henry et al. generated bitransgenic mice by breeding Whey Acidic Protein (WAP)-*Cre* mice with Rosa-*LacZ* reporter mice. The system uses Cre-lox technology in which Cre recombinase excises the DNA between two lox sites. WAP expression is induced when mammary alveolar cells differentiate during the second half of pregnancy (Wagner et al., 1997). Thus, when alveolar cells differentiate, induction of the WAP promoter causes transient expression of Cre recombinase which will, in turn, excise the floxed stop sequence between the Rosa promoter and the β-galactosidase encoding gene (*LacZ*), thus permanently labeling differentiated cells (Soriano, 1999; Wagner et al., 1997). We could generate triple transgenic mice (WAP-*Cre*/Rosa-*lacZ*/*LH*) by breeding WAP-*Cre*/Rosa-*LacZ* bitransgenics with LH-overexpressing mice. Then, we could stain both whole mammary glands and histological sections with X-gal to identify

differentiated cells (Wagner et al., 1997). We would expect to see a large population of cells that are positively stained by X-gal indicating they have undergone differentiation in the LH-overexpressing hormonal environment. One essential property of this susceptible cell population is retention during involution of the mammary gland (Henry et al., 2004). Thus, it will be critical to determine whether these cells are retained in mammary glands upon removal of ovarian hormones by ovariectomy. Furthermore, mammary tumors should also be stained with X-gal to determine whether the susceptible cell population does indeed become an overt tumor. Collectively, these may uncover a significant mechanism for hormonal modulation of ErbB2/Neu-induced tumorigenesis. Identification of a population of cells that is particularly susceptible to transformation by ErbB2/Neu could be a huge milestone for discovery of cancer drug targets. This cell population could be isolated and analyzed so that we could identify pathways that are uniquely altered in the susceptible cell population compared to normal cells, and thus therapeutically target this susceptible cell population, achieving the ultimate goal of drug design selectively targeting cancer cells while preserving normal cells.

In summary, this thesis has uncovered novel findings regarding mechanisms of ErbB2/Neu oncogenesis and, in so doing, generated several testable hypotheses that should provide additional insight into potential oncogenic mechanisms of ErbB2/Neu-intiated mammary tumorigenesis.

REFERENCES

(2005). Trastuzumab plus chemotherapy improves survival in early-stage HER2-positive breast cancer patients. Oncology (Williston. Park) *19*, 851, 862.

Adam,L., Vadlamudi,R., Kondapaka,S.B., Chernoff,J., Mendelsohn,J., and Kumar,R. (1998). Heregulin regulates cytoskeletal reorganization and cell migration through the p21-activated kinase-1 via phosphatidylinositol-3 kinase. J. Biol. Chem. *273*, 28238-28246.

Adelsman,M.A., McCarthy,J.B., and Shimizu,Y. (1999). Stimulation of beta1-integrin function by epidermal growth factor and heregulin-beta has distinct requirements for erbB2 but a similar dependence on phosphoinositide 3-OH kinase. Mol. Biol. Cell *10*, 2861-2878.

Akhurst,R.J. and Derynck,R. (2001). TGF-beta signaling in cancer--a double-edged sword. Trends Cell Biol. *11*, S44-S51.

Al Mehdi,A.B., Tozawa,K., Fisher,A.B., Shientag,L., Lee,A., and Muschel,R.J. (2000). Intravascular origin of metastasis from the proliferation of endothelium-attached tumor cells: a new model for metastasis. Nat. Med *6*, 100-102.

Alimandi,M., Romano,A., Curia,M.C., Muraro,R., Fedi,P., Aaronson,S.A., Di Fiore,P.P., and Kraus,M.H. (1995). Cooperative signaling of ErbB3 and ErbB2 in neoplastic transformation and human mammary carcinomas. Oncogene *10*, 1813-1821.

Allred,D.C., Clark,G.M., Molina,R., Tandon,A.K., Schnitt,S.J., Gilchrist,K.W., Osborne,C.K., Tormey,D.C., and McGuire,W.L. (1992). Overexpression of HER-2/neu and its relationship with other prognostic factors change during the progression of in situ to invasive breast cancer. Hum. Pathol *23*, 974-979.

Alroy,I. and Yarden,Y. (1997). The ErbB signaling network in embryogenesis and oncogenesis: signal diversification through combinatorial ligand-receptor interactions. FEBS Lett. *410*, 83-86.

Andrechek,E.R., Laing,M.A., Girgis-Gabardo,A.A., Siegel,P.M., Cardiff,R.D., and Muller,W.J. (2003). Gene Expression Profiling of Neu-induced Mammary Tumors from Transgenic Mice Reveals Genetic and Morphological Similarities to ErbB2-expressing Human Breast Cancers. Cancer Res *63*, 4920-4926.

Anisimov,V.N., Popovich,I.G., Alimova,I.N., Zabezhinski,M.A., Semenchenko,A.V., and Yashin,A.I. (2003). Number of pregnancies and ovariectomy modify mammary carcinoma development in transgenic HER-2/neu female mice. Cancer Lett. *193*, 49-55.

Azuma,M., Tamatani,T., Fukui,K., Yuki,T., Yoshida,H., Bando,T., Hoque,M.O., Kamogashira,T., Ogino,K., Nishino,N., and . (1994). Identification of EGF as an angiogenic factor present in conditioned medium from human salivary gland adenocarcinoma cell clones with varying degrees of metastatic potential. Cancer Lett. *84*, 189-198.

Ball,E.M. and Risbridger,G.P. (2001). Activins as regulators of branching morphogenesis. Dev. Biol. *238*, 1-12.

Barbacci,E.G., Guarino,B.C., Stroh,J.G., Singleton,D.H., Rosnack,K.J., Moyer,J.D., and Andrews,G.C. (1995). The structural basis for the specificity of epidermal growth factor and heregulin binding. J Biol. Chem. *270*, 9585-9589.

Barbacci,E.G., Pustilnik,L.R., Rossi,A.M., Emerson,E., Miller,P.E., Boscoe,B.P., Cox,E.D., Iwata,K.K., Jani,J.P., Provoncha,K., Kath,J.C., Liu,Z., and Moyer,J.D. (2003). The biological and biochemical effects of CP-654577, a selective erbB2 kinase inhibitor, on human breast cancer cells. Cancer Res *63*, 4450-4459.

Barcellos-Hoff,M.H. and Ewan,K.B. (2000). Transforming growth factor-beta and breast cancer: Mammary gland development. Breast Cancer Res *2*, 92-99.

Bargmann,C.I., Hung,M.C., and Weinberg,R.A. (1986). Multiple independent activations of the neu oncogene by a point mutation altering the transmembrane domain of p185. Cell *45*, 649-657.

Bargmann,C.I. and Weinberg,R.A. (1988). Increased tyrosine kinase activity associated with the protein encoded by the activated neu oncogene. Proc. Natl. Acad. Sci. U. S. A *85*, 5394-5398.

Baselga,J., Tripathy,D., Mendelsohn,J., Baughman,S., Benz,C.C., Dantis,L., Sklarin,N.T., Seidman,A.D., Hudis,C.A., Moore,J., Rosen,P.P., Twaddell,T., Henderson,I.C., and Norton,L. (1996). Phase II study of weekly intravenous recombinant humanized anti-p185HER2 monoclonal antibody in patients with HER2/neu-overexpressing metastatic breast cancer. J Clin. Oncol. *14*, 737-744.

Basso,A.D., Solit,D.B., Munster,P.N., and Rosen,N. (2002). Ansamycin antibiotics inhibit Akt activation and cyclin D expression in breast cancer cells that overexpress HER2. Oncogene *21*, 1159-1166.

Bates,S.E., Davidson,N.E., Valverius,E.M., Freter,C.E., Dickson,R.B., Tam,J.P., Kudlow,J.E., Lippman,M.E., and Salomon,D.S. (1988). Expression of transforming growth factor alpha and its messenger ribonucleic acid in human breast cancer: its regulation by estrogen and its possible functional significance. Mol. Endocrinol. *2*, 543-555.

Baulida,J., Kraus,M.H., Alimandi,M., Di Fiore,P.P., and Carpenter,G. (1996). All ErbB receptors other than the epidermal growth factor receptor are endocytosis impaired. J Biol. Chem. *271*, 5251-5257.

Beckmann,M.W., Niederacher,D., Schnurch,H.G., Gusterson,B.A., and Bender,H.G. (1997). Multistep carcinogenesis of breast cancer and tumour heterogeneity. J Mol Med *75*, 429-439.

Beerli,R.R. and Hynes,N.E. (1996). Epidermal growth factor-related peptides activate distinct subsets of ErbB receptors and differ in their biological activities. J Biol. Chem. *271*, 6071-6076.

Berra,E., Pages,G., and Pouyssegur,J. (2000). MAP kinases and hypoxia in the control of VEGF expression. Cancer Metastasis Rev. *19*, 139-145.

Bertucci,F., Borie,N., Ginestier,C., Groulet,A., Charafe-Jauffret,E., Adelaide,J., Geneix,J., Bachelart,L., Finetti,P., Koki,A., Hermitte,F., Hassoun,J., Debono,S., Viens,P., Fert,V., Jacquemier,J., and Birnbaum,D. (2004). Identification and validation of an ERBB2 gene expression signature in breast cancers. Oncogene *23*, 2564-2575.

Bjornsti,M.A. and Houghton,P.J. (2004). The TOR pathway: a target for cancer therapy. Nat. Rev. Cancer *4*, 335-348.

Board,M., Humm,S., and Newsholme,E.A. (1990). Maximum activities of key enzymes of glycolysis, glutaminolysis, pentose phosphate pathway and tricarboxylic acid cycle in normal, neoplastic and suppressed cells. Biochem. J *265*, 503-509.

Boggio,K., Nicoletti,G., Di Carlo,E., Cavallo,F., Landuzzi,L., Melani,C., Giovarelli,M., Rossi,I., Nanni,P., De Giovanni,C., Bouchard,P., Wolf,S., Modesti,A., Musiani,P., Lollini,P.L., Colombo,M.P., and Forni,G. (1998). Interleukin 12-mediated Prevention of Spontaneous Mammary Adenocarcinomas in Two Lines of Her-2/neu Transgenic Mice. J. Exp. Med. *188*, 589-596.

Bouchard,L., Lamarre,L., Tremblay,P.J., and Jolicoeur,P. (1989). Stochastic appearance of mammary tumors in transgenic mice carrying the MMTV/c-neu oncogene. Cell *57*, 931-936.

Boutros,R., Fanayan,S., Shehata,M., and Byrne,J.A. (2004). The tumor protein D52 family: many pieces, many puzzles. Biochem. Biophys. Res Commun. *325*, 1115-1121.

Brazma,A., Hingamp,P., Quackenbush,J., Sherlock,G., Spellman,P., Stoeckert,C., Aach,J., Ansorge,W., Ball,C.A., Causton,H.C., Gaasterland,T., Glenisson,P., Holstege,F.C., Kim,I.F., Markowitz,V., Matese,J.C., Parkinson,H., Robinson,A., Sarkans,U., Schulze-Kremer,S., Stewart,J., Taylor,R., Vilo,J., and Vingron,M. (2001). Minimum information about a microarray experiment (MIAME)-toward standards for microarray data. Nat. Genet. *29*, 365-371.

Brunet,A., Datta,S.R., and Greenberg,M.E. (2001). Transcription-dependent and -independent control of neuronal survival by the PI3K-Akt signaling pathway. Curr. Opin. Neurobiol. *11*, 297-305.

Bulavin,D.V., Phillips,C., Nannenga,B., Timofeev,O., Donehower,L.A., Anderson,C.W., Appella,E., and Fornace,A.J., Jr. (2004). Inactivation of the Wip1 phosphatase inhibits mammary tumorigenesis through p38 MAPK-mediated activation of the p16(Ink4a)-p19(Arf) pathway. Nat. Genet. *36*, 343-350.

Burgess,A.W., Cho,H.S., Eigenbrot,C., Ferguson,K.M., Garrett,T.P., Leahy,D.J., Lemmon,M.A., Sliwkowski,M.X., Ward,C.W., and Yokoyama,S. (2003). An open-and-shut case? Recent insights into the activation of EGF/ErbB receptors. Mol. Cell *12*, 541-552.

Bussmann,U.A., Lanuza,G.M., and Bussmann,L.E. (2004). Activin and follistatin in rat mammary gland. Mol Cell Endocrinol *221*, 9-19.

Calin,G.A., di Iasio,M.G., Caprini,E., Vorechovsky,I., Natali,P.G., Sozzi,G., Croce,C.M., Barbanti-Brodano,G., Russo,G., and Negrini,M. (2000). Low frequency of alterations of the alpha (PPP2R1A) and beta (PPP2R1B) isoforms of the subunit A of the serine-threonine phosphatase 2A in human neoplasms. Oncogene *19*, 1191-1195.

Cameron,V.A., Nishimura,E., Mathews,L.S., Lewis,K.A., Sawchenko,P.E., and Vale,W.W. (1994). Hybridization histochemical localization of activin receptor subtypes in rat brain, pituitary, ovary, and testis. Endocrinology *134*, 799-808.

Cao,Y., Dave,K.B., Doan,T.P., and Prescott,S.M. (2001). Fatty acid CoA ligase 4 is up-regulated in colon adenocarcinoma. Cancer Res *61*, 8429-8434.

Cao,Y., Pearman,A.T., Zimmerman,G.A., McIntyre,T.M., and Prescott,S.M. (2000). Intracellular unesterified arachidonic acid signals apoptosis. Proc. Natl Acad. Sci U. S. A *97*, 11280-11285.

Cardiff,R.D., Anver,M.R., Gusterson,B.A., Hennighausen,L., Jensen,R.A., Merino,M.J., Rehm,S., Russo,J., Tavassoli,F.A., Wakefield,L.M., Ward,J.M., and Green,J.E. (2000). The mammary pathology of genetically engineered mice: the consensus report and recommendations from the Annapolis meeting [see comments]. Oncogene *19*, 968-988.

Cardiff,R.D. and Wellings,S.R. (1999). The comparative pathology of human and mouse mammary glands. J. Mammary. Gland. Biol. Neoplasia. *4*, 105-122.

Cardone,M.H., Roy,N., Stennicke,H.R., Salvesen,G.S., Franke,T.F., Stanbridge,E., Frisch,S., and Reed,J.C. (1998). Regulation of cell death protease caspase-9 by phosphorylation. Science *282*, 1318-1321.

Carlomagno,C., Perrone,F., Gallo,C., De Laurentiis,M., Lauria,R., Morabito,A., Pettinato,G., Panico,L., D'Antonio,A., Bianco,A.R., and De Placido,S. (1996). c-erbB2 overexpression decreases the benefit of adjuvant tamoxifen in early-stage breast cancer without axillary lymph node metastases. J. Clin. Oncol. *14*, 2702-2708.

Carraway,K.L., III and Cantley,L.C. (1994). A neu acquaintance for erbB3 and erbB4: a role for receptor heterodimerization in growth signaling. Cell *78*, 5-8.

Carraway,K.L., III, Sliwkowski,M.X., Akita,R., Platko,J.V., Guy,P.M., Nuijens,A., Diamonti,A.J., Vandlen,R.L., Cantley,L.C., and Cerione,R.A. (1994). The erbB3 gene product is a receptor for heregulin. J Biol. Chem. *269*, 14303-14306.

Carter,P., Presta,L., Gorman,C.M., Ridgway,J.B., Henner,D., Wong,W.L., Rowland,A.M., Kotts,C., Carver,M.E., and Shepard,H.M. (1992). Humanization of an anti-p185HER2 antibody for human cancer therapy. Proc. Natl Acad. Sci U. S. A *89*, 4285-4289.

Carter,W.B., Hoying,J.B., Boswell,C., and Williams,S.K. (2001). HER2/neu over-expression induces endothelial cell retraction. Int. J Cancer *91*, 295-299.

Chambers,A.F., Groom,A.C., and MacDonald,I.C. (2002). Dissemination and growth of cancer cells in metastatic sites. Nat. Rev. Cancer *2*, 563-572.

Chambers,R.C., Leoni,P., Kaminski,N., Laurent,G.J., and Heller,R.A. (2003). Global expression profiling of fibroblast responses to transforming growth factor-beta1 reveals the induction of inhibitor of differentiation-1 and provides evidence of smooth muscle cell phenotypic switching. Am J Pathol *162*, 533-546.

Chang,H., Riese,D.J., Gilbert,W., Stern,D.F., and McMahan,U.J. (1997). Ligands for ErbB-family receptors encoded by a neuregulin-like gene. Nature *387*, 509-512.

Cheng,N., Bhowmick,N.A., Chytil,A., Gorksa,A.E., Brown,K.A., Muraoka,R., Arteaga,C.L., Neilson,E.G., Hayward,S.W., and Moses,H.L. (2005). Loss of TGF-beta type II receptor in fibroblasts promotes mammary carcinoma growth and invasion through upregulation of TGF-alpha-, MSP- and HGF-mediated signaling networks. Oncogene *24*, 5053-5068.

Cho,H.S., Mason,K., Ramyar,K.X., Stanley,A.M., Gabelli,S.B., Denney,D.W., Jr., and Leahy,D.J. (2003). Structure of the extracellular region of HER2 alone and in complex with the Herceptin Fab. Nature *421*, 756-760.

Clynes,R.A., Towers,T.L., Presta,L.G., and Ravetch,J.V. (2000). Inhibitory Fc receptors modulate in vivo cytoxicity against tumor targets. Nat. Med *6*, 443-446.

Cobleigh,M.A., Vogel,C.L., Tripathy,D., Robert,N.J., Scholl,S., Fehrenbacher,L., Wolter,J.M., Paton,V., Shak,S., Lieberman,G., and Slamon,D.J. (1999).

Multinational study of the efficacy and safety of humanized anti-HER2 monoclonal antibody in women who have HER2-overexpressing metastatic breast cancer that has progressed after chemotherapy for metastatic disease. J Clin. Oncol. *17*, 2639-2648.

Cocolakis,E., Lemay,S., Ali,S., and Lebrun,J.J. (2001). The p38 MAPK pathway is required for cell growth inhibition of human breast cancer cells in response to activin. J Biol. Chem. *276*, 18430-18436.

Cohen,B.D., Kiener,P.A., Green,J.M., Foy,L., Fell,H.P., and Zhang,K. (1996). The relationship between human epidermal growth-like factor receptor expression and cellular transformation in NIH3T3 cells. J Biol. Chem. *271*, 30897-30903.

Coussens,L., Yang-Feng,T.L., Liao,Y.C., Chen,E., Gray,A., McGrath,J., Seeburg,P.H., Libermann,T.A., Schlessinger,J., Francke,U., and . (1985). Tyrosine kinase receptor with extensive homology to EGF receptor shares chromosomal location with neu oncogene. Science *230*, 1132-1139.

Dalal,B.I., Keown,P.A., and Greenberg,A.H. (1993). Immunocytochemical localization of secreted transforming growth factor-beta 1 to the advancing edges of primary tumors and to lymph node metastases of human mammary carcinoma. Am J Pathol *143*, 381-389.

Danielsen,A.J. and Maihle,N.J. (2002). The EGF/ErbB receptor family and apoptosis. Growth Factors *20*, 1-15.

Datta,S.R., Brunet,A., and Greenberg,M.E. (1999). Cellular survival: a play in three Akts. Genes Dev. *13*, 2905-2927.

Datta,S.R., Dudek,H., Tao,X., Masters,S., Fu,H., Gotoh,Y., and Greenberg,M.E. (1997). Akt phosphorylation of BAD couples survival signals to the cell-intrinsic death machinery. Cell *91*, 231-241.

de Caestecker,M.P., Piek,E., and Roberts,A.B. (2000). Role of transforming growth factor-beta signaling in cancer. J Natl Cancer Inst *92*, 1388-1402.

de Kretser,D.M., Hedger,M.P., and Phillips,D.J. (1999). Activin A and follistatin: their role in the acute phase reaction and inflammation. J Endocrinol *161*, 195-198.

De Placido,S., De Laurentiis,M., Carlomagno,C., Gallo,C., Perrone,F., Pepe,S., Ruggiero,A., Marinelli,A., Pagliarulo,C., Panico,L., Pettinato,G., Petrella,G., and Bianco,A.R. (2003). Twenty-year results of the Naples GUN randomized trial: predictive factors of adjuvant tamoxifen efficacy in early breast cancer. Clin. Cancer Res *9*, 1039-1046.

de Winter,J.P., Roelen,B.A., ten Dijke,P., van der,B.B., and van den Eijnden-van Raaij AJ (1997). DPC4 (SMAD4) mediates transforming growth factor-beta1 (TGF-beta1) induced growth inhibition and transcriptional response in breast tumour cells. Oncogene *14*, 1891-1899.

Debnath,J., Mills,K.R., Collins,N.L., Reginato,M.J., Muthuswamy,S.K., and Brugge,J.S. (2002). The role of apoptosis in creating and maintaining luminal space within normal and oncogene-expressing mammary acini. Cell *111*, 29-40.

Derynck,R., Akhurst,R.J., and Balmain,A. (2001). TGF-beta signaling in tumor suppression and cancer progression. Nat. Genet. *29*, 117-129.

Desai,K.V., Xiao,N., Wang,W., Gangi,L., Greene,J., Powell,J.I., Dickson,R., Furth,P., Hunter,K., Kucherlapati,R., Simon,R., Liu,E.T., and Green,J.E. (2002). Initiating oncogenic event determines gene-expression patterns of human breast cancer models. PNAS *99*, 6967.

Di Fiore,P.P., Pierce,J.H., Kraus,M.H., Segatto,O., King,C.R., and Aaronson,S.A. (1987). erbB-2 is a potent oncogene when overexpressed in NIH/3T3 cells. Science *237*, 178-182.

Di Marco,E., Pierce,J.H., Knicley,C.L., and Di Fiore,P.P. (1990). Transformation of NIH 3T3 cells by overexpression of the normal coding sequence of the rat neu gene. Mol Cell Biol. *10*, 3247-3252.

Dickson,R.B., Kasid,A., Huff,K.K., Bates,S.E., Knabbe,C., Bronzert,D., Gelmann,E.P., and Lippman,M.E. (1987). Activation of growth factor secretion in tumorigenic states of breast cancer induced by 17 beta-estradiol or v-Ha-ras oncogene. Proc. Natl Acad. Sci U. S. A *84*, 837-841.

Dickson,R.B. and Lippman,M.E. (1987). Estrogenic regulation of growth and polypeptide growth factor secretion in human breast carcinoma. Endocr. Rev. *8*, 29-43.

Diehl,J.A., Cheng,M., Roussel,M.F., and Sherr,C.J. (1998). Glycogen synthase kinase-3beta regulates cyclin D1 proteolysis and subcellular localization. Genes Dev. *12*, 3499-3511.

DiGiovanna,M.P., Lerman,M.A., Coffey,R.J., Muller,W.J., Cardiff,R.D., and Stern,D.F. (1998). Active signaling by Neu in transgenic mice. Oncogene *17*, 1877-1884.

Dougall,W.C., Qian,X., Peterson,N.C., Miller,M.J., Samanta,A., and Greene,M.I. (1994). The neu-oncogene: signal transduction pathways, transformation mechanisms and evolving therapies. Oncogene *9*, 2109-2123.

Dowdy,S.C., Mariani,A., and Janknecht,R. (2003). HER2/Neu- and TAK1-mediated Up-regulation of the Transforming Growth Factor {beta} Inhibitor Smad7 via the ETS Protein ER81. J. Biol. Chem. *278*, 44377-44384.

Dressman,M.A., Baras,A., Malinowski,R., Alvis,L.B., Kwon,I., Walz,T.M., and Polymeropoulos,M.H. (2003). Gene Expression Profiling Detects Gene Amplification and Differentiates Tumor Types in Breast Cancer. Cancer Res *63*, 2194.

Druker,B.J., Talpaz,M., Resta,D.J., Peng,B., Buchdunger,E., Ford,J.M., Lydon,N.B., Kantarjian,H., Capdeville,R., Ohno-Jones,S., and Sawyers,C.L. (2001). Efficacy and safety of a specific inhibitor of the BCR-ABL tyrosine kinase in chronic myeloid leukemia. N Engl J Med *344*, 1031-1037.

Dutu,R., Nedelea,M., Veluda,G., and Burculet,V. (1980). Cytoenzymologic investigations on carcinomas of the cervix uteri. Acta Cytol. *24*, 160-166.

Eisen,M.B., Spellman,P.T., Brown,P.O., and Botstein,D. (1998). Cluster analysis and display of genome-wide expression patterns. Proc. Natl. Acad. Sci. U. S. A *95*, 14863-14868.

Elenius,K., Paul,S., Allison,G., Sun,J., and Klagsbrun,M. (1997). Activation of HER4 by heparin-binding EGF-like growth factor stimulates chemotaxis but not proliferation. EMBO J *16*, 1268-1278.

Esteva,F.J., Valero,V., Booser,D., Guerra,L.T., Murray,J.L., Pusztai,L., Cristofanilli,M., Arun,B., Esmaeli,B., Fritsche,H.A., Sneige,N., Smith,T.L., and Hortobagyi,G.N. (2002). Phase II study of weekly docetaxel and trastuzumab for patients with HER-2-overexpressing metastatic breast cancer. J Clin. Oncol. *20*, 1800-1808.

Evan,G.I. and Vousden,K.H. (2001). Proliferation, cell cycle and apoptosis in cancer. Nature *411*, 342-348.

Finkenzeller,G., Weindel,K., Zimmermann,W., Westin,G., and Marme,D. (2004). Activated Neu/ErbB-2 induces expression of the vascular endothelial growth factor gene by functional activation of the transcription factor Sp 1. Angiogenesis. *7*, 59-68.

Franklin,M.C., Carey,K.D., Vajdos,F.F., Leahy,D.J., de Vos,A.M., and Sliwkowski,M.X. (2004). Insights into ErbB signaling from the structure of the ErbB2-pertuzumab complex. Cancer Cell *5*, 317-328.

French,A.R., Tadaki,D.K., Niyogi,S.K., and Lauffenburger,D.A. (1995). Intracellular trafficking of epidermal growth factor family ligands is directly influenced by the pH sensitivity of the receptor/ligand interaction. J Biol. Chem. *270*, 4334-4340.

Garrett,T.P., McKern,N.M., Lou,M., Elleman,T.C., Adams,T.E., Lovrecz,G.O., Kofler,M., Jorissen,R.N., Nice,E.C., Burgess,A.W., and Ward,C.W. (2003). The crystal structure of a truncated ErbB2 ectodomain reveals an active conformation, poised to interact with other ErbB receptors. Mol. Cell *11*, 495-505.

Gebre-Medhin,M., Kindblom,L.G., Wennbo,H., Tornell,J., and Meis-Kindblom,J.M. (2001). Growth hormone receptor is expressed in human breast cancer. Am J Pathol *158*, 1217-1222.

Gobbi,H., Arteaga,C.L., Jensen,R.A., Simpson,J.F., Dupont,W.D., Olson,S.J., Schuyler,P.A., Plummer,W.D., Jr., and Page,D.L. (2000). Loss of expression of transforming growth factor beta type II receptor correlates with high tumour grade in human breast in-situ and invasive carcinomas. Histopathology *36*, 168-177.

Gobbi,H., Dupont,W.D., Simpson,J.F., Plummer,W.D., Jr., Schuyler,P.A., Olson,S.J., Arteaga,C.L., and Page,D.L. (1999). Transforming growth factor-beta and breast cancer risk in women with mammary epithelial hyperplasia. J Natl Cancer Inst *91*, 2096-2101.

Goldenberg,M.M. (1999). Trastuzumab, a recombinant DNA-derived humanized monoclonal antibody, a novel agent for the treatment of metastatic breast cancer. Clin. Ther. *21*, 309-318.

Goldman,C.K., Kim,J., Wong,W.L., King,V., Brock,T., and Gillespie,G.Y. (1993). Epidermal growth factor stimulates vascular endothelial growth factor production by human malignant glioma cells: a model of glioblastoma multiforme pathophysiology. Mol Biol. Cell *4*, 121-133.

Goldman,R., Levy,R.B., Peles,E., and Yarden,Y. (1990). Heterodimerization of the erbB-1 and erbB-2 receptors in human breast carcinoma cells: a mechanism for receptor transregulation. Biochemistry *29*, 11024-11028.

Graus-Porta,D., Beerli,R.R., Daly,J.M., and Hynes,N.E. (1997). ErbB-2, the preferred heterodimerization partner of all ErbB receptors, is a mediator of lateral signaling. EMBO J. *16*, 1647-1655.

Green,D.R. and Evan,G.I. (2002). A matter of life and death. Cancer Cell *1*, 19-30.

Groenen,L.C., Nice,E.C., and Burgess,A.W. (1994). Structure-function relationships for the EGF/TGF-alpha family of mitogens. Growth Factors *11*, 235-257.

Gunzburg,W.H. and Salmons,B. (1992). Factors controlling the expression of mouse mammary tumour virus. Biochem. J. *283 (Pt 3)*, 625-632.

Guy,C.T., Cardiff,R.D., and Muller,W.J. (1996). Activated neu induces rapid tumor progression. J Biol. Chem. *271*, 7673-7678.

Guy,C.T., Webster,M.A., Schaller,M., Parsons,T.J., Cardiff,R.D., and Muller,W.J. (1992). Expression of the neu protooncogene in the mammary epithelium of transgenic mice induces metastatic disease. Proc. Natl. Acad. Sci. U. S. A *89*, 10578-10582.

Guy,P.M., Platko,J.V., Cantley,L.C., Cerione,R.A., and Carraway,K.L., III (1994). Insect cell-expressed p180erbB3 possesses an impaired tyrosine kinase activity. Proc. Natl. Acad. Sci. U. S. A *91*, 8132-8136.

Hanahan,D. and Weinberg,R.A. (2000). The hallmarks of cancer. Cell *100*, 57-70.

Hancock,S.L., Tucker,M.A., and Hoppe,R.T. (1993). Breast cancer after treatment of Hodgkin's disease
1. J Natl Cancer Inst *85*, 25-31.

Harari,D., Tzahar,E., Romano,J., Shelly,M., Pierce,J.H., Andrews,G.C., and Yarden,Y. (1999). Neuregulin-4: a novel growth factor that acts through the ErbB-4 receptor tyrosine kinase. Oncogene *18*, 2681-2689.

Harris,A.L. (2002). Hypoxia--a key regulatory factor in tumour growth. Nat. Rev. Cancer *2*, 38-47.

Hennighausen,L. and Robinson,G.W. (2001). Signaling pathways in mammary gland development. Dev. Cell *1*, 467-475.

Hennipman,A., Smits,J., van Oirschot,B., van Houwelingen,J.C., Rijksen,G., Neyt,J.P., Van Unnik,J.A., and Staal,G.E. (1987). Glycolytic enzymes in breast cancer, benign breast disease and normal breast tissue. Tumour. Biol. *8*, 251-263.

Henry,M.D., Triplett,A.A., Oh,K.B., Smith,G.H., and Wagner,K.U. (2004). Parity-induced mammary epithelial cells facilitate tumorigenesis in MMTV-neu transgenic mice. Oncogene *23*, 6980-6985.

Hermanto,U., Zong,C.S., and Wang,L.H. (2001). ErbB2-overexpressing human mammary carcinoma cells display an increased requirement for the phosphatidylinositol 3-kinase signaling pathway in anchorage-independent growth
1. Oncogene *20*, 7551-7562.

Hewitt,S.C., Bocchinfuso,W.P., Zhai,J., Harrell,C., Koonce,L., Clark,J., Myers,P., and Korach,K.S. (2002). Lack of ductal development in the absence of functional estrogen receptor alpha delays mammary tumor formation induced by transgenic expression of ErbB2/neu. Cancer Res *62*, 2798-2805.

Higashiyama,S., Abraham,J.A., Miller,J., Fiddes,J.C., and Klagsbrun,M. (1991). A heparin-binding growth factor secreted by macrophage-like cells that is related to EGF. Science *251*, 936-939.

Hirata,A., Ogawa,S., Kometani,T., Kuwano,T., Naito,S., Kuwano,M., and Ono,M. (2002). ZD1839 (Iressa) induces antiangiogenic effects through inhibition of epidermal growth factor receptor tyrosine kinase. Cancer Res *62*, 2554-2560.

Holbro,T., Civenni,G., and Hynes,N.E. (2003). The ErbB receptors and their role in cancer progression. Exp. Cell Res *284*, 99-110.

Houston,S.J., Plunkett,T.A., Barnes,D.M., Smith,P., Rubens,R.D., and Miles,D.W. (1999). Overexpression of c-erbB2 is an independent marker of resistance to endocrine therapy in advanced breast cancer. Br. J. Cancer *79*, 1220-1226.

Hudziak,R.M., Lewis,G.D., Winget,M., Fendly,B.M., Shepard,H.M., and Ullrich,A. (1989). p185HER2 monoclonal antibody has antiproliferative effects in vitro and sensitizes human breast tumor cells to tumor necrosis factor. Mol Cell Biol. *9*, 1165-1172.

Hudziak,R.M., Schlessinger,J., and Ullrich,A. (1987). Increased expression of the putative growth factor receptor p185HER2 causes transformation and tumorigenesis of NIH 3T3 cells. Proc. Natl. Acad. Sci. U. S. A *84*, 7159-7163.

Hynes,N.E. and Lane,H.A. (2005). ERBB receptors and cancer: the complexity of targeted inhibitors. Nat. Rev. Cancer *5*, 341-354.

Hynes,N.E. and Stern,D.F. (1994). The biology of erbB-2/neu/HER-2 and its role in cancer. Biochim. Biophys. Acta *1198*, 165-184.

Ignatoski,K.M., Lapointe,A.J., Radany,E.H., and Ethier,S.P. (1999). erbB-2 overexpression in human mammary epithelial cells confers growth factor independence. Endocrinology *140*, 3615-3622.

Ishizawar,R. and Parsons,S.J. (2004). c-Src and cooperating partners in human cancer. Cancer Cell *6*, 209-214.

Izumi,Y., Xu,L., di Tomaso,E., Fukumura,D., and Jain,R.K. (2002). Tumour biology: herceptin acts as an anti-angiogenic cocktail. Nature *416*, 279-280.

Jacquemier,J., Ginestier,C., Rougemont,J., Bardou,V.J., Charafe-Jauffret,E., Geneix,J., Adelaide,J., Koki,A., Houvenaeghel,G., Hassoun,J., Maraninchi,D., Viens,P., Birnbaum,D., and Bertucci,F. (2005). Protein expression profiling identifies subclasses of breast cancer and predicts prognosis. Cancer Res *65*, 767-779.

Johnson,G.R., Kannan,B., Shoyab,M., and Stromberg,K. (1993). Amphiregulin induces tyrosine phosphorylation of the epidermal growth factor receptor and p185erbB2. Evidence that amphiregulin acts exclusively through the epidermal growth factor receptor at the surface of human epithelial cells. J Biol. Chem. *268*, 2924-2931.

Jones,J.T., Akita,R.W., and Sliwkowski,M.X. (1999). Binding specificities and affinities of egf domains for ErbB receptors. FEBS Lett. *447*, 227-231.

Kalkhoven,E., Roelen,B.A., de Winter,J.P., Mummery,C.L., van den Eijnden-van Raaij AJ, van der Saag,P.T., and van der,B.B. (1995). Resistance to transforming growth factor beta and activin due to reduced receptor expression in human breast tumor cell lines. Cell Growth Differ. *6*, 1151-1161.

Karunagaran,D., Tzahar,E., Beerli,R.R., Chen,X., Graus-Porta,D., Ratzkin,B.J., Seger,R., Hynes,N.E., and Yarden,Y. (1996). ErbB-2 is a common auxiliary subunit of NDF and EGF receptors: implications for breast cancer. EMBO J *15*, 254-264.

Katsuura,M. and Tanaka,S. (1989). Topographic analysis of human epidermal growth factor by monospecific antibodies and synthetic peptides. J Biochem. (Tokyo) *106*, 87-92.

Kauraniemi,P., Barlund,M., Monni,O., and Kallioniemi,A. (2001). New amplified and highly expressed genes discovered in the ERBB2 amplicon in breast cancer by cDNA microarrays. Cancer Res *61*, 8235-8240.

Kauraniemi,P., Hautaniemi,S., Autio,R., Astola,J., Monni,O., Elkahloun,A., and Kallioniemi,A. (2004). Effects of Herceptin treatment on global gene expression patterns in HER2-amplified and nonamplified breast cancer cell lines. Oncogene *23*, 1010-1013.

Keelan,J.A., Zhou,R.L., and Mitchell,M.D. (2000). Activin A exerts both pro- and anti-inflammatory effects on human term gestational tissues. Placenta *21*, 38-43.

Kelsey,J.L., Gammon,M.D., and John,E.M. (1993). Reproductive factors and breast cancer. Epidemiol. Rev. *15*, 36-47.

Kero,J., Poutanen,M., Zhang,F.P., Rahman,N., McNicol,A.M., Nilson,J.H., Keri,R.A., and Huhtaniemi,I.T. (2000). Elevated luteinizing hormone induces expression of its receptor and promotes steroidogenesis in the adrenal cortex. J. Clin. Invest *105*, 633-641.

Klapper,L.N., Glathe,S., Vaisman,N., Hynes,N.E., Andrews,G.C., Sela,M., and Yarden,Y. (1999). The ErbB-2/HER2 oncoprotein of human carcinomas may function solely as a shared coreceptor for multiple stroma-derived growth factors. Proc. Natl. Acad. Sci. U. S. A *96*, 4995-5000.

Klapper,L.N., Vaisman,N., Hurwitz,E., Pinkas-Kramarski,R., Yarden,Y., and Sela,M. (1997). A subclass of tumor-inhibitory monoclonal antibodies to ErbB-2/HER2 blocks crosstalk with growth factor receptors. Oncogene *14*, 2099-2109.

Klapper,L.N., Waterman,H., Sela,M., and Yarden,Y. (2000). Tumor-inhibitory antibodies to HER-2/ErbB-2 may act by recruiting c-Cbl and enhancing ubiquitination of HER-2. Cancer Res *60*, 3384-3388.

Klos,K.S., Zhou,X., Lee,S., Zhang,L., Yang,W., Nagata,Y., and Yu,D. (2003). Combined trastuzumab and paclitaxel treatment better inhibits ErbB-2-mediated angiogenesis in breast carcinoma through a more effective inhibition of Akt than either treatment alone. Cancer *98*, 1377-1385.

Kokai,Y., Myers,J.N., Wada,T., Brown,V.I., LeVea,C.M., Davis,J.G., Dobashi,K., and Greene,M.I. (1989). Synergistic interaction of p185c-neu and the EGF receptor leads to transformation of rodent fibroblasts. Cell *58*, 287-292.

Komatsu,M., Jepson,S., Arango,M.E., Carothers Carraway,C.A., and Carraway,K.L. (2001). Muc4/sialomucin complex, an intramembrane modulator of ErbB2/HER2/Neu, potentiates primary tumor growth and suppresses apoptosis in a xenotransplanted tumor. Oncogene *20*, 461-470.

Kraus,M.H., Issing,W., Miki,T., Popescu,N.C., and Aaronson,S.A. (1989). Isolation and characterization of ERBB3, a third member of the ERBB/epidermal growth factor receptor family: evidence for overexpression in a subset of human mammary tumors. Proc. Natl Acad. Sci U. S. A *86*, 9193-9197.

Krishnamurthy,S. and Sneige,N. (2002). Molecular and biologic markers of premalignant lesions of human breast. Adv. Anat. Pathol *9*, 185-197.

Kumar-Sinha,C., Ignatoski,K.W., Lippman,M.E., Ethier,S.P., and Chinnaiyan,A.M. (2003). Transcriptome Analysis of HER2 Reveals a Molecular Connection to Fatty Acid Synthesis. Cancer Res *63*, 132-139.

Kurokawa,Y., Matoba,R., Nakamori,S., Takemasa,I., Nagano,H., Dono,K., Umeshita,K., Sakon,M., Monden,M., and Kato,K. (2004). PCR-array gene expression profiling of hepatocellular carcinoma. J Exp. Clin. Cancer Res *23*, 135-141.

Lambe,M., Hsieh,C., Trichopoulos,D., Ekbom,A., Pavia,M., and Adami,H.O. (1994). Transient increase in the risk of breast cancer after giving birth. N Engl J Med *331*, 5-9.

Land,C.E., Tokunaga,M., Koyama,K., Soda,M., Preston,D.L., Nishimori,I., and Tokuoka,S. (2003). Incidence of female breast cancer among atomic bomb survivors, Hiroshima and Nagasaki, 1950-1990. Radiat. Res *160*, 707-717.

Landis,M.D., Seachrist,D.D., Montanez-Wiscovich,M.E., Danielpour,D., and Keri,R.A. (2005). Gene expression profiling of cancer progression reveals intrinsic regulation of transforming growth factor-[beta] signaling in ErbB2//Neu-induced tumors from transgenic mice. Oncogene *24*, 5173-5190.

Lane,H.A., Beuvink,I., Motoyama,A.B., Daly,J.M., Neve,R.M., and Hynes,N.E. (2000). ErbB2 potentiates breast tumor proliferation through modulation of p27(Kip1)-Cdk2 complex formation: receptor overexpression does not determine growth dependency. Mol. Cell Biol. *20*, 3210-3223.

Laughner,E., Taghavi,P., Chiles,K., Mahon,P.C., and Semenza,G.L. (2001). HER2 (neu) signaling increases the rate of hypoxia-inducible factor 1alpha (HIF-1alpha) synthesis: novel mechanism for HIF-1-mediated vascular endothelial growth factor expression. Mol Cell Biol. *21*, 3995-4004.

Le,X.F., Claret,F.X., Lammayot,A., Tian,L., Deshpande,D., LaPushin,R., Tari,A.M., and Bast,R.C., Jr. (2003). The role of cyclin-dependent kinase inhibitor p27Kip1 in anti-HER2 antibody-induced G1 cell cycle arrest and tumor growth inhibition. J Biol. Chem. *278*, 23441-23450.

Lee,R.J., Albanese,C., Fu,M., D'Amico,M., Lin,B., Watanabe,G., Haines,G.K., Siegel,P.M., Hung,M.C., Yarden,Y., Horowitz,J.M., Muller,W.J., and Pestell,R.G. (2000). Cyclin D1 is required for transformation by activated Neu and is induced through an E2F-dependent signaling pathway. Mol. Cell Biol. *20*, 672-683.

Lemmon,M.A., Bu,Z., Ladbury,J.E., Zhou,M., Pinchasi,D., Lax,I., Engelman,D.M., and Schlessinger,J. (1997). Two EGF molecules contribute additively to stabilization of the EGFR dimer. EMBO J *16*, 281-294.

Lemoine,N.R., Staddon,S., Dickson,C., Barnes,D.M., and Gullick,W.J. (1990). Absence of activating transmembrane mutations in the c-erbB-2 proto- oncogene in human breast cancer. Oncogene *5*, 237-239.

Lenferink,A.E., Busse,D., Flanagan,W.M., Yakes,F.M., and Arteaga,C.L. (2001). ErbB2/neu kinase modulates cellular p27(Kip1) and cyclin D1 through multiple signaling pathways. Cancer Res. *61*, 6583-6591.

Lenferink,A.E., Pinkas-Kramarski,R., van de Poll,M.L., van Vugt,M.J., Klapper,L.N., Tzahar,E., Waterman,H., Sela,M., van Zoelen,E.J., and Yarden,Y. (1998). Differential endocytic routing of homo- and hetero-dimeric ErbB tyrosine kinases confers signaling superiority to receptor heterodimers. EMBO J *17*, 3385-3397.

Lenferink,A.E., Simpson,J.F., Shawver,L.K., Coffey,R.J., Forbes,J.T., and Arteaga,C.L. (2000). Blockade of the epidermal growth factor receptor tyrosine kinase suppresses tumorigenesis in MMTV/Neu + MMTV/TGF-alpha bigenic mice. Proc. Natl Acad. Sci U. S. A *97*, 9609-9614.

Lesniak,M.S. and Brem,H. (2004). Targeted therapy for brain tumours. Nat. Rev. Drug Discov. *3*, 499-508.

Levkowitz,G., Waterman,H., Ettenberg,S.A., Katz,M., Tsygankov,A.Y., Alroy,I., Lavi,S., Iwai,K., Reiss,Y., Ciechanover,A., Lipkowitz,S., and Yarden,Y. (1999). Ubiquitin ligase activity and tyrosine phosphorylation underlie suppression of growth factor signaling by c-Cbl/Sli-1. Mol Cell *4*, 1029-1040.

Levkowitz,G., Waterman,H., Zamir,E., Kam,Z., Oved,S., Langdon,W.Y., Beguinot,L., Geiger,B., and Yarden,Y. (1998). c-Cbl/Sli-1 regulates endocytic sorting and ubiquitination of the epidermal growth factor receptor. Genes Dev. *12*, 3663-3674.

Li,B., Rosen,J.M., McMenamin-Balano,J., Muller,W.J., and Perkins,A.S. (1997). neu/ERBB2 cooperates with p53-172H during mammary tumorigenesis in transgenic mice. Mol. Cell Biol. *17*, 3155-3163.

Li,Y.M., Zhou,B.P., Deng,J., Pan,Y., Hay,N., and Hung,M.C. (2005). A hypoxia-independent hypoxia-inducible factor-1 activation pathway induced by phosphatidylinositol-3 kinase/Akt in HER2 overexpressing cells. Cancer Res. *65*, 3257-3263.

Liang,J., Zubovitz,J., Petrocelli,T., Kotchetkov,R., Connor,M.K., Han,K., Lee,J.H., Ciarallo,S., Catzavelos,C., Beniston,R., Franssen,E., and Slingerland,J.M. (2002). PKB/Akt phosphorylates p27, impairs nuclear import of p27 and opposes p27-mediated G1 arrest. Nat. Med. *8*, 1153-1160.

Liang,Y.C., Wu,C.H., Chu,J.S., Wang,C.K., Hung,L.F., Wang,Y.J., Ho,Y.S., Chang,J.G., and Lin,S.Y. (2005). Involvement of fatty acid-CoA ligase 4 in hepatocellular carcinoma growth: roles of cyclic AMP and p38 mitogen-activated protein kinase. World J Gastroenterol. *11*, 2557-2563.

Liu,Q., Wuu,J., Lambe,M., Hsieh,S.F., Ekbom,A., and Hsieh,C.C. (2002). Transient increase in breast cancer risk after giving birth: postpartum period with the highest risk (Sweden). Cancer Causes Control *13*, 299-305.

Liu,Q.Y., Niranjan,B., Gomes,P., Gomm,J.J., Davies,D., Coombes,R.C., and Buluwela,L. (1996). Inhibitory effects of activin on the growth and morpholgenesis of primary and transformed mammary epithelial cells. Cancer Res *56*, 1155-1163.

Lonardo,F., Di Marco,E., King,C.R., Pierce,J.H., Segatto,O., Aaronson,S.A., and Di Fiore,P.P. (1990). The normal erbB-2 product is an atypical receptor-like tyrosine kinase with constitutive activity in the absence of ligand. New Biol. *2*, 992-1003.

Loureiro,R.M., Maharaj,A.S., Dankort,D., Muller,W.J., and D'Amore,P.A. (2005). ErbB2 overexpression in mammary cells upregulates VEGF through the core promoter. Biochem. Biophys. Res Commun. *326*, 455-465.

MacDonald,I.C., Groom,A.C., and Chambers,A.F. (2002). Cancer spread and micrometastasis development: quantitative approaches for in vivo models. Bioessays *24*, 885-893.

Macheda,M.L., Rogers,S., and Best,J.D. (2005). Molecular and cellular regulation of glucose transporter (GLUT) proteins in cancer. J Cell Physiol *202*, 654-662.

Mackay,A., Jones,C., Dexter,T., Silva,R.L., Bulmer,K., Jones,A., Simpson,P., Harris,R.A., Jat,P.S., Neville,A.M., Reis,L.F., Lakhani,S.R., and O'Hare,M.J. (2003). cDNA microarray analysis of genes associated with ERBB2 (HER2/neu) overexpression in human mammary luminal epithelial cells. Oncogene *22*, 2680-2688.

Marmor,M.D., Skaria,K.B., and Yarden,Y. (2004). Signal transduction and oncogenesis by ErbB/HER receptors. Int. J Radiat. Oncol. Biol. Phys. *58*, 903-913.

Martinez-Lacaci,I., Saceda,M., Plowman,G.D., Johnson,G.R., Normanno,N., Salomon,D.S., and Dickson,R.B. (1995). Estrogen and phorbol esters regulate amphiregulin expression by two separate mechanisms in human breast cancer cell lines. Endocrinology *136*, 3983-3992.

Massague,J. (1998). TGF-beta signal transduction. Annu. Rev. Biochem. *67*, 753-791.

Massague,J. (2000). How cells read TGF-beta signals. Nat. Rev. Mol Cell Biol. *1*, 169-178.

Massague,J. and Pandiella,A. (1993). Membrane-anchored growth factors. Annu. Rev. Biochem. *62*, 515-541.

Mathews,L.S. and Vale,W.W. (1993). Molecular and functional characterization of activin receptors. Receptor *3*, 173-181.

Matzuk,M.M., Kumar,T.R., Vassalli,A., Bickenbach,J.R., Roop,D.R., Jaenisch,R., and Bradley,A. (1995). Functional analysis of activins during mammalian development. Nature *374*, 354-356.

Mazumdar,A., Adam,L., Boyd,D., and Kumar,R. (2001). Heregulin regulation of urokinase plasminogen activator and its receptor: human breast epithelial cell invasion. Cancer Res *61*, 400-405.

Mazurek,S., Grimm,H., Boschek,C.B., Vaupel,P., and Eigenbrodt,E. (2002). Pyruvate kinase type M2: a crossroad in the tumor metabolome. Br. J Nutr. *87 Suppl 1*, S23-S29.

McDermott,E.W., Barron,E.T., Smyth,P.P., and O'Higgins,N.J. (1990). Premorphological metabolic changes in human breast carcinogenesis. Br. J Surg. *77*, 1179-1182.

Menard,S., Aiello,P., Tagliabue,E., Rumio,C., Lollini,P.L., Colnaghi,M.I., and Balsari,A. (2000). Tamoxifen chemoprevention of a hormone-independent tumor in the proto- neu transgenic mice model. Cancer Res. *60*, 273-275.

Meyer,D. and Birchmeier,C. (1995). Multiple essential functions of neuregulin in development. Nature *378*, 386-390.

Milliken,E.L., Ameduri,R.K., Landis,M.D., Behrooz,A., Abdul-Karim,F.W., and Keri,R.A. (2002). Ovarian hyperstimulation by LH leads to mammary gland hyperplasia and cancer predisposition in transgenic mice. Endocrinology *143*, 3671-3680.

Moasser,M.M., Basso,A., Averbuch,S.D., and Rosen,N. (2001). The tyrosine kinase inhibitor ZD1839 ("Iressa") inhibits HER2-driven signaling and suppresses the growth of HER2-overexpressing tumor cells. Cancer Res. *61*, 7184-7188.

Molina,M.A., Codony-Servat,J., Albanell,J., Rojo,F., Arribas,J., and Baselga,J. (2001). Trastuzumab (herceptin), a humanized anti-Her2 receptor monoclonal antibody, inhibits basal and activated Her2 ectodomain cleavage in breast cancer cells. Cancer Res. *61*, 4744-4749.

Morrison,B.W. and Leder,P. (1994). neu and ras initiate murine mammary tumors that share genetic markers generally absent in c-myc and int-2-initiated tumors. Oncogene *9*, 3417-3426.

Motoyama,A.B., Hynes,N.E., and Lane,H.A. (2002). The efficacy of ErbB receptor-targeted anticancer therapeutics is influenced by the availability of epidermal growth factor-related peptides. Cancer Res. *62*, 3151-3158.

Muller,W.J., Sinn,E., Pattengale,P.K., Wallace,R., and Leder,P. (1988). Single-step induction of mammary adenocarcinoma in transgenic mice bearing the activated c-neu oncogene. Cell *54*, 105-115.

Munster,P.N., Marchion,D.C., Basso,A.D., and Rosen,N. (2002). Degradation of HER2 by ansamycins induces growth arrest and apoptosis in cells with HER2 overexpression via a HER3, phosphatidylinositol 3'-kinase-AKT-dependent pathway. Cancer Res. *62*, 3132-3137.

Muraoka,R.S., Koh,Y., Roebuck,L.R., Sanders,M.E., Brantley-Sieders,D., Gorska,A.E., Moses,H.L., and Arteaga,C.L. (2003). Increased Malignancy of

Neu-Induced Mammary Tumors Overexpressing Active Transforming Growth Factor {beta}1. Mol. Cell. Biol. *23*, 8691-8703.

Muthuswamy,S.K., Gilman,M., and Brugge,J.S. (1999). Controlled dimerization of ErbB receptors provides evidence for differential signaling by homo- and heterodimers. Mol Cell Biol. *19*, 6845-6857.

Muthuswamy,S.K., Li,D., Lelievre,S., Bissell,M.J., and Brugge,J.S. (2001). ErbB2, but not ErbB1, reinitiates proliferation and induces luminal repopulation in epithelial acini. Nat. Cell Biol. *3*, 785-792.

Neve,R.M., Sutterluty,H., Pullen,N., Lane,H.A., Daly,J.M., Krek,W., and Hynes,N.E. (2000). Effects of oncogenic ErbB2 on G1 cell cycle regulators in breast tumour cells. Oncogene *19*, 1647-1656.

Olayioye,M.A., Badache,A., Daly,J.M., and Hynes,N.E. (2001). An essential role for Src kinase in ErbB receptor signaling through the MAPK pathway. Exp. Cell Res. *267*, 81-87.

Olayioye,M.A., Beuvink,I., Horsch,K., Daly,J.M., and Hynes,N.E. (1999). ErbB receptor-induced activation of stat transcription factors is mediated by Src tyrosine kinases. J. Biol. Chem. *274*, 17209-17218.

Olayioye,M.A., Neve,R.M., Lane,H.A., and Hynes,N.E. (2000). The ErbB signaling network: receptor heterodimerization in development and cancer. EMBO J. *19*, 3159-3167.

Paria,B.C., Elenius,K., Klagsbrun,M., and Dey,S.K. (1999). Heparin-binding EGF-like growth factor interacts with mouse blastocysts independently of ErbB1: a possible role for heparan sulfate proteoglycans and ErbB4 in blastocyst implantation. Development *126*, 1997-2005.

Peles,E., Ben Levy,R., Tzahar,E., Liu,N., Wen,D., and Yarden,Y. (1993). Cell-type specific interaction of Neu differentiation factor (NDF/heregulin) with Neu/HER-2 suggests complex ligand-receptor relationships. EMBO J. *12*, 961-971.

Perou,C.M., Sorlie,T., Eisen,M.B., van de,R.M., Jeffrey,S.S., Rees,C.A., Pollack,J.R., Ross,D.T., Johnsen,H., Akslen,L.A., Fluge,O., Pergamenschikov,A., Williams,C., Zhu,S.X., Lonning,P.E., Borresen-Dale,A.L., Brown,P.O., and Botstein,D. (2000). Molecular portraits of human breast tumours. Nature *406*, 747-752.

Petraglia,F., Sacerdote,P., Cossarizza,A., Angioni,S., Genazzani,A.D., Franceschi,C., Muscettola,M., and Grasso,G. (1991). Inhibin and activin modulate human monocyte chemotaxis and human lymphocyte interferon-gamma production. J Clin. Endocrinol Metab *72*, 496-502.

Phillips,D.J. (2000). Regulation of activin's access to the cell: why is mother nature such a control freak? Bioessays *22*, 689-696.

Phillips,D.J. and de Kretser,D.M. (1998). Follistatin: a multifunctional regulatory protein. Front Neuroendocrinol. *19*, 287-322.

Pimentel,R.C., Yamada,K.A., Kleber,A.G., and Saffitz,J.E. (2002). Autocrine regulation of myocyte Cx43 expression by VEGF. Circ. Res *90*, 671-677.

Pinkas-Kramarski,R., Soussan,L., Waterman,H., Levkowitz,G., Alroy,I., Klapper,L., Lavi,S., Seger,R., Ratzkin,B.J., Sela,M., and Yarden,Y. (1996). Diversification of Neu differentiation factor and epidermal growth factor signaling by combinatorial receptor interactions. EMBO J. *15*, 2452-2467.

Plowman,G.D., Culouscou,J.M., Whitney,G.S., Green,J.M., Carlton,G.W., Foy,L., Neubauer,M.G., and Shoyab,M. (1993a). Ligand-specific activation of HER4/p180erbB4, a fourth member of the epidermal growth factor receptor family. Proc. Natl. Acad. Sci. U. S. A *90*, 1746-1750.

Plowman,G.D., Green,J.M., Culouscou,J.M., Carlton,G.W., Rothwell,V.M., and Buckley,S. (1993b). Heregulin induces tyrosine phosphorylation of HER4/p180erbB4. Nature *366*, 473-475.

Prenzel,N., Zwick,E., Daub,H., Leserer,M., Abraham,R., Wallasch,C., and Ullrich,A. (1999). EGF receptor transactivation by G-protein-coupled receptors requires metalloproteinase cleavage of proHB-EGF. Nature *402*, 884-888.

Ramaswamy,S., Ross,K.N., Lander,E.S., and Golub,T.R. (2003). A molecular signature of metastasis in primary solid tumors. Nat. Genet. *33*, 49-54.

Reed,W., Sandstad,B., Holm,R., and Nesland,J.M. (2003). The prognostic impact of hormone receptors and c-erbB-2 in pregnancy-associated breast cancer and their correlation with BRCA1 and cell cycle modulators. Int. J Surg. Pathol *11*, 65-74.

Reginato,M.J., Mills,K.R., Becker,E.B., Lynch,D.K., Bonni,A., Muthuswamy,S.K., and Brugge,J.S. (2005). Bim regulation of lumen formation in cultured mammary epithelial acini is targeted by oncogenes. Mol Cell Biol. *25*, 4591-4601.

Reis,F.M., Luisi,S., Carneiro,M.M., Cobellis,L., Federico,M., Camargos,A.F., and Petraglia,F. (2004). Activin, inhibin and the human breast. Mol Cell Endocrinol *225*, 77-82.

Reiss,M. (1999). TGF-beta and cancer. Microbes. Infect. *1*, 1327-1347.

Revillion,F., Bonneterre,J., and Peyrat,J.P. (1998). ERBB2 oncogene in human breast cancer and its clinical significance. Eur. J. Cancer *34*, 791-808.

Riese,D.J., Bermingham,Y., van Raaij,T.M., Buckley,S., Plowman,G.D., and Stern,D.F. (1996a). Betacellulin activates the epidermal growth factor receptor and erbB-4, and induces cellular response patterns distinct from those stimulated by epidermal growth factor or neuregulin-beta. Oncogene *12*, 345-353.

Riese,D.J., Kim,E.D., Elenius,K., Buckley,S., Klagsbrun,M., Plowman,G.D., and Stern,D.F. (1996b). The epidermal growth factor receptor couples transforming growth factor-alpha, heparin-binding epidermal growth factor-like factor, and amphiregulin to Neu, ErbB-3, and ErbB-4. J Biol. Chem. *271*, 20047-20052.

Riese,D.J. and Stern,D.F. (1998). Specificity within the EGF family/ErbB receptor family signaling network. Bioessays *20*, 41-48.

Riese,D.J., van Raaij,T.M., Plowman,G.D., Andrews,G.C., and Stern,D.F. (1995). The cellular response to neuregulins is governed by complex interactions of the erbB receptor family. Mol. Cell Biol. *15*, 5770-5776.

Risma,K.A., Clay,C.M., Nett,T.M., Wagner,T., Yun,J., and Nilson,J.H. (1995). Targeted overexpression of luteinizing hormone in transgenic mice leads to infertility, polycystic ovaries, and ovarian tumors. Proc. Natl. Acad. Sci. U. S. A *92*, 1322-1326.

Roberts,A.B. and Wakefield,L.M. (2003). The two faces of transforming growth factor beta in carcinogenesis. Proc. Natl. Acad. Sci. U. S. A *100*, 8621-8623.

Robertson,C., Primic-Zakelj,M., Boyle,P., and Hsieh,C.C. (1997). Effect of parity and age at delivery on breast cancer risk in Slovenian women aged 25-54 years. Int. J Cancer *73*, 1-9.

Robinson,G.W. and Hennighausen,L. (1997). Inhibins and activins regulate mammary epithelial cell differentiation through mesenchymal-epithelial interactions. Development *124*, 2701-2708.

Russo,I.H. and Russo,J. (1998). Role of hormones in mammary cancer initiation and progression. J. Mammary. Gland. Biol. Neoplasia. *3*, 49-61.

Russo,J. and Russo,I.H. (1996). Experimentally induced mammary tumors in rats. Breast Cancer Res Treat. *39*, 7-20.

Salomon,D.S., Brandt,R., Ciardiello,F., and Normanno,N. (1995). Epidermal growth factor-related peptides and their receptors in human malignancies. Crit Rev. Oncol. Hematol. *19*, 183-232.

Schechter,A.L., Stern,D.F., Vaidyanathan,L., Decker,S.J., Drebin,J.A., Greene,M.I., and Weinberg,R.A. (1984). The neu oncogene: an erb-B-related gene encoding a 185,000-Mr tumour antigen. Nature *312*, 513-516.

Schreiber,A.B., Winkler,M.E., and Derynck,R. (1986). Transforming growth factor-alpha: a more potent angiogenic mediator than epidermal growth factor. Science *232*, 1250-1253.

Segatto,O., King,C.R., Pierce,J.H., Di Fiore,P.P., and Aaronson,S.A. (1988). Different structural alterations upregulate in vitro tyrosine kinase activity and transforming potency of the erbB-2 gene. Mol Cell Biol. *8*, 5570-5574.

Seton-Rogers,S.E., Lu,Y., Hines,L.M., Koundinya,M., LaBaer,J., Muthuswamy,S.K., and Brugge,J.S. (2004). Cooperation of the ErbB2 receptor and transforming growth factor beta in induction of migration and invasion in mammary epithelial cells. Proc. Natl Acad. Sci U. S. A *101*, 1257-1262.

Shepard,H.M., Lewis,G.D., Sarup,J.C., Fendly,B.M., Maneval,D., Mordenti,J., Figari,I., Kotts,C.E., Palladino,M.A., Jr., Ullrich,A., and . (1991). Monoclonal antibody therapy of human cancer: taking the HER2 protooncogene to the clinic. J Clin. Immunol. *11*, 117-127.

Shepherd,T.G., Kockeritz,L., Szrajber,M.R., Muller,W.J., and Hassell,J.A. (2001). The pea3 subfamily ets genes are required for HER2/Neu-mediated mammary oncogenesis. Curr. Biol. *11*, 1739-1748.

Shin,I., Yakes,F.M., Rojo,F., Shin,N.Y., Bakin,A.V., Baselga,J., and Arteaga,C.L. (2002). PKB/Akt mediates cell-cycle progression by phosphorylation of p27(Kip1) at threonine 157 and modulation of its cellular localization. Nat. Med. *8*, 1145-1152.

Shing,Y., Christofori,G., Hanahan,D., Ono,Y., Sasada,R., Igarashi,K., and Folkman,J. (1993). Betacellulin: a mitogen from pancreatic beta cell tumors. Science *259*, 1604-1607.

Shoyab,M., Plowman,G.D., McDonald,V.L., Bradley,J.G., and Todaro,G.J. (1989). Structure and function of human amphiregulin: a member of the epidermal growth factor family. Science *243*, 1074-1076.

Siegel,P.M., Dankort,D.L., Hardy,W.R., and Muller,W.J. (1994). Novel activating mutations in the neu proto-oncogene involved in induction of mammary tumors. Mol. Cell Biol. *14*, 7068-7077.

Siegel,P.M. and Massague,J. (2003). Cytostatic and apoptotic actions of TGF-beta in homeostasis and cancer. Nat. Rev. Cancer *3*, 807-821.

Siegel,P.M., Ryan,E.D., Cardiff,R., and Muller,W. (1999). Elevated expression of activated forms of Neu/ErbB-2 and ErbB-3 are involved in the induction of mammary tumors in transgenic mice: implications for human breast cancer. EMBO J. *18*, 2149-2164.

Siegel,P.M., Shu,W., Cardiff,R.D., Muller,W.J., and Massague,J. (2003). Transforming growth factor {beta} signaling impairs Neu-induced mammary tumorigenesis while promoting pulmonary metastasis. PNAS *100*, 8430-8435.

Singletary,K.W., McNary,M.Q., Odoms,A.M., Nelshoppen,J., and Wallig,M.A. (1991). Ethanol consumption and DMBA-induced mammary carcinogenesis in rats. Nutr. Cancer *16*, 13-23.

Sjogren,S., Inganas,M., Lindgren,A., Holmberg,L., and Bergh,J. (1998). Prognostic and predictive value of c-erbB-2 overexpression in primary breast cancer, alone and in combination with other prognostic markers. J Clin. Oncol. *16*, 462-469.

Slamon,D.J., Clark,G.M., Wong,S.G., Levin,W.J., Ullrich,A., and McGuire,W.L. (1987). Human breast cancer: correlation of relapse and survival with amplification of the HER-2/neu oncogene. Science *235*, 177-182.

Slamon,D.J., Godolphin,W., Jones,L.A., Holt,J.A., Wong,S.G., Keith,D.E., Levin,W.J., Stuart,S.G., Udove,J., Ullrich,A., and et al. (1989). Studies of the HER-2/neu proto-oncogene in human breast and ovarian cancer. Science *244*, 707-712.

Slamon,D.J., Leyland-Jones,B., Shak,S., Fuchs,H., Paton,V., Bajamonde,A., Fleming,T., Eiermann,W., Wolter,J., Pegram,M., Baselga,J., and Norton,L. (2001). Use of chemotherapy plus a monoclonal antibody against HER2 for metastatic breast cancer that overexpresses HER2. N Engl J Med *344*, 783-792.

Sliwkowski,M.X., Lofgren,J.A., Lewis,G.D., Hotaling,T.E., Fendly,B.M., and Fox,J.A. (1999). Nonclinical studies addressing the mechanism of action of trastuzumab (Herceptin). Semin. Oncol. *26*, 60-70.

Sliwkowski,M.X., Schaefer,G., Akita,R.W., Lofgren,J.A., Fitzpatrick,V.D., Nuijens,A., Fendly,B.M., Cerione,R.A., Vandlen,R.L., and Carraway,K.L., III (1994). Coexpression of erbB2 and erbB3 proteins reconstitutes a high affinity receptor for heregulin. J Biol. Chem. *269*, 14661-14665.

Soltoff,S.P., Carraway,K.L., III, Prigent,S.A., Gullick,W.G., and Cantley,L.C. (1994). ErbB3 is involved in activation of phosphatidylinositol 3-kinase by epidermal growth factor. Mol. Cell Biol. *14*, 3550-3558.

Soriano,P. (1999). Generalized lacZ expression with the ROSA26 Cre reporter strain. Nat. Genet. *21*, 70-71.

Sorkin,A., Di Fiore,P.P., and Carpenter,G. (1993). The carboxyl terminus of epidermal growth factor receptor/erbB-2 chimerae is internalization impaired. Oncogene *8*, 3021-3028.

Spencer,K.S., Graus-Porta,D., Leng,J., Hynes,N.E., and Klemke,R.L. (2000). ErbB2 is necessary for induction of carcinoma cell invasion by ErbB family receptor tyrosine kinases. J. Cell Biol. *148*, 385-397.

Stighall,M., Manetopoulos,C., Axelson,H., and Landberg,G. (2005). High ID2 protein expression correlates with a favourable prognosis in patients with primary breast cancer and reduces cellular invasiveness of breast cancer cells. Int. J Cancer *115*, 403-411.

Sung,Y.K., Hwang,S.Y., Park,M.K., Bae,H.I., Kim,W.H., Kim,J.C., and Kim,M. (2003). Fatty acid-CoA ligase 4 is overexpressed in human hepatocellular carcinoma. Cancer Sci *94*, 421-424.

Tai,Y.T. and Gould,M.N. (1995). Hormonal modulation of neu-induced mammary carcinogenesis: evidence against a single-step induction of mammary cancer by neu. Carcinogenesis *16*, 1455-1459.

Tamayo,P., Slonim,D., Mesirov,J., Zhu,Q., Kitareewan,S., Dmitrovsky,E., Lander,E.S., and Golub,T.R. (1999). Interpreting patterns of gene expression with self-organizing maps: methods and application to hematopoietic differentiation. Proc. Natl. Acad. Sci. U. S. A *96*, 2907-2912.

Tang,B., Vu,M., Booker,T., Santner,S.J., Miller,F.R., Anver,M.R., and Wakefield,L.M. (2003). TGF-{beta} switches from tumor suppressor to prometastatic factor in a model of breast cancer progression. J. Clin. Invest. *112*, 1116-1124.

Tham,Y.L., Verani,M.S., and Chang,J. (2002). Reversible and irreversible cardiac dysfunction associated with trastuzumab in breast cancer. Breast Cancer Res Treat. *74*, 131-134.

Tokunaga,M., Norman,J.E., Jr., Asano,M., Tokuoka,S., Ezaki,H., Nishimori,I., and Tsuji,Y. (1979). Malignant breast tumors among atomic bomb survivors, Hiroshima and Nagasaki, 1950-74. J Natl Cancer Inst *62*, 1347-1359.

Toyoda,H., Komurasaki,T., Uchida,D., Takayama,Y., Isobe,T., Okuyama,T., and Hanada,K. (1995). Epiregulin. A novel epidermal growth factor with mitogenic activity for rat primary hepatocytes. J Biol. Chem. *270*, 7495-7500.

Treurniet,H.F., Rookus,M.A., Peterse,H.L., Hart,A.A., and van Leeuwen,F.E. (1992). Differences in breast cancer risk factors to neu (c-erbB-2) protein overexpression of the breast tumor. Cancer Res *52*, 2344-2345.

Tzahar,E., Moyer,J.D., Waterman,H., Barbacci,E.G., Bao,J., Levkowitz,G., Shelly,M., Strano,S., Pinkas-Kramarski,R., Pierce,J.H., Andrews,G.C., and Yarden,Y. (1998). Pathogenic poxviruses reveal viral strategies to exploit the ErbB signaling network. EMBO J *17*, 5948-5963.

Tzahar,E., Pinkas-Kramarski,R., Moyer,J.D., Klapper,L.N., Alroy,I., Levkowitz,G., Shelly,M., Henis,S., Eisenstein,M., Ratzkin,B.J., Sela,M., Andrews,G.C., and Yarden,Y. (1997). Bivalence of EGF-like ligands drives the ErbB signaling network. EMBO J *16*, 4938-4950.

Tzahar,E., Waterman,H., Chen,X., Levkowitz,G., Karunagaran,D., Lavi,S., Ratzkin,B.J., and Yarden,Y. (1996). A hierarchical network of interreceptor interactions determines signal transduction by Neu differentiation factor/neuregulin and epidermal growth factor. Mol. Cell. Biol. *16*, 5276-5287.

Ueda,Y., Wang,S., Dumont,N., Yi,J.Y., Koh,Y., and Arteaga,C.L. (2004). Overexpression of HER2 (erbB2) in human breast epithelial cells unmasks transforming growth factor beta-induced cell motility. J Biol. Chem. *279*, 24505-24513.

Ullrich,A., Coussens,L., Hayflick,J.S., Dull,T.J., Gray,A., Tam,A.W., Lee,J., Yarden,Y., Libermann,T.A., Schlessinger,J., and . (1984). Human epidermal growth factor receptor cDNA sequence and aberrant expression of the amplified gene in A431 epidermoid carcinoma cells. Nature *309*, 418-425.

van der,G.P., Hunter,T., and Lindberg,R.A. (1994). Receptor protein-tyrosine kinases and their signal transduction pathways. Annu. Rev. Cell Biol. *10*, 251-337.

Verrecchia,F., Chu,M.L., and Mauviel,A. (2001). Identification of novel TGF-beta /Smad gene targets in dermal fibroblasts using a combined cDNA microarray/promoter transactivation approach. J Biol. Chem. *276*, 17058-17062.

Vieira,A.V., Lamaze,C., and Schmid,S.L. (1996). Control of EGF receptor signaling by clathrin-mediated endocytosis. Science *274*, 2086-2089.

Viglietto,G., Motti,M.L., Bruni,P., Melillo,R.M., D'Alessio,A., Califano,D., Vinci,F., Chiappetta,G., Tsichlis,P., Bellacosa,A., Fusco,A., and Santoro,M. (2002). Cytoplasmic relocalization and inhibition of the cyclin-dependent kinase inhibitor p27(Kip1) by PKB/Akt-mediated phosphorylation in breast cancer. Nat. Med. *8*, 1136-1144.

Vogel,C.L., Cobleigh,M.A., Tripathy,D., Gutheil,J.C., Harris,L.N., Fehrenbacher,L., Slamon,D.J., Murphy,M., Novotny,W.F., Burchmore,M., Shak,S., Stewart,S.J., and Press,M. (2002). Efficacy and safety of trastuzumab as a single agent in first-line treatment of HER2-overexpressing metastatic breast cancer. J Clin. Oncol. *20*, 719-726.

Wada,T., Qian,X.L., and Greene,M.I. (1990). Intermolecular association of the p185neu protein and EGF receptor modulates EGF receptor function. Cell *61*, 1339-1347.

Wagner,K.U., Wall,R.J., St Onge,L., Gruss,P., Wynshaw-Boris,A., Garrett,L., Li,M., Furth,P.A., and Hennighausen,L. (1997). Cre-mediated gene deletion in the mammary gland. Nucleic Acids Res. *25*, 4323-4330.

Wakefield,L.M. and Roberts,A.B. (2002). TGF-beta signaling: positive and negative effects on tumorigenesis. Curr. Opin. Genet. Dev. *12*, 22-29.

Wakefield,L.M. and Sporn,M.B. (1990). Suppression of carcinogenesis: a role for TGF-beta and related molecules in prevention of cancer. Immunol. Ser. *51*, 217-243.

Wakefield,L.M., Yang,Y.A., and Dukhanina,O. (2000). Transforming growth factor-beta and breast cancer: Lessons learned from genetically altered mouse models. Breast Cancer Res *2*, 100-106.

Wang,B., Kennan,W.S., Yasukawa-Barnes,J., Lindstrom,M.J., and Gould,M.N. (1992). Difference in the response of neu and ras oncogene-induced rat mammary carcinomas to early and late ovariectomy. Cancer Res. *52*, 4102-4105.

Wang,N., Kudryavtseva,E., Ch'en,I.L., McCormick,J., Sugihara,T.M., Ruiz,R., and Andersen,B. (2004). Expression of an engrailed-LMO4 fusion protein in mammary epithelial cells inhibits mammary gland development in mice. Oncogene *23*, 1507-1513.

Wang,S.E., Wu,F.Y., Shin,I., Qu,S., and Arteaga,C.L. (2005). Transforming growth factor {beta} (TGF-{beta})-Smad target gene protein tyrosine phosphatase receptor type kappa is required for TGF-{beta} function. Mol Cell Biol. *25*, 4703-4715.

Warburg,O. (1956). On the origin of cancer cells. Science *123*, 309-314.

Waterman,H., Sabanai,I., Geiger,B., and Yarden,Y. (1998). Alternative intracellular routing of ErbB receptors may determine signaling potency. J Biol. Chem. *273*, 13819-13827.

Weinstein,E.J., Kitsberg,D.I., and Leder,P. (2000). A mouse model for breast cancer induced by amplification and overexpression of the neu promoter and transgene. Mol Med *6*, 4-16.

Wellings,S.R. and Jensen,H.M. (1973). On the origin and progression of ductal carcinoma in the human breast. J Natl Cancer Inst *50*, 1111-1118.

Welt,C.K. and Crowley,W.F., Jr. (1998). Activin: an endocrine or paracrine agent? Eur. J Endocrinol *139*, 469-471.

Wilson,K.S., Roberts,H., Leek,R., Harris,A.L., and Geradts,J. (2002). Differential Gene Expression Patterns in HER2/neu-Positive and -Negative Breast Cancer Cell Lines and Tissues. Am J Pathol *161*, 1171.

Wong,C.W., Song,C., Grimes,M.M., Fu,W., Dewhirst,M.W., Muschel,R.J., and Al Mehdi,A.B. (2002). Intravascular location of breast cancer cells after spontaneous metastasis to the lung. Am J Pathol *161*, 749-753.

Worthylake,R., Opresko,L.K., and Wiley,H.S. (1999). ErbB-2 amplification inhibits down-regulation and induces constitutive activation of both ErbB-2 and epidermal growth factor receptors. J. Biol. Chem. *274*, 8865-8874.

Wright,C., Nicholson,S., Angus,B., Sainsbury,J.R., Farndon,J., Cairns,J., Harris,A.L., and Horne,C.H. (1992). Relationship between c-erbB-2 protein product expression and response to endocrine therapy in advanced breast cancer. Br. J. Cancer *65*, 118-121.

Wu,K., Zhang,Y., Xu,X.C., Hill,J., Celestino,J., Kim,H.T., Mohsin,S.K., Hilsenbeck,S.G., Lamph,W.W., Bissonette,R., and Brown,P.H. (2002). The retinoid X receptor-selective retinoid, LGD1069, prevents the development of estrogen receptor-negative mammary tumors in transgenic mice. Cancer Res *62*, 6376-6380.

Xiong,S., Grijalva,R., Zhang,L., Nguyen,N.T., Pisters,P.W., Pollock,R.E., and Yu,D. (2001). Up-regulation of vascular endothelial growth factor in breast cancer cells by the heregulin-beta1-activated p38 signaling pathway enhances endothelial cell migration. Cancer Res *61*, 1727-1732.

Xu,F.J., Stack,S., Boyer,C., O'Briant,K., Whitaker,R., Mills,G.B., Yu,Y.H., and Bast,R.C., Jr. (1997). Heregulin and agonistic anti-p185(c-erbB2) antibodies inhibit proliferation but increase invasiveness of breast cancer cells that overexpress p185(c-erbB2): increased invasiveness may contribute to poor prognosis. Clin. Cancer Res *3*, 1629-1634.

Yakes,F.M., Chinratanalab,W., Ritter,C.A., King,W., Seelig,S., and Arteaga,C.L. (2002). Herceptin-induced inhibition of phosphatidylinositol-3 kinase and Akt Is required for antibody-mediated effects on p27, cyclin D1, and antitumor action. Cancer Res. *62*, 4132-4141.

Yamamoto,T., Ikawa,S., Akiyama,T., Semba,K., Nomura,N., Miyajima,N., Saito,T., and Toyoshima,K. (1986). Similarity of protein encoded by the human c-erb-B-2 gene to epidermal growth factor receptor. Nature *319*, 230-234.

Yang,G., Cai,K.Q., Thompson-Lanza,J.A., Bast,R.C., Jr., and Liu,J. (2004). Inhibition of breast and ovarian tumor growth through multiple signaling pathways by using retrovirus-mediated small interfering RNA against Her-2/neu gene expression. J Biol. Chem. *279*, 4339-4345.

Yang,X., Edgerton,S.M., Kosanke,S.D., Mason,T.L., Alvarez,K.M., Liu,N., Chatterton,R.T., Liu,B., Wang,Q., Kim,A., Murthy,S., and Thor,A.D. (2003). Hormonal and Dietary Modulation of Mammary Carcinogenesis in Mouse Mammary Tumor Virus-c-erbB-2 Transgenic Mice. Cancer Res *63*, 2425-2433.

Yang,Y.a., Dukhanina,O., Tang,B., Mamura,M., Letterio,J.J., MacGregor,J., Patel,S.C., Khozin,S., Liu,Z.y., Green,J., Anver,M.R., Merlino,G., and Wakefield,L.M. (2002). Lifetime exposure to a soluble TGF-{beta} antagonist protects mice against metastasis without adverse side effects. J. Clin. Invest. *109*, 1607-1615.

Yarden,Y. (2001). The EGFR family and its ligands in human cancer. signalling mechanisms and therapeutic opportunities. Eur. J Cancer *37 Suppl 4*, S3-S8.

Yarden,Y. and Sliwkowski,M.X. (2001). Untangling the ErbB signalling network. Nat. Rev. Mol. Cell Biol. *2*, 127-137.

Yen,L., Benlimame,N., Nie,Z.R., Xiao,D., Wang,T., Al Moustafa,A.E., Esumi,H., Milanini,J., Hynes,N.E., Pages,G., and Alaoui-Jamali,M.A. (2002). Differential regulation of tumor angiogenesis by distinct ErbB homo- and heterodimers. Mol Biol. Cell *13*, 4029-4044.

Yen,L., You,X.L., Al Moustafa,A.E., Batist,G., Hynes,N.E., Mader,S., Meloche,S., and Alaoui-Jamali,M.A. (2000). Heregulin selectively upregulates vascular endothelial growth factor secretion in cancer cells and stimulates angiogenesis. Oncogene *19*, 3460-3469.

Yu,D. and Hung,M.C. (2000). Overexpression of ErbB2 in cancer and ErbB2-targeting strategies. Oncogene *19*, 6115-6121.

Yu,D., Jing,T., Liu,B., Yao,J., Tan,M., McDonnell,T.J., and Hung,M.C. (1998a). Overexpression of ErbB2 blocks Taxol-induced apoptosis by upregulation of p21Cip1, which inhibits p34Cdc2 kinase. Mol Cell *2*, 581-591.

Yu,D., Liu,B., Jing,T., Sun,D., Price,J.E., Singletary,S.E., Ibrahim,N., Hortobagyi,G.N., and Hung,M.C. (1998b). Overexpression of both p185c-erbB2 and p170mdr-1 renders breast cancer cells highly resistant to taxol. Oncogene *16*, 2087-2094.

Yu,H. and Jove,R. (2004). The STATs of cancer--new molecular targets come of age. Nat. Rev. Cancer *4*, 97-105.

Yu,Q., Geng,Y., and Sicinski,P. (2001). Specific protection against breast cancers by cyclin D1 ablation. Nature *411*, 1017-1021.

Yue,J. and Mulder,K.M. (2001). Transforming growth factor-beta signal transduction in epithelial cells. Pharmacol. Ther. *91*, 1-34.

Zha,J., Harada,H., Yang,E., Jockel,J., and Korsmeyer,S.J. (1996). Serine phosphorylation of death agonist BAD in response to survival factor results in binding to 14-3-3 not BCL-X(L). Cell *87*, 619-628.

Zhang,D., Sliwkowski,M.X., Mark,M., Frantz,G., Akita,R., Sun,Y., Hillan,K., Crowley,C., Brush,J., and Godowski,P.J. (1997). Neuregulin-3 (NRG3): a novel neural tissue-enriched protein that binds and activates ErbB4. Proc. Natl Acad. Sci U. S. A *94*, 9562-9567.

Zhang,K., Sun,J., Liu,N., Wen,D., Chang,D., Thomason,A., and Yoshinaga,S.K. (1996). Transformation of NIH 3T3 cells by HER3 or HER4 receptors requires the presence of HER1 or HER2. J Biol. Chem. *271*, 3884-3890.

Zhou,B.P., Hu,M.C., Miller,S.A., Yu,Z., Xia,W., Lin,S.Y., and Hung,M.C. (2000). HER-2/neu blocks tumor necrosis factor-induced apoptosis via the Akt/NF-kappaB pathway. J. Biol. Chem. *275*, 8027-8031.

Zhou,B.P., Liao,Y., Xia,W., Spohn,B., Lee,M.H., and Hung,M.C. (2001a). Cytoplasmic localization of p21Cip1/WAF1 by Akt-induced phosphorylation in HER-2/neu-overexpressing cells. Nat. Cell Biol. *3*, 245-252.

Zhou,B.P., Liao,Y., Xia,W., Zou,Y., Spohn,B., and Hung,M.C. (2001b). HER-2/neu induces p53 ubiquitination via Akt-mediated MDM2 phosphorylation. Nat. Cell Biol. *3*, 973-982.

Zoll,B., Kynast,B., Corell,B., Marx,D., Fischer,G., and Schauer,A. (1992). Alterations of the c-erbB2 gene in human breast cancer. J. Cancer Res. Clin. Oncol. *118*, 468-473.